

Osteoarthritis:

at the crossroads of metabolism and inflammation

Anne Elisabeth Kozijn

Osteoarthritis: at the crossroads of metabolism and inflammation

Artrose:
op het snijvlak van metabolisme en ontsteking
(met een samenvatting in het Nederlands)

Anne Elisabeth Kozijn

Osteoarthritis: at the crossroads of metabolism and inflammation
ISBN/EAN 978-94-6380-678-7

PhD thesis, Utrecht University, University Medical Center Utrecht, Utrecht, the Netherlands
© 2020 Anne Elisabeth Kozijn

The work described in this thesis was conducted at the Metabolic Health Research expertise group of the Netherlands Organization for Applied Scientific Research (TNO) and the University Medical Center Utrecht, Department of Orthopaedics and Department of Rheumatology & Clinical Immunology.

The research described in this thesis was financially supported by the TNO Research Program Predictive Health Technologies and the European Union's Seventh Framework Programme for research, technological development and demonstration under grant agreement No. 305815-D-BOARD.

Printing of this thesis was financially supported by the Metabolic Health Research expertise group of the Netherlands Organization for Applied Scientific Research (TNO).

Cover illustration: Martine Riphagen
Cover design: Jaiwey Nuij (https://www.jaiweynuij.com)
and Dennis Hendriks / ProefschriftMaken.nl

Printed by ProefschriftMaken on FSC-certified paper

Osteoarthritis:
at the crossroads of metabolism and inflammation

Artrose:
op het snijvlak van metabolisme en ontsteking
(met een samenvatting in het Nederlands)

Proefschrift

ter verkrijging van de graad van doctor aan de Universiteit Utrecht op gezag van de rector magnificus, prof. dr. H.R.B.M. Kummeling, ingevolge het besluit van het college voor promoties in het openbaar te verdedigen op

dinsdag 4 februari 2020 des ochtends te 10.30 uur

door

Anne Elisabeth Kozijn
geboren op 17 november 1985
te Apeldoorn

Promotoren:	Prof. dr. H. Weinans
	Prof. dr. F.P.J.G. Lafeber
Copromotoren:	Dr. R. Stoop
	Dr. I. Bobeldijk-Pastorova



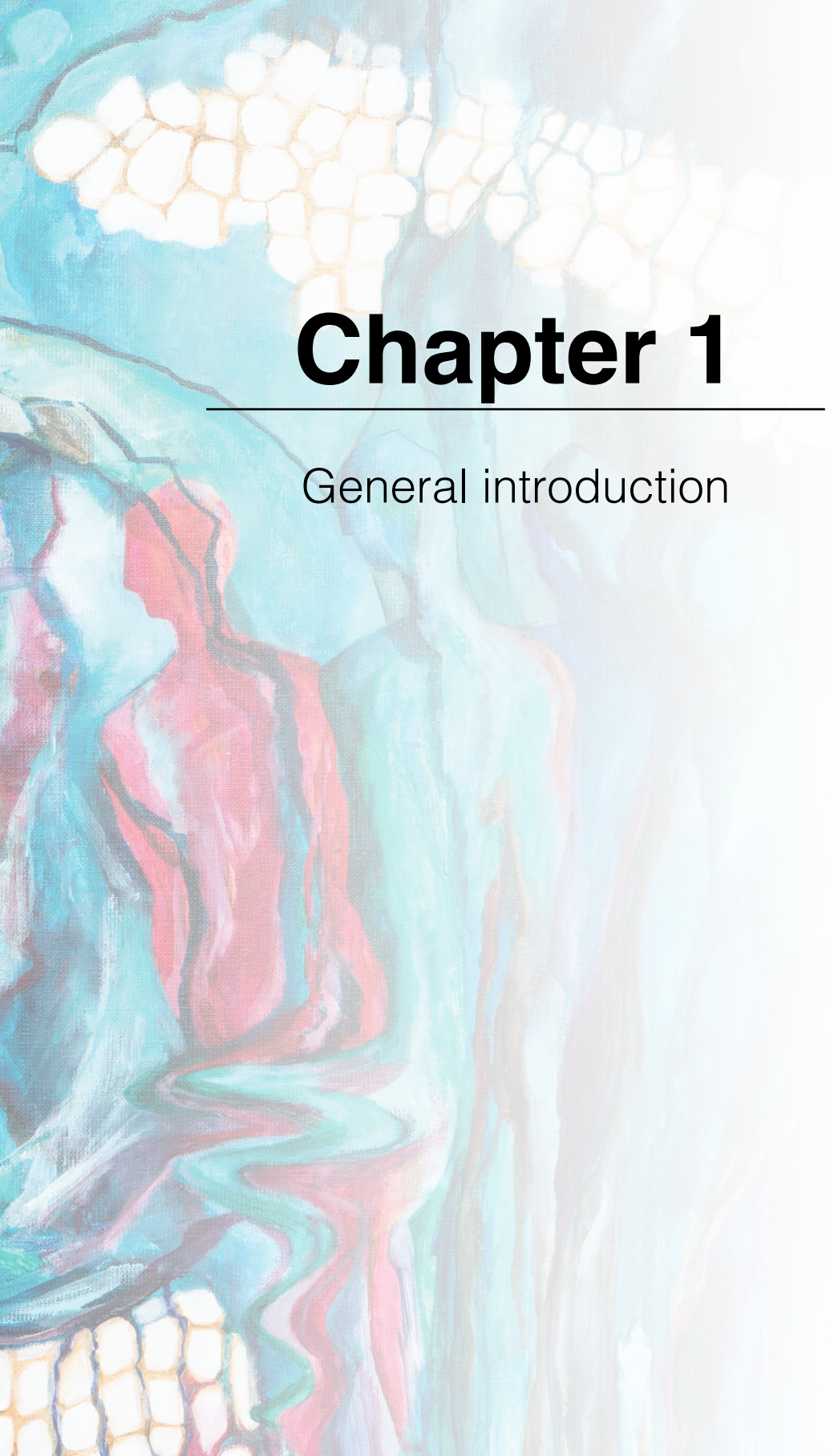
Thesis cover design: An artist's interpretation of my PhD research (by Martine Riphagen)

Free-moving people can be seen at the top of the painting. Unfortunately, the movement becomes stiffer and changes to a static position on the left hand side of the canvas. These people are trapped in fat cells. At the top right, the fat cells pose a threat to the free-moving people. In the centre is a circle, a "wheel", representing movement. On top of the wheel are mice, which have made an indispensable contribution to my research. In the middle, crown-like structures and other structures are visible that depict the search for answers to my research questions. I am the seated figure in red, literally connected with lines and intertwined with my research. My seat has the shape of the staff of Asclepius (symbol of medicine). Next to me are people who symbolize the support of others during this period – such as colleagues, family and friends. At the far right stand a vague, indefinite figure who has turned away, symbolising the less positive contributions to my research. The colours used refer to the (immuno)histological results that I have achieved. The blending of colours unifies the entire artwork: me and my research!

Table of contents

Chapter 1	General introduction	9
Chapter 2	Variable cartilage degradation in mice with diet-induced metabolic dysfunction: food for thought	39
Chapter 3	High-fat dietary consumption promotes disease progression in a surgical joint destabilisation murine model of osteoarthritis: role of systemic eicosanoids and circulating monocytes	83
Chapter 4	Increased inflammation in the infrapatellar fat pad in a surgical mouse model of osteoarthritis upon high-fat feeding	115
Chapter 5	Human C-reactive protein aggravates osteoarthritis development in mice on a high-fat diet	137
Chapter 6	Intensive therapeutic lowering of cholesterol does not affect progression of diet-induced osteoarthritis in a translational dyslipidemia model	175
Chapter 7	Discussion and outlook	193
	Summary	211
	Nederlandse samenvatting	213
	Dankwoord	215
	Curriculum vitae	219
	List of abbreviations	220





Chapter 1

General introduction

Osteoarthritis: prevalence, diagnosis and impact

Pathogenesis, symptoms and risk factors of osteoarthritis

Osteoarthritis (OA) is a debilitating joint disorder that is characterised by a loss of articular cartilage, which may be accompanied by remodelling of articular cartilage and/or adjacent bone, osteophyte formation, synovial inflammation, and pain[1]. While it can occur in any synovial joint, OA is most frequently observed in de knee, hip or hand[2–4]. To date, OA remains challenging to treat and its definition, risk factors and pathophysiology are still evolving[5].

The definition of OA was long centred on the changes in the articular cartilage but OA is now considered a disease of the whole joint, including alterations in the articular cartilage, subchondral bone, ligaments, capsule and synovial membrane, ultimately leading to joint failure[5]. The range and severity of symptoms are diverse and can change over time. In addition, clinical symptoms do not always correlate with the structural integrity of a joint[6], especially in the early phase of the disease: individuals with clinical presentations of pain and symptoms do not always have radiographic evidence of disease (i.e. symptomatic OA), and many asymptomatic individuals can present with severe structural OA changes (i.e. radiographic OA)[7]. In an attempt to define this heterogenenous condition, a distinction has been proposed between OA "disease" and "illness"[1,8]. The "disease" of OA is defined as the measurable abnormalities that could lead to the illness. These characteristic changes are found radiographically as joint space narrowing, subchondral sclerosis, subchondral cysts, and osteophyte formation. The "illness" of OA is defined as the symptoms that bring the patient to the physician, such as pain or immobility.

Because patients generally seek medical care after symptoms develop, it remains challenging to identify and treat patients early in the disease or illness process. In general, OA is more common in women than men, increases with age (i.e. occurring after the age of 40-50 years), and is greater in developed than developing countries[3,9]. Risk factors for OA can be broadly categorised as either: 1) systemic, including age, gender, genetics and ethnicity; 2) mechanical, including joint structure/alignment, abnormal loading, trauma, physical activity and repetitive joint use through occupation; and 3) environmental, including smoking, sedentary lifestyle, obesity, and nutrition[4,9]. The factors that initiate OA are likely to vary depending on the joint site.

Changes in cartilage, bone, synovium and infrapatellar fat pad in knee osteoarthritis

A joint is the connection between bones in the body that allow different degrees and types of movements. In synovial joints, the most common joints of the body, the articulating surfaces of the bones come into contact with each other within a joint

cavity that is filled with a lubricating fluid10. This thesis focuses on the knee joint, as OA is most prevalent in the knee[2–4] and association between OA and obesity has been particularly marked for this joint[11].

Together with the synovial fluid, thin layers of articular cartilage that cover the surfaces of the bones reduce the friction between bones during joint movement. Loss of these articular cartilage layers remains the signature pathological feature of OA, which is assessed radiographically as a reduction in joint space width and is a major determinant in the Kellgren-Lawrence grading system for OA severity[12,13]. Cartilage consists solely out of chondrocytes, which synthesize and maintain the collagen-based extracellular matrix, and the tissue is not vascularized or innervated[14]. Instead, compression of the articular cartilage generates fluid flow, providing nutrients to the chondrocytes by diffusion[15]. Partly as a result of these properties, articular cartilage has a low reparative potential14 and failure of chondrocytes to maintain homeostasis between synthesis and degradation of extracellular matrix components underlies osteoarthritis[16]. It is not known what initiates the imbalance between the degradation and the repair of cartilage, but pathways of OA-induced cartilage destruction include cell death, activation and abnormal differentiation of remaining chondrocytes, degradation of the extracellular matrix, and production of inflammatory mediators[17]. Localized areas of loss of cartilage can increase focal stress across the joint, leading to further cartilage loss and malalignment, creating a vicious cycle of joint damage that ultimately can lead to joint failure[18].

Along with progressive loss of articular cartilage, OA is characterised by increased subchondral bone sclerosis. The subchondral bone is distally connected to the overlying articular cartilage through a layer of calcified cartilage. These structures are suggested to act as a functional osteochondral unit, displaying molecular crosstalk and distributing mechanical forces to minimize shear stresses on the articular cartilage layer[19–21]. Longitudinal studies in patients will need to confirm whether disrupted homeostasis of this unit is involved in the onset or progression of OA[22]. Joint disruption leads to subchondral bone sclerosis, with thickening of the subchondral bone plate, extensive remodelling of the trabeculae (internal structure of the trabecular bone), development of subchondral bone cysts, and the formation of osteophytes, in an attempt at repair[23]. Changes in the subchondral bone plate and trabeculae are associated with activation of the bone remodelling cycle, probably to adapt to changes in the biomechanics or to repair microdamage[19]. Osteophytes are new bony outgrowths at the joint margins, where the cartilage and bone come together, and are very common in OA – being a more prominent feature than for example in rheumatoid arthritis[24]. In addition, the occurrence of osteophytes in affected joints is an important criterion for the diagnosis of OA, but their pathophysiology and function is not completely understood[24,25]. Osteophytes may reflect the adaptation of a joint to instability or originate from

an altered, pro-inflammatory internal joint milieu that promotes chondrogenesis of precursor cells in the periosteum and synovial lining[25–27]. These abnormal bone remodelling processes, together with increased bone turnover and vascularisation, contribute to stiffening and reduced mobility of the joint that further aggravate the disease[28,29].

It remains unclear whether the morphological changes that occur in the synovium during OA pathogenesis are primary or whether they are the result of joint inflammation, cartilage degradation and lesions of the subchondral bone[30,31]. The synovium is connective tissue membrane that lines the cavity of a synovial joint[32]. It is highly vascular, well-innervated, and consists out of one to three layers of specialized fibroblast-like synoviocytes that are interspersed with macrophages[33,34]. The synovium allows for smooth movement by preventing joint capsule adherence with cartilage and maintaining a constant synovial fluid volume that provides nutrition and lubrication to the cartilage[32,35]. Synovial inflammation is common in OA patients[36] and is characterised by proliferation and hyperplasia of the lining cells along with moderate inflammatory cell infiltration and increased vascularity[35]. Although the role of inflammation in osteoarthritis (OA) has been heavily debated[37,38], mounting evidence suggests that synovitis and the resultant pro-inflammatory and pro-catabolic mediators are important in the pathogenesis of OA with effects on articular cartilage[39]. The role of activated synovial macrophages herein is increasingly appreciated, with a recent study demonstrating in vivo that macrophage number significantly associated with knee OA pain, joint space narrowing, and osteophytes[40]. The factors released during synovial inflammation attract immune cells, increase angiogenesis and induce a phenotypic shift in chondrocytes that produce additional cytokines and proteolytic enzymes, creating a vicious cycle of further cartilage degradation and synovial inflammation[39]. Eventually, the inflammatory processes result in reduced levels of lubricin and impaired lubricating ability of synovial fluid, thus leading to joint friction and chondrocyte apoptosis[41]. Synovitis is associated with OA pain in humans, but it is as yet unclear whether synovitis-mediated stimulation or sensitisation of sensory nerves is a direct (via the synovial neuronal network) or indirect (via pro-inflammatory factors) mechanism[42,43].

In the past decade, the infrapatellar fat pad (IFP or IPFP; also known as Hoffa's fat pad) has come to light as a potential source of pro-inflammatory and pro-catabolic mediators[44,45]. Like the synovial membrane, the IFP is a well-innervated, highly vascularised, intracapsular soft tissue located close to the articular cartilage. Like other adipose tissues, the main cell types in the IFP are adipocytes, fibroblasts, and immune cells (i.e. macrophages, mast cells, and lymphocytes)[46]. The function of the IFP is unknown and purely theoretical. Due to its anatomical position, it has long been believed to serve a structural function by absorbing shocks[47] and aiding in the

distribution of synovial fluid[48], without any presumption of metabolic activity[45]. But, several reports have now indicated that IFP displays both basal and hormone-induced lipolysis[46,49] and is proposed to represent a potential endocrine link between obesity and knee OA[50]. There are compelling indications that the IFP contributes to OA pathogenesis, but the mechanism remains unclear. Most evidence comes from clinical studies in late-stage knee OA patients, where the IFP was found to be more inflamed, vascularized and fibrous compared with those of control patients without OA[51,52], as well as between obese and lean OA patients[53]. However, a recent preclinical study showed little to no involvement of the IFP in early OA pathogenesis[54], suggesting that the IFP can play different roles during the course of the disease.

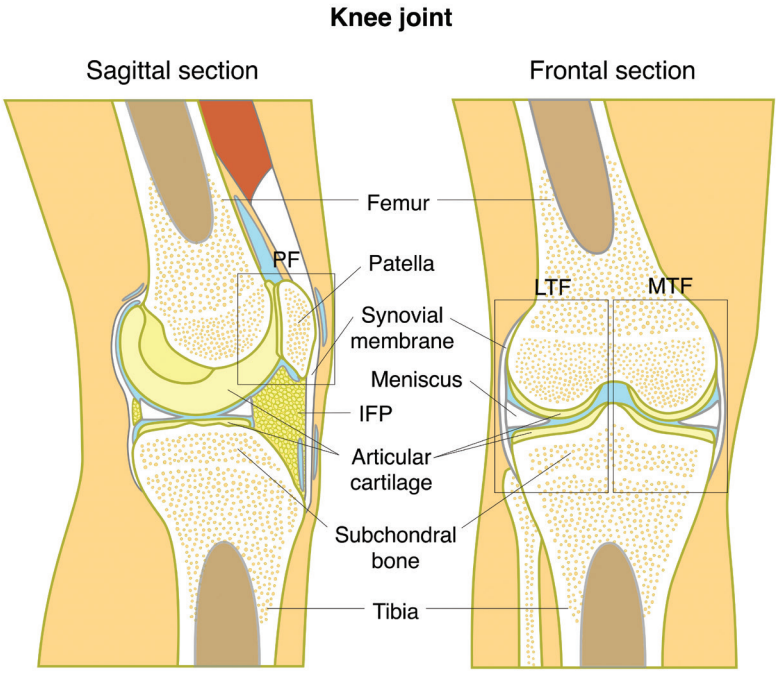


Figure 1 Anatomy of a healthy human knee joint. The highlighted structures can be affected by OA and will be referred to frequently in this thesis. Severity scoring of OA in the mouse is primarily based on the articular cartilage. Articular cartilage is divided into three compartments which are comparable in location to the human knee depicted here: the lateral tibiofemoral compartment (LTF), the medial tibiofemoral compartment (MTF), and the patellofemoral compartment (PF). The locations of articular cartilage (yellow), subchondral bone (beige), menisci (white), synovial membrane (white), synovial fluid (blue) and infrapatellar fat pad (IFP, yellow) are shown.

Social and economical impact of osteoarthritis

Disease progression is irreversible once the osteoarthritic process is initiated, thus progressively impairing quality of life. Prevalence and incidence estimates for OA differ greatly due to variation in OA definition and joint sites under consideration5 and should therefore be interpreted with caution. Worldwide estimates are that 9.6% of men and 18.0% of women over the age of 60 years have symptomatic OA[55]. Approximately 80% of those with OA will have limitations in movement, and 25% cannot perform their major activities of daily life[55]. In addition, OA-related disability is associated with higher all-cause mortality and OA patients have a greater risk at developing depression[56–58]. In the Netherlands, nearly 1.4 out of 17.1 million people (8.2%) were diagnosed and registered with OA at the general practices in 2017[59]. With the aging of the population in developed and developing countries and the increase in certain risk factors for OA, particularly obesity and a sedentary lifestyle, it is expected that the number of people living with OA will increase considerably over the coming decades. Not surprisingly, this has substantial economic impact: in the United States, the loss of productivity due to the OA pain and disability, together with the costs of care, has been estimated at 27 billion dollars annually[60]. In the Netherlands, the costs of care for OA were 1.3 billion euros in 2015, corresponding to 1.6% of the total national health care costs[61].

This social and economical burden is not easily wavered, because no disease-modifying OA treatment (that is, treatment that will reduce symptoms in addition to slowing or stopping disease progression) has yet received approval by the regulatory agencies[5,62]. Current pharmacological treatments are therefore mainly targeted to relief of symptoms[63,64]. Non-pharmacologic approaches such as exercise and weight loss can improve symptoms but to date have not been found to impact disease progression[65,66,64]. The same is true for pharmacological treatments, including acetaminophen (paracetamol), nonsteroidal anti-inflammatory drugs (NSAIDs), COX-2 inhibitors, opioid analgesics, and intra-articular drugs[62,65,67]. Surgical interventions like total joint replacement are considered as the definitive treatment of OA, typically limited to patients with end-stage OA[68,69]. The most recently developed therapies have focussed on stem cells in the management of OA, however, due to the lack of standardised methodology, the application of these therapies has so far been discouraged[70,71]. The complexity and variability of OA aetiology suggests the need for patient-specific, aetiology-based treatment and necessitates research efforts to better understand disease development and progression.

Exploring patient phenotypes in osteoarthritis

The broad definition of OA – as a "group of overlapping distinct joint disorders with similar biological, morphological and clinical outcomes" – already reflects the difficulty in determining the appropriate treatment strategy for each patient. Identifying phenotypes of patients is therefore paramount to enable the detection of OA in its

early stages as well as distinguish individuals who are at higher risk of progression, which in turn could be used to guide clinical decision-making and allow more effective and specific therapeutic interventions to be designed5. Computational "big data" approaches, integrating data from various sources (i.e. clinical, imaging, "omics" data), are believed to advance identification of OA phenotypes in the future[72–75]. As there is no generally accepted classification system for OA phenotypes yet[76,77], conventional stratification based on the risk factors that underlie OA (such as obesity, age, or joint injury), structural features, or symptomatic presentation may remain clinically relevant for the time being[1,77]. The truth probably lies somewhere in between, as different categorisations can serve different purposes (e.g. diagnosis, treatment, prognosis) and mutually exclusive phenotypes conflict with the multifactorial nature of OA[77]. For the sake of simplicity we consider, in this thesis, a conventional OA phenotype termed 'metabolic OA', also described as metabolic syndrome- or obesity-associated OA. Metabolic OA is herein characterised by prevalence of a metabolic disorder (e.g. obesity, dyslipidemia, diabetes, hypercholesteremia) in association with systemic low-grade inflammation (elevated plasma leptin, C-reactive protein, erythrocyte sedimentation rate)[74].

The role of metabolism in the pathogenesis of osteoarthritis

Osteoarthritis and obesity

The historical concept of 'wear-and-tear' was built upon the high incidence of knee OA observed in obese people, linking the excessive weight to detrimental joint loading[78]. However, the recent paradigm shift to 'OA as a disease of the entire joint' instigated recognition that metabolic and inflammatory processes also play a significant role in metabolic OA. A population-based study demonstrated that obesity approximately doubles the lifetime risk of developing symptomatic knee OA compared with those who are of normal weight or are underweight[79]. Also, weight loss is known to induce pain relief and improved physical function in obese OA patients, along with decreased low-grade inflammation[80]. These observations can be dedicated to the reduction of mechanical forces, but weight bearing alone cannot explain the significantly higher rate of metabolic syndrome in the OA compared with non-OA population (59 vs. 23%)[81], the frequently observed mild to severe synovitis in OA which intensity correlates with prognosis[82], and the association of hand OA with metabolic diseases regardless of weight[83]. It is currently believed that the systemic low-grade inflammation that accompanies visceral obesity, dyslipidemia, and insulin resistance is responsible for the higher risk of OA development in obese individuals, but whether this inflammation is cause or consequence of metabolic OA remains unknown.

Diet-induced mouse model to study metabolic osteoarthritis

With the identification of increasingly more metabolic and inflammatory mechanisms involved, the relationship between obesity and OA has become more complex[11]. Preclinical models are critical tools both in advancing our understanding through basic research and in treatment development. When modelling OA in small animals, it must be taken into account that distinct mechanisms may drive distinct OA phenotypes[84]. Metabolic OA has therefore been predominantly studied with the diet-induced obesity model in small animals. Silberberg *et al.* first linked high-fat diet (HFD) feeding with accelerated OA onset and progression in the 1950s[85,86]. Literature on metabolic OA models has been scarce since then[87], with the vast majority of reports dating from the past decade. However, use of the model is far from standardised with literature showing a plethora of conditions that have been employed in as many combinations. The C57BL/6J mouse strain or genetic variants with this background have been most frequently employed for this model, as the readily obtained obesity observed in these mice closely parallels the metabolic adaptations seen in human disease pathogenesis[88]. At large, most researchers have employed a very-high-fat diet (VHFD, 60 kcal% from fat) to induce metabolic OA, sometimes combined with an increased mechanical burden through surgery or exercise. Many variations in study length are represented, although most report on a period of at least 12 weeks of VHFD feeding. Last but not least, a key difference between all publications is the scoring of OA severity. Despite initiatives for a common system for OA severity scoring in the mouse[89], many groups employ their own scoring system or use one of many adaptations to the Mankin scoring system designed for human cartilage[90], thus complicating interpretation of results and comparisons between studies. In addition to classic methods such as histological examination, several other approaches have been newly developed or adopted to the small size of mice, like high-throughput 'omics' technologies, that enable comprehensive analyses of many outcome parameters in OA[91].

Lipids, cholesterol, and eicosanoids in metabolic osteoarthritis

Lipids and cholesterol, next to being essential structural components of cell membranes and the main source of energy storage, are now increasingly recognized as potent signalling molecules that regulate a multitude of cellular responses and participate in the crosstalk between inflammation and metabolism92. Cholesterol is a hydrophobic molecule and needs to be associated with a lipoprotein particle to be transported in the plasma. Plasma lipoproteins are divided into five major classes: chylomicrons, very-low-density lipoproteins (VLDL), intermediate-density lipoproteins (IDL), low-density lipoproteins (LDL), and high-density lipoproteins (HDL). Increased levels of cholesterol contained in (V)LDL particles promote cholesterol accumulation and an inflammatory response, while HDL-associated cholesterol (HDL-C) opposes this

process and reduces inflammation by promoting the cellular efflux of cholesterol[93]. Fatty acids are lipid "building blocks" and are the main contributors to dietary fat in humans[94]. Fatty acids are hydrocarbon chains of varying lengths and degrees of unsaturation (i.e. the presence of double bonds), with a carboxyl group at one end and a methyl (ω or n) group at the other[95]. The extent of unsaturation may vary from 1 double bond (monounsaturated fatty acids, or MUFAs) to two or more double bonds (polyunsaturated fatty acids, or PUFAs)[95]. Additional complexity in the structure of fatty acids may arise from the position of the double bonds and from the cis or trans orientation of the double bonds[95]. The number, position and orientation of double bonds can curve the fatty acid chain, thus altering its packing in lipid membranes and modifying its biophysical properties, such as its melting temperature[95]. Structural variation among complex lipids and among fatty acids gives rise to functional differences that result in different impacts upon metabolism and upon cell and tissue responses[95], resulting in different reports on the effects of fatty acids in distinct conditions.

Lipidomics is one of the systems biology methodologies that has become available for use in small animal models thanks to prodigious technological progress in recent years. Lipidomics is a branch of metabolomics that focuses on lipid metabolism. It has been defined as "the full characterization of lipid molecular species and of their biological roles with respect to expression of proteins involved in lipid metabolism and function, including gene regulation"[96]. There are different analytical methods available: untargeted lipid profiling with which especially the membrane lipids, present in relatively high concentrations in plasma, serum and tissues, can be analysed (e.g. phospholipids, triglycerides, cholesteryl esters, free fatty acids), and targeted methods focusing on the analysis of low-abundant lipid mediators such as eicosanoids. With the increased sensitivity achieved in recent years, lipidomics provides a powerful tool to quantify the changes in individual lipids[92,97] and has been a key analytic approach in the research presented in this thesis. Lipidomic analysis of a sample gives a 'lipid profile', which contains information on the lipid composition and abundance of individual lipids present in the starting material.

In obese persons, free fatty acid clearance and cholesterol metabolism is compromised[98], making lipid accumulation and the ensuing dyslipidemia important features of obesity. Elucidating the role of lipid metabolism in the pathogenesis of obesity-related, metabolic OA is therefore of great importance. Hypercholesterolemia is an important aspect of dyslipidemia which has been associated with an increased risk of OA[99–101]. Cholesterol accumulates in OA cartilage because of deregulation of the cholesterol efflux in affected chondrocytes[102,103]. Evidence for a contribution of high cholesterol levels to OA development and progression comes primarily from animal studies, whereas only few observational studies were performed in humans. In mice, a diet enriched in cholesterol in combination with a genetic background allowing for an

atherogenic lipid profile (high (V)LDL-C) has been shown to induce[104] or aggravate[105] OA. LDL can be oxidized in an inflammatory milieu and hence oxidized LDL (oxLDL) was postulated to be involved in OA processes such as synovial inflammation, cartilage destruction and osteophyte formation[105,106].

Until now, most of the evidence linking individual lipids or lipid classes to OA pathogenesis has been derived from animal in vitro and intervention studies[107]. It has been shown that fatty acids can have effects on both OA symptoms and structural abnormalities – with different fatty acid types exerting distinct effects[107]. Saturated free fatty acids, especially palmitic acid, were found to induce toll-like receptor 4 (TLR-4, a potent stimulator of inflammatory responses) signalling and extracellular matrix degradation[107,98]. In general, n-3 PUFAs seem to reduce inflammatory markers and cartilage degradation, while SFAs and n-6 PUFAs show opposing effects[107]. However, a recent randomised, double blind, multicentre trial revealed no additional benefit of high-dose compared with low-dose n-3 PUFA supplementation on structural outcome in OA patients, while, unexpectedly, the low-dose n-3 PUFA group showed a higher decrease in pain outcome[108]. These results might be explained by the enrichment of the low-dose supplementation with oleic acid, a n-9 PUFA suggested to have anti-inflammatory effects[98]. Nevertheless, this study demonstrates our gaps in knowledge and the need for additional research with high-quality methods (like lipidomics) in higher numbers OA patients.

The major mediators of PUFA effects in the body are oxylipins, which are a family of PUFA oxidation products formed via one or more mono- or dioxygen-dependent reactions[109]. Oxylipins in animals, referred to as eicosanoids (Greek icosa; twenty) because of their formation from 20-carbon essential fatty acids, can be enzymatically metabolized into secondary products which can be potently bioactive. Eicosanoids have a large range of biological functions, including promoting and enhancing inflammatory responses, regulating pregnancy and child-birth, controlling blood pressure and the secretion of stomach mucus and acid, contracting or relaxing smooth muscle[110]. Due to their immune modulatory capacity[111], eicosanoids have been proposed to mediate the link between metabolism and immunity in obesity-associated complications[112]. Eicosanoids are generated by three separate enzyme families, lipoxygenase (LOX), cyclooxygenase (COX) and cytochrome P450 (CYP450), which expression is highly tissue-localised and varies with inflammatory activation state[113]. Non-steroidal anti-inflammatory drugs (NSAIDs), one of the drug classes currently used to alleviate symptoms in OA, work by inhibiting the activity of COX enzymes[114]. The COX-2 enzyme is significantly elevated in both the synovial fluid and the synovium from affected joints of OA patients compared to healthy controls and even RA patients[115]. An important COX metabolite is arachidonic acid (AA), which has been shown to accumulate in OA joints[116]. COX enzymes metabolize AA to form prostaglandin precursor prostaglandin H2 (PGH2)

and inhibition of this process by NSAIDs leads to decreased pain and inflammation in OA patients. PGH2 is metabolized by prostaglandin E synthase into inflammatory mediator prostaglandin E2 (PGE2). PGE2 results in decreased proteoglycan content in cartilage explants[117,118] and is likely to contribute to OA pathology by promoting inflammation, apoptosis, bone resorption, and angiogenesis[114,119]. In plasma, systemic AA levels were positively associated with synovitis severity in knees from patients with or at risk of OA[120]. Likewise, systemic levels of the COX metabolite PGE2 and 15-LOX metabolite 15-HETE were found to be increased in OA patients compared to healthy controls121. Inhibition of the LOX pathway, which is a primary source of pro-inflammatory leukotrienes, has shown to be beneficial for OA patients as well[122].

However, despite clear involvement of lipid signalling in the pathogenesis of OA, lipid mediators have scarcely been studied in OA. Increased proinflammatory as well as proresolving lipid mediators have been reported in OA joints[123] and their relative contribution to OA pathogenesis is as yet unclear. In addition, reported studies show significant differences in subjects (e.g. between patient cohorts, various animal models, early vs. late OA) and methodological approach (e.g. lipid subtypes, lipidomic technique, statistical methodology and sampling sites). In line with this, our group demonstrated in a rat diet-induced OA model that local eicosanoid signatures in the synovial fluid differ significantly from systemic eicosanoid signatures in the plasma[124]. Such differential roles add to the complexity of lipid involvement in OA and these seemingly paradoxical results have contributed to the debate as to the existence of metabolic OA[125]. There is a great diversity in the methods and approaches which adds an extra complexity level to the interpretation of the results observed in OA (but also other inflammatory disease) studies. Greater coherence between studies together with omics techniques, such as lipidomics in combination with bioinformatics, will help in identifying the underlying metabolic changes in OA and defining the metabolic phenotype of OA.

Given the changes in metabolism observed in OA, the particularly important role of lipid changes in driving the most significant comorbidities, and their pleiotropic biological actions, free fatty acids and cholesterol are indicated as promising candidates for future therapeutic interventions in metabolic OA[126]. Although the experimental evidence both in preclinical models and humans is still scarce, studies aimed at understanding the involvement of obesity in OA pathogenesis focus more and more on lipids[126]. For now, it is clear that nutritional status is an essential factor involved in the modulation of the immune response and may therefore be determinant in the development and application of (personalised) therapeutic strategies for metabolic OA.

Metabolic osteoarthritis and immunity

The classification of OA as a non-inflammatory arthritis is an unfortunate consequence of early observations noting fewer leukocytes in OA synovial fluid compared with that of rheumatoid arthritis, reactive arthritis, and even septic arthritis[127]. Although synovial inflammation was already reported in so-called 'post-traumatic' synovitis decades ago[128] and technological advances in molecular biology in the 1990s revealed cytokine and prostaglandin involvement in cartilage degradation, synovitis only became accepted as a critical feature of OA in the early 21st century[38]. The involvement of an inflammatory component is now well recognized and, interestingly, the source and type of inflammatory mediators may differ by OA phenotype[2].

Local inflammation: noncellular immune responses

It is as yet unclear whether local inflammation can be the driver of OA, but its presence is associated with more severe pain, increased joint dysfunction, and even accelerated cartilage degeneration in certain patient populations[129]. In view of the entire synovial joint as an organ[130], abnormal biomechanical stress induced by changes in periarticular musculature and (peri)articular tendons and ligaments, exacerbated by the loss of other joint homeostatic functions (e.g. lubricant production)131, can contribute to local inflammation. Several studies have indicated that local inflammation can be driven by cartilage matrix molecules or degradation products through the activation of innate immune responses[131,132]. An illustrative example is aggrecan, a major component of the cartilage extracellular matrix, which is cleaved at a specific aggrecanase site by several members of ADAMTS family of metalloproteases. ADAMTS5 was found to be the primary aggrecanase responsible for aggrecan degradation in a murine model of post-traumatic OA, as deletion of active ADAMTS5 abrogated the course of cartilage degradation compared with wild-type controls[133]. Other danger-associated molecular patterns (DAMPs), such as degradation products like fibronectin134 and tenascin-C fragments135, low-molecular-weight HA[136], multiple alarmins (e.g. HMGB1137, S100A8 and S100A9[138]), free fatty acids[107,139,140], and others, are increased in concentration in OA joints as well. In conjunction with abnormal mechanical and oxidative stresses, DAMPs induce numerous inflammatory mediators, including cytokines (such as TNF, IL-1β, IL-6), and chemokines (IL-8)[131]. These inflammatory mediators in turn induce the synthesis of other inflammatory mediators, pro-matrix metalloproteinases (pro-MMPs) and other proteinases by chondrocytes141, increase the synthesis of PGE2 (by stimulating COX2)[142], microsomal PGE synthase-1 (mPGES-1)[143], and soluble phospholipase A2 (sPLA2)[144], and upregulate the production of free radical nitric oxide via inducible nitric oxide synthase (iNOS)[130,132]. These processes subsequently add to OA progression by altering chondrocyte differentiation, function and viability and by promoting synovitis[131,145].

The complement system, a noncellular part of the innate immune system that functions as a first-line host defence against pathogenic microbes, can be activated in OA joints by DAMPs, synovial fluid crystals, and also by apoptotic cells and the resulting cell debris[131]. Complement activation appears critical in OA pathogenesis, especially in early OA[146], through the formation of membrane attack complex (MAC) on chondrocytes and induction of the expression of proinflammatory and degradative molecules in chondrocytes[146–148]. Moreover, complement also appears to contribute to obesity-associated metabolic disturbances and adipose tissue inflammation, possibly provoking insulin resistance[149,150]. By applying injury-induced OA in mice genetically deficient for complement components C5, C6, or CD59a (an inhibitor of MAC), it was elegantly shown that generation of C5a and of the MAC (C5b-9) is implicated in OA progression[146]. Increased levels of C3a and C5b-9 in synovial fluid, presence of MAC in cartilage and synovium, and a markedly higher expression of complement effectors together with a lower expression of complement inhibitors in the synovial membranes from OA compared to healthy individuals corroborated these preclinical results[146].

Local inflammation: cellular immune responses

Cytokines have long been known to be involved in cartilage destruction and synovitis, causing inflammatory reactions and pain[151,152]. Interleukin-1β (IL-1β), IL-6 and tumor necrosis factor alpha (TNF-α) represent the main pro-inflammatory and catabolic cytokines, although others, like IL-15, IL-17, IL-18, IL-21 and chemokines like IL-8, CCL-2, CCL7, and CCL8, have also been implicated in OA[82,151,153]. Local sources of such inflammatory mediators are the synovium and intra-articular adipose tissues like the infrapatellar fat pad (IFP or IPFP; also known as Hoffa's fat pad), which are innervated and well-vascularized joint tissues. Especially the IFP has gained much interest in the past few years, evolving in general perception from an inert fat storage depot and shock absorber to an active endocrine organ that is able to exert metabolic effects on the joint tissues[45]. The IFP has the typical histological structure of adipose tissue where adipocytes make up most of the cell population, next to fibroblasts, which produce the extracellular matrix, and immune cells such as macrophages, mast cells, and lymphocytes. In OA patients the IFP has been shown to represent a source of inflammatory molecules and to be more inflamed and vascularized compared to non-OA controls[46,52,154,155]. Paradoxically, despite its heightened inflammatory state in OA pathogenesis, removal of the IFP has been reported to cause adverse effects on cartilage metabolism and to provoke patellar tendon shortening[156,157]. However, as for obvious ethical reasons these reports are based on IFP tissues from cadaveric studies or from end-stage OA patients who undergo total joint replacement, it is as yet unknown if these findings are general IFP characteristics or whether the IFP may fulfill different metabolic functions during different OA phases[82,158].

The OA synovial membrane is characterized by increased hyperplasia, fibrosis, vascularization, and immune cells infiltration as well as inflammatory molecules and neuropeptides production[159]. Synovitis correlates with OA symptoms and is characterized by increased pain sensitivity[39,160]. Infiltration of immune cells like monocytes and macrophages in the synovial tissue and the increase of cytokines and chemokines in the synovial tissue and synovial fluid are at the basis of synovitis development[161,162]. Infiltration of immune cells in the OA synovium primarily reflects migration rather than local proliferation and therefore is dependent on soluble mediators, especially chemokines[151,163]. Alternatively, complement activation can also recruit immune cells and is described to play an important role in early inflammatory processes in both adipose and synovial tissue during OA[146,148]. Correspondingly, elevated levels of C-reactive protein (CRP) have been correlated with local synovial inflammation in patients with OA[164]. The acute phase protein CRP activates complement via C1q165, which has been implicated in bone remodelling and OA pathogenesis[166–168]. In addition, CRP acts as a direct chemoattractant to monocytes and can regulate innate and adaptive responses by stimulating endothelial cells to express monocyte chemoattractant protein-1 (MCP-1), promoting monocyte chemotactic activity and recruiting circulating leukocytes to areas of inflammation[169]. Both IL-6 and IL-1β, key pro-inflammatory cytokines in OA pathogenesis, are known to promote production of CRP: with IL-6 being the essential inducer of CRP gene expression and IL-1β enhancing the effect[170,171]. Together with TNFα, IL-6 and IL-1β directly facilitate persistent joint inflammation and joint cartilage destruction in OA by initiating low-grade inflammation and degradation of extracellular matrix components by inducing various pro-MMPs and cytokines through activated synovial macrophages, synovial fibroblasts, or the chondrocytes themselves[148,172,173].

As the various catabolic processes affect and reinforce one another, cartilage degradation and inflammation become intertwined and disentangling becomes difficult if not impossible. In this respect, a new emerging concept reconsiders the link between the IFP and the synovium as being constitutive elements of a single anatomofunctional unit and not two separate tissues[159,174,175]. It was recently suggested that inflammation in this anatomofunctional unit may drive peripheral and central pain sensitization in knee OA, proposing early targeting of inflammation as a strategy to prevent the sensitization and thereby reduce pain severity in knee OA[159].

Systemic inflammation

Given the local role of inflammatory mediators in knee OA and the trafficking of immune cells through OA synovium and back into the circulation, it is reasonable to think that local inflammation may be reflected in the blood of OA patients by one or more systemic inflammatory markers. Especially for the metabolic OA phenotype[176],

with obesity and metabolic disorders known to be related to systemic low-grade inflammation. Whether local inflammation may indeed be reflected systemically is still under debate, as researchers have reported evidence supporting[120,164,177] and opposing[178,179] this concept. Others refined that low-grade systemic inflammation may play a greater role in symptoms180 and quality of life[181] rather than radiographic changes in OA.

Phenotyping of peripheral blood leukocytes (PBLs) from knee OA patients and healthy controls showed that cytotoxic and memory CD8+ T cell population frequencies were increased[182]. Age-related declines in T-lymphocytes seen in healthy controls in this study were not observed in knee osteoarthritis patients, suggesting alteration by the disease process[182,183]. One group showed reduced OA severity in both CD4- and CD8-deficient C57BL/6J mice in a surgically induced model[184,185]. Another study found increased PBL inflammatory activity and elevated systemic levels of lipid mediators 15-HETE and PGE2 to be associated with symptomatic knee OA[121]. These results are interesting but need to be replicated, particularly in 'preradiographic' disease wherein identifying active inflammation as the cause of joint pain may be difficult[183].

The exact role of inflammation in OA pathogenesis thus remains challenging to define, not least because basal inflammatory processes in OA are generally low-grade and molecular with many usual suspects implicated. Other mechanisms, not directly related to local inflammation, also need to be considered. Genetic and epigenetic modifications in OA pathogenesis for example, which include DNA methylation, histone modification, and non-coding RNAs[186]. Another variable that could influence the systemic inflammatory state is dietary intake, with a more proinflammatory diet associated with higher prevalence of radiographic symptomatic knee OA[187]. Correspondingly, another cohort study demonstrated that systemic levels of n-3 and n-6 fatty acids, which are influenced by diet, may be related to selected structural findings in knees with or at risk of OA[120].

How much of the influence on OA pathogenesis is local, and how much is systemic, remains to be further investigated. Both local and systemic inflammation are probably involved and noncellular as well as cellular immune responses go hand in hand and even reinforce each other. Nevertheless, biomarkers for early diagnosis of OA that can be detected via minimally invasive techniques (e.g. in urine or peripheral blood) are still the holy grail of OA research. There is also the general hope to find biomarkers that can identify more rapid progressors and classify patients into subgroups based on the expected treatment response, in order to provide more targeted treatment. Inflammatory mediators can conceivably meet these characteristics and systemic levels for IL-6, adiponectin, LP-PLA2, and TNF-RII have been proposed as possible markers for some OA phenotypes[178]. However, it is probable that the efficacy of these biomarkers will depend on disease stage and clinical phenotypes, as synovitis is most frequently observed in symptomatic OA with moderate to severe radiographic OA[39].

Specific targeting of inflammatory pathways, and perhaps subtyping patients based on inflammatory profiles, may expand treatment options for OA[183]. Clearly, the number and diversity of inflammatory mediators in OA joints, the complex roles of some of these molecules in tissue damage and repair, and the physiological roles of some mediators in host defence makes targeting them individually for OA therapy a daunting task[131]. Perhaps for this reason, there is a paucity of randomized, placebo-controlled trials investigating the efficacy of anti-cytokine therapies[188]. Tissue engineering and cell therapy aside, most of the currently ongoing clinical trials employ immunotherapy or gene therapy as anti-inflammatory treatment for OA of the knee or hands. A recently completed clinical trial evaluated the efficacy and safety of otilimab, a fully human monoclonal antibody against GM-CSF, in patients with inflammatory hand OA(NCT02683785)[188]. This treatment was well tolerated and resulted in pain reduction and function improvement although the results were not statistically significant[189]. Other biologicals like adalimumab, a fully human anti-TNF-α monoclonal antibody (NCT02471118), tocilizumab, an anti-IL-6 receptor monoclonal antibody (NCT02477059), and MEDI7352, a bispecific monoclonal antibody able to bind nerve growth factor (NGF) and TNF-α (NCT02508155), are assessed in randomized, double-blind, placebo-controlled studies in patients with painful OA of the knee or hand. Novel approaches consist of gene therapy strategies for IL-1Ra (NCT02790723) and IL-10 (NCT0347748), which could lead to sustained levels of these anti-inflammatory mediators in the affected joint[188]. An anti-TNF-α gene therapy, using an adenoviral vector encoding TNF-α receptor type 2 fused to the immunoglobulin IgG1 Fc domain (rAAV2-TNFR:Fc), was halted due to safety concerns[188,190].

Future treatment would ideally combine treatment of pain, tissue damage, and inflammation. Although the therapies from current clinical trials showed promise in preclinical research, their true efficacy in patients still needs to be determined. Therefore, current treatment options in OA remain limited and focused around pain and symptom management. Based on the complexity of the disease and the pathways involved, it is also very likely that OA diagnosis and prognosis will continue to be based on a combined panel of biomarkers and/or imaging markers in the foreseeable future.

Thesis aim

The present thesis aims to investigate how metabolic overload contributes to the pathophysiology of knee OA. As described in the previous sections, it has become increasingly recognized that aberrations in metabolism and immunity contribute critically to OA pathogenesis. We explored the role of these independent yet intertwined processes using novel lipidomic and cellular imaging approaches in mouse models of

diet-induced OA. The comprehensive analysis of multiple metabolic and inflammatory mediators, both systemically and locally, furthers our understanding of these factors in obesity-related OA pathogenesis. This knowledge is a prerequisite to identify possible novel biomarkers for the early detection and prediction of the course of the disease. In the future, this knowledge may guide the selection of targets for disease-modifying therapies.

Thesis outline

First, the diet-induced OA model was evaluated for its robustness and repeatability by comparing OA features observed in twelve preclinical studies (**Chapter 2**). These studies were performed in wild-type C57BL/6J mice and genetically modified mice (hCRP, LDLr–/–.Leiden and ApoE*3Leiden.CETP mice) based on C57BL/6J background, which received various high-caloric dietary regimens at variable duration. By comparing the various study designs, we explored the most optimal conditions to induce obesity-related OA. We then sought to evaluate whether and how nutritional fat could aggravate OA progression. Hence, low- and high-fat feeding regimens were combined with a microsurgical destabilization of the medial meniscus in C57BL/6J mice to assure OA development (**Chapter 3**). This post-traumatic OA (PTOA) model is low invasive and sufficiently sensitive to study subtle changes in disease progression by mild triggers like genetic background and diet.
To unravel the effects of a dysregulated lipid metabolism on the inflammatory state, we studied the development of metabolic inflammation both locally and systemically. In **Chapter 4** we focussed on the inflammatory status of the infrapatellar fat pad (IFP) during OA progression, as evidence is emerging that the IFP can be a potential local source of inflammatory mediators in the knee. Next, we addressed the involvement of the innate immune system in the development of diet-induced OA. For this we provided male mice from a human C-reactive protein (hCRP) knock-in strain with a high-fat diet for 38 weeks (**Chapter 5**). Lastly, to investigate the contribution of altered lipoprotein handling on diet-induced cartilage degradation, we assessed the contribution of elevated plasma cholesterol levels to the severity of diet-induced OA (**Chapter 6**). Cholesterol is involved in lipid metabolism as well as inflammation and is described to attenuate OA progression. Novel high-intensive cholesterol-lowering strategies were evaluated for their efficacy in halting or reducing aggravation of pre-existent, diet-induced OA. The results obtained in these studies are discussed and placed into the context of the current state of the field in **Chapter 7**.

References

1. Lane, N. E. *et al.* OARSI-FDA initiative: defining the disease state of osteoarthritis. *Osteoarthritis Cartilage* **19**, 478–482 (2011).
2. Bijlsma, J. W., Berenbaum, F. & Lafeber, F. P. Osteoarthritis: an update with relevance for clinical practice. *The Lancet* **377**, 2115–2126 (2011).
3. Allen, K. D. & Golightly, Y. M. Epidemiology of osteoarthritis: state of the evidence. *Curr. Opin. Rheumatol.* **27**, 276–283 (2015).
4. O'Neill, T. W., McCabe, P. S. & McBeth, J. Update on the epidemiology, risk factors and disease outcomes of osteoarthritis. *Best Pract. Res. Clin. Rheumatol.* **32**, 312–326 (2018).
5. Martel-Pelletier, J. *et al.* Osteoarthritis. *Nat. Rev. Dis. Primer* **2**, 16072 (2016).
6. Creamer, P., Lethbridge-Cejku, M. & Hochberg, M. C. Determinants of pain severity in knee osteoarthritis: effect of demographic and psychosocial variables using 3 pain measures. *J. Rheumatol.* **26**, 1785–1792 (1999).
7. Bedson, J. & Croft, P. R. The discordance between clinical and radiographic knee osteoarthritis: a systematic search and summary of the literature. *BMC Musculoskelet. Disord.* **9**, 116 (2008).
8. Kraus, V. B., Blanco, F. J., Englund, M., Karsdal, M. A. & Lohmander, L. S. Call for standardized definitions of osteoarthritis and risk stratification for clinical trials and clinical use. *Osteoarthritis Cartilage* **23**, 1233–1241 (2015).
9. Palazzo, C., Nguyen, C., Lefevre-Colau, M.-M., Rannou, F. & Poiraudeau, S. Risk factors and burden of osteoarthritis. *Ann. Phys. Rehabil. Med.* **59**, 134–138 (2016).
10. Chapter 9.1 Classification of Joints. in *Anatomy and Physiology* (BCCampus).
11. Courties, A., Sellam, J. & Berenbaum, F. Metabolic syndrome-associated osteoarthritis. *Curr. Opin. Rheumatol.* **29**, 214–222 (2017).
12. Kellgren, J. H. & Lawrence, J. S. Radiological assessment of osteo-arthrosis. *Ann. Rheum. Dis.* **16**, 494–502 (1957).
13. Felson, D. T., Niu, J., Guermazi, A., Sack, B. & Aliabadi, P. Defining radiographic incidence and progression of knee osteoarthritis: suggested modifications of the Kellgren and Lawrence scale. *Ann. Rheum. Dis.* **70**, 1884–1886 (2011).
14. Archer, C. W. & Francis-West, P. The chondrocyte. *Int. J. Biochem. Cell Biol.* **35**, 401–404 (2003).
15. Sophia Fox, A. J., Bedi, A. & Rodeo, S. A. The Basic Science of Articular Cartilage. *Sports Health* **1**, 461–468 (2009).
16. Heijink, A. *et al.* Biomechanical considerations in the pathogenesis of osteoarthritis of the knee. *Knee Surg. Sports Traumatol. Arthrosc.* **20**, 423–435 (2012).
17. Lotz, M. & Carames, B. Autophagy and Cartilage Homeostasis Mechanisms in Joint Health, Aging and Osteoarthritis. *Nat. Rev. Rheumatol.* **7**, 579–587 (2011).
18. Felson, D. T. Osteoarthritis of the Knee. *N. Engl. J. Med.* **354**, 841–848 (2006).
19. Lories, R. J. & Luyten, F. P. The bone–cartilage unit in osteoarthritis. *Nat. Rev. Rheumatol.* **7**, 43–49 (2011).
20. Weinans, H. *et al.* Pathophysiology of peri-articular bone changes in osteoarthritis. *Bone* **51**, 190–196 (2012).

21. Stewart, H. L. & Kawcak, C. E. The Importance of Subchondral Bone in the Pathophysiology of Osteoarthritis. *Front. Vet. Sci.* **5**, (2018).
22. Findlay, D. M. & Kuliwaba, J. S. Bone–cartilage crosstalk: a conversation for understanding osteoarthritis. *Bone Res.* **4**, 16028 (2016).
23. Sharma, A. R., Jagga, S., Lee, S.-S. & Nam, J.-S. Interplay between Cartilage and Subchondral Bone Contributing to Pathogenesis of Osteoarthritis. *Int. J. Mol. Sci.* **14**, 19805–19830 (2013).
24. Junker, S. *et al.* Differentiation of osteophyte types in osteoarthritis - proposal of a histological classification. *Jt. Bone Spine Rev. Rhum.* **83**, 63–67 (2016).
25. van der Kraan, P. M. & van den Berg, W. B. Osteophytes: relevance and biology. *Osteoarthritis Cartilage* **15**, 237–244 (2007).
26. Hsia, A. W. *et al.* Osteophyte formation after ACL rupture in mice is associated with joint restabilization and loss of range of motion. *J. Orthop. Res. Off. Publ. Orthop. Res. Soc.* **35**, 466–473 (2017).
27. Markhardt, B. K., Li, G. & Kijowski, R. The Clinical Significance of Osteophytes in Compartments of the Knee Joint With Normal Articular Cartilage. *AJR Am. J. Roentgenol.* **210**, W164–W171 (2018).
28. Burr, D. B. & Gallant, M. A. Bone remodelling in osteoarthritis. *Nat. Rev. Rheumatol.* **8**, 665–673 (2012).
29. Donell, S. Subchondral bone remodelling in osteoarthritis. *EFORT Open Rev.* **4**, 221–229 (2019).
30. Sutton, S. *et al.* The contribution of the synovium, synovial derived inflammatory cytokines and neuropeptides to the pathogenesis of osteoarthritis. *Vet. J. Lond. Engl. 1997* **179**, 10–24 (2009).
31. Man, G. & Mologhianu, G. Osteoarthritis pathogenesis – a complex process that involves the entire joint. *J. Med. Life* **7**, 37–41 (2014).
32. Smith, M. D. The Normal Synovium. *Open Rheumatol. J.* **5**, 100–106 (2011).
33. Smith, M. *et al.* Microarchitecture and protective mechanisms in synovial tissue from clinically and arthroscopically normal knee joints. *Ann. Rheum. Dis.* **62**, 303–307 (2003).
34. Orr, C. *et al.* Synovial tissue research: a state-of-the-art review. *Nat. Rev. Rheumatol.* **13**, 463–475 (2017).
35. Hügle, T. & Geurts, J. What drives osteoarthritis?—synovial versus subchondral bone pathology. *Rheumatology* **56**, 1461–1471 (2017).
36. Sarmanova, A., Hall, M., Moses, J., Doherty, M. & Zhang, W. Synovial changes detected by ultrasound in people with knee osteoarthritis – a meta-analysis of observational studies. *Osteoarthritis Cartilage* **24**, 1376–1383 (2016).
37. Dequeker, J. & Luyten, F. P. The history of osteoarthritis-osteoarthrosis. *Ann. Rheum. Dis.* **67**, 5–10 (2008).
38. Berenbaum, F. Osteoarthritis as an inflammatory disease (osteoarthritis is not osteoarthrosis!). *Osteoarthritis Cartilage* **21**, 16–21 (2013).
39. Mathiessen, A. & Conaghan, P. G. Synovitis in osteoarthritis: current understanding with therapeutic implications. *Arthritis Res. Ther.* **19**, (2017).
40. Kraus, V. B. *et al.* Direct In Vivo Evidence of Activated Macrophages in Human Osteoarthritis. *Osteoarthr. Cartil. OARS Osteoarthr. Res. Soc.* **24**, 1613–1621 (2016).
41. Szychlinska, M. A., Leonardi, R., Al-Qahtani, M., Mobasheri, A. & Musumeci, G. Altered joint tribology in osteoarthritis: Reduced lubricin synthesis due to the inflammatory process. New horizons for therapeutic approaches. *Ann. Phys. Rehabil. Med.*

59, 149–156 (2016).
42. Eitner, A., Pester, J., Nietzsche, S., Hofmann, G. O. & Schaible, H.-G. The innervation of synovium of human osteoarthritic joints in comparison with normal rat and sheep synovium. *Osteoarthritis Cartilage* **21**, 1383–1391 (2013).
43. O'Neill, T. W. & Felson, D. T. Mechanisms of Osteoarthritis (OA) Pain. *Curr. Osteoporos. Rep.* **16**, 611–616 (2018).
44. Clockaerts, S. *et al.* The infrapatellar fat pad should be considered as an active osteoarthritic joint tissue: a narrative review. *Osteoarthritis Cartilage* **18**, 876–882 (2010).
45. Ioan-Facsinay, A. & Kloppenburg, M. An emerging player in knee osteoarthritis: the infrapatellar fat pad. *Arthritis Res. Ther.* **15**, 225 (2013).
46. Eymard, F. & Chevalier, X. Inflammation of the infrapatellar fat pad. *Joint Bone Spine* **83**, 389–393 (2016).
47. Teichtahl, A. J. *et al.* A large infrapatellar fat pad protects against knee pain and lateral tibial cartilage volume loss. *Arthritis Res. Ther.* **17**, (2015).
48. Saddik, D., McNally, E. G. & Richardson, M. MRI of Hoffa's fat pad. *Skeletal Radiol.* **33**, 433–444 (2004).
49. Ioan-Facsinay, A. *et al.* Adipocyte-derived lipids modulate CD4+ T-cell function. *Eur. J. Immunol.* **43**, 1578–1587 (2013).
50. Burda, B. *et al.* Variance in infra-patellar fat pad volume: Does the body mass index matter?—Data from osteoarthritis initiative participants without symptoms or signs of knee disease. *Ann. Anat. - Anat. Anz.* **213**, 19–24 (2017).
51. Klein-Wieringa, I. R. *et al.* The infrapatellar fat pad of patients with osteoarthritis has an inflammatory phenotype. *Ann. Rheum. Dis.* **70**, 851–857 (2011).
52. Favero, M. *et al.* Infrapatellar fat pad features in osteoarthritis: a histopathological and molecular study. *Rheumatology* **56**, 1784–1793 (2017).
53. Harasymowicz, N. S. *et al.* Regional Differences Between Perisynovial and Infrapatellar Adipose Tissue Depots and Their Response to Class II and Class III Obesity in Patients With Osteoarthritis. *Arthritis Rheumatol. Hoboken NJ* **69**, 1396–1406 (2017).
54. Barboza, E. *et al.* Profibrotic Infrapatellar Fat Pad Remodeling Without M1 Macrophage Polarization Precedes Knee Osteoarthritis in Mice With Diet-Induced Obesity. *Arthritis Rheumatol.* **69**, 1221–1232 (2017).
55. Wittenauer, R., Smith, L. & Aden, K. *World Health Organisation update on 2004 Background Paper, BP 6.12 Osteoarthritis*. (2013).
56. Veronese, N. *et al.* Association between lower limb osteoarthritis and incidence of depressive symptoms: data from the osteoarthritis initiative. *Age Ageing* **46**, 470–476 (2017).
57. Cleveland, R. J. & Callahan, L. F. Can Osteoarthritis Predict Mortality? *N. C. Med. J.* **78**, 322–325 (2017).
58. Vina, E. R. & Kwoh, C. K. Epidemiology of Osteoarthritis: Literature Update. *Curr. Opin. Rheumatol.* **30**, 160–167 (2018).
59. Nivel Zorgregistraties eerste lijn. (2017). Available at: https://www.nivel.nl/nl/nivel-zorgregistraties-eerste-lijn/nivel-zorgregistraties-eerste-lijn. (Accessed: 24th June 2019)
60. Losina, E. *et al.* Lifetime medical costs of knee osteoarthritis management in the United States: Impact of extending indications for total knee arthroplasty. *Arthritis Care Res.* **67**, 203–215 (2015).
61. Volksgezondheidenzorg.info. (2015). Available at: https://www.volksgezondheidenzorg.info/onderwerp/

artrose/kosten/kosten#node-kosten-van-zorg-naar-vorm-van-artrose. (Accessed: 24th June 2019)
62. Oo, W. M., Yu, S. P.-C., Daniel, M. S. & Hunter, D. J. Disease-modifying drugs in osteoarthritis: current understanding and future therapeutics. *Expert Opin. Emerg. Drugs* **23**, 331–347 (2018).
63. Karsdal, M. A. *et al.* Disease-modifying treatments for osteoarthritis (DMOADs) of the knee and hip: lessons learned from failures and opportunities for the future. *Osteoarthritis Cartilage* **24**, 2013–2021 (2016).
64. Shah, K., Zhao, A. G. & Sumer, H. New Approaches to Treat Osteoarthritis with Mesenchymal Stem Cells. *Stem Cells Int.* **2018**, (2018).
65. McAlindon, T. E. *et al.* OARSI guidelines for the non-surgical management of knee osteoarthritis. *Osteoarthritis Cartilage* **22**, 363–388 (2014).
66. Hunter, D. J. *et al.* The Intensive Diet and Exercise for Arthritis (IDEA) trial: 18-month radiographic and MRI outcomes. *Osteoarthritis Cartilage* **23**, 1090–1098 (2015).
67. Loeser, R. F. The Role of Aging in the Development of Osteoarthritis. *Trans. Am. Clin. Climatol. Assoc.* **128**, 44–54 (2017).
68. Yusuf, E. Pharmacologic and Non-Pharmacologic Treatment of Osteoarthritis. *Curr. Treat. Options Rheumatol.* **2**, 111–125 (2016).
69. Quinn, R. H., Murray, J. N., Pezold, R. & Sevarino, K. S. Surgical Management of Osteoarthritis of the Knee: *J. Am. Acad. Orthop. Surg.* **26**, e191–e193 (2018).
70. Wolfstadt, J. I., Cole, B. J., Ogilvie-Harris, D. J., Viswanathan, S. & Chahal, J. Current Concepts: The Role of Mesenchymal Stem Cells in the Management of Knee Osteoarthritis. *Sports Health* **7**, 38–44 (2015).
71. Pas, H. I. *et al.* Stem cell injections in knee osteoarthritis: a systematic review of the literature. *Br. J. Sports Med.* **51**, 1125–1133 (2017).
72. Zhang, W. *et al.* Classification of osteoarthritis phenotypes by metabolomics analysis. *BMJ Open* **4**, e006286 (2014).
73. Ren, G. & Krawetz, R. Applying computation biology and "big data" to develop multiplex diagnostics for complex chronic diseases such as osteoarthritis. *Biomarkers* **20**, 533–539 (2015).
74. Dell'Isola, A., Allan, R., Smith, S. L., Marreiros, S. S. P. & Steultjens, M. Identification of clinical phenotypes in knee osteoarthritis: a systematic review of the literature. *BMC Musculoskelet. Disord.* **17**, (2016).
75. Van Spil, W. E., Kubassova, O., Boesen, M., Bay-Jensen, A.-C. & Mobasheri, A. Osteoarthritis phenotypes and novel therapeutic targets. *Biochem. Pharmacol.* **165**, 41–48 (2019).
76. Deveza, L. A. *et al.* Knee osteoarthritis phenotypes and their relevance for outcomes: a systematic review. *Osteoarthritis Cartilage* **25**, 1926–1941 (2017).
77. Bierma-Zeinstra, S. M. & van Middelkoop, M. Osteoarthritis: In search of phenotypes. *Nat. Rev. Rheumatol.* **13**, 705–706 (2017).
78. Radin, E. L., Paul, I. L. & Rose, R. M. Role of mechanical factors in pathogenesis of primary osteoarthritis. *Lancet Lond. Engl.* **1**, 519–522 (1972).
79. Murphy, L. *et al.* Lifetime risk of symptomatic knee osteoarthritis. *Arthritis Rheum.* **59**, 1207–1213 (2008).
80. Wang, X., Hunter, D., Xu, J. & Ding, C. Metabolic triggered inflammation in osteoarthritis. *Osteoarthritis Cartilage* **23**, 22–30 (2015).
81. Puenpatom, R. A. & Victor, T. W.

Increased prevalence of metabolic syndrome in individuals with osteoarthritis: an analysis of NHANES III data. *Postgrad. Med.* **121**, 9–20 (2009).
82. Berenbaum, F., Griffin, T. M. & Liu-Bryan, R. Review: Metabolic Regulation of Inflammation in Osteoarthritis. *Arthritis Rheumatol.* **69**, 9–21 (2017).
83. Visser, A. W. *et al.* The relative contribution of mechanical stress and systemic processes in different types of osteoarthritis: the NEO study. *Ann. Rheum. Dis.* **74**, 1842–1847 (2015).
84. Malfait, A.-M. & Little, C. B. On the predictive utility of animal models of osteoarthritis. *Arthritis Res. Ther.* **17**, 225 (2015).
85. Silberberg, R. & Silberberg, M. Skeletal growth and articular changes in mice receiving a high-fat diet. *Am. J. Pathol.* **26**, 113–131, incl 4 pl (1950).
86. Silberberg, M. & Silberberg, R. Degenerative joint disease in mice fed a high-fat diet at various ages. *Exp. Med. Surg.* **10**, 76–87 (1952).
87. Griffin, T. M. & Guilak, F. Why is obesity associated with osteoarthritis? Insights from mouse models of obesity. *Biorheology* **45**, 387–398 (2008).
88. Wang, C.-Y. & Liao, J. K. A mouse model of diet-induced obesity and insulin resistance. *Methods Mol. Biol. Clifton NJ* **821**, 421–433 (2012).
89. Glasson, S. S., Chambers, M. G., Van Den Berg, W. B. & Little, C. B. The OARSI histopathology initiative – recommendations for histological assessments of osteoarthritis in the mouse. *Osteoarthritis Cartilage* **18**, S17–S23 (2010).
90. Mankin, H. J. Biochemical and metabolic aspects of osteoarthritis. *Orthop. Clin. North Am.* **2**, 19–31 (1971).
91. Fang, H. & Beier, F. Mouse models of osteoarthritis: modelling risk factors and assessing outcomes. *Nat. Rev. Rheumatol.* **10**, 413–421 (2014).
92. Zhang, C. *et al.* Lipid metabolism in inflammation-related diseases. *The Analyst* **143**, 4526–4536 (2018).
93. Tall, A. R. & Yvan-Charvet, L. Cholesterol, inflammation and innate immunity. *Nat. Rev. Immunol.* **15**, 104–116 (2015).
94. Calder, P. C. Functional Roles of Fatty Acids and Their Effects on Human Health. *J. Parenter. Enter. Nutr.* **39**, 18S-32S (2015).
95. Burdge, G. C. & Calder, P. C. Introduction to fatty acids and lipids. *World Rev. Nutr. Diet.* **112**, 1–16 (2015).
96. Spener, F., Lagarde, M., Géloên, A. & Record, M. Editorial: What is lipidomics? *Eur. J. Lipid Sci. Technol.* **105**, 481–482 (2003).
97. Hu, T. & Zhang, J.-L. Mass-spectrometry-based lipidomics. *J. Sep. Sci.* **41**, 351–372 (2018).
98. Felson, D. T. & Bischoff-Ferrari, H. A. Dietary fatty acids for the treatment of OA, including fish oil. *Ann. Rheum. Dis.* **75**, 1–2 (2016).
99. Hart, D. J., Doyle, D. V. & Spector, T. D. Association between metabolic factors and knee osteoarthritis in women: the Chingford Study. *J. Rheumatol.* **22**, 1118–1123 (1995).
100. Stürmer, T. *et al.* Serum cholesterol and osteoarthritis. The baseline examination of the Ulm Osteoarthritis Study. *J. Rheumatol.* **25**, 1827–1832 (1998).
101. Addimanda, O. *et al.* Clinical associations in patients with hand osteoarthritis. *Scand. J. Rheumatol.* **41**, 310–313 (2012).
102. Tsezou, A., Iliopoulos, D., Malizos, K. N. & Simopoulou, T. Impaired expression of genes regulating cholesterol efflux in human osteoarthritic chondrocytes. *J. Orthop. Res. Off. Publ. Orthop. Res. Soc.* **28**, 1033–1039 (2010).
103. Triantaphyllidou, I.-E. *et al.* Perturba-

tions in the HDL metabolic pathway predispose to the development of osteoarthritis in mice following long-term exposure to western-type diet. *Osteoarthritis Cartilage* **21**, 322–330 (2013).
104. Gierman, L. M. *et al.* Osteoarthritis development is induced by increased dietary cholesterol and can be inhibited by atorvastatin in APOE*3Leiden. CETP mice--a translational model for atherosclerosis. *Ann. Rheum. Dis.* **73**, 921–927 (2014).
105. de Munter, W. *et al.* Cholesterol accumulation caused by low density lipoprotein receptor deficiency or a cholesterol-rich diet results in ectopic bone formation during experimental osteoarthritis. *Arthritis Res. Ther.* **15**, R178 (2013).
106. de Munter, W., van der Kraan, P. M., van den Berg, W. B. & van Lent, P. L. E. M. High systemic levels of low-density lipoprotein cholesterol: fuel to the flames in inflammatory osteoarthritis? *Rheumatology* **55**, 16–24 (2016).
107. Loef, M., Schoones, J. W., Kloppenburg, M. & Ioan-Facsinay, A. Fatty acids and osteoarthritis: different types, different effects. *Jt. Bone Spine Rev. Rhum.* **86**, 451–458 (2019).
108. Hill, C. L. *et al.* Fish oil in knee osteoarthritis: a randomised clinical trial of low dose versus high dose. *Ann. Rheum. Dis.* **75**, 23–29 (2016).
109. Gabbs, M., Leng, S., Devassy, J. G., Monirujjaman, M. & Aukema, H. M. Advances in Our Understanding of Oxylipins Derived from Dietary PUFAs. *Adv Nutr* **6**, 513–40 (2015).
110. de Carvalho, C. C. C. R. & Caramujo, M. J. The Various Roles of Fatty Acids. *Mol. J. Synth. Chem. Nat. Prod. Chem.* **23**, (2018).
111. Dennis, E. A. & Norris, P. C. Eicosanoid Storm in Infection and Inflammation. *Nat. Rev. Immunol.* **15**, 511–523 (2015).
112. de Jong, A. J., Kloppenburg, M., Toes, R. E. M. & Ioan-Facsinay, A. Fatty Acids, Lipid Mediators, and T-Cell Function. *Front. Immunol.* **5**, (2014).
113. Maskrey, B. H. & O'Donnell, V. B. Analysis of eicosanoids and related lipid mediators using mass spectrometry. *Biochem. Soc. Trans.* **36**, 1055–1059 (2008).
114. Nakata, K. *et al.* Disease-modifying effects of COX-2 selective inhibitors and non-selective NSAIDs in osteoarthritis: a systematic review. *Osteoarthritis Cartilage* **26**, 1263–1273 (2018).
115. Fan, H., Liu, G., Zhao, C., Li, X. T. F. & Yang, X. Y. Differential expression of COX-2 in osteoarthritis and rheumatoid arthritis. *Genet. Mol. Res. GMR* **14**, 12872–12879 (2015).
116. Lippiello, L., Walsh, T. & Fienhold, M. The association of lipid abnormalities with tissue pathology in human osteoarthritic articular cartilage. *Metabolism.* **40**, 571–576 (1991).
117. Hardy, M. M. *et al.* Cyclooxygenase 2-dependent prostaglandin E2 modulates cartilage proteoglycan degradation in human osteoarthritis explants. *Arthritis Rheum.* **46**, 1789–1803 (2002).
118. Attur, M. *et al.* Prostaglandin E2 exerts catabolic effects in osteoarthritis cartilage: evidence for signaling via the EP4 receptor. *J. Immunol. Baltim. Md 1950* **181**, 5082–5088 (2008).
119. Martel-Pelletier, J., Pelletier, J.-P. & Fahmi, H. Cyclooxygenase-2 and prostaglandins in articular tissues. *Semin. Arthritis Rheum.* **33**, 155–167 (2003).
120. Baker, K. R. *et al.* Association of Plasma n-6 and n-3 polyunsaturated fatty acids with synovitis in the knee: the MOST Study. *Osteoarthr. Cartil. OARS Osteoarthr. Res. Soc.* **20**, 382–387 (2012).

121. Attur, M. *et al.* Low-grade inflammation in symptomatic knee osteoarthritis: prognostic value of inflammatory plasma lipids and peripheral blood leukocyte biomarkers. *Arthritis Rheumatol* **67**, 2905–15 (2015).
122. Bannuru, R. R., Osani, M. C., Al-Eid, F. & Wang, C. Efficacy of curcumin and Boswellia for knee osteoarthritis: Systematic review and meta-analysis. *Semin. Arthritis Rheum.* **48**, 416–429 (2018).
123. Mustonen, A.-M. *et al.* Distinct fatty acid signatures in infrapatellar fat pad and synovial fluid of patients with osteoarthritis versus rheumatoid arthritis. *Arthritis Res. Ther.* **21**, 124 (2019).
124. de Visser, H. M. *et al.* Local and systemic inflammatory lipid profiling in a rat model of osteoarthritis with metabolic dysregulation. *PLoS One* **13**, e0196308 (2018).
125. Metabolic OA; Does it Exist? - Osteoarthritis and Cartilage. Available at: https://www.oarsijournal.com/article/S1063-4584(17)30069-9/fulltext. (Accessed: 2nd August 2019)
126. Ioan-Facsinay, A. & Kloppenburg, M. Bioactive lipids in osteoarthritis: risk or benefit? *Curr. Opin. Rheumatol.* **30**, 108–113 (2018).
127. Sokolove, J. & Lepus, C. M. Role of inflammation in the pathogenesis of osteoarthritis: latest findings and interpretations. *Ther. Adv. Musculoskelet. Dis.* **5**, 77–94 (2013).
128. Soren, A., Klein, W. & Huth, F. Microscopic comparison of the synovial changes in posttraumatic synovitis and osteoarthritis. *Clin. Orthop.* 191–195 (1976).
129. Scanzello, C. R. & Loeser, R. F. Editorial: Inflammatory Activity in Symptomatic Knee Osteoarthritis: Not All Inflammation Is Local: EDITORIAL. *Arthritis Rheumatol.* **67**, 2797–2800 (2015).
130. Loeser, R. F., Goldring, S. R., Scanzello, C. R. & Goldring, M. B. Osteoarthritis: A Disease of the Joint as an Organ. *Arthritis Rheum.* **64**, 1697–1707 (2012).
131. Liu-Bryan, R. & Terkeltaub, R. Emerging regulators of the inflammatory process in osteoarthritis. *Nat. Rev. Rheumatol.* **11**, 35–44 (2015).
132. Goldring, M. B. & Otero, M. Inflammation in osteoarthritis. *Curr. Opin. Rheumatol.* **23**, 471–478 (2011).
133. Glasson, S. S. *et al.* Deletion of active ADAMTS5 prevents cartilage degradation in a murine model of osteoarthritis. *Nature* **434**, 644–648 (2005).
134. Chevalier, X., Claudepierre, P., Groult, N., Zardi, L. & Hornebeck, W. Presence of ED-A containing fibronectin in human articular cartilage from patients with osteoarthritis and rheumatoid arthritis. *J. Rheumatol.* **23**, 1022–1030 (1996).
135. Sofat, N. *et al.* Tenascin-C fragments are endogenous inducers of cartilage matrix degradation. *Rheumatol. Int.* **32**, 2809–2817 (2012).
136. Dahl, I. M. & Husby, G. Hyaluronic acid production in vitro by synovial lining cells from normal and rheumatoid joints. *Ann. Rheum. Dis.* **44**, 647–657 (1985).
137. Li, Z.-C. *et al.* Correlation of synovial fluid HMGB-1 levels with radiographic severity of knee osteoarthritis. *Clin. Investig. Med. Med. Clin. Exp.* **34**, E298 (2011).
138. van Lent, P. L. E. M. *et al.* Active involvement of alarmins S100A8 and S100A9 in the regulation of synovial activation and joint destruction during mouse and human osteoarthritis. *Arthritis Rheum.* **64**, 1466–1476 (2012).
139. Medina-Luna, D. *et al.* Hyperlipidem-

ic microenvironment conditionates damage mechanisms in human chondrocytes by oxidative stress. *Lipids Health Dis.* **16**, 114 (2017).
140. Valdes, A. M. *et al.* Omega-6 oxylipins generated by soluble epoxide hydrolase are associated with knee osteoarthritis. *J. Lipid Res.* **59**, 1763–1770 (2018).
141. Vuolteenaho, K. *et al.* High synovial fluid interleukin-6 levels are associated with increased matrix metalloproteinase levels and severe radiographic changes in osteoarthritis patients. *Osteoarthritis Cartilage* **25**, S92–S93 (2017).
142. Li, X. *et al.* PGE2 And Its Cognate EP Receptors Control Human Adult Articular Cartilage Homeostasis and Are Linked to the Pathophysiology of Osteoarthritis. *Arthritis Rheum.* **60**, 513–523 (2009).
143. Gosset, M. *et al.* Prostaglandin E2 synthesis in cartilage explants under compression: mPGES-1 is a mechanosensitive gene. *Arthritis Res. Ther.* **8**, R135 (2006).
144. Pruzanski, W., Bogoch, E., Wloch, M. & Vadas, P. The role of phospholipase A2 in the physiopathology of osteoarthritis. *J. Rheumatol. Suppl.* **27**, 117–119 (1991).
145. Husa, M., Liu-Bryan, R. & Terkeltaub, R. Shifting HIFs in osteoarthritis. *Nat. Med.* **16**, 641–644 (2010).
146. Wang, Q. *et al.* Identification of a central role for complement in osteoarthritis. *Nat. Med.* **17**, 1674–1679 (2011).
147. Blom, A. M. The role of complement inhibitors beyond controlling inflammation. *J. Intern. Med.* **282**, 116–128 (2017).
148. Silawal, S., Triebel, J., Bertsch, T. & Schulze-Tanzil, G. Osteoarthritis and the Complement Cascade. *Clin. Med. Insights Arthritis Musculoskelet. Disord.* **11**, (2018).
149. Ghosh, P., Sahoo, R., Vaidya, A., Chorev, M. & Halperin, J. A. Role of complement and complement regulatory proteins in the complications of diabetes. *Endocr. Rev.* **36**, 272–288 (2015).
150. Moreno-Navarrete, J. M. & Fernández-Real, J. M. The complement system is dysfunctional in metabolic disease: Evidences in plasma and adipose tissue from obese and insulin resistant subjects. *Semin. Cell Dev. Biol.* **85**, 164–172 (2019).
151. Lopes, E. B. P., Filiberti, A., Husain, S. A. & Humphrey, M. B. Immune Contributions to Osteoarthritis. *Curr. Osteoporos. Rep.* **15**, 593–600 (2017).
152. Syx, D., Tran, P. B., Miller, R. E. & Malfait, A.-M. Peripheral Mechanisms Contributing to Osteoarthritis Pain. *Curr. Rheumatol. Rep.* **20**, 9 (2018).
153. Kapoor, M., Martel-Pelletier, J., Lajeunesse, D., Pelletier, J.-P. & Fahmi, H. Role of proinflammatory cytokines in the pathophysiology of osteoarthritis. *Nat. Rev. Rheumatol.* **7**, 33–42 (2011).
154. Gierman, L. M. *et al.* Metabolic profiling reveals differences in concentrations of oxylipins and fatty acids secreted by the infrapatellar fat pad of donors with end-stage osteoarthritis and normal donors. *Arthritis Rheum.* **65**, 2606–2614 (2013).
155. Belluzzi, E. *et al.* Conditioned media from human osteoarthritic synovium induces inflammation in a synoviocyte cell line. *Connect. Tissue Res.* **60**, 136–145 (2019).
156. Bastiaansen-Jenniskens, Y. M. *et al.* Infrapatellar fat pad of patients with end-stage osteoarthritis inhibits catabolic mediators in cartilage. *Ann. Rheum. Dis.* **71**, 288–294 (2012).
157. Gwyn, R., Kotwal, R. S., Holt, M. D. & Davies, A. P. Complete excision of the infrapatellar fat pad is associated

with patellar tendon shortening after primary total knee arthroplasty. *Eur. J. Orthop. Surg. Traumatol.* **26**, 545–549 (2016).
158. Ye, C. *et al.* Influence of the Infrapatellar Fat Pad Resection during Total Knee Arthroplasty: A Systematic Review and Meta-Analysis. *PloS One* **11**, e0163515 (2016).
159. Belluzzi, E. *et al.* Contribution of Infrapatellar Fat Pad and Synovial Membrane to Knee Osteoarthritis Pain. *BioMed Res. Int.* **2019**, (2019).
160. Neogi, T. *et al.* Association of Joint Inflammation With Pain Sensitization in Knee Osteoarthritis: The Multicenter Osteoarthritis Study. *Arthritis Rheumatol. Hoboken NJ* **68**, 654–661 (2016).
161. Rahmati, M., Mobasheri, A. & Mozafari, M. Inflammatory mediators in osteoarthritis: A critical review of the state-of-the-art, current prospects, and future challenges. *Bone* **85**, 81–90 (2016).
162. Raghu, H. *et al.* CCL2/CCR2, but not CCL5/CCR5, mediates monocyte recruitment, inflammation and cartilage destruction in osteoarthritis. *Ann. Rheum. Dis.* **76**, 914–922 (2017).
163. Bernardini, G., Benigni, G., Scrivo, R., Valesini, G. & Santoni, A. The Multifunctional Role of the Chemokine System in Arthritogenic Processes. *Curr. Rheumatol. Rep.* **19**, 11 (2017).
164. Pearle, A. *et al.* Elevated C-reactive protein levels in osteoarthritis are associated with local joint inflammation. *Arthritis Res. Ther.* **6**, 56 (2004).
165. Marnell, L., Mold, C. & Du Clos, T. W. C-reactive protein: Ligands, receptors and role in inflammation. *Clin. Immunol.* **117**, 104–111 (2005).
166. Ganova, P., Gyurkovska, V., Belenska-Todorova, L. & Ivanovska, N. Functional complement activity is decisive for the development of chronic synovitis, osteophyte formation and processes of cell senescence in zymosan-induced arthritis. *Immunol. Lett.* **190**, 213–220 (2017).
167. Lourido, L. *et al.* Discovery of circulating proteins associated to knee radiographic osteoarthritis. *Sci. Rep.* **7**, 137 (2017).
168. Minguzzi, M. *et al.* Emerging Players at the Intersection of Chondrocyte Loss of Maturational Arrest, Oxidative Stress, Senescence and Low-Grade Inflammation in Osteoarthritis. *Oxid. Med. Cell. Longev.* **2018**, (2018).
169. Sproston, N. R. & Ashworth, J. J. Role of C-Reactive Protein at Sites of Inflammation and Infection. *Front. Immunol.* **9**, 754 (2018).
170. Weinhold, B., Bader, A., Poli, V. & Rüther, U. Interleukin-6 is necessary, but not sufficient, for induction of the humanC-reactive protein gene in vivo. *Biochem. J.* **325 (Pt 3)**, 617–621 (1997).
171. Szalai, A. J. *et al.* Testosterone and IL-6 requirements for human C-reactive protein gene expression in transgenic mice. *J. Immunol. Baltim. Md 1950* **160**, 5294–5299 (1998).
172. Fernandes, J. C., Martel-Pelletier, J. & Pelletier, J.-P. The role of cytokines in osteoarthritis pathophysiology. *Biorheology* **39**, 237–246 (2002).
173. Mrosewski, I. *et al.* Regulation of osteoarthritis-associated key mediators by TNFα and IL-10: effects of IL-10 overexpression in human synovial fibroblasts and a synovial cell line. *Cell Tissue Res.* **357**, 207–223 (2014).
174. Eymard, F. *et al.* Knee and hip intra-articular adipose tissues (IAATs) compared with autologous subcutaneous adipose tissue: a specific phenotype for a central player in osteoarthritis. *Ann. Rheum. Dis.* **76**, 1142–1148 (2017).

175. Geraghty, R. M. & Spear, M. Evidence for plical support of the patella. *J. Anat.* **231**, 698–707 (2017).
176. June, R. K., Liu-Bryan, R., Long, F. & Griffin, T. M. Emerging Role of Metabolic Signaling in Synovial Joint Remodeling and Osteoarthritis. *J. Orthop. Res. Off. Publ. Orthop. Res. Soc.* **34**, 2048–2058 (2016).
177. Daghestani, H. N., Pieper, C. F. & Kraus, V. B. Soluble macrophage biomarkers indicate inflammatory phenotypes in patients with knee osteoarthritis. *Arthritis Rheumatol* **67**, 956–65 (2015).
178. Vlad, S. C., Neogi, T., Aliabadi, P., Fontes, J. D. T. & Felson, D. T. No Association Between Markers of Inflammation and Osteoarthritis of the Hands and Knees. *J. Rheumatol.* **38**, 1665–1670 (2011).
179. Shadyab, A. H. *et al.* Prospective Associations of C-Reactive Protein (CRP) Levels and CRP Genetic Risk Scores with Risk of Total Knee and Hip Replacement for Osteoarthritis in a Diverse Cohort. *Osteoarthritis Cartilage* **26**, 1038–1044 (2018).
180. Jin, X. *et al.* Circulating C reactive protein in osteoarthritis: a systematic review and meta-analysis. *Ann. Rheum. Dis.* **74**, 703–710 (2015).
181. Lee, J.-H. *et al.* Relationship between oxidative balance score and quality of life in patients with osteoarthritis. *Medicine (Baltimore)* **98**, (2019).
182. Ponchel, F. *et al.* Changes in peripheral blood immune cell composition in osteoarthritis. *Osteoarthritis Cartilage* **23**, 1870–1878 (2015).
183. Scanzello, C. R. Role of low-grade inflammation in osteoarthritis. *Curr. Opin. Rheumatol.* **29**, 79 (2017).
184. Shen, P.-C. *et al.* T helper cells promote disease progression of osteoarthritis by inducing macrophage inflammatory protein-1γ. *Osteoarthritis Cartilage* **19**, 728–736 (2011).
185. Hsieh, J.-L. *et al.* CD8+ T Cell-Induced Expression of Tissue Inhibitor of Metalloproteinses-1 Exacerbated Osteoarthritis. *Int. J. Mol. Sci.* **14**, 19951–19970 (2013).
186. Raman, S., FitzGerald, U. & Murphy, J. M. Interplay of Inflammatory Mediators with Epigenetics and Cartilage Modifications in Osteoarthritis. *Front. Bioeng. Biotechnol.* **6**, 22 (2018).
187. Veronese, N. *et al.* The Relationship Between the Dietary Inflammatory Index and Prevalence of Radiographic Symptomatic Osteoarthritis: Data from the Osteoarthritis Initiative. *Eur. J. Nutr.* **58**, 253–260 (2019).
188. Alcaraz, M. J., Guillén, M. I. & Ferrándiz, M. L. Emerging therapeutic agents in osteoarthritis. *Biochem. Pharmacol.* **165**, 4–16 (2019).
189. Schett, G. *et al.* A Phase IIa Study of Anti-GM-CSF Antibody GSK3196165 in Subjects with Inflammatory Hand Osteoarthritis. *ACR Meeting Abstracts*
190. Mease, P. J. *et al.* Safety, Tolerability, and Clinical Outcomes after Intraarticular Injection of a Recombinant Adeno-associated Vector Containing a Tumor Necrosis Factor Antagonist Gene: Results of a Phase 1/2 Study. *J. Rheumatol.* **37**, 692–703 (2010).



Chapter 2

Variable cartilage degradation in mice with diet-induced metabolic dysfunction: food for thought

Kozijn A.E., Gierman L.M., van der Ham F., Mulder P., Morrison M.C., Kühnast S., van der Heijden R.A., Stavro P.M., van Koppen A., Pieterman E.J., van den Hoek A.M., Kleemann R., Princen H.M.G., Mastbergen S.C., Lafeber F.P.J.G., Zuurmond A.M., Bobeldijk I., Weinans H., Stoop R.

Published as:
Kozijn A.E., Gierman L.M., van der Ham F., Mulder P., Morrison M.C., Kühnast S., van der Heijden R.A., Stavro P.M., van Koppen A., Pieterman E.J., van den Hoek A.M., Kleemann R., Princen H.M.G., Mastbergen S.C., Lafeber F.P.J.G., Zuurmond A.M., Bobeldijk I., Weinans H., Stoop R.
Variable cartilage degradation in mice with diet-induced metabolic dysfunction: food for thought. *Osteoarthritis Cartilage. 2018 Jan;26(1):95-107.*

Abstract

Background. Human cohort studies have demonstrated a role for systemic metabolic dysfunction in osteoarthritis (OA) pathogenesis in obese patients. To explore the mechanisms underlying this metabolic phenotype of OA, we examined cartilage degradation in the knees of mice from different genetic backgrounds in which a metabolic phenotype was established by various dietary approaches.

Methods. Wild-type C57BL/6J mice and genetically modified mice (hCRP, LDLr$^{-/-}$. Leiden and ApoE*3Leiden. CETP mice) based on C57BL/6J background were used to investigate the contribution of inflammation and altered lipoprotein handling on diet-induced cartilage degradation. High-caloric diets of different macronutrient composition (i.e. high-carbohydrate or high-fat) were given in regimens of varying duration to induce a metabolic phenotype with aggravated cartilage degradation relative to controls.

Results. Metabolic phenotypes were confirmed in all studies as mice developed obesity, hypercholesteremia, glucose intolerance and/or insulin resistance. Aggravated cartilage degradation was only observed in two out of the twelve experimental setups, specifically in long-term studies in male hCRP and female ApoE*3Leiden. CETP mice. C57BL/6J and LDLr$^{-/-}$.Leiden mice did not develop HFD-induced OA under the conditions studied. Osteophyte formation and synovitis scores showed variable results between studies, but also between strains and gender.

Conclusions. Long-term feeding of high-caloric diets consistently induced a metabolic phenotype in various C57BL/6J(-based) mouse strains. In contrast, the induction of articular cartilage degradation proved variable, which suggests that an additional trigger might be necessary to accelerate diet-induced OA progression. Gender and genetic modifications that result in a humanized pro-inflammatory state (human CRP) or lipoprotein metabolism (human-E3L.CETP) were identified as important contributing factors.

Introduction

Osteoarthritis (OA) is a progressive joint disease that is characterised by focal loss of articular cartilage, which impedes smooth joint movement and causes stiffness and pain. The most important risk factors for OA are age, gender and obesity. The latter being of specific interest in developed countries, where prolonged life expectancy and a progressive sedentary lifestyle in combination with a high caloric diet is predicted to exponentially increase the number of obese individuals and hence the prevalence of OA[1]. The most common subtype of OA in obese individuals is metabolically induced OA[2], here referred to as 'metabolic OA'.

The association between knee OA and obesity has been comprehensively studied in humans. Weight loss was found to significantly reduce pain and increase mobility in knee OA patients3 and reduced the risk of onset of the disease4. In obese adults, weight loss combined with exercise appears to be the most promising treatment and is therefore recommended by several international guidelines on the management of metabolic OA[5 6]. Moreover, overweight was found to be associated with hand OA as well, indicating a possible underlying systemic factor in disease pathogenesis7. The involvement of both metabolic and systemic aspects was demonstrated in cohort studies, where knee OA development did not depend on weight or BMI but was strongly related to concurrent dysregulation of glucose and lipid metabolism[8].

Even though the association between OA and obesity is evident, the underlying mechanisms have yet to be resolved. Animal models can help fill this knowledge gap. Combining all observations in humans, a translational animal model for metabolic OA should display obesity in concurrence with metabolic dysfunction. Various species have been used to examine metabolic OA, all relying on diet-induced obesity, with the mouse being the most comprehensively studied. Silberberg *et al.* laid the foundation of the current diet-induced metabolic OA mouse model in the 1950s by linking a high-fat diet with accelerated OA onset and progression[9]. Literature on metabolic OA models has been scarce after this promising start[10], with the majority of reports dating from the past decade.

It can be ascertained from literature that there is no consensus on the best species or the optimal study design for in vivo metabolic OA models. The animal model most thoroughly examined in the context of metabolic OA is the C57BL/6J mouse strain, or genetic variants based on this background, as the readily obtained obesity observed in C57BL/6J mice closely parallels the metabolic adaptations seen in human disease pathogenesis[11]. Most researchers have employed the very high-fat diet (VHFD), a high-fat diet with a supraphysiological fat content of 60kcal% energy from fat, to induce metabolic OA in male mice – occasionally combined with an increased mechanical burden through surgery or exercise[12 13]. In contrast, published experimental designs vary greatly in study duration and age at start, which are important determinants of the

capacity for metabolic adaptation and ultimately of the severity of metabolic OA. The methodology used for determination of OA severity presents another striking difference between publications. Despite international initiatives for a common scoring system, many groups employ their own scoring system or use one of many adaptations to the Mankin scoring system[14]. Taken together, although in humans the link between obesity and OA is confirmed and appropriate animal models for both diseases are available, research on metabolic OA in animal models is still in its infancy.

Here we aim to explore the suitability of the mouse as a preclinical model for metabolic OA and to define important contributing factors to disease development. To this end, we examined OA features in the knees of mice that received various high-caloric dietary regimens at variable duration. All evaluated mouse strains were C57BL/6J or based on this background, bearing genetic modifications that humanize the strains to increase translatability to the human situation. High-caloric diets ranged in fat content from more physiological to supraphysiological, with a focus on the former for translatability purposes.

Materials and methods

A detailed methods section is available at the end of this Chapter.

Mice and diets

Twelve experiments were performed in which a high-caloric diet was used to induce overweight and metabolic dysfunction in wild-type C57BL/6J mice and genetically modified mice (hCRP, LDLr$^{-/-}$.Leiden and ApoE*3Leiden.CETP mice) based on a C57BL/6J background. The high-caloric diets applied in our studies differed in macronutrient composition (Table 1).

Table 1. Main composition of the experimental diets without any supplementations.

		Type of diet[a]					
		Chow	**LFD**	**WTD**	**MFD**	**HFD**	**VHFD**
	Supplier	Ssniff GmbH	Research Diets, Inc	ABdiets	Research Diets, Inc	Research Diets, Inc	Research Diets, Inc
	Catalogue number	V1534	D12450B	4021.04	D03101604	D12451	D12492
	Used in Study	1, 2, 4, 8, 11, 12	3, 5	12	5	1-8*†	9-11
Energy source (kcal%)	Diet components (g/kg)						
Fat		**9**	**10**	**16**	**30**	**45**	**60**
	Crude fat	33	-	-	-	-	-
	Lard	-	19.0	-	116.7	206.8	316.6
	Cacao butter	-	-	150.0	-	-	-
	Corn oil	-	-	10.0	-	-	-
	Soybean oil	-	23.7	-	26.5	29.1	32.3
	Cholesterol^	-	0.05	0.07	0.08	0.20	0.30
Protein		**33**	**20**	**20**	**20**	**20**	**20**
	Crude protein	190	-	-	-	-	-
	Casein	-	189.6	200.0	212.2	233.1	258.4
	L-Cystine	-	2.8	0.5	3.2	3.5	3.9
Carbohydrate		**58**	**70**	**56**	**50**	**35**	**20**
	Corn starch	365	298.6	100.0	226.8	84.8	0
	Sucrose	-	331.7	405.0	264.0	201.4	88.9
	Sugar	47	-	-	-	-	-
	Maltodextrin 10	-	33.2	-	37.1	116.5	161.5
Fibre							
	Crude fibre	49	-	-	-	-	-
	Cellulose	-	47.4	62.0	53.0	58.3	64.6

* Study 4: the HFD was supplied via BioServices, which resembles the HFD from Research Diets, Inc.
† Study 6: D12451 was modified by the supplier for the intervention groups: soybean oil was changed into corn oil and 43.5 gm% of lard was replaced by either of the oils of interest (to a total of 15 gm% lard and 9 gm% oil).
^ Natural cholesterol content of the basic diet, additional cholesterol supplementation is specified in Table 2.
a LFD, low-fat diet; WTD, Western-type diet; MFD, mid-fat diet; HFD, high-fat diet; VHFD, very high-fat diet.

Evaluated studies

The experiments were designed to examine various diet-induced metabolic disorders and therefore differed in original research question and design (Table 2).

Table 2. Overview of the evaluated mouse studies ranked by mouse strain and study duration.

Study	Original design	Age at start (weeks)	Weeks on study diet	Mice/ group	Diet intervention groups[a]	Gender[b]
C57BL/6J						
1	Early detection of type II diabetes and its complications	12	0	12	chow	M
			6	12 12	chow HFD	
			12	12 12	chow HFD	
			24	12 12	chow HFD	
2[59]	The role of adipose tissue inflammation in NAFLD	12	24	10 15	chow HFD	M
3[17]	Aging	12	52	10-15	LFD HFD	M
hCRP						
4[16‡]	Metabolic syndrome	10-14	38	10 10	chow HFD	M
				10 10	chow HFD	F
LDLr$^{-/-}$.Leiden						
5	Diabetic nephropathy	8	20	10 10 10	LFD MFD HFD	M
6	Type II diabetes	12	20	15 15 15 15 15	HFD HFD + refined soybean oil HFD + unrefined soybean oil HFD + refined palm oil HFD + unrefined palm oil	M
7	Diabetic nephropathy	12	20	10 10 10 10	HFD HFD + fructose HFD + 0,2% cholesterol HFD + 1,0% cholesterol 20w	M
			31	10	HFD + 1,0% cholesterol 31w	
8	Metabolic syndrome	13-15	30	6 15	chow HFD	M
ApoE*3Leiden.CETP						
9	Metabolic syndrome	10-16	26*	10	VHFD + fructose	M

10	Insulin resistance and dyslipidemia	10-12	32†	8	VHFD + fructose	M
11	Osteoarthritis	15	32	12 12 12 12	chow VHFD VHFD + chow VHFD low-MetS	M
12[54‡]	Atherosclerosis and OA	8-12	38	12 12 17	Chow group WTD + 0,4% cholesterol WTD + 1,0% cholesterol	M
				12 12 17	Chow group WTD + 0,1% cholesterol WTD + 0,3% cholesterol	F

* Study 9: during the final 16 weeks 10% fructose was added to the drinking water.
† Study 10: during the final 24 weeks 10% fructose was added to the drinking water.
‡ Previously published OA data.
a LFD, low-fat diet (10kcal% energy from fat); WTD, Western-type diet (16kcal% energy from fat); MFD, mid-fat diet (30kcal% energy from fat); HFD, high-fat diet (45kcal% energy from fat); VHFD, very high-fat diet (60kcal% energy from fat); low-MetS, mice showing inexplicably low metabolic adaptation to the VHFD; b M, male and F, female.

Analysis of metabolic dysfunction and osteoarthritis

Metabolic dysfunction is defined as a significant increase in either body weight and fasted plasma cholesterol, glucose and/or insulin levels compared with normal values as observed in chow- or low fat diet (LFD, 10kcal% energy from fat)-fed controls.
Articular cartilage degradation, osteophyte formation and synovitis were scored on coronal 5 μm knee joint sections, stained with Haematoxylin, Fast Green and Safranin-O, according to OARSI histopathology initiative recommendations for the mouse[15].

Statistical analysis

Statistical analysis was performed using IBM SPSS software (v23.0, IBM SPSS Inc., Chicago, IL, USA) or GraphPad Prism (v7.01, GraphPad, San Diego, USA). Data analysis revealed that the assumptions of normality and homoscedasticity could not be satisfied in any of our studies. Therefore, depending on study design, non-parametric Mann-Whitney U-test for comparison of 2 groups or Kruskal-Wallis test for >2 groups was used for both the metabolic parameters and histopathological scores. A probability value <0.05 was considered statistically significant. Data are presented as median with interquartile ranges (IQR). For the OA scores, mean ± standard deviations (SD) are reported as well.

Results

Variability in diet-induced osteoarthritis severity

Ten out of the twelve diet-induced metabolic dysfunction approaches did not result in an aggravated development of OA compared with matched controls (Table 3; representative images in Figure 1). The higher OA severity scores in these studies are accompanied by relatively large standard deviations, indicating large biological variation among mice (see also Figure S1). Severity scores demonstrated clear mouse-strain-dependent effects: in our hands, C57BL/6J mice on a high-fat diet (HFD, 45kcal% energy from fat) regimen up to 52 weeks did not develop aggravated cartilage degradation (Figure 1A). Severity scores did increase over time, but were comparable to chow and LFD controls at each time point.

The human C-reactive protein (hCRP) knock-in mouse strain (Study 4) had previously shown diet-induced aggravation of OA[16]. Mice of both genders received either chow or HFD for 38 weeks. At endpoint, HFD-fed male hCRP mice had developed significantly more OA compared with chow controls (Figure 1B). In female hCRP mice HFD feeding had no effect on OA severity, which was comparable to males on chow.

LDLr-/-.Leiden mice predominantly received lard-based synthetic diets, for a period of 20-31 weeks. In studies 6 and 7 the diets were adjusted by replacing dietary lard partly with specific oils or by supplementing the diet with fructose or cholesterol, respectively. Although an overall reduction in proteoglycan content was noticeable (Figure 1C), none of these dietary approaches aggravated OA development compared with chow- or LFD-fed mice. No diet-induced cartilage degradation was observed in LDLr$^{-/-}$.Leiden mice up to 31 weeks.

Male ApoE*3Leiden.CETP mice displayed high OA severity scores in general, independent of diet (Figure 1E). Compartmental subscores demonstrated a proportional distribution across all compartments, showing no preference for the medial or lateral side (Table S1). Female ApoE*3Leiden.CETP mice demonstrated less joint damage in the chow control compared with males and an accelerated OA development in the 0.3% but not 0.1% cholesterol-supplemented group (Study 12, Figure 1D).

Table 3. Overview of knee OA severity scores from twelve independent mouse studies with various approaches for diet-induced metabolic dysfunction.

Study	Age at start (weeks)	Weeks on study diet	Diet intervention groups[a]	Gender[b]	Total OA severity score	
C57BL/6J					**Median [IQR]**	**Mean ± SD**
1	12	0	chow	M	1.25 [0.75-1.50]	1.31 ± 0.70
		6	chow		2.19 [1.34-2.46]	2.06 ± 1.05
			HFD		2.00 [1.13-3.29]	2.18 ± 1.07
		12	chow		3.25 [2.42-4.50]	4.53 ± 4.26
			HFD		2.82 [1.97-4.28]	3.25 ± 1.45
		24	chow		4.94 [3.94-5.72]	5.51 ± 3.22
			HFD		4.40 [3.60-5.43]	4.38 ± 1.29
2[59]	12	24	chow	M	3.69 [3.29-5.60]	4.19 ± 1.37
			HFD		4.00 [3.50-5.00]	4.22 ± 1.15
3[17]	12	52	LFD	M	4.69 [3.88-6.22]	4.12 ± 1.65
			HFD		5.88 [5.00-7.50]	5.20 ± 1.58
hCRP						
4[16‡]	10-14	38	chow	M	4.83 [3.17-5.17]	4.45 ± 1.33
			HFD		**6.33 [4.42-12.25]**	**7.81 ± 4.54**
			chow	F	3.33 [3.25-4.75]	3.70 ± 0.86
			HFD		3.50 [2.50-4.75]	3.69 ± 1.20
LDLr$^{-/-}$.Leiden						
5	8	20	LFD	M	3.50 [3.20-4.25]	3.55 ± 0.67
			MFD		4.00 [2.90-4.64]	3.70 ± 1.36
			HFD		3.75 [2.63-5.02]	3.80 ± 1.49
6	12	20	HFD	M	3.00 [2.25-4.00]	3.43 ± 1.30
			HFD + refined soybean oil		3.50 [2.63-4.38]	3.83 ± 0.58
			HFD + unrefined soybean oil		3.75 [2.37-4.75]	2.78 ± 1.84
			HFD + refined palm oil		3.50 [2.75-4.00]	3.50 ± 0.87
			HFD + unrefined palm oil		3.25 [2.50-3.75]	2.88 ± 0.70
7	12	20	HFD	M	3.29 [2.67-4.27]	3.45 ± 0.88
			HFD + fructose		3.67 [2.81-4.93]	4.22 ± 2.39
			HFD + 0.2% cholesterol		3.38 [2.77-3.81]	3.90 ± 2.05
			HFD + 1.0% cholesterol 20w		3.33 [2.42-3.49]	3.09 ± 0.99
		31	HFD + 1.0% cholesterol 31w		4.08 [2.89-4.48]	4.20 ± 1.71
8	13-15	30	chow	M	3.50 [2.59-5.67]	4.06 ± 1.47
			HFD		4.75 [4.00-5.83]	6.17 ± 4.31

ApoE*3Leiden.CETP						
9	10-16	26*	VHFD + fructose	M	5.88 [4.38-7.94]	7.39 ± 5.21
10	10-12	32†	VHFD + fructose	M	5.00 [4.00-14.75]	8.32 ± 5.23
11	15	32	chow	M	6.38 [5.00-17.63]	8.81 ± 4.89
			VHFD		5.50 [3.63-8.50]	6.53 ± 2.20
			VHFD + chow		5.50 [4.25-8.50]	7.80 ± 3.63
			VHFD, low-MetS		7.63 [5.00-12.25]	9.97 ± 5.07
12[54‡]	8-12	38	Chow group	M	7.82 [5.94-9.81]	8.26 ± 2.29
			WTD + 0.4% cholesterol		6.88 [5.19-7.63]	7.37 ± 3.48
			WTD + 1.0% cholesterol		7.75 [6.03-8.72]	8.45 ± 3.87
			Chow group	F	5.01 [4.69-6.04]	5.35 ± 1.16
			WTD + 0.1% cholesterol		6.13 [5.63-6.88]	5.98 ± 1.04
			WTD + 0.3% cholesterol		**6.69 [5.13-7.81]**	**6.81 ± 2.25**

Total OA severity scores presented here are group medians with interquartile ranges and group averages with standard deviation of the averaged sum scores for the tibiofemoral knee compartments (max. 24, OARSI histopathology recommendations for the mouse[15]). Bold font indicates statistically significant changed OA severity compared with chow controls. Statistical significance level was set to $p<0.05$.

* Study 9: during the final 16 weeks 10% fructose was added to the drinking water.

† Study 10: during the final 24 weeks 10% fructose was added to the drinking water.

‡ Previously published OA data.

a LFD, low-fat diet (10kcal% energy from fat); WTD, Western-type diet (16kcal% energy from fat); MFD, mid-fat diet (30kcal% energy from fat); HFD, high-fat diet (45kcal% energy from fat); VHFD, very high-fat diet (60kcal% energy from fat); low-MetS, mice showing inexplicably low metabolic adaptation to the VHFD; b M, male and F, female.

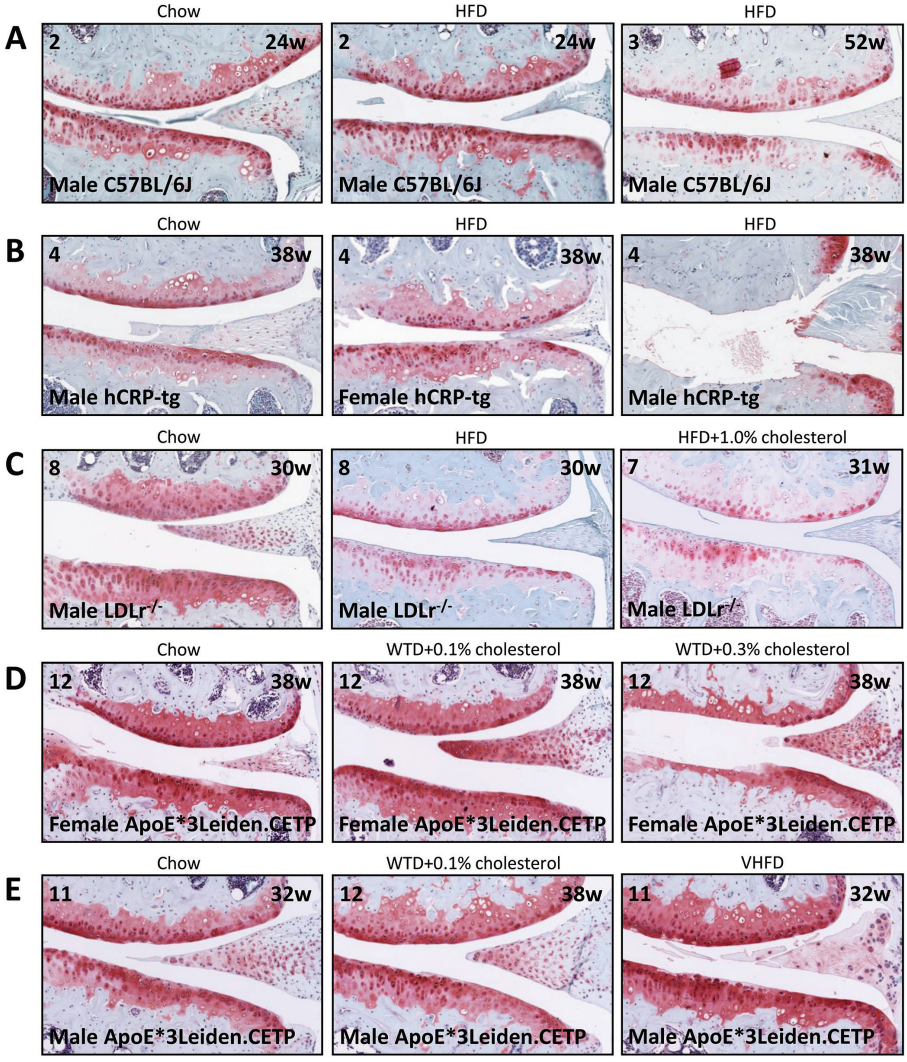


Figure 1. Representative coronal sections of the medial tibiofemoral compartments, stained with Fast-Green/Safranin-O. Additional information for each image: study number in upper left corner, duration (weeks) in upper right corner, gender and strain in lower left corner. Magnification for all microphotographs was 40x. A) HFD does not induce aggravated cartilage degeneration at 24 or 52 weeks of feeding in male wild-type C57BL/6J mice. B) Male hCRP transgenic mice developed aggravated cartilage degeneration when fed a HFD compared with chow diet for 38 weeks, while female hCRP transgenic mice did not. C) HFD without or with additional cholesterol did not accelerate cartilage degeneration in male LDLr-/- mice compared to chow-fed controls. D) Aggravated diet-induced cartilage degeneration was observed in female ApoE*3Leiden.CETP mice fed a WTD with additional dietary cholesterol for 38 weeks, showing a cholesterol-dependent increase in severity. E) Male ApoE*3Leiden.CETP mice showed surface fibrillation and loss of surface lamina, independent of the dietary interventions investigated.

Presence of metabolic dysfunction

To monitor the development and extent of the diet-induced metabolic dysfunction, time-dependent effects of all dietary interventions on body weight and fasted plasma levels of cholesterol, glucose and insulin were regularly measured over the course of each study (Figures 1 and 2). Obesity was established by all high-fat diet regimens, in combination with at least one of the following comorbidities: hypercholesterolemia, glucose intolerance or insulin resistance. ApoE*3Leiden.CETP mice fed a WTD (Study 12) remained lean. Nonetheless, metabolic dysfunction in the form of hypercholesteremia was clearly observed in these mice, especially in females receiving additional 0.3% dietary cholesterol.

C57BL/6J mice (Study 1-2) rapidly responded to HFD and became obese within 12 weeks compared with age-matched chow controls. Cholesterol levels gradually increased up to three-fold compared with chow-fed controls over the course of 12 weeks and remained at this level until the end of the study. While blood glucose of HFD-fed mice remained at a constant high level, insulin levels continued to increase, indicative of insulin resistance. In Study 1, development of insulin resistance and glucose intolerance in HFD-fed mice was confirmed by insulin and glucose tolerance tests at 24 weeks (data not shown). Study 3 showed that this insulin sensitivity was attenuated upon prolonged HFD feeding, as the HFD group initially showed a similar increase in insulin levels but then recuperation to LFD-fed control levels as of week 4017. Also, HFD-fed mice steadily increased their body weight during the first 40 weeks, after which body weight stabilised until the end of the study. Cholesterol levels remained significantly elevated compared with control during the entire study period.

hCRP transgenic mice (Study 4) reached obesity after 18 weeks on a HFD, with modest to no changes in glucose and insulin levels up to 10 weeks. At week 36, a glucose tolerance test showed a delayed clearance of glucose in HFD-mice of both sexes compared with their chow controls (data not shown), indicative of glucose intolerance. Males exhibited higher absolute levels of glucose and insulin than females.

In LDLr-/-.Leiden mice (Study 5), the fat percentage in a synthetic diet positively associated with the observed increase in body weight, plasma glucose and insulin levels. Cholesterol levels changed significantly on a HFD but not on a mid-fat diet (MFD, 30kcal% energy from fat) compared with LFD controls, suggesting that a synthetic diet needs to provide in more than 30kcal% energy from fat to induce hypercholesterolemia. Modifications to the dietary fatty acid composition (Study 6) induced metabolic changes over a period of 20 weeks. Refined soybean oil lowered all metabolic parameters except plasma glucose. Palm oil greatly induced all measured plasma parameters, with additional increases in insulin levels upon feeding unrefined palm oil.

Fructose supplementation for 20 weeks (Study 7) slightly reduced body weight

increase, marginally increased cholesterol levels, but drastically increased insulin levels compared with controls. Cholesterol supplementation dose-dependently increased plasma cholesterol levels compared with controls, changing the metabolic state towards a more hypercholesterolemic phenotype without insulin resistance. In Study 8 HFD-fed male LDLr-/-.Leiden mice continuously gained weight, reaching markedly higher weights than chow controls. Cholesterol levels increased almost 4-fold over time compared with controls. Insulin levels varied over time, but were significantly higher compared with chow control mice as of week 6.

Studies performed in ApoE*3Leiden.CETP mice were of longer duration than aforementioned studies, the shortest being 26 weeks (Study 9, Table 2). In both Studies 9 and 10, fructose was added to the drinking water on top of a very high-fat diet (VHFD, 60kcal% energy from fat). On this regimen, male ApoE*3Leiden.CETP mice rapidly gained weight during the first 16 weeks and stabilized from then onwards. Fasted plasma cholesterol levels were tripled within 12 weeks compared with baseline values. Fructose treatment provoked a steep insulin increase in Study 9, though this was not as apparent in Study 10. Insulin and glucose tolerance tests at endpoint confirmed dysregulation of glucose metabolism in both studies (data not shown).

Male ApoE*3Leiden.CETP mice demonstrated similar increases in weight and cholesterol levels on a VHFD without fructose supplementation (Study 11). Cholesterol levels showed a 2.5-fold increase compared with chow controls at endpoint. When switched from VHFD to chow diet ('VHFD+chow'), body weight and cholesterol levels decreased to near chow control levels within 12 weeks. Low-MetS mice – ApoE*3Leiden.CETP mice with low metabolic adaptations to VHFD – indeed presented low body weight gain and cholesterol levels on a VHFD, albeit consistently elevated compared with chow controls.

Cholesterol supplementation continuously increased plasma cholesterol levels in both ApoE*3Leiden.CETP genders over time without effect on weight gain (Study 12). Females were more susceptible to dietary cholesterol than their male counterparts, showing plasma cholesterol increases of 7.5-fold and 4.5-fold compared with chow controls, respectively. Blood sugar regulation parameters were not available for the latter two studies.

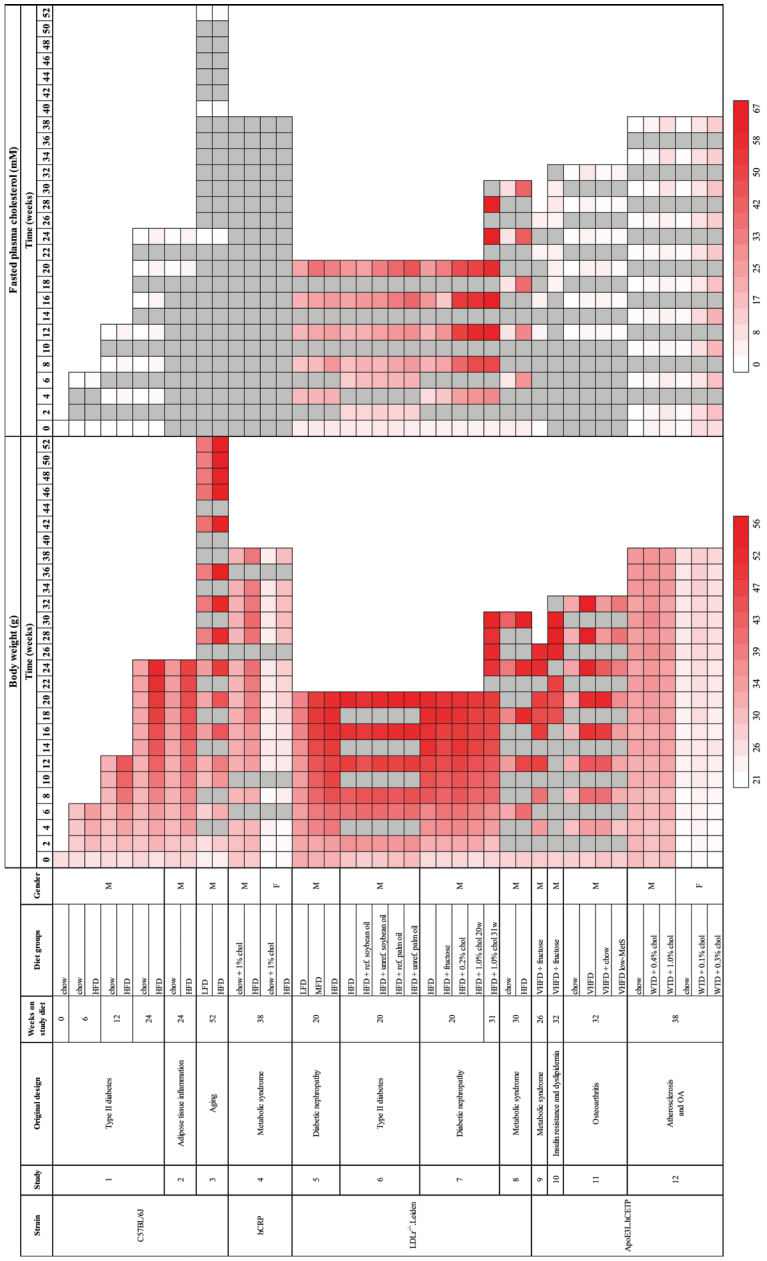


Figure 2. Biweekly overview of the changes in body weight and total fasting cholesterol plasma levels for diet interventions of all studies investigated, ranked by mouse strain. Colour intensity matches the measured concentration for each parameter, as visualized by the scale at the bottom of each heat map. Grey indicates no data available. Table S2 bears the actual values of the group medians with interquartile ranges for selected time points.

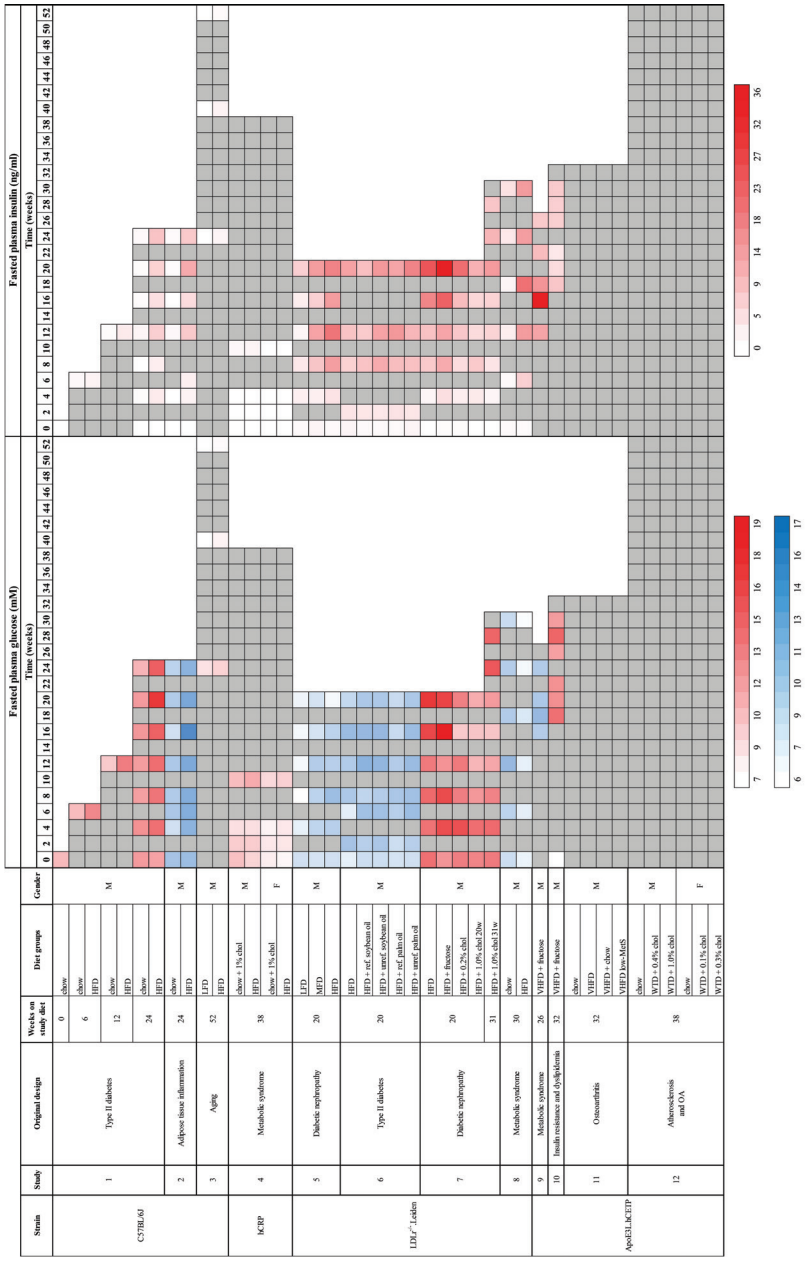


Figure 3. Biweekly overview of the changes in fasting glucose and insulin plasma levels for diet interventions of all studies investigated, ranked by mouse strain. For the glucose heatmap, red indicates results that were immediately measured using a hand-held glucose analyser (blood glucose), while blue represents values measured by enzymatic assay at the end of the study (plasma glucose). Colour intensity matches the measured concentration for each parameter, as visualized by the scale at the bottom of each heat map. Grey indicates no data available. Table S3 bears the actual values of the group medians with interquartile ranges for selected time points.

Variability in induction of inflammatory OA features on HFD

To better understand how metabolic dysfunction impacts OA pathology, osteophyte formation and synovitis were additionally scored. A HFD is known to increase these inflammatory OA features in mice[18 19], which can be distinguished before changes in cartilage structure become visible[20]. In general, both features showed high variability in our studies (Figures 4 and 5).

In wild-type C57BL/6J mice, synovitis seemed to increase due to HFD feeding from 12 to 24 weeks in Study 1, as compared with chow controls. Study 2 confirmed a significant increase in synovitis scores between these two diets at 24 weeks. This difference in synovial inflammation is not visible after 52 weeks of HFD feeding (Study 3), suggesting a return to LFD control levels. The presence of osteophytes increased over time in C57BL/6J mice, but HFD feeding only aggravated this process in Study 1.

Male hCRP mice from Study 4, demonstrating significantly increased OA severity, did not show corresponding significant increases in osteophyte formation and synovitis. Although the mice with the highest OA scores also showed the highest osteophyte and synovitis scores, this association was not applicable in general. Female hCRP mice on a HFD showed a non-significant trend (p=0.087) towards an increase in synovitis score compared with chow controls, but did not differ from controls in osteophyte formation.

In LDLr-/- mice, additional scoring of osteophyte formation and synovitis provided a profounder picture of disease pathogenesis. Osteophyte formation increased significantly on a HFD compared with chow in Studies 5 and 8. Synovitis seemed to increase as well in these mice, with a significant difference observed between HFD- and chow-fed mice in Study 5. This difference was less clear in Study 8, where the HFD-fed mice showed an aberrant, lower synovitis scores compared to HFD-fed mice in Studies 5-7 – despite longer study duration.

Male ApoE*3Leiden.CETP mice, as with OA severity, showed overall high scores for both osteophyte formation and synovitis, independent of diet. Interestingly, female ApoE*3Leiden.CETP mice showed a discrepancy in these two features, with high synovitis scores – to the level of their male counterparts – but almost no osteophyte formation.

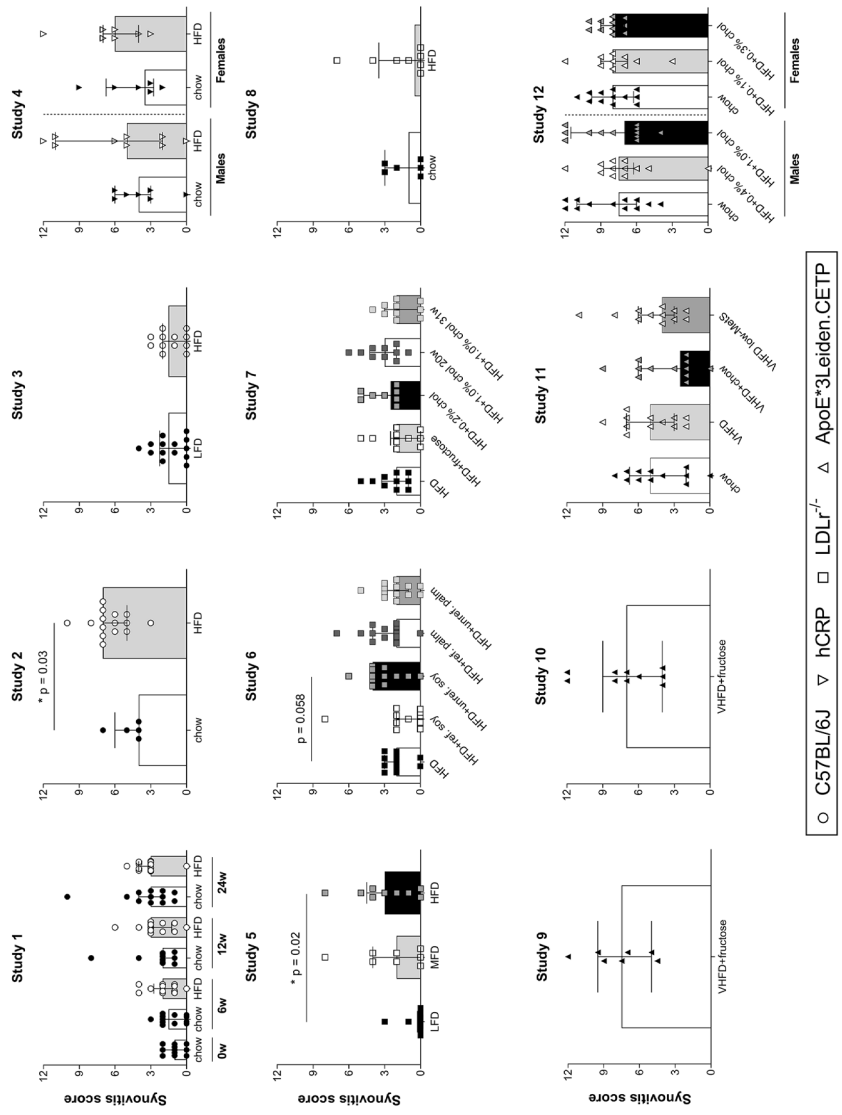


Figure 4. Overview of synovitis scores for each study group, arranged per study. Total synovitis scores presented per study in separate scatterplots showing the individual summed score for the tibiofemoral knee compartments for each animal per study group (max. 12, OARSI histopathology recommendations for the mouse[15]). Group medians (indicated by bars) and interquartile ranges are also shown. * indicates statistical significance relative to control at the same time point ($p<0.05$). LFD, low-fat diet (10 kcal% energy from fat); WTD, Western-type diet (16 kcal% energy from fat); MFD, mid-fat diet (30 kcal% energy from fat); HFD, high-fat diet (45 kcal% energy from fat); VHFD, very high-fat diet (60 kcal% energy from fat); w, time in weeks; ref., refined oil; unref., unrefined oil; low-MetS, mice showing inexplicably low metabolic adaptation to the VHFD.

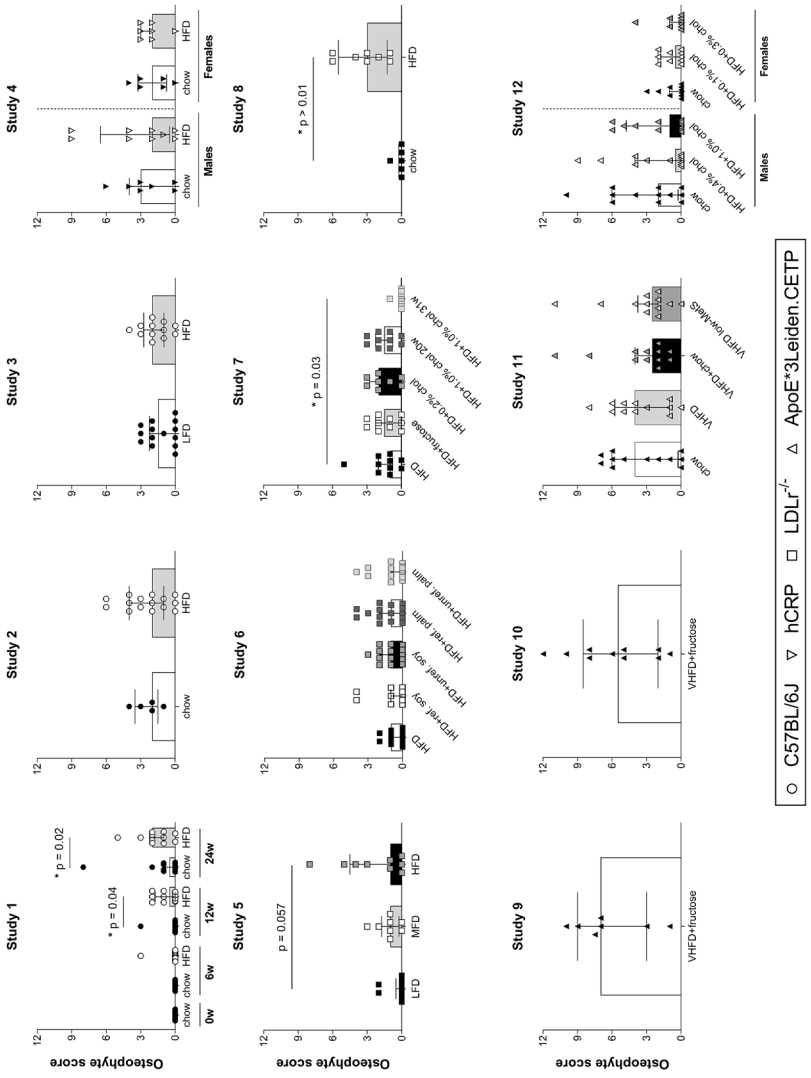


Figure 5. Overview of osteophyte scores for each study group, arranged per study. Total osteophyte scores presented per study in separate scatterplots showing the individual summed score for the tibiofemoral knee compartments for each animal per study group (max. 12, OARSI histopathology recommendations for the mouse[15]). Group medians (indicated by bars) and interquartile ranges are also shown. * indicates statistical significance relative to control at the same time point (p<0.05).LFD, low-fat diet (10 kcal% energy from fat); WTD, Western-type diet (16 kcal% energy from fat); MFD, mid-fat diet (30 kcal% energy from fat); HFD, high-fat diet (45 kcal% energy from fat); VHFD, very high-fat diet (60 kcal% energy from fat); w, time in weeks; ref., refined oil; unref., unrefined oil; low-MetS, mice showing inexplicably low metabolic adaptation to the VHFD.

Discussion

We report on the variable induction of diet-induced articular cartilage degradation in twelve mouse experiments originally designed to examine various diet-induced metabolic disorders. The link between obesity and OA has become evident in human cohort studies as well as obesity-induced animal models. We postulated that a translational animal model for metabolic OA should display obesity in concurrence with hallmarks of metabolic dysfunction. All our studies confirmed the manifestation of a metabolic phenotype, leaving the absence of accelerated cartilage degradation unexplained. Osteophyte formation and synovitis showed variable results as well, both between HFD-fed mice and controls as between HFD-fed groups within each strain. Rather, our results suggest that an additional trigger – on top of a high-caloric dietary stressor – is necessary to evoke metabolic OA. We found that diet-induced cartilage degradation developed in two mouse models that express human genes (i.e. hCRP and ApoE*3Leiden.CETP mice), suggesting that the corresponding gene products contribute to disease development. These results challenge the general consensus that HFD feeding per se is sufficient to evoke OA development.

To improve the translatability of our results, we made use of relevant humanized mouse strains[21 22] and high-caloric diets with more physiological fat content. We acknowledge that our options to explore all contributing factors and perform further mechanistic research was limited due to the broad variation in experimental design and the fact that most of our studies were not preconceived to assess OA development. Also, the OARSI 2010 scoring system we employed, specifically designed for the comparison of OA severity across the various murine OA models, focuses primarily on the condition of articular cartilage. Being a milder form of OA, diet-induced OA has been evaluated using alternative scoring systems that are more sensitive at discriminating the depth and breadth of mild to moderate OA pathology. To compensate for the cartilage-centered approach, osteophyte formation and synovitis were scored as additional OA features to examine the impact of metabolic dysfunction on different aspects of OA pathology. There may be many explanations for the discrepancy between our results and current literature[23] on diet-induced OA in small animal models, like differences between experiments and laboratories as reviewed in detail by van der Kraan[24]. The type of scoring system applied can also affect interpretation. Nevertheless, we have encountered several other research groups for which diet-induced metabolic overload in mice did not result in OA development either. Hence, it is certainly possible that OA literature has a publication bias concerning this model; a known issue in the OA field[25] and research in general[26].

The large number of studies – with substantial group sizes – and the consistently applied methodology in our studies enabled us to deduce major confounding factors like strain

and gender. Firstly, the C57BL/6J background is a relevant factor shared across all studies. Secondly, most of our studies were conducted in male mice, mainly because males are more prone to develop metabolic dysfunction than females. Thirdly, while duration varied, dietary exposure exceeded 12 weeks in all experiments – a commonly described end point for diet-induced OA in C57BL/6J mice[19 27-29]. However, diet-induced OA studies typically employ VHFDs that contain supraphysiological quantities of fat (i.e. 60kcal% energy from fat). In contrast, we chose to predominantly use high-fat diets in our studies with 45kcal% energy from fat, which better approximate the fat content observed in certain human diets[30]. Moreover, in a comprehensive review on high-fat diets, Buettner *et al.*[31] considered it appropriate to state that semi-purified diets with a fat content of more than 40% energy based on animal fats and ω-6/ω-9 fatty acid-containing plant oils will lead to metabolic dysregulation in rodents. The fat fractions of the diets in our studies were all based on lard, in one study partially replaced by soybean or palm oils rich in ω-6/ω-9 fatty acids. Taken together, we believe that all studies described here employed vindicated approaches for diet-induced metabolic dysfunction.

One of the humanized mouse strains used here expresses the human transgene for C-reactive protein (hCRP). As an acute-phase protein, hCRP is able to exert proinflammatory effects through complement activation[32]. Although hCRP is not directly linked to a metabolic pathway, the protein was found to have great impact on the murine metabolic state and cartilage degradation. Obesity development on a HFD was delayed in transgenic hCRP compared with wild-type C57BL/6J mice, with the average body weight after 38 weeks of HFD feeding equating to 12 weeks of HFD feeding in C57BL/6J. Induction of insulin resistance was also delayed in hCRP mice. Together with the absence of diet-induced OA in C57BL/6J and LDLr-/-.Leiden mice, this indicates that the severity of metabolic dysfunction is not a major determinant of OA development in the models investigated. Despite the delayed metabolic dysfunction male hCRP mice showed significant OA aggravation upon HFD feeding, whereas females gained notably less weight and did not develop diet-induced OA. Accordingly, male hCRP mice expressed 50-fold higher levels of hCRP than females[33]. A role for hCRP in OA pathogenesis is further supported by an earlier finding by our group that two different types of drugs with anti-inflammatory properties prevented OA development in hCRP male mice[16]. These results suggest that the general inflammatory status associates with the onset and progression of metabolic OA. Interestingly, the inflammatory OA features osteophyte formation and synovitis were not very pronounced in these mice. Many cohort studies have investigated the relationship between CRP and OA, but reports are contradictory and the role of CRP is still under debate[34-37], making further investigation into this link necessary. A meta-analysis of 32 reported clinical studies by Jin and colleagues further complicates the role of CRP in OA pathogenesis, as it was

concluded that low-grade systemic inflammation may play a more prominent role in symptoms of OA[38].

In line with expectations[39], ApoE*3Leiden.CETP mice, a model with humanized lipoprotein metabolism, rapidly developed obesity and metabolic dysfunction on a VHFD. In general, ApoE*3Leiden.CETP mice were highly prone to cartilage degradation, independent of the level of diet-induced metabolic dysfunction. Specifically in males, OA scores were consistently higher than in other strains investigated, even on a chow diet. The same overall high scores were found for both osteophyte formation and synovitis, again independent of the level of diet-induced metabolic dysfunction. The ApoE*3Leiden.CETP mouse expresses three human transgenes when compared with the wild-type C57BL/6J mouse (i.e. ApoE*3Leiden, CETP and APOC1)[40], suggesting that one or more of these gene products contribute to OA development. For instance, we and others have reported that the apoCI apolipoprotein may augment the general inflammatory state[41-44]. ApoE has also been implicated in systemic inflammatory processes, although it can exert both anti- and proinflammatory actions depending on the specific isoform[45 46]. Alternatively, the higher male susceptibility may also be explained by higher androgen levels, which exacerbate OA in mice[47]. Human studies also support a role of sex hormones in OA, showing increased OA prevalence and severity in postmenopausal women compared with premenopausal women and age-matched men[48 49]. Moreover, androgens and ApoE isoforms have been shown to be functionally intertwined in inflammatory processes[46 50], providing a possible rationale as to why ApoE*3Leiden.CETP males show more cartilage degradation in response to metabolic challenges compared with females.

Contrary to the males, female ApoE*3Leiden.CETP transgenic mice showed less cartilage degradation on chow but were susceptible to diet-induced OA. The inflammatory OA features showed deviant results, as ApoE*3Leiden.CETP females developed almost no osteophytes but demonstrated overall high synovitis scores independent of diet. These results contradict current literature in which excessive bone formation and synovitis due to high LDL cholesterol levels is described[51]. The gender differences may partly be explained by the significantly higher diet-induced plasma cholesterol levels observed in ApoE*3Leiden.CETP females, a discrepancy driven by sex hormones[52]. Together with the unfavourable LDL/HDL ratio in these mice, this observation is in agreement with higher OA incidence in women with elevated waist circumference and low HDL cholesterol[53]. Moreover, we previously reported suppression of WTD-induced OA development in ApoE*3Leiden. CETP females upon preventive treatment with the cholesterol-lowering anti-inflammatory drug atorvastatin (Study 12), while cholesterol-lowering alone by ezetimibe did not show this effect[54]. Again, this advocates a role for inflammation in OA development, as previously argued for the hCRP strain. For OA patients the benefit of statin therapy is unclear at present, as human studies

investigating the effect of statins on OA development are scarce and a beneficial effect is not observed in all studies[55]. Potential beneficial effects might however be missed due to underdosing, as we have previously shown that the optimal lipid-lowering statin dose is much lower than the threshold for the anti-inflammatory effects[56]. Accordingly, in a population-based longitudinal study, Kadam *et al.* demonstrated that a higher mean daily statin dose was significantly associated with a decreased likelihood of clinical OA during a 10-year follow-up[57].

In conclusion, we have demonstrated that diet-induced metabolic dysfunction per se does not necessarily lead to aggravated articular cartilage degradation in mice on a C57BL/6J background. Whereas most of the studies evaluated here were not designed specifically for OA research, there are reports using diet-induced metabolic dysregulation as the only trigger to induce OA in small animal models[23]. In light of our results and the relatively small amount of publications since the 1950s, it is likely that the OA literature has a bias and tends to selective reporting on this issue. Nonetheless, our results support the current concept that metabolic OA is driven by low-grade inflammation[58], although metabolic factors alone might not be enough to generate progressive OA. We suggest that an additional trigger, other than high-caloric feeding alone, is necessary to evoke metabolic OA. In addition to mechanical stressors, as described in literature, we showed that gender and inflammatory factors encoded by the human transgenes in hCRP and ApoE*3Leiden.CETP mice might also trigger metabolic OA development.

Acknowledgements

We thank our colleague Marjolein van Rotterdam for her contribution to this manuscript concerning the technical and operational aspects of the animal facilities. We thank our colleagues Tanja Krone and Sabina Bijlsma from the Statistics Department for their continued statistical support. We thank Jos Runhaar at the Erasmus University Medical Center Rotterdam for his editorial assistance. The authors acknowledge that due to space limitations only a subselection of references is included in this manuscript.

Authors' contributions

AEK, LMG, PM, MCM, SK, MPS, AVK, EJP, AMH, RK, HMGP, AMZ and RS have designed the experiments. AEK, LMG, FH, PM, MCM and SK have carried out experimental procedures. AEK has been the primary person responsible for writing the manuscript. All authors were involved in revising the manuscript critically for important intellectual content and approved the final version to be published.

Funding

This manuscript was supported by funding from the Netherlands Organization for Applied Scientific Research (TNO) and the European Union's Seventh Framework Programme for research, technological development and demonstration under grant agreement No. 305815-D-BOARD.

Competing interests

The authors declare that they have no conflict of interest.

References

1. Murphy L, Schwartz TA, Helmick CG, Renner JB, Tudor G, Koch G, *et al.* Lifetime risk of symptomatic knee osteoarthritis. *Arthritis Rheum* 2008;59(9):1207-13. doi: 10.1002/art.24021
2. Bijlsma JW, Berenbaum F, Lafeber FP. Osteoarthritis: an update with relevance for clinical practice. *Lancet* 2011;377(9783):2115-26. doi: 10.1016/S0140-6736(11)60243-2 [published Online First: 16 June 2011]
3. Christensen R, Bartels EM, Astrup A, Bliddal H. Effect of weight reduction in obese patients diagnosed with knee osteoarthritis: a systematic review and meta-analysis. *Ann Rheum Dis* 2007;66(4):433-9. doi: 10.1136/ard.2006.065904
4. Runhaar J, de Vos BC, van Middelkoop M, Vroegindeweij D, Oei EH, Bierma-Zeinstra SM. Moderate weight loss prevents incident knee osteoarthritis in overweight and obese females. *Arthritis Care Res (Hoboken)* 2016 doi: 10.1002/acr.22854
5. Gay C, Chabaud A, Guilley E, Coudeyre E. Educating patients about the benefits of physical activity and exercise for their hip and knee osteoarthritis. Systematic literature review. *Ann Phys Rehabil Med* 2016;59(3):174-83. doi: 10.1016/j.rehab.2016.02.005
6. McAlindon TE, Bannuru RR, Sullivan MC, Arden NK, Berenbaum F, Bierma-Zeinstra SM, *et al.* OARSI guidelines for the non-surgical management of knee osteoarthritis. *Osteoarthritis Cartilage* 2014;22(3):363-88. doi: 10.1016/j.joca.2014.01.003
7. Visser AW, de Mutsert R, le Cessie S, den Heijer M, Rosendaal FR, Kloppenburg M, *et al.* The relative contribution of mechanical stress and systemic processes in different types of osteoarthritis: the NEO study. *Ann Rheum Dis* 2015;74(10):1842-7. doi: 10.1136/annrheumdis-2013-205012
8. Sowers M, Karvonen-Gutierrez CA, Palmieri-Smith R, Jacobson JA, Jiang Y, Ashton-Miller JA. Knee osteoarthritis in obese women with cardiometabolic clustering. *Arthritis Rheum* 2009;61(10):1328-36. doi: 10.1002/art.24739
9. Silberberg M, Silberberg R. Degenerative joint disease in mice fed a high-fat diet at various ages. *Exp Med Surg* 1952;10(1):76-87.
10. Griffin TM, Guilak F. Why is obesity associated with osteoarthritis? Insights from mouse models of obesity. *Biorheology* 2008;45(3-4):387-98.
11. Wang CY, Liao JK. A mouse model of diet-induced obesity and insulin resistance. *Methods Mol Biol* 2012;821:421-33. doi: 10.1007/978-1-61779-430-8_27
12. de Visser HM, Mastbergen SC, Kozijn AE, Coeleveld K, Pouran B, van Rijen MH, *et al.* Metabolic dysregulation accelerates injury-induced joint degeneration, driven by local inflammation; an in vivo rat study. *J Orthop Res* 2017 doi: 10.1002/jor.23712
13. Griffin TM, Huebner JL, Kraus VB, Yan Z, Guilak F. Induction of osteoarthritis and metabolic inflammation by a very high-fat diet in mice: effects of short-term exercise. *Arthritis Rheum* 2012;64(2):443-53. doi: 10.1002/art.33332

14. Mankin HJ. Biochemical and metabolic aspects of osteoarthritis. *Orthop Clin North Am* 1971;2(1):19-31.
15. Glasson SS, Chambers MG, Van Den Berg WB, Little CB. The OARSI histopathology initiative - recommendations for histological assessments of osteoarthritis in the mouse. *Osteoarthritis Cartilage* 2010;18 Suppl 3:S17-23. doi: 10.1016/j.joca.2010.05.025
16. Gierman LM, van der Ham F, Koudijs A, Wielinga PY, Kleemann R, Kooistra T, *et al.* Metabolic stress-induced inflammation plays a major role in the development of osteoarthritis in mice. *Arthritis Rheum* 2012;64(4):1172-81. doi: 10.1002/art.33443
17. van der Heijden RA, Sheedfar F, Morrison MC, Hommelberg PP, Kor D, Kloosterhuis NJ, *et al.* High-fat diet induced obesity primes inflammation in adipose tissue prior to liver in C57BL/6j mice. *Aging (Albany NY)* 2015;7(4):256-68. doi: 10.18632/aging.100738
18. Hamada D, Maynard R, Schott E, Drinkwater CJ, Ketz JP, Kates SL, *et al.* Suppressive Effects of Insulin on Tumor Necrosis Factor-Dependent Early Osteoarthritic Changes Associated With Obesity and Type 2 Diabetes Mellitus. *Arthritis Rheumatol* 2016;68(6):1392-402. doi: 10.1002/art.39561
19. Iwata M, Ochi H, Hara Y, Tagawa M, Koga D, Okawa A, *et al.* Initial responses of articular tissues in a murine high-fat diet-induced osteoarthritis model: pivotal role of the IPFP as a cytokine fountain. *PLoS One* 2013;8(4):e60706. doi: 10.1371/journal.pone.0060706
20. Sokolove J, Lepus CM. Role of inflammation in the pathogenesis of osteoarthritis: latest findings and interpretations. *Ther Adv Musculoskelet Dis* 2013;5(2):77-94. doi: 10.1177/1759720X12467868
21. Kuhnast S, van der Tuin SJ, van der Hoorn JW, van Klinken JB, Simic B, Pieterman E, *et al.* Anacetrapib reduces progression of atherosclerosis, mainly by reducing non-HDL-cholesterol, improves lesion stability and adds to the beneficial effects of atorvastatin. *Eur Heart J* 2015;36(1):39-48. doi: 10.1093/eurheartj/ehu319
22. Zadelaar S, Kleemann R, Verschuren L, de Vries-Van der Weij J, van der Hoorn J, Princen HM, *et al.* Mouse models for atherosclerosis and pharmaceutical modifiers. *Arterioscler Thromb Vasc Biol* 2007;27(8):1706-21. doi: 10.1161/ATVBAHA.107.142570
23. Berenbaum F, Griffin TM, Liu-Bryan R. Review: Metabolic Regulation of Inflammation in Osteoarthritis. *Arthritis Rheumatol* 2017;69(1):9-21. doi: 10.1002/art.39842
24. van der Kraan PM. Factors that influence outcome in experimental osteoarthritis. *Osteoarthritis Cartilage* 2017;25(3):369-75. doi: 10.1016/j.joca.2016.09.005
25. Vincent T, Malfait AM. Time to be positive about negative data? *Osteoarthritis Cartilage* 2017;25(3):351-53. doi: 10.1016/j.joca.2017.01.016
26. Ioannidis JP. Why most published research findings are false. *PLoS Med* 2005;2(8):e124. doi: 10.1371/journal.pmed.0020124
27. Aibibula Z, Ailixiding M, Iwata M, Piao J, Hara Y, Okawa A, *et al.* Xanthine oxidoreductase activation is implicated in the onset of metabolic arthritis. *Biochem Biophys Res Commun* 2016;472(1):26-32. doi: 10.1016/j.bbrc.2016.02.039
28. Kc R, Li X, Forsyth CB, Voigt RM, Summa KC, Vitaterna MH, *et al.* Osteoarthritis-like pathologic changes

in the knee joint induced by environmental disruption of circadian rhythms is potentiated by a high-fat diet. *Sci Rep* 2015;5:16896. doi: 10.1038/srep16896
29. Miao H, Chen L, Hao L, Zhang X, Chen Y, Ruan Z, *et al.* Stearic acid induces proinflammatory cytokine production partly through activation of lactate-HIF1alpha pathway in chondrocytes. *Sci Rep* 2015;5:13092. doi: 10.1038/srep13092
30. Hu FB, Manson JE, Willett WC. Types of dietary fat and risk of coronary heart disease: a critical review. *J Am Coll Nutr* 2001;20(1):5-19.
31. Buettner R, Schölmerich J, Bollheimer LC. High-fat Diets: Modeling the Metabolic Disorders of Human Obesity in Rodents. *Obesity* 2007;15(4):798-808. doi: 10.1038/oby.2007.608
32. Rhodes B, Furnrohr BG, Vyse TJ. C-reactive protein in rheumatology: biology and genetics. *Nat Rev Rheumatol* 2011;7(5):282-9. doi: 10.1038/nrrheum.2011.37
33. Trion A, de Maat MP, Jukema JW, van der Laarse A, Maas MC, Offerman EH, *et al.* No effect of C-reactive protein on early atherosclerosis development in apolipoprotein E*3-leiden/human C-reactive protein transgenic mice. *Arterioscler Thromb Vasc Biol* 2005;25(8):1635-40. doi: 10.1161/01.ATV.0000171992.36710.1e
34. Saberi Hosnijeh F, Siebuhr AS, Uitterlinden AG, Oei EH, Hofman A, Karsdal MA, *et al.* Association between biomarkers of tissue inflammation and progression of osteoarthritis: evidence from the Rotterdam study cohort. *Arthritis Res Ther* 2016;18:81. doi: 10.1186/s13075-016-0976-3
35. Spector TD, Hart DJ, Nandra D, Doyle DV, Mackillop N, Gallimore JR, *et al.* Low-level increases in serum C-reactive protein are present in early osteoarthritis of the knee and predict progressive disease. *Arthritis Rheum* 1997;40(4):723-7. doi:10.1002/1529-0131(199704)40:4<723::AID-ART18>3.0.CO;2-L
36. Pearle AD, Scanzello CR, George S, Mandl LA, DiCarlo EF, Peterson M, *et al.* Elevated high-sensitivity C-reactive protein levels are associated with local inflammatory findings in patients with osteoarthritis. *Osteoarthritis Cartilage* 2007;15(5):516-23. doi: 10.1016/j.joca.2006.10.010
37. Kerkhof HJ, Bierma-Zeinstra SM, Castano-Betancourt MC, de Maat MP, Hofman A, Pols HA, *et al.* Serum C reactive protein levels and genetic variation in the CRP gene are not associated with the prevalence, incidence or progression of osteoarthritis independent of body mass index. *Ann Rheum Dis* 2010;69(11):1976-82. doi: 10.1136/ard.2009.125260
38. Jin X, Beguerie JR, Zhang W, Blizzard L, Otahal P, Jones G, *et al.* Circulating C reactive protein in osteoarthritis: a systematic review and meta-analysis. *Ann Rheum Dis* 2015;74(4):703-10. doi: 10.1136/annrheumdis-2013-204494
39. van den Hoek AM, van der Hoorn JW, Maas AC, van den Hoogen RM, van Nieuwkoop A, Droog S, *et al.* APOE*3Leiden.CETP transgenic mice as model for pharmaceutical treatment of the metabolic syndrome. *Diabetes Obes Metab* 2014;16(6):537-44. doi: 10.1111/dom.12252
40. Jong MC, Dahlmans VE, van Gorp PJ, Breuer ML, Mol MJ, van der Zee A, *et al.* Both lipolysis and hepatic uptake of VLDL are impaired in transgenic mice coexpressing human apolipoprotein E*3Leiden and human apolipoprotein C1. *Arterioscler Thromb Vasc Biol* 1996;16(8):934-40.
41. Westerterp M, Berbee JF, Pires NM,

van Mierlo GJ, Kleemann R, Romijn JA, *et al.* Apolipoprotein C-I is crucially involved in lipopolysaccharide-induced atherosclerosis development in apolipoprotein E-knockout mice. *Circulation* 2007;116(19):2173-81. doi: 10.1161/CIRCULATIONAHA.107.693382
42. Ligthart S, de Vries PS, Uitterlinden AG, Hofman A, group CIw, Franco OH, *et al.* Pleiotropy among common genetic loci identified for cardiometabolic disorders and C-reactive protein. *PLoS One* 2015;10(3):e0118859. doi: 10.1371/journal.pone.0118859
43. Schippers EF, Berbee JF, van Disseldorp IM, Versteegh MI, Havekes LM, Rensen PC, *et al.* Preoperative apolipoprotein CI levels correlate positively with the proinflammatory response in patients experiencing endotoxemia following elective cardiac surgery. *Intensive Care Med* 2008;34(8):1492-7. doi: 10.1007/s00134-008-1077-9
44. Olsson B, Gigante B, Mehlig K, Bergsten A, Leander K, de Faire U, *et al.* Apolipoprotein C-I genotype and serum levels of triglycerides, C-reactive protein and coronary heart disease. *Metabolism* 2010;59(12):1736-41. doi: 10.1016/j.metabol.2010.04.017
45. Huang ZH, Reardon CA, Getz GS, Maeda N, Mazzone T. Selective suppression of adipose tissue apoE expression impacts systemic metabolic phenotype and adipose tissue inflammation. *J Lipid Res* 2015;56(2):215-26. doi: 10.1194/jlr.M050567
46. Zhang H, Wu LM, Wu J. Cross-talk between apolipoprotein E and cytokines. *Mediators Inflamm* 2011;2011:949072. doi: 10.1155/2011/949072
47. Ma HL, Blanchet TJ, Peluso D, Hopkins B, Morris EA, Glasson SS. Osteoarthritis severity is sex dependent in a surgical mouse model. *Osteoarthritis Cartilage* 2007;15(6):695-700. doi: 10.1016/j.joca.2006.11.005
48. Oliveria SA, Felson DT, Reed JI, Cirillo PA, Walker AM. Incidence of symptomatic hand, hip, and knee osteoarthritis among patients in a health maintenance organization. *Arthritis Rheum* 1995;38(8):1134-41.
49. Srikanth VK, Fryer JL, Zhai G, Winzenberg TM, Hosmer D, Jones G. A meta-analysis of sex differences prevalence, incidence and severity of osteoarthritis. *Osteoarthritis Cartilage* 2005;13(9):769-81. doi: 10.1016/j.joca.2005.04.014
50. Brown CM, Xu Q, Okhubo N, Vitek MP, Colton CA. Androgen-mediated immune function is altered by the apolipoprotein E gene. *Endocrinology* 2007;148(7):3383-90. doi: 10.1210/en.2006-1200
51. de Munter W, van den Bosch MH, Sloetjes AW, Croce KJ, Vogl T, Roth J, *et al.* High LDL levels lead to increased synovial inflammation and accelerated ectopic bone formation during experimental osteoarthritis. *Osteoarthritis Cartilage* 2016;24(5):844-55. doi: 10.1016/j.joca.2015.11.016
52. van Vlijmen BJ, van 't Hof HB, Mol MJ, van der Boom H, van der Zee A, Frants RR, *et al.* Modulation of very low density lipoprotein production and clearance contributes to age- and gender- dependent hyperlipoproteinemia in apolipoprotein E3-Leiden transgenic mice. *J Clin Invest* 1996;97(5):1184-92. doi: 10.1172/JCI118532
53. Gkretsi V, Simopoulou T, Tsezou A. Lipid metabolism and osteoarthritis: lessons from atherosclerosis. *Prog Lipid Res* 2011;50(2):133-40. doi: 10.1016/j.plipres.2010.11.001
54. Gierman LM, Kuhnast S, Koudijs A, Pieterman EJ, Kloppenburg M, van

Osch GJ, *et al.* Osteoarthritis development is induced by increased dietary cholesterol and can be inhibited by atorvastatin in APOE*3Leiden. CETP mice--a translational model for atherosclerosis. *Ann Rheum Dis* 2014;73(5):921-7. doi: 10.1136/annrheumdis-2013-203248

55. de Munter W, van der Kraan PM, van den Berg WB, van Lent PL. High systemic levels of low-density lipoprotein cholesterol: fuel to the flames in inflammatory osteoarthritis? *Rheumatology (Oxford)* 2016;55(1):16-24. doi: 10.1093/rheumatology/kev270
56. van der Meij E, Koning GG, Vriens PW, Peeters MF, Meijer CA, Kortekaas KE, *et al.* A clinical evaluation of statin pleiotropy: statins selectively and dose-dependently reduce vascular inflammation. *PLoS One* 2013;8(1):e53882. doi: 10.1371/journal.pone.0053882
57. Kadam UT, Blagojevic M, Belcher J. Statin use and clinical osteoarthritis in the general population: a longitudinal study. *J Gen Intern Med* 2013;28(7):943-9. doi: 10.1007/s11606-013-2382-8
58. Courties A, Sellam J, Berenbaum F. Metabolic syndrome-associated osteoarthritis. *Curr Opin Rheumatol* 2017 doi: 10.1097/BOR.0000000000000373
59. Mulder P, Morrison MC, Wielinga PY, van Duyvenvoorde W, Kooistra T, Kleemann R. Surgical removal of inflamed epididymal white adipose tissue attenuates the development of non-alcoholic steatohepatitis in obesity. *Int J Obes (Lond)* 2016;40(4):675-84. doi: 10.1038/ijo.2015.226

Supplemental Material and methods

General study characteristics

Twelve experiments were performed in which a high-caloric diet was used to induce obesity and metabolic dysfunction in mice. The experiments were designed to study various aspects of the metabolic syndrome (MetS) and therefore varied in experimental design. All experiments were approved by the institutional Animal Care and Use Committee of TNO and were in compliance with European Community specifications regarding the use of laboratory animals.

Mice

The experiments were carried out in wild-type C57BL/6J mice and genetically modified mice (hCRP, LDLr$^{-/-}$.Leiden and ApoE*3Leiden.CETP mice) based on C57BL/6J background. Depending on the study male mice or both genders were used (Table 2). Age at the start of the study varied between studies from 8 to 16 weeks (Table 2). Control mice were always of same sex and age as the treatment groups. Wild-type C57BL/6J mice were purchased from Charles River Laboratories (L'Arbresle Cedex, France) and received a 2-week acclimatization period after transfer to the animal facility. Inbred human C-reactive protein (hCRP) transgenic mice, low density lipoprotein receptor-deficient (LDLr$^{-/-}$.Leiden) mice and ApoE*3Leiden.CETP mice were obtained from the in-house breeding colony (TNO Metabolic Health Research, Leiden, The Netherlands). Human CRP transgenic mice specifically express hCRP in the liver. Human CRP is an acute-phase protein, used mainly as a general inflammation marker, and is upregulated in hCRP transgenic mice upon diet-induced metabolic overload[1].

The LDLr$^{-/-}$.Leiden strain is a translational model for obesity-associated diseases[2] and shows impaired clearance of lipoproteins due to the lack of LDL receptors, which results in marked hypercholesterolemia. In addition, Western-type and high-fat diets cause insulin resistance in LDLr$^{-/-}$ mice[3].

Heterozygous ApoE*3Leiden.CETP mice were obtained in our animal facility by crossbreeding heterozygous ApoE*3Leiden mice, characterized by an enzyme-linked immunosorbent assay (ELISA) for human ApoE, with homozygous human cholesteryl ester transfer protein (CETP) transgenic mice. By combining an impaired lipoprotein clearance (ApoE*3Leiden) with a shift in cholesterol distribution from HDL to (V)LDL particles (CETP) a more translational model for lipoprotein metabolism is obtained[4 5]. ApoE*3Leiden.CETP double transgenic mice are prone to develop obesity, insulin resistance and dyslipidemia on high-fat and high-cholesterol diets and demonstrate human-like responses to different anti-diabetic and hypolipidemic drugs[6].

Animals were monitored at least once a day and humane endpoints were established and applied in case of severe pain or suffering. These were behavioral or pathophysiological endpoints, amongst others: inertia, ruffled haircoat, hunched posture, weight loss of

20% or more in two consecutive days, severe fighting injuries, apparent pain7 or stress signs like excessive grooming.

Housing

Studies 4, 10, 11 and 12 were performed in a non-specific pathogen-free (SPF) animal facility, while Studies 1-3 and 5-9 were executed in an AAALAC-accredited SPF animal facility (Table 1). The commissioning of the SPF animal facility was effectuated in 2012. For the relocation to the SPF animal facility, all inbred strains underwent rederivation by embryo transfer until an SPF microbiological status was reached according to FELASA2012 guidelines for health monitoring[8].

Mice were housed in open polycarbonate cages (Type II in non-SPF and Type II L in SPF animal facility) with 3-4 animals/cage. The bedding material differed between the animal facilities, with Lignocel® S9 sawdust used in the non-SPF and Lignocel® BK8-15 sawdust used in the SPF animal facility. In both facilities mice were maintained under standard conditions with a 12 h light-dark cycle beginning at 07:00 UTC+1. Mice received acidified water (pH 2.8, non-SPF animal facility) or autoclaved water (SPF facility) and food ad libitum. Cages were set up in temperature-controlled (non-SPF: 22 ± 2.0°C, SPF: 21 ± 0.5°C) and humidity-controlled (non-SPF: 40-70%, SPF: 45 ± 2%) rooms, with 8 (non-SPF) or 15 (SPF) air changes/hour under filtered positive pressure ventilation. To reduce distress from unexpected noises, radio featuring alternating music and talk was played continuously.

Microbiological status of both animal facilities was monitored using sentinel mice and random sampling of the breeding colonies. In every conventional animal room in which animals were housed, two sentinels of same species and sex were housed for a minimum of 8 weeks. Quarterly health screens of sentinels as well as random mice from the breeding stock were conducted by a certified company, according to FELASA guidelines. Furthermore, periodical surface screens were performed to evaluate cleaning procedures and detect possible sources of contamination. By default, the health status of mice purchased from commercial animal breeders was inspected upon entry.

Diets

Body weight and food intake were monitored throughout each study. Experiments were carried out in male mice or mice of both genders. ApoE*3Leiden.CETP transgenic mice first received a run-in period of minimally 4 weeks on study diet, after which mice were randomized into groups for fasted plasma cholesterol (CHOD-PAP 11491458, Roche Diagnostics, Woerden, the Netherlands), fasted plasma triglycerides (GPO-PAP 11488872, Roche Diagnostics) and body weight. Mice of other strains were matched into study groups based on body weight. Mice were fed either control or high-caloric diets, as displayed in Table 1. The applied chow diet was grain based, supplemented with sugar

beet and soybean meal as additional sources for fiber, protein and fat, respectively. Note that the fat content of the purified Western-type diet (WTD) is derived from vegetable sources, while the synthetic diets are predominantly lard-based. Duration and exposure to study diet varied among studies from 0 to 38 weeks (Table 2). A few of the studies had not incorporated a chow or low-fat diet (LFD, 10 kcal% energy from fat) control group (Table 2, Study 6, 7, 9 and 10). In studies 9 and 10, mice received 10% w/v fructose in the drinking water on top of the dietary intervention to increase VLDL production. Mice remained on their respective diets until the completion of the study.

Evaluated studies

The experiments described in this manuscript differ in research question and design (Table 2). Nevertheless, since MetS-related diseases develop in a similar setting, all studies share a common approach: high-caloric dietary intervention. Four different strains of mice were used to model for the various metabolic comorbidities (see "Mice"). Next to strain, also the duration and type of diet differed between studies. OA development was assessed at the final endpoint of each study, unless stated otherwise. At the endpoint of each study mice were euthanised using gradual-fill CO_2 asphyxiation. Previously published data were included to provide a context for comparison and are indicated by a double dagger (‡) next to the referencing in the tables (Study 4 and 12).

Study 1 was a time-course study in male C57BL/6J mice designed to study the early metabolic events leading to high-fat diet (HFD, 45 kcal% energy from fat)-induced type 2 diabetes up to 24 weeks. To correct for the effect of aging, chow-fed control groups were included. OA severity was monitored at each time point. In Study 2, comparable to Study 1 in strain, gender, diet and duration, HFD-induced non-alcoholic fatty liver disease (NAFLD) was examined with the specific aim to investigate the effect of surgical removal of inflamed adipose tissue on the progression of NAFLD9.

Study 3 was designed to examine the onset and progression of metabolic inflammation in the liver and adipose tissues during diet-induced obesity10. After a 6-week run-in period on LFD, male C57BL/6J mice were either continued on the LFD or switched to a HFD regimen for 52 weeks.

In Study 4 the hCRP mouse strain was employed to study the effects of HFD-induced metabolic syndrome on inflammation. hCRP transgenic mice of both genders received either chow supplemented with 1% cholesterol or a HFD for 38 weeks. Significant OA development in the knees of these mice was the first indication in our hands that metabolic stress-induced inflammation plays a role in disease pathogenesis11.

Studies 5 and 7 are linked in the effort to develop a translational mouse model for diabetic nephropathy. Study 5 aimed to define the best in vivo model currently available and Study 7 aimed to aggravate disease development. In Study 5, the effect of dietary fat content on the induction of diabetic nephropathy was examined in male LDLr−/−.

Leiden mice over a period of 20 weeks. In Study 7, disease development in male LDLr$^{-/-}$. Leiden mice was monitored for a longer period (31 weeks) to determine the increase in disease severity. Furthermore, the HFD was supplemented with fructose or cholesterol to aggravate the progression of diabetic nephropathy. These aims required no low-fat diet control group, as the intervention groups were compared to a HFD control group.
In Study 6, the effects of refined and unrefined vegetable oils were studied in the context of HFD-induced type 2 diabetes in male LDLr$^{-/-}$.Leiden mice, as unrefined oils were found to greatly reduce cardiovascular risk factors in comparison with their refined form. As these dietary interventions were compared to the original HFD, this study included no low-fat diet control group.
Study 8, a time-course study, was designed for the early detection of diet-induced diabetes type II and its comorbidities, like non-alcoholic steatohepatitis (NASH), atherosclerosis and diabetic retinopathy. To this end, male LDLr$^{-/-}$.Leiden mice were fed a chow or HFD diet up to 30 weeks.
In Study 9 and 10 male ApoE*3Leiden.CETP mice were given a VHFD for 26 or 32 weeks, supplemented with 10% (w/v) fructose in the drinking water for the final 16 or 24 weeks, respectively. Both studies compared a HFD control group to HFD-fed groups which received various pharmaceutical interventions. No low-fat diet control group was included in either study.
Studies 11 and 12 are the only listed experiments that were originally designed to study OA development, although in Study 12 atherosclerosis was concurrently studied. Study 11 was designed to examine the effects of VHFD-induced changes in lipid metabolism on OA development. Next to a VHFD-fed group and a chow control a 'metabolic rescue' group was included, in which mice were started on a VHFD and switched to chow after 20 weeks. A fourth group consisted of mice showing inexplicably low metabolic adaptation to the VHFD (low body weight, low fasted cholesterol and triglycerides levels), hereafter called 'low-MetS' mice. It is known from previous experiments that these mice do not develop diet-induced atherosclerosis, but the effect thereof was not yet known for OA development. Study 12 compared metabolic OA progression in ApoE*3Leiden.CETP mice of either gender over the course of 38 weeks11. It was the only evaluated study using a WTD, which is lower in fat but higher in carbohydrate content compared to a HFD (Table 1). Diet intervention groups received a WTD supplemented with a sex-specific high or low percentage of cholesterol, while control mice received chow.

Metabolic parameters

We define metabolic dysfunction here as a significant increase in either body weight and/or fasting cholesterol, glucose and/or insulin plasma levels compared with normal values as observed in chow- or LFD-fed controls.

EDTA plasma samples were collected after a 4-5 hour fasting period by tail vein incision at various time points throughout each study. Blood glucose was measured either immediately per time point using a hand-held glucose analyser (FreeStyle Disectronic, Vianen, The Netherlands) or all time points at once by the hexokinase method using commercial reagents (No. 2319 and 2942, Instruchemie, Delfzijl, The Netherlands; No. G6918, Sigma-Aldrich, Zwijndrecht, The Netherlands). Total cholesterol (No. 11491458216, Roche Diagnostics Nederland BV, Woerden, The Netherlands) and total triglycerides (No-11488872, Roche Diagnostics) were determined with enzymatic assays directly upon plasma collection according to manufacturer's instructions. Insulin levels were determined using an ELISA for mouse insulin (Cat.no. 10-1113-01, Mercodia, Uppsala, Sweden). Data are shown in heat maps (Figures 1 and 2).

Histology

Specimens used were knee joint sections cut, stained and scored specifically for this research, combined with archival sections from published (Study 4 and 12) and unpublished (Study 9) data to add to the general context. Knee joints of the hind limbs were harvested, fixed in a 10% formalin neutral buffered solution (Sigma-Aldrich, USA) for a minimal of 24 hours, decalcified in Kristensen's solution, dehydrated and embedded in paraffin. Before the decalcification step, knee joints were randomized and blinded. Serial coronal 5 µm sections were collected throughout the joint and stained with Weigert's Hematoxylin, Fast Green and Safranin-O, according to OARSI recommendations[12].

We employed the OA scoring system specifically designed for the mouse as described by the OARSI histopathology initiative[12]. Therefore, cartilage degeneration was rescored in studies 4 and 9 according to the OARSI 2010 recommendations. Two to three sections (dependent on the quality of the sections) were scored per animal, of which the average score represents the final score per animal. Specific sections for grading were selected from the central weight-bearing region of the tibial plateau, which was determined using the presence of the anterior cruciate ligament, femoral growth rings and anatomy of the menisci as anatomical landmarks.. All sections from all studies were scored by the same independent investigators (AEK and FvdH), who were blinded for group assignment, specifically for the current research. The joint was scored at 6 locations: femoral condyles and tibial plateaus at the lateral and medial sides, trochlear groove and the patella (score 0-6 per location). Due to incomplete patellar scores for all mice, we report the averaged sum of the medial and lateral scores as the total tibiofemoral cartilage degeneration score (Table 3, maximum total score 24).

The OARSI 2010 scoring system is an universal scoring system to grade OA severity, focusing primarily on the condition of the articular cartilage. Therefore, as additional features of OA, osteophyte formation and synovial inflammation were scored separately

to examine the impact of obesity and metabolic dysfunction on different aspects of OA pathology. In line with the OARSI 2010 recommendations, osteophyte formation and synovial inflammation were scored using a 0-3 scoring paradigm where 0 is normal, 1 = mild, 2 = moderate and 3 = severe changes. These changes were separately evaluated for the lateral femur, medial femur, lateral tibia and medial tibia by one independent blinded grader (AEK). Reported total scores represent the summed scores for the tibiofemoral part of the knee joint (maximum total score 12).

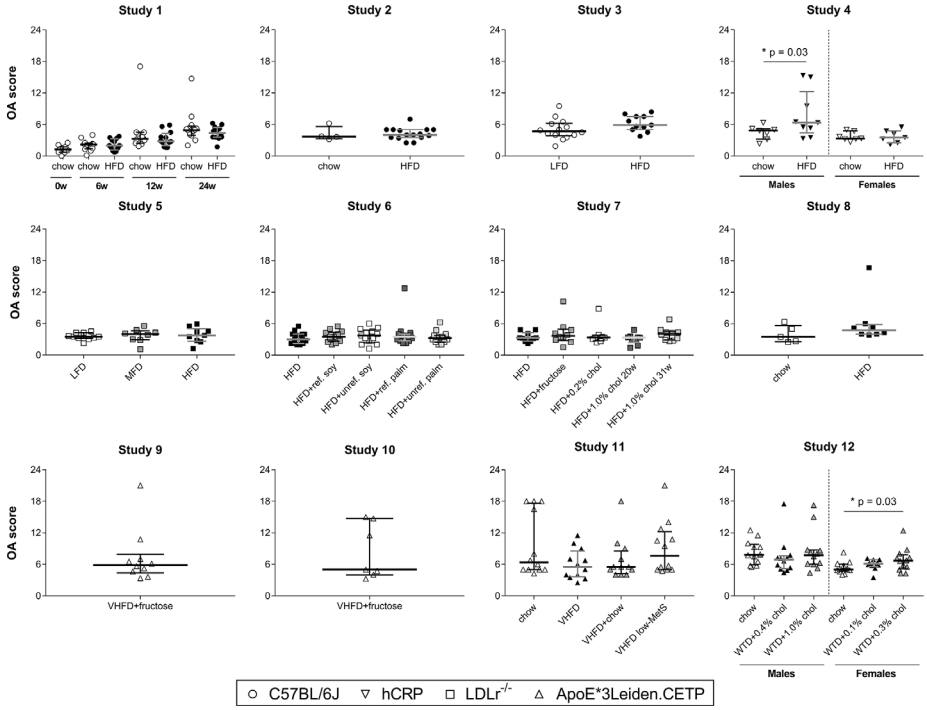


Figure S1. Overview of OA severity scores for each study group, arranged per study. Total OA severity scores presented per study in separate scatterplots showing the individual summed score for the tibiofemoral knee compartments for each animal per study group (max. 24, OARSI histopathology recommendations for the mouse12). Group medians (indicated by bars) and interquartile ranges are also shown. * indicates statistical significance relative to control at the same time point ($p<0.05$).

LFD, low-fat diet (10 kcal% energy from fat); WTD, Western-type diet (16 kcal% energy from fat); MFD, mid-fat diet (30 kcal% energy from fat); HFD, high-fat diet (45 kcal% energy from fat); VHFD, very high-fat diet (60 kcal% energy from fat); w, time in weeks; ref., refined oil; unref., unrefined oil; low-MetS, mice showing inexplicably low metabolic adaptation to the VHFD.

Table S1 Overview of compartmental knee OA severity scores from twelve independent mouse studies with various approaches for diet-induced metabolic dysfunction. Osteoarthritis severity scores presented here are group medians and interquartile ranges per knee joint compartment (max. score 6 per compartment, OARSI histopathology recommendations for the mouse12). Statistical significance level was set to $p<0.05$.

Study	Weeks on study diet	Diet intervention groups[a]	Gender[b]	OA severity score							
				Medial side				Lateral side			
				Femoral condyle		Tibia plateau		Femoral condyle		Tibia plateau	
				Median	IQR	Median	IQR	Median	IQR	Median	IQR
C57BL/6J											
1	0	chow	M	0.25	[0.15 - 0.25]	0.50	[0.38 - 0.69]	0.13	[0.00 - 0.25]	0.25	[0.21 - 0.44]
	6	chow		0.63	[0.19 - 0.91]	0.75	[0.50 - 0.88]	0.38	[0.09 - 0.53]	0.38	[0.19 - 0.50]
		HFD		1.00	[0.50 - 1.50]	0.63	[0.50 - 0.81]	0.25	[0.09 - 0.50]	0.25	[0.22 - 0.56]
	12	chow		1.00	[0.88 - 2.00]	1.13	[0.94 - 1.50]	0.50	[0.25 - 0.56]	0.63	[0.31 - 0.69]
		HFD		1.00	[1.00 - 1.50]	0.88	[0.63 - 1.56]	0.38	[0.25 - 0.50]	0.63	[0.34 - 1.16]
	24	chow		2.00	[1.25 - 2.00]	1.38	[0.97 - 2.06]	0.63	[0.50 - 0.75]	0.75	[0.53 - 1.03]
		HFD		1.25	[0.96 - 2.00]	1.13	[0.73 - 1.27]	0.69	[0.50 - 0.78]	1.00	[0.81 - 1.22]
2[9]	24	chow	M	0.50	[0.50 - 0.50]	1.25	[0.88 - 1.88]	1.17	[0.88 - 1.38]	1.19	[1.01 - 1.28]
		HFD		0.50	[0.50 - 0.75]	0.83	[0.50 - 1.17]	1.42	[1.25 - 2.00]	1.25	[1.00 - 1.42]
3[10]	52	LFD	M	0.50	[0.50 - 0.50]	1.00	[0.75 - 1.50]	1.00	[1.00 - 1.50]	1.00	[0.75 - 2.00]
		HFD		0.63	[0.50 - 0.75]	1.00	[0.75 - 1.31]	1.50	[0.88 - 1.75]	2.00	[0.94 - 2.75]
hCRP											
4[†‡]	38	chow + 1.0% chol	M	1.67	[1.33 - 2.00]	1.17	[0.67 - 1.33]	0.50	[0.50 - 0.67]	0.83	[0.50 - 0.83]
		HFD		1.50	[1.33 - 2.00]	2.00	[1.67 - 2.50]	1.00	[0.75 - 2.50]	0.83	[0.75 - 2.00]
		chow + 1.0% chol	F	1.33	[1.08 - 1.83]	0.83	[0.75 - 1.17]	0.50	[0.50 - 0.67]	0.83	[0.67 - 1.00]
		HFD		1.00	[0.83 - 1.42]	0.83	[0.71 - 1.33]	0.50	[0.50 - 0.63]	0.67	[0.67 - 0.75]

LDLr$^{-/-}$.Leiden											
5	20	LFD MFD HFD	M	1.00	[0.69 - 1.19]	0.88	[0.63 - 1.25]	0.50	[0.50 - 0.59]	0.81	[0.50 - 1.53]
				1.50	[0.88 - 1.58]	0.81	[0.50 - 1.03]	1.25	[0.83 - 1.38]	0.75	[0.59 - 1.06]
				0.88	[0.81 - 1.00]	1.00	[0.72 - 1.06]	0.94	[0.59 - 1.34]	0.63	[0.63 - 1.38]
6	20	HFD HFD + ref. soybean HFD + unref. soybean HFD + ref. palm HFD + unref. palm	M	0.75	[0.50 - 0.75]	0.50	[0.50 - 0.75]	0.75	[0.50 - 1.13]	0.75	[0.50 - 0.75]
				0.50	[0.50 - 0.75]	0.50	[0.50 - 1.00]	0.75	[0.50 - 1.50]	1.00	[0.50 - 1.00]
				0.75	[0.50 - 1.25]	0.75	[0.50 - 1.00]	0.75	[0.50 - 1.00]	0.75	[0.75 - 1.50]
				0.50	[0.50 - 1.00]	0.75	[0.50 - 1.13]	0.75	[0.75 - 1.25]	1.00	[0.50 - 1.00]
				0.75	[0.50 - 1.00]	0.75	[0.50 - 1.13]	0.75	[0.50 - 1.00]	0.75	[0.50 - 1.00]
7	20	HFD HFD + fructose HFD + 0.2% chol HFD + 1.0% chol 20w	M	0.50	[0.50 - 0.92]	0.75	[0.52 - 1.00]	1.08	[0.88 - 1.33]	0.83	[0.75 - 0.98]
				0.50	[0.50 - 1.17]	0.71	[0.50 - 0.96]	1.00	[0.83 - 1.48]	0.92	[0.77 - 1.31]
				0.58	[0.50 - 0.94]	0.50	[0.42 - 0.58]	1.33	[1.13 - 1.44]	0.88	[0.73 - 1.00]
				0.58	[0.50 - 0.67]	0.75	[0.67 - 1.08]	0.92	[0.67 - 1.00]	0.75	[0.67 - 1.00]
	31	HFD + 1.0% chol 31w		0.58	[0.50 - 0.73]	0.71	[0.53 - 0.94]	1.17	[1.00 - 1.33]	0.96	[0.83 - 1.40]
8	30	chow HFD	M	0.50	[0.50 - 0.75]	0.83	[0.71 - 0.83]	1.08	[0.75 - 1.54]	1.33	[1.00 - 1.67]
				0.75	[0.63 - 1.04]	1.33	[1.00 - 1.50]	1.00	[1.00 - 1.42]	1.67	[1.25 - 1.83]
ApoE*3Leiden.CETP											
9	26	VHFD + fructose	M	0.88	[0.63 - 1.22]	0.75	[0.66 - 1.38]	2.00	[1.81 - 2.50]	2.13	[1.19 - 2.81]
10	32	VHFD + fructose	M	2.00	[1.25 - 6.00]	2.00	[1.25 - 3.63]	2.00	[0.63 - 2.00]	0.75	[0.50 - 1.25]
11	32	chow VHFD VHFD + chow VHFD, low-MetS	M	1.06	[0.50 - 5.81]	1.50	[1.13 - 6.00]	1.88	[1.50 - 2.00]	1.75	[1.75 - 2.00]
				0.88	[0.72 - 2.00]	1.50	[1.16 - 2.00]	2.00	[1.44 - 2.00]	1.63	[1.09 - 2.00]
				1.06	[0.84 - 1.63]	1.25	[1.06 - 2.13]	2.00	[1.75 - 2.00]	2.00	[1.75 - 2.81]
				2.38	[1.41 - 3.75]	3.00	[1.44 - 4.88]	1.88	[1.69 - 2.00]	1.88	[1.50 - 2.00]

12[11‡]	38	chow WTD + 0.4% chol WTD + 1.0% chol	M	2.25	[0.75 - 2.56]	2.00	[2.00 - 2.50]	2.00	[1.50 - 2.06]	2.00	[1.69 - 2.31]
				0.94	[0.72 - 1.63]	1.63	[1.47 - 2.06]	1.75	[1.46 - 2.00]	2.00	[1.69 - 2.44]
				1.69	[1.13 - 2.00]	1.88	[1.34 - 2.13]	2.00	[2.00 - 2.50]	2.00	[1.88 - 2.25]
		chow WTD + 0.1% chol WTD + 0.3% chol	F	0.69	[0.47 - 0.91]	1.19	[1.00 - 1.56]	1.75	[1.50 - 2.00]	1.75	[1.19 - 2.00]
				1.31	[0.88 - 1.50]	1.50	[1.28 - 1.75]	1.75	[1.41 - 2.00]	1.50	[1.03 - 2.00]
				1.50	[0.84 - 1.88]	1.88	[1.50 - 2.06]	1.38	[1.19 - 1.81]	1.50	[1.44 - 2.00]

‡ Previously published OA data; a chol, cholesterol and ref., refined oil; LFD, low-fat diet (10 kcal% energy from fat); WTD, Western-type diet (16 kcal% energy from fat); MFD, mid-fat diet (30 kcal% energy from fat); HFD, high-fat diet (45 kcal% energy from fat); VHFD, very high-fat diet (60 kcal% energy from fat); low-MetS, mice showing inexplicably low metabolic adaptation to the VHFD; b M, male and F, female.

Table S2

Changes in body weight and total fasting cholesterol plasma levels presented here are the actual values of the group medians and interquartile ranges, as shown in color code in Figure 2. For presentation purposes, time points were selected with high overlap between studies. Grey indicates no data available.

Strain	Study	Original design	Weeks on study diet	Diet groups	Gender	Body weight (g)													
						Time (weeks)													
						0	6	12	20	24	26	30	32	38	52				
C57BL/6J	1	Type II diabetes	0	chow	M	25.7 [25.1 - 26.1]													
			6	chow		26.1 [25.6 - 26.6]	29.8 [29.4 - 30.5]												
				HFD		25.2 [24.3 - 26.3]	34.4 [33.0 - 37.6]												
			12	chow		26.6 [26.1 - 27.7]	30.3 [28.9 - 31.7]	31.5 [30.3 - 33.3]											
				HFD		25.7 [25.3 - 27.1]	35.9 [34.4 - 38.0]	44.2 [41.6 - 47.6]											
			24	chow		27.1 [25.6 - 27.9]	30.9 [29.3 - 31.3]	31.8 [30.5 - 32.4]	33.0 [32.1 - 33.6]	33.2 [32.5 - 34.1]									
				HFD		25.5 [24.4 - 27.0]	34.8 [33.8 - 38.1]	42.9 [40.1 - 45.5]	49.4 [47.9 - 51.3]	51.9 [49.2 - 53.7]									
	2	Adipose tissue inflammation	24	chow	M	27.4 [27.0 - 27.7]	30.9 [30.6 - 31.2]	32.1 [31.5 - 34.3]	35.3 [32.3 - 35.5]	35.6 [30.9 - 35.8]									
				HFD		27.1 [26.3 - 27.5]	35.9 [34.2 - 39.6]	40.6 [38.1 - 45.1]	46.2 [42.3 - 50.0]	48.0 [45.1 - 51.5]									
	3	Aging	52	LFD	M	23.8 [23.1 - 24.6]	28.0 [27.5 - 29.0]	31.7 [28.7 - 31.7]	33.1 [29.8 - 34.2]	34.7 [32.8 - 35.9]									
				HFD		23.8 [23.4 - 24.6]	32.0 [31.0 - 32.4]	38.6 [35.6 - 39.9]	44.8 [41.1 - 47.2]	48.7 [45.9 - 50.2]									
hCRP	4	Metabolic syndrome	38	chow + 1% chol	M	28.9 [28.1 - 30.6]		32.0 [31.5 - 33.6]	31.0 [30.7 - 32.8]	31.7 [30.5 - 32.0]		31.8 [31.1 - 31.9]	31.8 [31.2 - 33.0]	31.4 [30.9 - 33.2]					
				HFD		28.4 [27.5 - 29.7]		34.3 [33.6 - 36.2]	38.3 [35.2 - 39.9]	40.6 [37.6 - 43.7]		41.7 [37.2 - 43.5]	39.6 [37.8 - 43.5]	39.8 [37.9 - 44.4]					
				chow + 1% chol	F	21.6 [21.4 - 23.5]		24.2 [23.3 - 25.3]	24.6 [23.4 - 25.5]	24.4 [23.9 - 26.0]		24.7 [23.8 - 25.9]	24.8 [24.0 - 25.6]	24.3 [24.0 - 26.9]					
				HFD		22.5 [22.0 - 22.7]		24.4 [24.1 - 25.2]	27.6 [26.2 - 35.9]	28.3 [27.7 - 37.9]		30.1 [28.1 - 35.5]	29.9 [27.8 - 35.1]	30.2 [30.2 - 31.6]					
LDLr$^{-/-}$.Leiden	5	Diabetic nephropathy	20	LFD	M	32.6 [30.2 - 35.8]	34.2 [29.0 - 37.4]	35.5 [30.8 - 39.9]	37.9 [35.4 - 42.6]										
				MFD		31.7 [29.6 - 36.7]	39.3 [36.5 - 44.4]	45.1 [42.5 - 49.5]	48.9 [46.9 - 53.2]										
				HFD		31.8 [29.9 - 35.6]	41.2 [39.1 - 44.3]	47.4 [43.0 - 50.4]	51.7 [49.4 - 55.7]										
	6	Type II diabetes	20	HFD	M	29.0 [25.1 - 33.6]	40.3 [34.0 - 43.8]	48.3 [42.4 - 50.2]	52.6 [49.7 - 55.7]										
				HFD + ref. soybean oil		27.9 [24.6 - 30.7]	41.4 [32.9 - 42.8]	45.4 [40.9 - 48.2]	50.7 [46.8 - 52.8]										
				HFD + unref. soybean oil		28.5 [27.5 - 30.1]	41.6 [38.9 - 43.5]	48.4 [45.8 - 49.8]	51.9 [49.8 - 53.3]										
				HFD + ref. palm oil		29.7 [27.2 - 31.9]	40.0 [39.1 - 43.9]	47.5 [46.1 - 50.3]	52.8 [50.9 - 56.7]										
				HFD + unref. palm oil		30.6 [27.4 - 31.8]	41.2 [39.3 - 45.6]	48.7 [45.6 - 50.7]	53.0 [49.6 - 54.6]										
	7	Diabetic nephropathy	20	HFD	M	26.4 [25.6 - 27.0]	37.3 [36.9 - 37.8]	47.4 [46.6 - 48.3]	52.3 [52.1 - 53.1]										
				HFD + fructose		26.6 [24.2 - 28.3]	39.9 [34.6 - 43.0]	46.1 [43.2 - 50.7]	50.3 [48.6 - 54.1]										
				HFD + 0.2% chol		27.0 [24.0 - 28.3]	40.2 [34.7 - 41.1]	48.1 [45.3 - 49.9]	50.5 [50.1 - 52.8]										
				HFD + 1.0% chol 20w		25.7 [24.1 - 28.3]	38.5 [34.4 - 42.3]	45.3 [43.6 - 50.5]	49.6 [47.4 - 53.2]										
			31	HFD + 1.0% chol 31w		26.9 [25.0 - 28.2]	38.7 [34.2 - 38.9]	44.3 [42.8 - 46.6]	49.1 [48.2 - 51.2]	50.2 [49.5 - 53.8]	51.8 [50.7 - 54.9]	52.9 [50.9 - 56.5]							
	8	Metabolic syndrome	30	chow	M	27.4 [26.4 - 28.8]	32.8 [29.2 - 34.2]	34.8 [31.6 - 36.3]		39.2 [35.5 - 45.2]		42.9 [38.5 - 47.7]							
				HFD		28.2 [26.9 - 29.8]	41.0 [39.5 - 42.4]	47.3 [45.5 - 49.7]		51.6 [49.6 - 56.0]		53.4 [51.0 - 58.0]							
	9	Metabolic syndrome	26	VHFD + fructose	M	28.2 [26.7 - 29.3]		47.9 [46.0 - 49.4]	48.3 [46.0 - 49.6]	51.2 [48.7 - 53.0]	51.4 [48.3 - 52.4]								
	10	Insulin resistance and dyslipidemia	32	VHFD + fructose	M	27.5 [26.2 - 28.6]			45.7 [45.2 - 48.5]		52.5 [50.6 - 56.5]	54.1 [52.0 - 55.7]							
ApoE3L.hCETP	11	Osteoarthritis	32	chow	M	28.0 [27.2 - 30.1]		31.9 [30.5 - 33.0]	32.4 [31.4 - 34.3]	33.3 [31.3 - 34.0]			32.8 [30.6 - 34.4]						
				VHFD		27.7 [26.2 - 29.3]		44.2 [42.4 - 50.5]	51.4 [50.4 - 54.4]	52.9 [50.1 - 55.4]			56.0 [52.4 - 58.4]						
				VHFD + chow		29.0 [26.4 - 29.9]		44.3 [42.1 - 47.6]	51.9 [49.8 - 54.5]	44.0 [42.6 - 47.5]			34.8 [34.0 - 37.0]						
				VHFD, low-MetS		27.8 [27.0 - 29.6]		33.2 [31.9 - 34.4]	37.0 [35.7 - 38.5]	38.6 [36.3 - 41.2]			39.7 [36.1 - 45.0]						
	12	Atherosclerosis and OA	38	chow	M	30.1 [29.3 - 30.4]	31.3 [31.1 - 32.1]	31.9 [31.6 - 33.1]	33.8 [32.4 - 35.0]	33.4 [32.0 - 35.0]	34.7 [32.9 - 37.0]	35.0 [33.1 - 37.6]	34.1 [32.5 - 36.2]	35.5 [33.4 - 37.6]					
				WTD + 0.4% chol		28.5 [28.1 - 29.7]	30.5 [30.1 - 32.3]	31.9 [31.2 - 34.1]	34.9 [32.8 - 36.2]	35.6 [33.2 - 36.4]	36.7 [34.9 - 37.8]	37.2 [34.4 - 38.7]	36.5 [33.4 - 38.3]	36.1 [34.9 - 39.3]					
				WTD + 1.0% chol		29.9 [28.3 - 30.4]	31.6 [30.3 - 32.6]	33.3 [30.7 - 33.7]	34.1 [32.9 - 36.4]	34.1 [32.2 - 35.7]	35.3 [33.6 - 37.3]	34.3 [33.4 - 36.6]	33.5 [33.1 - 35.6]	35.2 [33.5 - 36.6]					
				chow	F	21.8 [20.9 - 23.6]	22.9 [21.6 - 24.1]	23.3 [22.6 - 24.8]	24.0 [23.4 - 27.3]	24.2 [23.4 - 26.5]	25.0 [23.1 - 27.8]	25.0 [23.4 - 28.8]	24.9 [24.2 - 27.4]	25.7 [23.7 - 28.7]					
				WTD + 0.1% chol		22.4 [20.8 - 23.0]	23.4 [22.1 - 24.1]	24.4 [22.6 - 25.2]	25.5 [23.6 - 27.6]	25.9 [23.8 - 29.1]	26.7 [24.7 - 30.1]	26.8 [25.0 - 29.2]	26.7 [25.4 - 29.7]	27.8 [26.5 - 30.2]					
				WTD + 0.3% chol		21.4 [21.0 - 22.0]	22.4 [21.7 - 23.9]	23.9 [22.2 - 24.6]	24.7 [23.0 - 26.8]	24.8 [23.3 - 26.5]	25.8 [23.9 - 27.0]	25.7 [24.3 - 27.1]	25.9 [24.6 - 27.4]	26.8 [24.6 - 28.1]					

Strain	Study	Original design	Weeks on study diet	Diet groups	Gender	Fasted plasma cholesterol (mM) Time (weeks) 0	6	12	20	24	26	30	32	38	52
C57BL/6J	1	Type II diabetes	0	chow	M	2.0 [1.9 - 2.1]									
			6	chow			1.9 [1.8 - 2.1]								
				HFD			3.7 [3.5 - 4.0]								
			12	chow		1.8 [1.7 - 1.9]		1.8 [1.7 - 2.0]							
				HFD		1.9 [1.8 - 1.9]		5.0 [4.2 - 5.2]							
			24	chow		2.0 [1.9 - 2.1]		2.1 [2.0 - 2.3]	2.2 [2.0 - 2.3]	2.3 [2.0 - 2.3]					
				HFD		1.9 [1.8 - 2.0]		4.6 [4.5 - 4.9]	5.3 [5.1 - 5.5]	5.8 [5.7 - 6.1]					
	2	Adipose tissue inflammation	24	chow	M				2.4 [2.3 - 2.6]	2.6 [2.4 - 2.6]					
				HFD					4.8 [3.9 - 5.4]	5.2 [4.8 - 6.1]					
	3	Aging	52	LFD	M					2.1 [1.9 - 2.3]					2.2 [2.1 - 2.6]
				HFD						2.8 [2.5 - 3.1]					3.0 [2.7 - 3.1]
hCRP	4	Metabolic syndrome	38	chow + 1% chol	M										
				HFD											
				chow + 1% chol	F										
				HFD											
LDLr$^{-/-}$.Leiden	5	Diabetic nephropathy	20	LFD	M	6.7 [6.4 - 9.2]		19.6 [14.4 - 26.8]	23.9 [14.3 - 39.3]						
				MFD		7.4 [6.2 - 7.9]		23.3 [11.1 - 28.9]	37.4 [30.9 - 37.7]						
				HFD		7.3 [6.5 - 8.5]		25.7 [21.3 - 35.6]	33.3 [32.0 - 53.0]						
	6	Type II diabetes	20	HFD	M	7.4 [6.6 - 7.9]	14.5 [10.5 - 17.0]	19.7 [16.5 - 21.1]	28.2 [21.3 - 34.0]						
				HFD + ref. soybean oil		7.2 [6.9 - 7.7]	17.8 [11.2 - 20.9]	21.2 [16.1 - 24.5]	25.3 [22.0 - 33.2]						
				HFD + unref. soybean oil		8.1 [7.1 - 8.7]	19.0 [15.4 - 20.1]	24.7 [21.7 - 29.0]	34.3 [27.8 - 40.1]						
				HFD + ref. palm oil		7.3 [6.9 - 7.9]	20.2 [17.1 - 23.7]	28.1 [23.6 - 31.9]	40.2 [35.0 - 42.9]						
				HFD + unref. palm oil		6.7 [6.1 - 7.8]	20.6 [16.1 - 24.7]	30.5 [22.4 - 35.2]	46.0 [31.3 - 49.8]						
	7	Diabetic nephropathy	20	HFD	M	5.6 [5.6 - 7.1]		19.8 [16.6 - 23.2]	26.5 [25.1 - 29.5]						
				HFD + fructose		5.9 [5.2 - 6.0]		28.8 [22.7 - 40.4]	33.6 [25.7 - 45.5]						
				HFD + 0.2% chol		5.8 [5.3 - 6.3]		52.0 [45.4 - 61.6]	47.9 [46.3 - 49.1]						
				HFD + 1.0% chol 20w		5.6 [5.4 - 6.3]		59.0 [46.6 - 64.8]	50.7 [46.6 - 55.7]						
			31	HFD + 1.0% chol 31w		6.0 [5.5 - 6.2]		60.3 [56.6 - 73.1]	57.5 [46.4 - 62.6]	64.4 [55.8 - 72.1]					
	8	Metabolic syndrome	30	chow	M	6.5 [5.8 - 8.2]	7.8 [7.0 - 8.4]	8.7 [7.0 - 9.7]		9.4 [8.8 - 10.0]		10.5 [9.2 - 11.1]			
				HFD		6.8 [6.6 - 7.1]	28.7 [23.6 - 32.1]	31.8 [26.9 - 35.1]		43.7 [37.6 - 46.4]		41.6 [33.8 - 45.6]			
ApoE3L.hCETP	9	Metabolic syndrome	26	VHFD + fructose	M	2.5 [2.3 - 2.6]		4.9 [4.5 - 5.2]			6.2 [5.7 - 7.2]				
	10	Insulin resistance and dyslipidemia	32	VHFD + fructose	M				5.5 [5.3 - 6.3]		4.9 [4.7 - 6.2]	6.9 [5.6 - 8.7]			
	11	Osteoarthritis	32	chow	M			2.0 [1.9 - 2.4]	2.2 [1.9 - 2.5]	2.8 [2.6 - 3.3]			2.8 [2.3 - 3.9]		
				VHFD				4.2 [3.8 - 4.6]	6.0 [4.9 - 8.2]	5.4 [5.1 - 7.5]			7.8 [6.3 - 8.4]		
				VHFD + chow				4.2 [4.1 - 4.6]	6.4 [5.8 - 7.1]	3.2 [3.0 - 3.6]			3.6 [3.4 - 5.7]		
				VHFD, low-MetS				3.0 [1.8 - 3.7]	3.6 [2.2 - 4.6]	3.6 [2.9 - 4.5]			5.1 [3.8 - 7.6]		
	12	Atherosclerosis and OA	38	chow	M	2.0 [1.5 - 2.3]	2.6 [2.3 - 2.8]				2.4 [2.0 - 2.9]	1.6 [1.5 - 2.0]		2.2 [2.1 - 2.5]	
				WTD + 0.4% chol		5.1 [4.3 - 6.6]	4.7 [3.7 - 6.3]				4.5 [3.7 - 5.6]	3.8 [3.4 - 5.5]		5.0 [3.5 - 6.8]	
				WTD + 1.0% chol		5.0 [4.5 - 6.6]	6.8 [5.9 - 7.4]				6.1 [5.4 - 8.3]	8.5 [6.7 - 9.6]		10.2 [8.1 - 13.4]	
				chow	F	3.6 [3.3 - 3.9]	3.2 [3.1 - 3.3]				2.8 [2.5 - 3.3]	2.6 [2.2 - 2.8]		2.0 [1.6 - 2.4]	
				WTD + 0.1% chol		10.5 [9.8 - 11.0]	8.3 [5.4 - 11.8]				9.1 [5.6 - 10.4]	8.3 [6.4 - 12.0]		8.3 [5.6 - 9.6]	
				WTD + 0.3% chol		10.2 [8.8 - 11.0]	16.9 [14.9 - 18.0]				14.3 [12.5 - 19.0]	16.2 [13.6 - 19.7]		14.3 [12.5 - 18.7]	

Table S2 Changes in body weight and total fasting cholesterol plasma levels at selected time points from twelve independent mouse studies with various approaches for diet-induced metabolic dysfunction.

Table S3

Changes in fasting glucose and insulin plasma levels presented here are the actual values of the group medians and interquartile ranges, as shown in color code in Figure 3. For presentation purposes, time points were selected with high overlap between studies. Grey indicates no data available.

Strain	Study	Original design	Weeks on study diet	Diet groups	Gender	Fasted glucose (mM)								
						Time (weeks)								
						0	6	12	20	24	26	30	32	38	52
C57BL/6J	1	Type II diabetes	0	chow	M	10.5 [10.1 - 11.0]									
			6	chow			10.4 [10.0 - 11.4]								
				HFD			12.9 [12.0 - 13.2]								
			12	chow				9.8 [8.6 - 11.1]							
				HFD		12.0 [11.3 - 12.7]		13.4 [12.1 - 14.0]							
			24	chow				11.9 [10.9 - 12.6]	12.0 [11.5 - 12.4]	10.8 [10.0 - 11.3]					
				HFD		11.6 [11.0 - 12.4]		14.1 [13.4 - 15.9]	17.1 [15.7 - 17.9]	14.9 [14.2 - 15.6]					
	2	Adipose tissue inflammation	24	chow	M	8.3 [8.2 - 8.3]	8.2 [8.1 - 8.3]	8.1 [7.7 - 8.1]	8.0 [7.8 - 8.1]	7.7 [7.0 - 8.0]					
				HFD		8.5 [8.2 - 8.8]	9.2 [7.8 - 9.7]	9.3 [8.7 - 9.4]	9.4 [8.7 - 10.4]	9.0 [8.5 - 9.6]					
	3	Aging	52	LFD	M					8.7 [8.3 - 9.1]					7.3 [6.8 - 8.1]
				HFD						9.4 [9.0 - 10.8]					7.6 [6.4 - 8.3]
ICRP	4	Metabolic syndrome	38	chow + 1% chol	M	10.2 [9.8 - 10.8]									
				HFD		9.3 [9.0 - 9.8]									
				chow + 1% chol	F	8.2 [8.0 - 8.4]									
				HFD		7.8 [7.3 - 8.3]									
LDLr$^{-/-}$.Leiden	5	Diabetic nephropathy	20	LFD	M	7.2 [6.1 - 7.6]		6.3 [5.7 - 6.7]	6.4 [5.7 - 6.5]						
				MFD		7.1 [6.3 - 8.0]		7.9 [6.6 - 8.2]	7.1 [6.2 - 7.4]						
				HFD		7.2 [6.6 - 7.7]		7.8 [7.5 - 7.8]	6.3 [5.7 - 6.6]						
	6	Type II diabetes	20	HFD	M	6.6 [6.3 - 7.7]	6.7 [6.2 - 8.2]	8.0 [7.6 - 8.9]	7.5 [6.6 - 8.1]						
				HFD + ref. soybean oil		7.3 [6.5 - 7.6]	8.4 [6.4 - 8.8]	9.0 [7.7 - 11.1]	8.1 [7.5 - 8.9]						
				HFD + unref. soybean oil		7.3 [7.1 - 7.7]	8.4 [8.1 - 8.9]	8.8 [8.3 - 9.0]	8.1 [7.3 - 8.5]						
				HFD + ref. palm oil		7.1 [6.2 - 7.5]	7.8 [7.5 - 8.4]	7.9 [6.6 - 9.0]	7.4 [7.1 - 7.8]						
				HFD + unref. palm oil		7.2 [6.4 - 7.8]	8.5 [7.9 - 8.8]	8.6 [7.7 - 8.9]	8.1 [7.5 - 8.5]						
	7	Diabetic nephropathy	20	HFD	M	14.0 [12.4 - 14.5]		13.6 [11.0 - 14.7]	17.1 [13.8 - 19.6]						
				HFD + fructose		12.3 [12.3 - 12.9]		12.4 [12.3 - 17.0]	16.4 [15.3 - 18.9]						
				HFD + 0.2% chol		13.3 [12.5 - 14.0]		13.6 [11.2 - 14.9]	13.2 [12.1 - 13.8]						
				HFD + 1.0% chol 20w		13.0 [12.2 - 14.0]		10.7 [9.8 - 11.5]	11.1 [10.8 - 12.3]						
			31	HFD + 1.0% chol 31w		13.5 [13.0 - 13.8]		11.4 [11.1 - 12.5]	12.0 [10.9 - 12.7]	15.3 [14.0 - 15.9]					
	8	Metabolic syndrome	30	chow	M	7.3 [7.1 - 7.9]	7.7 [7.3 - 8.5]	8.7 [8.5 - 8.8]		7.9 [7.7 - 8.1]		7.4 [7.2 - 7.8]			
				HFD		6.5 [6.2 - 6.7]	6.7 [5.7 - 7.1]	6.6 [6.1 - 6.7]		6.3 [6.0 - 7.2]		6.1 [5.9 - 6.6]			
	9	Metabolic syndrome	26	VHFD + fructose	M				8.1 [7.5 - 8.3]	8.0 [7.6 - 8.7]					
	10	Insulin resistance and dyslipidemia	32	VHFD + fructose	M	7.2 [6.8 - 8.2]			12.6 [12.3 - 13.2]		11.7 [11.5 - 11.9]	11.9 [9.8 - 12.7]			
ApoE3L.hCETP	11	Osteoarthritis	32	chow	M										
				VHFD											
				VHFD + chow											
				VHFD, low-MetS											
	12	Atherosclerosis and OA	38	chow	M										
				WTD + 0.4% chol											
				WTD + 1.0% chol											
				chow	F										
				WTD + 0.1% chol											
				WTD + 0.3% chol											

Strain	Study	Original design	Weeks on study diet	Diet groups	Gender	Fasted plasma insulin (ng/ml) Time (weeks) 0	6	12	20	24	26	30	32	38	52
C57BL/6J	1	Type II diabetes	0	chow	M	0.4 [0.3 - 0.7]									
			6	chow			1.5 [1.2 - 1.7]								
				HFD			2.2 [1.4 - 2.7]								
			12	chow				1.0 [0.9 - 1.5]							
				HFD				3.2 [2.4 - 7.0]							
			24	chow		0.5 [0.4 - 0.6]		2.0 [1.0 - 2.5]	1.0 [0.8 - 1.1]	1.4 [1.0 - 2.3]					
				HFD		0.5 [0.3 - 0.6]		6.9 [4.7 - 8.0]	6.6 [6.1 - 7.8]	8.4 [8.0 - 8.7]					
	2	Adipose tissue inflammation	24	chow	M	0.8 [0.7 - 1.0]		1.6 [1.2 - 2.5]	1.1 [0.7 - 2.5]	1.2 [1.1 - 1.3]					
				HFD		0.9 [0.6 - 1.1]	2.6 [1.7 - 4.5]	7.6 [3.8 - 17.7]	12.0 [5.6 - 19.3]	7.7 [5.5 - 24.4]					
	3	Aging	52	LFD	M					0.9 [0.7 - 1.2]					0.7 [0.6 - 0.8]
				HFD						1.8 [1.0 - 4.3]					1.2 [0.8 - 1.7]
hCRP	4	Metabolic syndrome	38	chow + 1% chol	M	0.5 [0.3 - 0.6]									
				HFD		0.5 [0.3 - 0.5]									
				chow + 1% chol	F	0.5 [0.1 - 0.8]									
				HFD		0.2 [0.1 - 0.3]									
LDLr$^{-/-}$.Leiden	5	Diabetic nephropathy	20	LFD	M	1.4 [0.7 - 1.9]		2.0 [1.1 - 3.7]	6.9 [4.4 - 13.7]						
				MFD		1.8 [1.0 - 2.4]		12.9 [5.3 - 18.3]	14.1 [12.3 - 15.1]						
				HFD		1.4 [1.1 - 2.6]		19.4 [16.1 - 35.0]	17.5 [16.9 - 27.2]						
	6	Type II diabetes	20	HFD	M	1.8 [1.1 - 2.6]		8.5 [5.4 - 16.0]	13.1 [6.0 - 22.9]						
				HFD + ref. soybean oil		1.3 [0.9 - 2.8]		7.4 [5.5 - 14.3]	9.0 [7.3 - 13.7]						
				HFD + unref. soybean oil		1.2 [1.1 - 1.4]		12.9 [10.7 - 14.8]	14.7 [11.6 - 18.6]						
				HFD + ref. palm oil		1.3 [1.0 - 2.3]		14.6 [9.3 - 17.1]	12.7 [11.2 - 19.6]						
				HFD + unref. palm oil		1.8 [1.1 - 2.8]		10.0 [5.9 - 13.4]	17.4 [10.0 - 35.4]						
	7	Diabetic nephropathy	20	HFD	M	0.8 [0.7 - 1.1]		8.8 [6.9 - 10.1]	24.2 [23.9 - 27.1]						
				HFD + fructose		1.0 [0.9 - 1.6]		12.5 [6.6 - 19.8]	36.2 [23.5 - 50.5]						
				HFD + 0.2% chol		1.0 [0.8 - 1.5]		7.9 [5.1 - 14.1]	20.4 [15.6 - 23.2]						
				HFD + 1.0% chol 20w		0.8 [0.5 - 1.3]		5.2 [3.6 - 7.6]	10.8 [9.7 - 14.7]						
			31	HFD + 1.0% chol 31w		0.9 [0.7 - 1.4]		6.3 [3.4 - 8.2]	14.3 [11.1 - 23.5]	10.4 [5.3 - 21.4]					
	8	Metabolic syndrome	30	chow	M	1.3 [0.8 - 2.2]	1.4 [1.1 - 2.0]	2.9 [1.7 - 3.2]		3.6 [2.0 - 5.3]		4.5 [3.2 - 5.6]			
				HFD		1.1 [0.9 - 1.6]	6.8 [4.5 - 10.9]	13.9 [9.4 - 22.7]		13.7 [11.2 - 24.5]		13.9 [11.3 - 15.5]			
ApoE3L.hCETP	9	Metabolic syndrome	26	VHFD + fructose	M			12.7 [11.1 - 16.1]			7.8 [5.2 - 11.1]				
	10	Insulin resistance and dyslipidemia	32	VHFD + fructose	M				5.1 [4.1 - 5.9]		7.0 [5.2 - 10.1]	7.5 [2.5 - 7.9]			
	11	Osteoarthritis	32	chow	M										
				VHFD											
				VHFD + chow											
				VHFD, low-MetS											
	12	Atherosclerosis and OA	38	chow	M										
				WTD + 0.4% chol											
				WTD + 1.0% chol											
				chow	F										
				WTD + 0.1% chol											
				WTD + 0.3% chol											

Table S3 Changes in fasting glucose and insulin plasma levels at selected time points from twelve independent mouse studies with various approaches for diet-induced metabolic dysfunction.

Supplemental References

1. Gierman LM, van der Ham F, Koudijs A, Wielinga PY, Kleemann R, Kooistra T, *et al.* Metabolic stress-induced inflammation plays a major role in the development of osteoarthritis in mice. *Arthritis Rheum* 2012;64(4):1172-81. doi: 10.1002/art.33443
2. Verschuren L, Kooistra T, Bernhagen J, Voshol PJ, Ouwens DM, van Erk M, *et al.* MIF deficiency reduces chronic inflammation in white adipose tissue and impairs the development of insulin resistance, glucose intolerance, and associated atherosclerotic disease. *Circ Res* 2009;105(1):99-107. doi: 10.1161/CIRCRESAHA.109.199166
3. Merat S, Casanada F, Sutphin M, Palinski W, Reaven PD. Western-type diets induce insulin resistance and hyperinsulinemia in LDL receptor-deficient mice but do not increase aortic atherosclerosis compared with normoinsulinemic mice in which similar plasma cholesterol levels are achieved by a fructose-rich diet. *Arterioscler Thromb Vasc Biol* 1999;19(5):1223-30.
4. van Vlijmen BJ, van den Maagdenberg AM, Gijbels MJ, van der Boom H, HogenEsch H, Frants RR, *et al.* Diet-induced hyperlipoproteinemia and atherosclerosis in apolipoprotein E3-Leiden transgenic mice. *J Clin Invest* 1994;93(4):1403-10. doi: 10.1172/JCI117117
5. van den Hoek AM, van der Hoorn JW, Maas AC, van den Hoogen RM, van Nieuwkoop A, Droog S, *et al.* APOE*3Leiden.CETP transgenic mice as model for pharmaceutical treatment of the metabolic syndrome. *Diabetes Obes Metab* 2014;16(6):537-44. doi: 10.1111/dom.12252
6. van de Steeg E, Kleemann R, Jansen HT, van Duyvenvoorde W, Offerman EH, Wortelboer HM, *et al.* Combined analysis of pharmacokinetic and efficacy data of preclinical studies with statins markedly improves translation of drug efficacy to human trials. *J Pharmacol Exp Ther* 2013;347(3):635-44. doi: 10.1124/jpet.113.208595
7. Langford DJ, Bailey AL, Chanda ML, Clarke SE, Drummond TE, Echols S, *et al.* Coding of facial expressions of pain in the laboratory mouse. *Nat Methods* 2010;7(6):447-9. doi: 10.1038/nmeth.1455
8. Mahler Convenor M, Berard M, Feinstein R, Gallagher A, Illgen-Wilcke B, Pritchett-Corning K, *et al.* FELASA recommendations for the health monitoring of mouse, rat, hamster, guinea pig and rabbit colonies in breeding and experimental units. *Lab Anim* 2014;48(3):178-92. doi: 10.1177/0023677213516312
9. Mulder P, Morrison MC, Wielinga PY, van Duyvenvoorde W, Kooistra T, Kleemann R. Surgical removal of inflamed epididymal white adipose tissue attenuates the development of non-alcoholic steatohepatitis in obesity. *Int J Obes (Lond)* 2016;40(4):675-84. doi: 10.1038/ijo.2015.226
10. van der Heijden RA, Sheedfar F, Morrison MC, Hommelberg PP, Kor D, Kloosterhuis NJ, *et al.* High-fat diet induced obesity primes inflammation in adipose tissue prior to liver in C57BL/6j mice. *Aging (Albany NY)* 2015;7(4):256-68. doi: 10.18632/aging.100738
11. Gierman LM, Kuhnast S, Koudijs A, Pieterman EJ, Kloppenburg M, van Osch GJ, *et al.* Osteoarthritis develop-

ment is induced by increased dietary cholesterol and can be inhibited by atorvastatin in APOE*3Leiden. CETP mice--a translational model for atherosclerosis. *Ann Rheum Dis* 2014;73(5):921-7. doi: 10.1136/annrheumdis-2013-203248

12. Glasson SS, Chambers MG, Van Den Berg WB, Little CB. The OARSI histopathology initiative - recommendations for histological assessments of osteoarthritis in the mouse. *Osteoarthritis Cartilage* 2010;18 Suppl 3:S17-23. doi: 10.1016/j.joca.2010.05.025



Chapter 3

High-fat dietary consumption promotes disease progression in a surgical joint destabilisation murine model of osteoarthritis: role of systemic eicosanoids and circulating monocytes

Kozijn A.E., de Visser H.M., Tartjiono M.T., Casbas F., Ravipati S., van der Ham F., Bacardit J., Bouwman J., Mastbergen S.C., Zuurmond A.M., Barrett D.A., Lafeber F.P.J., Bobeldijk I., Stoop R., Mobasheri A., Weinans H.

Submitted for publication

Abstract

Background. In this study we investigated the contribution of high-fat diet-induced metabolic overload to osteoarthritis (OA) progression originally caused by mild mechanical trauma to the mouse knee joint. We hypothesized that metabolic stress would induce a proinflammatory environment by altering systemic lipid levels and immune cell populations.

Methods. Twelve-week-old male C57BL/6J mice (n=20) were given a low-fat diet (LFD, 10%kcal from fat) or high-fat diet (HFD, 45%kcal from fat) for 18 weeks. OA was initiated by transecting the medial meniscotibial ligament of the right knee joint at t=10 weeks. OA severity and changes in M1/M2 polarization of synovial macrophage populations were determined in serial coronal FFPE-mounted sections. Eicosanoid levels and monocyte populations were evaluated before and after ligament transection.

Results. Diet-induced metabolic stress assessed by body weight, systemic cholesterol levels, and insulin resistance index was significantly higher in HFD mice. This group also showed increased cartilage damage, synovitis, and osteophyte formation compared with LFD controls. High-fat feeding elevated systemic arachidonic acid levels, which mainly resulted in increased levels of its cytochrome P450-catalysed diol metabolites 5,6-dihydroxyeicosatrienoic acid (DHET) and 8,9-DHET. High-fat feeding also triggered an increase in pro-inflammatory intermediate $CD43^{++}Ly6C^{int}$ monocytes after ligament resection. Ligament resection in addition to high-fat feeding induced increased expression of the activation marker CD11c selectively on non-classical $CD43^{++}Ly6C^{low}$ monocytes. No significant changes in synovial macrophage polarization were observed.

Conclusions. Metabolic stress resulted in a proinflammatory environment and aggravated injury-induced OA progression. Our results suggest that a CYP450-focused eicosanoid metabolism and activated circulating monocytes may be drivers of this metabolic stress-induced OA progression, contributing to the mechanistic understanding and potentially serving as future diagnostic and prognostic biomarkers for metabolic OA.

Introduction

Obesity is the second most significant risk factor for the development of osteoarthritis (OA), the most common form of arthritis[1]. Besides mechanical overload of the joints due to excess body weight, obesity contributes to OA pathogenesis through metabolic disbalance[2], also termed metabolic stress. Metabolic stress is thought to be a major contributor in a subtype of OA referred to as metabolic OA[3–6], an OA phenotype that is characterized by a systemic low-grade inflammation – although this classification is still under debate[7]. Metabolic OA prevalence is highest in developed countries, where the incidence of obesity progressively increases due to a sedentary lifestyle, low levels of physical activity, and high-caloric diet[8]. The pathogenesis of metabolic OA has been linked to several features of the metabolic syndrome, such as central obesity, insulin resistance and dyslipidemia[2, 9, 10]. Even though the association between OA and metabolic stress is demonstrated by many studies, the underlying pathophysiologic mechanisms are still vague.

Animal models of diet-induced OA can help elucidate the mechanisms underlying metabolic OA. It is suggested that high-fat feeding induces an overall primed state and the associated metabolic stress undermines the body's capacity to adequately cope with insults like knee injury[11, 12]. The obesity-prone C57BL6/J mouse is widely used to study metabolic OA and applied diets are typically high in caloric content, like Western-type diets or high-fat diets (45-60 kcal% energy from fat)[13]. Diet-induced OA severity is typically mild in animal models provided with a high fat diet only and we found that increased articular cartilage damage compared with low-fat diet (LFD) controls is not assured[14]. Rather, our results suggested that an additional trigger, over and above a high-caloric dietary stressor, is necessary to evoke metabolic OA.

In this study we investigated the contribution of metabolic stress to OA progression induced by mild trauma to the knee joint. We placed C57BL/6J mice on a low-fat diet (LFD, 10kcal% energy from fat) or high-fat diet (HFD, 45kcal% energy from fat) and induced OA onset by surgical destabilization of the medial meniscus (DMM). This post-traumatic OA (PTOA) model is low invasive and sufficiently sensitive to study subtle changes in disease progression by mild triggers like genetic background and diet[15, 16]. As obesity is associated with a systemic low-grade inflammation, we hypothesized that diet-induced metabolic stress would induce a proinflammatory environment by altering systemic lipid levels and immune cell populations. We determined systemic eicosanoid levels, lipid mediators best known for their pivotal role in inflammation[17], and circulating monocyte populations. Peripheral blood monocytes are precursor cells for macrophages: an immune cell that plays a role in OA pathogenesis and is known to shift towards the pro-inflammatory (M1) phenotype during adipose-related inflammation[18, 19]. Therefore, we also explored changes in M1/M2 polarization of synovial macrophage populations in PTOA.

Material and methods

Please refer to the end of this Chapter for a detailed methods section.

The experiment was approved by the institutional Animal Care and Use Committee of TNO and was in compliance with ARRIVE guidelines and European Community specifications regarding the use of laboratory animals. The experiment was carried out in wild-type male C57BL/6J mice purchased from Charles River Laboratories (L'Arbresle Cedex, France) that received a 2-week acclimatization period after transfer to a specific pathogen-free (SPF) animal facility. Twelve-week old male C57BL/6J mice (n=10 per group) were given a synthetic high-fat diet (HFD, 45% kcal from fat) or low-fat diet (LFD, 10% kcal from fat) for 18 weeks. Ten weeks after starting the diet, OA was surgically induced in the right knee joint by transecting the medial meniscotibial ligament (MMTL) and destabilizing the medial meniscus (DMM). The left knee joint served as an experimental control and received all surgical procedures except for the MMTL transection (sham surgery). Mice were euthanized 8 weeks post-surgery using gradual-fill CO_2 asphyxiation.
Metabolic stress was assessed throughout the experiment by monitoring changes in body weight, body composition, and systemic total cholesterol, glucose and insulin levels. Serial coronal 5 µm FFPE sections were collected throughout the joint at 60 µm intervals, stained, and evaluated for cartilage degradation, osteophyte formation and synovitis using the OARSI scoring system specifically designed for the mouse[20]. Eicosanoid profiling was performed in fasted plasma samples as described previously[21]. Monocyte subpopulations were analysed in heparin-buffered peripheral blood samples stained with the antibody panel shown in Table 1. Data was obtained using a 3-laser FACSCanto™ II flow cytometer and analysed with FlowJo v10.2 software.

Table 1. Monoclonal antibody panel used for the analysis of peripheral monocyte subpopulations.

Marker	Fluorochrome	Dilution	Clone	Manufacturer	Catalogue number
CD11c	Horizon V450	1:100	HL3	BD Biosciences	560521
CD206*	AF488	1:200	C068C2	BioLegend	141710
CD115	PE	1:400	AFS98	eBioscience	12-1152-83
CD43	PE/Cy7	1:100	S7	BD Biosciences	562866
Ly6C	PerCP	1:50	HK1.4	BioLegend	128028
CD11b	APC	1:400	M1/70	eBioscience	17-0112-83

Abbreviations: AF, Alexa Fluor; PE, phycoerythrin; Cy, cyanine; PerCP, peridinin chlorophyll protein complex; APC, allophycocyanin.
*Intracellular staining.

FFPE sections from DMM-operated knee joints were triple-stained with primary antibodies targeting F4/80 (pan-macrophage), iNOS (M1) and CD206 (M2). Quantification was performed in the lateral patellofemoral synovial lining (ROI), unmixed colour spectra were obtained with a Nuance multispectral imaging system (40x magnification), and analysed with ImageJ 1.51n software. Statistical analysis was performed using IBM SPSS software. In all analyses, a probability value < 0.05 was considered statistically significant. Unless stated otherwise, data are presented by the median with interquartile range (range between the 25th to 75th percentiles).

Results

Metabolic stress aggravates PTOA development

Diet-induced metabolic stress was observed in the HFD group, as demonstrated by the metabolic profile of the HFD animals at the end of the study (Table 2). Metabolic stress was already present before surgery: body weight, cholesterol levels, and HOMA-IR were significantly increased in HFD mice compared with LFD controls after 9 weeks (data not shown). Body composition analysis revealed that the increase in body weight was completely attributed to an increase in body fat mass.

Articular cartilage damage was assessed by histological examination to evaluate the effect of HFD on DMM-induced cartilage damage. In the sham-operated contralateral knee joints hardly any cartilage damage was observed (Figure 1). DMM surgery on the other hand induced clear OA development in both groups, with diet-induced spatial differences in cartilage damage (Figure 1). Cartilage damage was significantly aggravated in HFD mice compared with controls, with median [interquartile range] OA scores of 19.4 [15.1-20.9] in HFD versus 13.8 [8.0-20.0] in LFD mice (p=0.049, Figure 2A). This difference could mainly be attributed to increased damage in the lateral tibiofemoral compartments (Figure 2B). HFD mice showed advanced cartilage erosion in both lateral compartments, extending to 25-50% of the articular surface (8.0 [4.9-10.0]; p=0.01), while LFD mice showed increased fibrillation, fissures and occasional cartilage loss <25% (3.8 [3.0-8.0]) (Figure 1). The medial knee compartments, typically more affected in the DMM model, were almost completely devoid of cartilage and reached close to the maximal score of 12 in both the HFD and LFD groups (Figure 2C). Therefore, even if potential diet-induced aggravation had occurred, this could not be inferred from the medial side as these were nearing maximal scores (HFD 11.0 [10.6-11.8]; LFD 10.0 [5.0-12.0]; p = 0.109). Synovial inflammation was significantly increased and more severe in HFD mice (7 out of 8 mice; 6.5 [5.3-8.5]) compared with LFD mice (4 out of 7 mice; 1.0 [0.0-6.0]; p=0.04, Figure 2D). Sham-operated contralateral knees showed no synovial thickening. Increased osteophyte formation was observed in the HFD group compared with the LFD controls (Figure 2E). Sham-operated contralateral knee joints showed hardly any osteophyte formation.

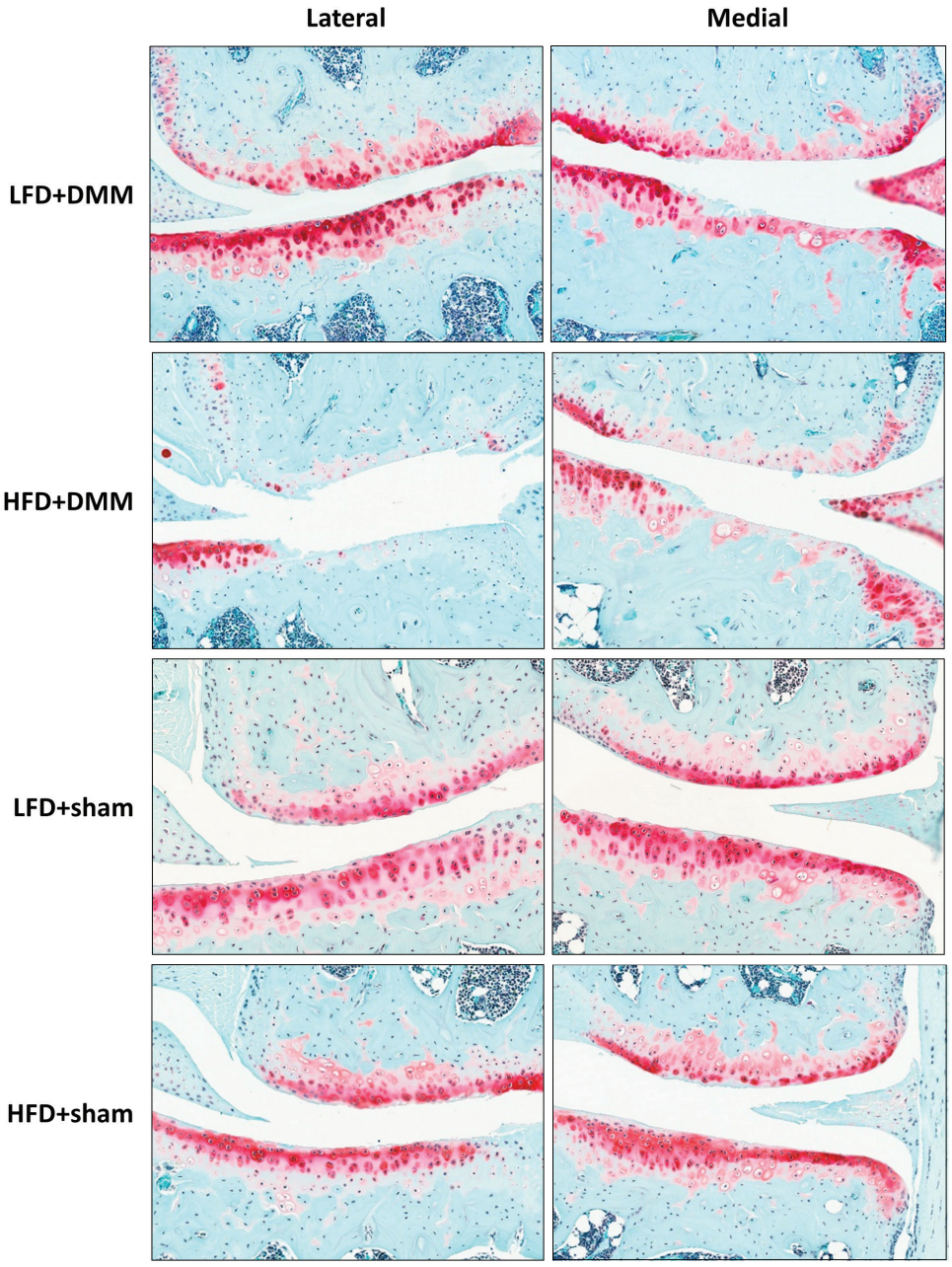


Figure 1 HFD feeding aggravates OA progression at the lateral but not the medial side of the destabilized knee. Representative Safranin-O, Fast Green and Hematoxylin-stained coronal sections showing detailed pictures of the lateral femur condyle and tibial plateau from sham and DMM knee joints of the LFD and HFD group. Original magnification ×20.

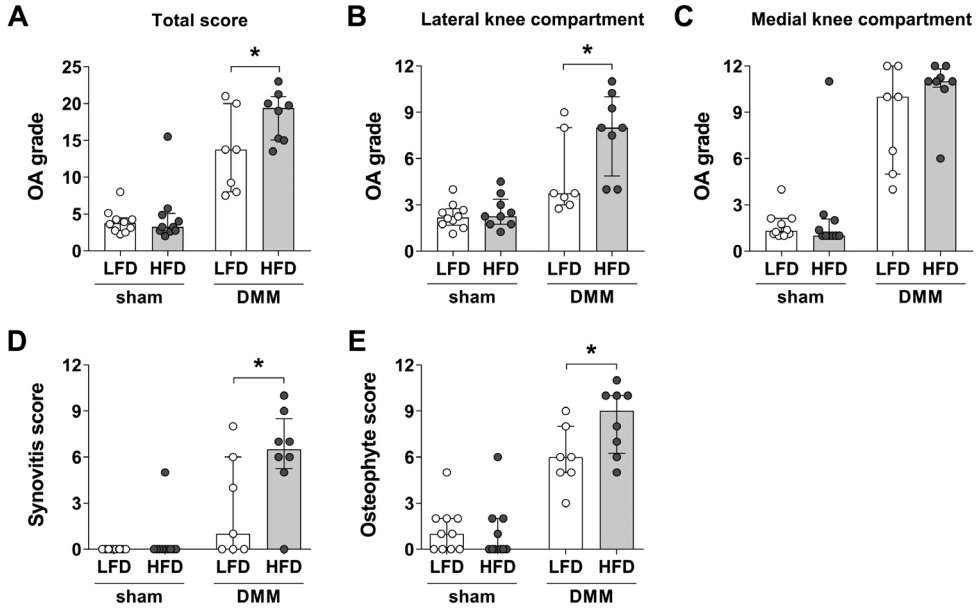


Figure 2 HFD feeding increased cartilage degeneration, osteophyte formation and synovial inflammation. A) Summed histopathological scores for the tibiofemoral knee compartments of the LFD and HFD mice. Cartilage damage was most pronounced at B) the lateral side of the joint in HFD animals, whereas C) the medial side was severely damaged in both groups. D) Total synovitis scores showing the individual summed score for the tibiofemoral knee compartments for each animal per study group. E) Total osteophyte scores showing the individual summed score for the tibiofemoral knee compartments for each animal per study group. Scoring was performed according to OARSI histopathology recommendations for the mouse16. Data are presented as group median (indicated by bars) with interquartile range (error bars). *Statistical significance was set to p<0.05.

Table 2. Metabolic parameters confirm HFD-induced metabolic stress at the end of the study.

	LFD		HFD		
	Mean ± SD	**IQR**	**Mean ± SD**	**IQR**	**Significance**
Body weight (g)	31.34 ± 1.99	[29.50 – 34.30]	40.06 ± 6.94	[27.90 – 49.20]	p < 0.01
Fat mass (g)	4.52 ± 1.91	[2.24 – 7.29]	12.48 ± 4.67	[5.70 – 17.62]	p < 0.01
Lean mass (g)	25.41 ± 1.72	[22.82 – 27.20]	26.60 ± 2.33	[22.65 – 30.46]	p = 0.64
Cholesterol (mM)	2.40 ± 0.99	[0.88 – 3.93]	3.99 ± 0.84	[2.09 – 4.84]	p < 0.01
HOMA-IR index	15.78 ± 7.77	[7.46 – 30.49]	62.79 ± 39.9	[6.71 – 122.49]	p = 0.02

Bold font indicates significant difference (p<0.05) between HFD group and LFD controls, determined by two-tailed Mann-Whitney non-parametric testing. SD, standard deviation; IQR, interquartile range.

Systemic changes in eicosanoid levels

Eicosanoids can exert both pro- and anti-inflammatory functions and have been implicated in the pathogenesis of a variety of immunometabolic disorders, like obesity[13-17]. Eicosanoids are formed from omega-3 (n-3) or n-6 polyunsaturated fatty acid (PUFA) precursors via the cyclooxygenase (COX), lipoxygenase (LOX), and cytochrome P450 pathways (CYP450, Figure 3)[22]. At large, n-6 PUFA-derived eicosanoids exhibit more pro-inflammatory and n-3 PUFA-derived eicosanoids more anti-inflammatory activity. Although a useful framework, this simplistic dichotomy does not cover the complexity of the physiological effects of eicosanoids *in vivo*[22].

Because of plasma volume limitations and the volume demands of the assay, we were able to reliably detect the levels of 24 eicosanoids. Overall, minor differences were observed between the diet groups. HFD induced a significant increase in arachidonic acid (AA) levels, a n-6 PUFA precursor, with 947 [765-1257] in LFD *versus* 1538 [1230-1935] in HFD mice ($p<0.01$) at 14 weeks. To find out how this increase affected total eicosanoid metabolism, we evaluated the changes in eicosanoid profiles of the mice before and after DMM surgery. Pathway analysis revealed that the increase in AA levels mainly translated into increased hydroxylation into the fatty acid diols 5,6-dihydroxyeicosatrienoic acid (DHET) and 8,9-DHET (Figure 3). In addition, 5-HETE and 13-OxoODE levels were increased in HFD mice compared with LFD mice. Similar plasma eicosanoid profiles were observed between 9 and 14 weeks (data not shown).

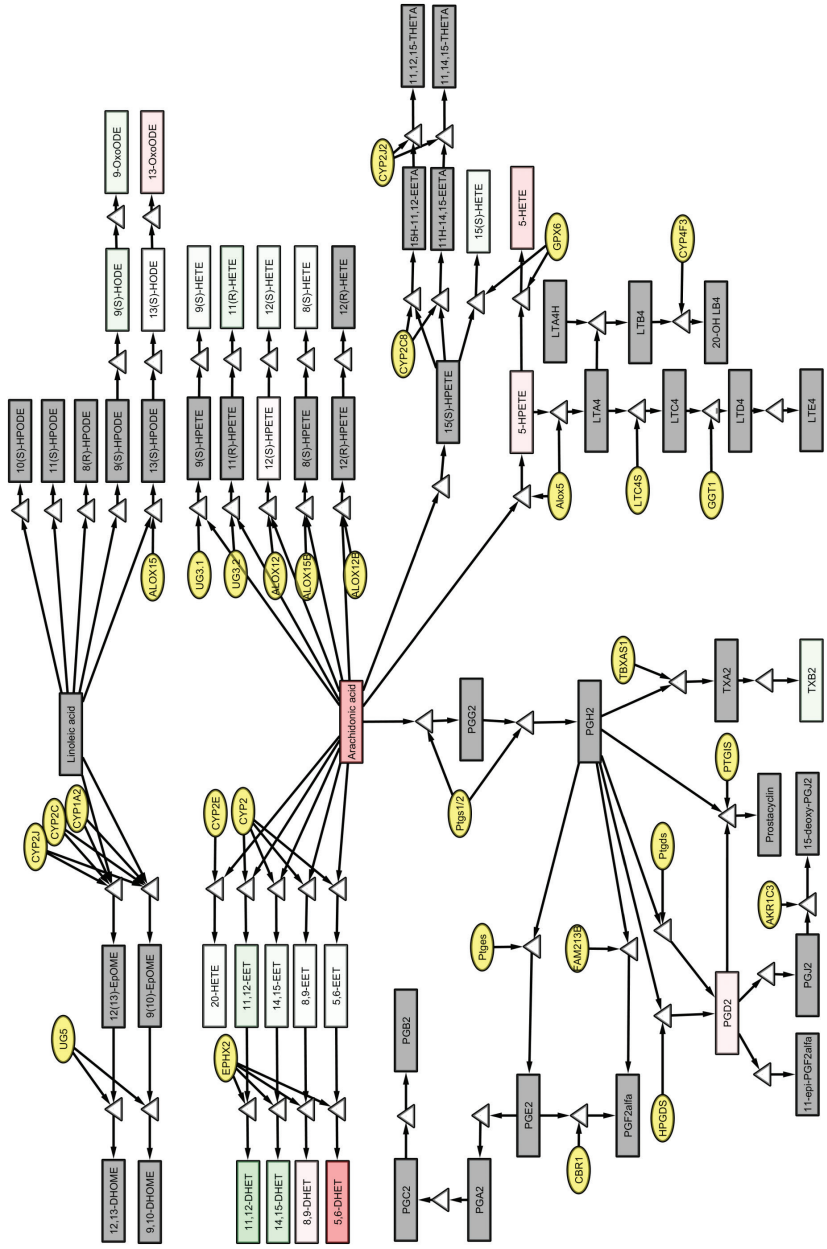


Figure 3 HFD increased plasma arachidonic acid levels and affected eicosanoid metabolism. Overview of the changes in murine plasma eicosanoid profiles between 0 and 9 weeks after LFD or HFD feeding. The following is indicated by the colours: grey, not detected or quantified; red, increased concentrations in HFD mice; green, decreased concentrations in HFD mice. Colour intensity reflects the extent to which eicosanoid levels have been elevated or decreased. CYP450, cytochrome P450; COX, cyclooxygenase; LOX, lipoxygenase.

Activation of circulating monocyte subpopulations

Monocytes are short-lived mononuclear phagocytes that constitute ~10% of peripheral leukocytes in humans and ~4% in mice[23]. Current nomenclature divides murine monocytes into three subpopulations based on their surface expression of CD43 and Ly6C receptors[24]: 1) $CD43^{+}Ly6C^{hi}$ classical monocytes; 2) $CD43^{++}Ly6C^{int}$ intermediate monocytes; 3) $CD43^{++}Ly6C^{low}$ non-classical monocytes. The three subpopulations share a developmental relationship (from classical via intermediate to non-classical) and are phenotypically and functionally different.

Monocyte subpopulation percentages showed subtle differences between the LFD and HFD groups over time (Figure 4A). The most pronounced effect of long-term HFD was an increase in circulating CD43++Ly6Cint intermediate monocytes at t=17 weeks, at the expense of the CD43++Ly6Clow non-classical subpopulation. This increase showed significance within the total CD115+CD11b+SSC-Alow monocyte fraction ($p = 0.044$, data not shown), but due to interindividual variability did not reach significance within the total leukocyte fraction ($p = 0.107$, Figure 4B).
The increase in intermediate monocytes concurred with a significantly increased expression of the monocyte activation marker CD11c in HFD mice compared with LFD controls (0.8 [0.7-1.4] *versus* 3.0 [1.6-3.9] at 9 weeks and 3.0 [1.9-3.4] *versus* 6.6 [4.6-7.7] at 17 weeks, respectively; Figure 4C). CD11c contributes to monocyte arrest on endothelial cells and, as such, is upregulated by activated monocytes during chemotaxis. Both high-fat diet and knee injury contributed to the increased expression of CD11c, respectively, as: 1) HFD mice showed significantly more CD11c expression compared with LFD controls at 9 and 17 weeks ($p<0.01$) and 2) LFD mice showed increased CD11c expression over time ($p=0.03$). Backgating (i.e. highlighting the final gated population within the population of its ancestors) of the $CD11c^{+}$ cells into the total $CD115^{+}CD11b^{+}SSC\text{-}A^{low}$ monocyte fraction revealed that this integrin was predominantly upregulated by the $CD43^{++}Ly6C^{low}$ non-classical monocytes (Figure 4D).

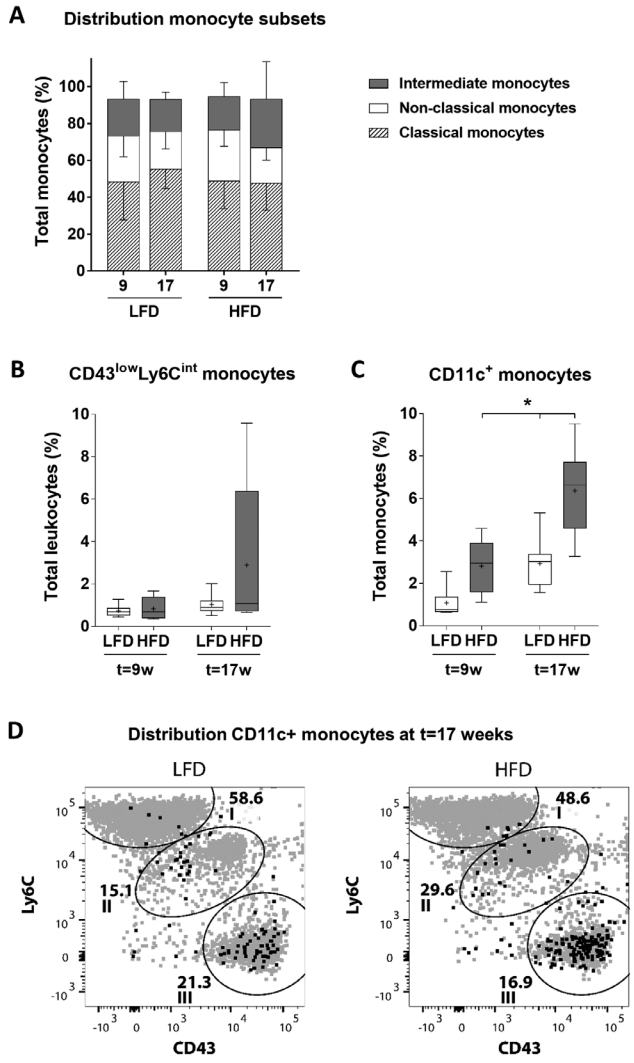


Figure 4 CD11c-expressing monocytes significantly increased in the HFD group and correlate with osteophytosis and synovial inflammation. A) Peripheral $CD115^{+}CD11b^{+}SSC\text{-}A^{low}$ monocyte subpopulations showed subtle changes in HFD mice compared with LFD mice over time. B) Increased frequency of $CD43^{++}Ly6C^{int}$ intermediate monocytes plotted as percentage of total leukocytes. C) CD11c-expressing monocytes significantly increased in both diet groups over time, but to a higher degree in the HFD group. D) Backgating of $CD11c^{+}$ cells (black dots) to pre-set monocyte gate at t=17w revealed an upregulation of CD11c expression by the non-classical $CD43^{++}Ly6C^{low}$ monocyte subset: I, classical monocytes; II, intermediate monocytes; III, non-classical monocytes. Stacked bars show mean values and standard deviation for each monocyte subset. Box-and-whiskers plots display a statistical summary of the mean (+ within box), median (line within box), interquartile range (box) and the minimum and maximum values (whiskers). *Statistical significance was set to $p<0.05$.

High-fat feeding induced no macrophage polarization

As activated monocytes may differentiate into macrophages upon tissue entry, the effects of the HFD on this immune cell type were investigated locally by evaluating the surface area percentage positivity of M1 (iNOS) and M2 (CD206) macrophage markers in the synovial lining of DMM-operated right knee joints.

Synovial thickening was increased in knee joints of HFD mice compared with LFD mice (Figure 5A). The ratio of the surface area percentages between M1 marker iNOS and M2 marker CD206 showed an increase in the HFD mice that did not reach significance (LFD 0.54 [0.39-1.34] *versus* HFD 1.28 [0.62-1.66]; p=0.12; Figure 5B). Pan-macrophage marker F4/80 positivity was predominantly observed in the upper synovial layer and showed a non-significant increase on HFD (0.94 [0.20-2.78] versus 2.49 [1.61-5.25]; Figure 5C). The subset-specific markers CD206 and iNOS were upregulated in the HFD group compared with LFD group as well, but none of the markers reached a significant difference between both groups. This was also observed within the $F4/80^+$ macrophage fraction, where the colocalization surface area percentages of CD206 and iNOS positivity were similar between diet groups (Figure 5D).

Correlation analyses revealed moderate to high positive associations for the total F4/80-stained surface area of the synovial lining with lateral OA degeneration and synovitis scores (Table S2). Both OA scores significantly correlated to the colocalization of the total area positivity of the three macrophage markers as well. Osteophyte scores showed no correlation with any of the macrophage stains. Within the $F4/80^+$ fraction, neither subset marker associated with the evaluated OA features.

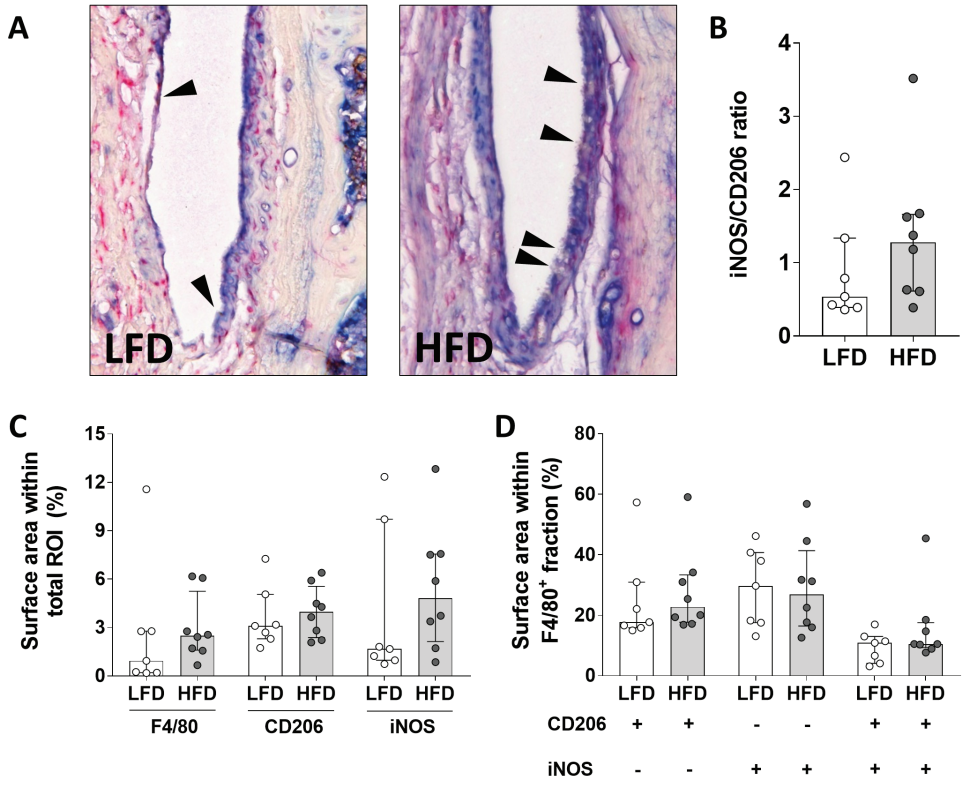


Figure 5 HFD feeding increased macrophage presence but induced no shift in macrophage subset ratio in the synovium. A) Representative images of the lateral patellofemoral synovial lining (ROI) from DMM-operated knees triple stained with pan-macrophage marker F4/80 (yellow, arrowheads), M1 subset marker iNOS (blue) and M2 subset marker CD206 (red). Original magnification ×40. B) Ratio between total iNOS and total CD206 percentage positivity was not significantly different between both groups. C) Percentage marker positivity within the ROI of LFD and HFD mice. D) Percentage CD206 and/or iNOS positivity within F4/80+ fraction shows no diet-induced shift in macrophage phenotypes. Data are presented as group median (indicated by bars) with interquartile range (error bars).

Discussion

In this study, we investigated to what degree metabolic stress aggravated disease progression in a post-traumatic OA (PTOA) model and which mechanisms could be involved. Mice on a HFD showed significantly more cartilage damage upon knee injury compared with those on a LFD. Increased OA severity also manifested itself in enhanced osteophyte formation and synovial inflammation. Modulation of eicosanoid metabolism towards the CYP450 pathway and activation of monocyte subpopulations reflected an aggravated state of systemic immune activation. Locally, HFD-induced synovial thickening resulted in an increase in macrophage markers that positively

associated with OA severity, but no clear macrophage polarization was observed. These results suggest that systemic changes, triggered by HFD-induced metabolic stress, aggravate injury-induced OA by dysregulating eicosanoid metabolism and by increasing immune activation.

Aggravation of local injury due to metabolic stress was evident from the observed spatial differences in OA features. HFD mice showed more generalized cartilage damage compared to LFD mice, which displayed the medially oriented cartilage damage known to the DMM model[15]. The observed diet-induced disease aggravation confirms results from other PTOA mouse models on a HFD regimen[16, 25] and is in line with faster disease progression reported for obese OA patients[26]. The clear increases in lateral cartilage damage, synovial inflammation, and osteophyte formation compared with LFD mice qualifies the HFD DMM model as a suitable preclinical mouse model to identify players and pathways involved in metabolic OA. As both the internal sham control joints and the LFD animals developed considerably smaller OA features for all measured parameters, we conclude that HFD feeding on its own has limited potential to induce OA but clearly creates a proinflammatory environment leading to aggravation of PTOA progression.

To identify which factors might contribute to a diet-induced proinflammatory environment, we explored changes in systemic eicosanoid levels. In addition to regulating a wide range of physiologic processes[27], eicosanoids can exert both pro- and anti-inflammatory functions[28]. Of note, synovial fluid eicosanoid profiles were not reflected systemically in a rat model of HFD-induced OA, which suggests differential roles of eicosanoids in local versus peripheral compartments[29]. Although local eicosanoid involvement has been reported in OA[30–33], their systemic role in OA pathogenesis is less explored. In our model, HFD sparked a clear increase in systemic arachidonic acid (AA) levels, a n-6 polyunsaturated fatty acid that can trigger a pro-inflammatory cascade. Increased AA hydroxylation by the enzyme soluble epoxide hydrolase (sEH) in the cytochrome P450 pathway generated increased levels of dihydroxyeicosatrienoic acids (DHETs). This probably reflects the diet-induced metabolic stress, as obesity has been shown to induce altered CYP-expression and increased sEH-generated DHET levels in models of metabolic syndrome[34–36]. Accordingly, metabolic syndrome was ameliorated by pharmacological inhibition of sEH[37, 38]. A similar dysregulation of CYP-mediated eicosanoid metabolism has also been observed in patients with cardiovascular disease, a metabolic condition that shares pathophysiological similarities with OA[39], for which sEH inhibitors (sEHi) have shown promising therapeutic effects[40]. Recently, increased synovial fluid levels of sEH-generated n-6 PUFAs were positively associated with knee OA[41], demonstrating a link between eicosanoid metabolism and OA progression as well. Although initially considered to be inactive EET degradation products, DHETs have been reported to promote CCL2-mediated monocyte chemotaxis in vivo and

to restore sEHi-blocked human monocyte migration *in vitro*[42]. This is particularly interesting, as the CCL2/CCR2 signalling axis has been shown to preferentially mediate monocyte trafficking and promote inflammation and tissue damage in OA[43]. Because circulating monocytes can replenish tissue-resident macrophage populations, which are important players in OA pathogenesis, high systemic DHET levels may directly or indirectly influence the progression of OA through the activation of peripheral monocyte subsets.

To investigate whether peripheral monocyte subsets were indeed affected in our model, we analysed changes in circulating monocyte subsets before and after knee injury. We observed significantly increased monocytic activation, reflected by the upregulation of β_2-integrin CD11c. HFD mice increased monocytic CD11c expression before DMM surgery, demonstrating a dietary effect. It is interesting that LFD mice showed more $CD11c^+$ monocytes at end point (8 weeks after DMM) than before DMM surgery. As it seems not likely that CD11c is a marker for ageing alone, this finding suggests that monocytic CD11c expression partly reflects the consequences of the DMM surgery. However, due to the lack of external sham-operated controls we were not able to verify this possibility in our study. Our finding that CD11c was predominantly expressed by non-classical monocytes is consistent with earlier reports[44] and points to tissue infiltration by this subset. It might be that the increase in the circulating intermediate $CD43^{++}Ly6C^{int}$ monocyte subpopulation indicates renewing of the non-classical monocyte pool by maturation of peripheral classical monocytes. Alternatively, the increase of this pro-inflammatory monocyte subset might indicate a role in metabolic OA pathogenesis. In humans, intermediate monocytes appear to be the main population to be perturbed in disease conditions[45], including metabolic syndrome, rheumatoid arthritis and atherosclerosis[46–48]. Though preliminary, our observations show consistency with current literature on the role of monocyte subsets in inflammation and OA. Elevated monocytic activation has also been reported in women with knee OA and positively associated with BMI[49]. Similar preclinical findings were made in a mouse model of diet-induced atherosclerosis, in which low-grade inflammation sustained elevated levels of $CD11b^+Ly6C^{hi}$ pro-inflammatory monocytes[50]. Here, similar low-grade inflammation instigated significant in vitro expansion of intermediate monocytes in human peripheral blood mononuclear cells[50]. Taken together, our data add to the current understanding that a systemic dysregulated lipid metabolism and immune activation may be independent yet intertwined processes that contribute to the progression of metabolic OA.

We hypothesized that M1 polarization as seen in obesity might drive local metabolic OA pathogenesis, but no significant increases or shift in synovial macrophage subpopulations were observed. The relative increase of synovial $F4/80^+$ macrophages in the HFD group is likely an underestimation, as significant synovial thickening

inherently affects surface area percentages in our image analysis. However, despite the low sample numbers with interindividual variability, our novel triple immunostaining provided a clear image of the local macrophage polarization. We observed a mixed pattern of both M1 and M2 macrophage markers together with increased iNOS deposition in the synovia of HFD mice (data not shown). These novel findings are in line with clinical studies showing that activated human macrophages in the OA knee joint express both M1 and M2 markers while displaying a pro-inflammatory cytokine profile[51, 52]. Therefore, the increased iNOS secretion in the HFD group might reflect altered macrophage activation (instead of polarization) and indicate a pro-inflammatory microenvironment in the knee joint.

In conclusion, we have demonstrated that metabolic stress as applied in this model on its own does not provide sufficient stress for OA development, but clearly aggravated PTOA progression by promoting cartilage damage, synovial inflammation, and osteophyte formation. HFD instigated a proinflammatory environment through systemic changes in lipid metabolism and activation of non-classical monocytes. Based on these results, we propose that a CYP450-focused eicosanoid metabolism and activated circulating monocytes may be drivers of metabolic OA progression. These systemic factors might have future potential as diagnostic and prognostic markers for metabolic OA, consistent with conclusions from a recent clinical study[53, 54]. For the clinical setting, our results imply that pharmacological inhibition of metabolic stress could benefit obese patients with secondary OA. Specifically, inhibition of soluble epoxide hydrolase could be a promising strategy to attenuate metabolic OA.

Acknowledgements
We are very grateful to Dr. Melina Daans for sharing her expertise and providing micro-surgical training to AEK. We thank Sabina Bijlsma and Eric Schoen for their continued statistical support. We thank Martien Caspers for his assistance with the phenotype database repository. We thank Jan Lindeman and Marlieke Geerts at the Leiden University Medical Center and for their help with the development of the triple chromogenic immunostaining for macrophages. We thank Anne Schwerk for her enthusiastic assistance concerning the histological part of the research.

Availability of data and material
The datasets used and/or analysed during the current study are available from the corresponding author on reasonable request. The lipidomic dataset is also stored in a phenotype database repository and is available by signing up via https://dashin.eu/interventionstudies/. After receiving credentials and logging in, the study can be accessed via https://dashin.eu/interventionstudies/study/show/39162914 or by searching the study code (HFD_DMM) or study title ("High-fat diet feeding aggravates osteoarthritis progression in a surgical mouse model: role of eicosanoids and circulating monocytes").

Authors' contributions
AEK, AMZ, IB and RS have designed the experiment. AEK, MT, FC, RS, FH, JB and JB have carried out experimental procedures. AEK has been the primary person responsible for writing the manuscript. HMV, SCM, AMZ, DAB, FPJL, IB, RS, AM and HW were involved in drafting the work or revising it critically for important intellectual content. All authors approved the final version to be published.

Funding
This manuscript was supported by funding from the Netherlands Organization for Applied Scientific Research (TNO) and the European Union's Seventh Framework Programme for research, technological development and demonstration under grant agreement No. 305815-D-BOARD. Funders did not have any additional role in the study design, data collection and analysis, decision to publish or preparation of the manuscript. Specific roles of the authors are described in the Authors' contributions section.

Competing interests
The authors declare that they have no competing interests.

References

1. Murphy LB, Cisternas MG, Greenlund KJ, Giles W, Hannan C, Helmick CG. Defining Arthritis for Public Health Surveillance: Methods and Estimates in Four US Population Health Surveys. Arthritis Care Res Hoboken. 2017;69:356–67.
2. Berenbaum F, Wallace IJ, Lieberman DE, Felson DT. Modern-day environmental factors in the pathogenesis of osteoarthritis. Nat Rev Rheumatol. 2018.
3. Bijlsma JW, Berenbaum F, Lafeber FP. Osteoarthritis: an update with relevance for clinical practice. The Lancet. 2011;377:2115–26.
4. Dell'Isola A, Allan R, Smith SL, Marreiros SS, Steultjens M. Identification of clinical phenotypes in knee osteoarthritis: a systematic review of the literature. BMC Musculoskelet Disord. 2016;17:425.
5. Appleton CT, Hawker GA, Hill CL, Pope JE. Editorial: "Weighing in" on the Framingham Osteoarthritis Study: Measuring Biomechanical and Metabolic Contributions to Osteoarthritis. Arthritis Rheumatol. 2017;69:1127–30.
6. Courties A, Sellam J, Berenbaum F. Metabolic syndrome-associated osteoarthritis. Curr Opin Rheumatol. 2017;29:214–22.
7. Li S, Felson DT. What Is the Evidence to Support the Association Between Metabolic Syndrome and Osteoarthritis? A Systematic Review. Arthritis Care Res. 2019;71:875–84.
8. Obesity: preventing and managing the global epidemic. Report of a WHO consultation. World Health Organ Tech Rep Ser. 2000;894:i–xii, 1–253.
9. Thijssen E, van Caam A, van der Kraan PM. Obesity and osteoarthritis, more than just wear and tear: pivotal roles for inflamed adipose tissue and dyslipidaemia in obesity-induced osteoarthritis. Rheumatol Oxf. 2015;54:588–600.
10. Schwarz S, Mrosewski I, Silawal S, Schulze-Tanzil G. The interrelation of osteoarthritis and diabetes mellitus: considering the potential role of interleukin-10 and in vitro models for further analysis. Inflamm Res. 2018;67:285–300.
11. Buettner R, Scholmerich J, Bollheimer LC. High-fat diets: modeling the metabolic disorders of human obesity in rodents. Obes Silver Spring. 2007;15:798–808.
12. Mulder P, Morrison MC, Wielinga PY, van Duyvenvoorde W, Kooistra T, Kleemann R. Surgical removal of inflamed epididymal white adipose tissue attenuates the development of non-alcoholic steatohepatitis in obesity. Int J Obes. 2016;40:675–84.
13. Wang CY, Liao JK. A mouse model of diet-induced obesity and insulin resistance. Methods Mol Biol. 2012;821:421–33.
14. Kozijn AE, Gierman LM, van der Ham F, Mulder P, Morrison MC, Kuhnast S, *et al.* Variable cartilage degradation in mice with diet-induced metabolic dysfunction: food for thought. Osteoarthritis Cartilage. 2018;26:95–107.
15. Glasson SS, Blanchet TJ, Morris EA. The surgical destabilization of the medial meniscus (DMM) model of osteoarthritis in the 129/SvEv mouse. Osteoarthritis Cartilage. 2007;15:1061–9.

16. Mooney R, Sampson E, Lerea J, Rosier R, Zuscik M. High-fat diet accelerates progression of osteoarthritis after meniscal/ligamentous injury. Arthritis Res Ther. 2011;13:R198.
17. Araujo AC, Wheelock CE, Haeggstrom JZ. The Eicosanoids, Redox-Regulated Lipid Mediators in Immunometabolic Disorders. Antioxid Redox Signal. 2018;29:275–96.
18. Dal-Secco D, Wang J, Zeng Z, Kolaczkowska E, Wong CH, Petri B, *et al.* A dynamic spectrum of monocytes arising from the in situ reprogramming of CCR2+ monocytes at a site of sterile injury. J Exp Med. 2015;212:447–56.
19. Urban H, Little CB. The role of fat and inflammation in the pathogenesis and management of osteoarthritis. Rheumatol Oxf. 2018;57 suppl_4:iv10–21.
20. Glasson SS, Chambers MG, Van Den Berg WB, Little CB. The OARSI histopathology initiative - recommendations for histological assessments of osteoarthritis in the mouse. Osteoarthritis Cartilage. 2010;18 Suppl 3:S17-23.
21. Kozijn AE, Tartjiono MT, Ravipati S, van der Ham F, Barrett DA, Mastbergen SC, *et al.* Human C-reactive protein aggravates osteoarthritis development in mice on a high-fat diet. Osteoarthritis Cartilage. 2019;27:118–28.
22. Gabbs M, Leng S, Devassy JG, Monirujjaman M, Aukema HM. Advances in Our Understanding of Oxylipins Derived from Dietary PUFAs. Adv Nutr. 2015;6:513–40.
23. Guilliams M, Mildner A, Yona S. Developmental and Functional Heterogeneity of Monocytes. Immunity. 2018;49:595–613.
24. Ziegler-Heitbrock L, Ancuta P, Crowe S, Dalod M, Grau V, Hart DN, *et al.* Nomenclature of monocytes and dendritic cells in blood. Blood. 2010;116:e74-80.
25. Louer CR, Furman BD, Huebner JL, Kraus VB, Olson SA, Guilak F. Diet-induced obesity significantly increases the severity of posttraumatic arthritis in mice. Arthritis Rheum. 2012;64:3220–30.
26. Messier SP. Obesity and osteoarthritis: disease genesis and nonpharmacologic weight management. Rheum Clin North Am. 2008;34:713–29.
27. Funk CD. Prostaglandins and leukotrienes: advances in eicosanoid biology. Science. 2001;294:1871–5.
28. Zivkovic AM, Telis N, German JB, Hammock BD. Dietary omega-3 fatty acids aid in the modulation of inflammation and metabolic health. Calif Agric. 2011;65:106–11.
29. de Visser HM, Mastbergen SC, Ravipati S, Welsing PMJ, Pinto FC, Lafeber F, *et al.* Local and systemic inflammatory lipid profiling in a rat model of osteoarthritis with metabolic dysregulation. PLoS One. 2018;13:e0196308.
30. Richardson D, Pearson R, Kurian N, Latif ML, Garle M, Barrett D, *et al.* Characterisation of the cannabinoid receptor system in synovial tissue and fluid in patients with osteoarthritis and rheumatoid arthritis. Arthritis Res Ther. 2008;10:R43.
31. Gierman LM, Wopereis S, van El B, Verheij ER, Werff-van der Vat BJ, Bastiaansen-Jenniskens YM, *et al.* Metabolic profiling reveals differences in concentrations of oxylipins and fatty acids secreted by the infrapatellar fat pad of donors with end-stage osteoarthritis and normal donors. Arthritis Rheum. 2013;65:2606–14.
32. Korotkova M, Jakobsson P-J. Persisting eicosanoid pathways in rheumatic diseases. Nat Rev Rheumatol. 2014;10:229–41.

33. Laufer S. Role of eicosanoids in structural degradation in osteoarthritis. Curr Opin Rheumatol. 2003;15:623–7.
34. Zha W, Edin ML, Vendrov KC, Schuck RN, Lih FB, Jat JL, *et al.* Functional characterization of cytochrome P450-derived epoxyeicosatrienoic acids in adipogenesis and obesity. J Lipid Res. 2014;55:2124–36.
35. Wang W, Yang J, Qi W, Yang H, Wang C, Tan B, *et al.* Lipidomic profiling of high-fat diet-induced obesity in mice: Importance of cytochrome P450-derived fatty acid epoxides. Obes Silver Spring. 2017;25:132–40.
36. Wang W, Yang J, Zhang J, Wang Y, Hwang SH, Qi W, *et al.* Lipidomic profiling reveals soluble epoxide hydrolase as a therapeutic target of obesity-induced colonic inflammation. Proc Natl Acad Sci U A. 2018;115:5283–8.
37. Iyer A, Kauter K, Alam MA, Hwang SH, Morisseau C, Hammock BD, *et al.* Pharmacological inhibition of soluble epoxide hydrolase ameliorates diet-induced metabolic syndrome in rats. Exp Diabetes Res. 2012;2012:758614.
38. Liu Y, Dang H, Li D, Pang W, Hammock BD, Zhu Y. Inhibition of soluble epoxide hydrolase attenuates high-fat-diet-induced hepatic steatosis by reduced systemic inflammatory status in mice. PLoS One. 2012;7:e39165.
39. Fernandes GS, Valdes AM. Cardiovascular disease and osteoarthritis: common pathways and patient outcomes. Eur J Clin Invest. 2015;45:405–14.
40. Theken KN, Schuck RN, Edin ML, Tran B, Ellis K, Bass A, *et al.* Evaluation of cytochrome P450-derived eicosanoids in humans with stable atherosclerotic cardiovascular disease. Atherosclerosis. 2012;222:530–6.
41. Valdes AM, Ravipati S, Pousinis P, Menni C, Mangino M, Abhishek A, *et al.* Omega-6 oxylipins generated by soluble epoxide hydrolase are associated with knee osteoarthritis. J Lipid Res. 2018;59:1763–70.
42. Kundu S, Roome T, Bhattacharjee A, Carnevale KA, Yakubenko VP, Zhang R, *et al.* Metabolic products of soluble epoxide hydrolase are essential for monocyte chemotaxis to MCP-1 in vitro and in vivo. J Lipid Res. 2013;54:436–47.
43. Raghu H, Lepus CM, Wang Q, Wong HH, Lingampalli N, Oliviero F, *et al.* CCL2/CCR2, but not CCL5/CCR5, mediates monocyte recruitment, inflammation and cartilage destruction in osteoarthritis. Ann Rheum Dis. 2017;76:914–22.
44. Sunderkotter C, Nikolic T, Dillon MJ, Van Rooijen N, Stehling M, Drevets DA, *et al.* Subpopulations of mouse blood monocytes differ in maturation stage and inflammatory response. J Immunol. 2004;172:4410–7.
45. Wong KL, Yeap WH, Tai JJY, Ong SM, Dang TM, Wong SC. The three human monocyte subsets: implications for health and disease. Immunol Res. 2012;53:41–57.
46. Stansfield BK, Ingram DA. Clinical significance of monocyte heterogeneity. Clin Transl Med. 2015;4:5.
47. Idzkowska E, Eljaszewicz A, Miklasz P, Musial WJ, Tycinska AM, Moniuszko M. The Role of Different Monocyte Subsets in the Pathogenesis of Atherosclerosis and Acute Coronary Syndromes. Scand J Immunol. 2015;82:163–73.
48. Tsukamoto M, Seta N, Yoshimoto K, Suzuki K, Yamaoka K, Takeuchi T. CD14(bright)CD16+ intermediate monocytes are induced by interleukin-10 and positively correlate with disease activity in rheumatoid arthritis. Arthritis Res Ther. 2017;19:28.
49. Loukov D, Karampatos S, Maly MR, Bowdish DME. Monocyte activation

is elevated in women with knee-osteoarthritis and associated with inflammation, BMI and pain. Osteoarthritis Cartilage. 2018;26:255–63.
50. Geng S, Chen K, Yuan R, Peng L, Maitra U, Diao N, *et al.* The persistence of low-grade inflammatory monocytes contributes to aggravated atherosclerosis. Nat Commun. 2016;7:13436.
51. de Jong AJ, Klein-Wieringa IR, Andersen SN, Kwekkeboom JC, Herb-van Toorn L, de Lange-Brokaar BJE, *et al.* Lack of high BMI-related features in adipocytes and inflammatory cells in the infrapatellar fat pad (IFP). Arthritis Res Ther. 2017;19:186.
52. Daghestani HN, Pieper CF, Kraus VB. Soluble Macrophage Biomarkers Indicate Inflammatory Phenotypes in Patients With Knee Osteoarthritis: Macrophage Markers in OA. Arthritis Rheumatol. 2015;67:956–65.
53. Attur M, Krasnokutsky S, Statnikov A, Samuels J, Li Z, Friese O, *et al.* Low-grade inflammation in symptomatic knee osteoarthritis: prognostic value of inflammatory plasma lipids and peripheral blood leukocyte biomarkers. Arthritis Rheumatol. 2015;67:2905–15.
54. Scanzello CR, Loeser RF. Editorial: Inflammatory Activity in Symptomatic Knee Osteoarthritis: Not All Inflammation Is Local: EDITORIAL. Arthritis Rheumatol. 2015;67:2797–800.

Supplemental Material and methods

Experimental animals and housing

The experiment was carried out in wild-type male C57BL/6J mice purchased from Charles River Laboratories (L'Arbresle Cedex, France) that received a 2-week acclimatization period after transfer to a specific pathogen-free (SPF) animal facility. Age at the start of the study was 12 weeks. Mice were housed in open polycarbonate cages (Type II L) with 2-3 animals/cage. Cages were set up in temperature- (21 ± 0.5°C) and humidity-controlled (45 ± 2%) rooms, with 15 air changes/hour under filtered positive pressure ventilation. Mice were maintained under standard conditions with a 12 h light-dark cycle (beginning at 07:00 UTC+1). The experiment was approved by the institutional Animal Care and Use Committee of TNO and was in compliance with ARRIVE guidelines and European Community specifications regarding the use of laboratory animals.

Diets and surgical intervention

Metabolic stress was induced by providing a high-fat diet (HFD, 45% kcal from fat; cat# D12451, Research Diets, Inc., New Brunswick, USA) to 12-week old male C57BL/6J mice (n=10) for 18 weeks. Ten control mice of same sex and age received a synthetic low-fat diet (LFD, 10% kcal from fat; cat# D12450B, Research Diets, Inc.) during that time period. Group sizes were determined based on variance obtained from pilot data. In turn, estimated effect size and variation of these data will be used to estimate the required sample size for future studies. Mice had access to clean water and food *ad libitum*.

Ten weeks after starting the diet OA was induced in the right knee only by destabilizing the medial meniscus (DMM) as previously described[12]. In short, the medial meniscotibial ligament (MMTL) of the right knee joint was transected, detaching the medial meniscus from the tibial plateau and inducing knee instability. The left knee joint served as an experimental control and received all surgical procedures except for the MMTL transection (sham surgery). Surgery was conducted in waves on several consecutive days, with groups equally divided over the days, time slots, and the groups to avoid effects of date or time on results. Surgery was performed under isoflurane anaesthesia and mice received analgesia 30 minutes before (subcutaneous (sc) injection of 0.05 mg/kg Temgesic) and 4-6 hours after surgery (sc injection of 0.01 mg/kg Temgesic) to minimize suffering. In some cases, equally distributed amongst both groups, analgesic treatment was prolonged for up to 3 days (sc injection of 0.01 mg/kg Temgesic every 12 hours), to prevent gnawing on the sutures and promote recovery. Wound healing and mobility were monitored daily up to 2 weeks after surgery. Mice were euthanized 8 weeks post-surgery using gradual-fill CO_2 asphyxiation.

Assessment of metabolic stress

We define metabolic stress as a significant increase in either body weight and/or fasting cholesterol, glucose and/or insulin plasma levels compared with values as observed in LFD controls. Body weight was determined every other week. Changes in body composition were assessed at 0, 9 and 17 weeks using the quantitative magnetic resonance method (EchoMRI, Echo Medical Systems LLC, Houston, TX, USA – measuring whole body fat, lean, free water, and total water masses in live animals). At regular intervals (t = 0/5/9/14/18 weeks), EDTA plasma samples were collected by tail vein incision after a 4-5 hour fasting period and residual plasma was stored at -80ºC. Total cholesterol was determined directly upon plasma collection by enzymatic assay (No. 11491458216, Roche Diagnostics Nederland BV, The Netherlands) according to manufacturer's instructions. Plasma glucose and insulin levels were measured for all time points at once. Glucose levels were determined by the hexokinase assy using commercially available reagents (No. 2319 and 2942, InstruChemie, The Netherlands; No. G6918, Sigma-Aldrich, The Netherlands). Insulin levels were determined using an ELISA for mouse insulin (Cat.no. 10-1113-01, Mercodia, Sweden). Insulin resistance index (HOMA-IR) was calculated according to the equation proposed by Matthews *et al.*[3]: HOMA-IR = (glucose (mmol/L) × insulin (mU/L)) / 22.5.

Histopathology of the mouse knee joint

Knee joints of the hind limbs were harvested, fixed in a 10% formalin neutral buffered solution (Sigma-Aldrich, USA) for 24 hours, decalcified in Kristensen's solution, dehydrated and embedded in paraffin. Serial coronal 5 µm sections were collected throughout the joint at 60 µm intervals and stained with Weigert's Hematoxylin, Fast Green and Safranin-O. Sections from the front of the knee, at the posterior side of the infrapatellar fat pad, were used to control for successful MMTL transection (Figure S1). Two HFD mice and three LFD control mice showed intact MMTL at their right leg and were excluded from further analysis (leaving n=8 and 7 for comparison). As expected, all sham knee joints showed intact MMTL.

At least two representative sections from the midcoronal region of each knee joint were evaluated for OA severity, using the OARSI histopathology initiative scoring system specifically designed for the mouse4. Grading was performed by two independent observers who were blinded for group assignment (AK and FH). The joint was scored at 6 locations: femoral condyles and tibial plateaus at the lateral and medial sides, trochlear groove and the patella (score 0-6 per articular cartilage compartment). Due to incomplete patellar scores for all mice, we report the sum of the medial and lateral scores as the total tibiofemoral cartilage degeneration score (maximum total score 24). Osteophyte formation and synovitis were scored separately on the same sections and at the same locations. We used the scoring method recommended by the OARSI

histopathology initiative4, where: 0 is normal, 1 = mild, 2 = moderate and 3 = severe changes. For these parameters too, we report the sum of the four compartmental sub scores as the total score (maximum total score 12).

Eicosanoid analyses in fasted plasma

Eicosanoid profiling was performed in the thawed (-80°C frozen) fasted plasma samples obtained at t=0, 9 and 17 weeks. Sample volumes of 50 µl were aliquoted from each plasma sample. Internal standards (10 µl of PGF2a-EA-d4 (2.49µM), 10 µl of AA-d8 (1µM), 10 µl of PGD2-d4 (1µM), 10 µl of 15-HETE-d8 (7.6µM) were added to each sample or blank sample (MilliQ water), along with 2 µl of formic acid (98% v/v) and 5 µl butylhydroxytoluene. Sample preparation and analysis was performed based on the method described by Wong et al.5. In summary, lipids were extracted by SPE, separated using reversed-phase HPLC and detected using tandem mass spectrometry in multiple reaction monitoring mode. Pooled QC samples (human plasma) were interspaced approximately after every 14 study samples to monitor the method performance. Concentrations of a total of 24 eicosanoids were calculated using external calibration standards for each of the analytes. The lipidomic dataset is also stored in a phenotype database repository and is available by signing up via https://dashin.eu/interventionstudies/. After receiving credentials and logging in, the study can be accessed via https://dashin.eu/interventionstudies/study/show/39162914 or by searching the study code (HFD_DMM) or study title ("High-fat diet feeding aggravates osteoarthritis progression in a surgical mouse model: role of eicosanoids and circulating monocytes").

Immunophenotyping of peripheral monocytes by flow cytometry

Monocytic subpopulations were analysed in peripheral blood samples at 9 and 17 weeks, to study changes over time. Blood (5 drops/animal) was drawn via tail incision into lithium heparin-coated Microvette tubes and were further processed within 8 h of collection. Following erythrocyte lysis, cells were washed and resuspended in staining buffer, consisting of a phosphate buffered saline solution with 2% newborn calf serum (PBS-NBCS). Cells were then transferred to a V-bottom 96-wells plate, washed and blocked for non-specific antibody binding with 50 µl normal mouse serum for 15 minutes at room temperature. Cell surface staining was performed with the antibody panel shown in Table 1 (except for CD206, which was used for intracellular staining). Anti-CD16/CD32 monoclonal antibody (clone 2.4G2, dilution 1:50, cat#553141, BD Biosciences, USA) was added to the antibody mix to reduce non-specific antibody binding to Fc gamma II/III receptors. For intracellular staining of the mannose receptor (CD206), cells were fixed and permeabilized using the Fix/Perm kit (BD Pharmingen) according to manufacturer's recommendations and incubated with the relevant

antibody (Table 1). Both staining incubations were performed in PBS-NBCS for 30 minutes at 4ºC. Pooled portions of samples were used for unstained, single-stained and fluorescence minus one (FMO) controls. Data acquisition was performed with a 3-laser FACSCantoTM II flow cytometer using the FACSDiva Software (Becton Dickinson) (Table S1). Cytometer Setup and Tracking beads and CompBeads antibody-capturing particles (both BD Biosciences) were used to standardize instrument and compensation settings, respectively. Flow cytometry data were analysed using FlowJo v10.2 (Treestar Inc., USA). Cell clumps were gated out on a pulse geometry gate (FSC-H x FSC-A). Debris sized <25K were excluded on low angle (forward scatter, FSC) versus 90º angle (side scatter, SSC; "live" gate). Monocytes were identified as positive for CD115 and CD11b expression. Monocyte populations of interest were subsequently defined based on their expression of CD43 and Ly6C (Figure S2). Activation of circulating monocytes was assessed with CD206, which is involved in phagocytosis, and β2-integrin CD11c, which contributes to monocyte arrest on endothelial cells.

Immunohistochemical evaluation of macrophage subsets in the knee

DMM-operated knee joints from both groups were stained for M1 and M2 macrophage subsets by triple-labelling immunohistochemistry (IHC), in which primary antibodies targeted murine macrophages (F4/80, 1:100, MF48000 (BM8), Invitrogen) and their subset-specific markers inducible nitric oxide synthase (iNOS; 1:400, ab136918 (K13-A), Abcam) for M1 macrophages or mannose receptor (CD206, 1:100, AF2535, R&D Systems) for M2 macrophages. Slides were deparaffinized with xylene for 5 min and rehydrated through graded alcohols to DI water. Heat-induced antigen retrieval was performed in the Dako PT Link System using the low pH Target Retrieval Solution (pH 6.0, Dako, CA, USA). After washing, primary antibodies against F4/80 and iNOS were added for overnight incubation at 4°C except for the first section on each slide that served as a negative control. Slides were washed the next day, blocked in 0.3% H_2O_2 for 15 min at RT, and incubated with appropriate AP- and HRP-conjugated secondary antibodies (RALP525 L, Biocare Medical; ab97057, Abcam). Positive reactions were visualized with Ferangi Blue (FB813H, Biocare Medical) for iNOS and StayYellow (ab169561, Abcam) for F4/80. To inactivate preceding labels, slides were incubated with antibody elution buffer (100 mM glycine/NaOH, pH 10.0) for 1 hour at 50°C. Following a washing step, primary antibody against CD206 was added for a 2-hour incubation at 37°C except for the first section on each slide that served as a negative control. Slides were washed and incubated with an appropriate AP-conjugated secondary antibody (ab6886, Abcam), which was visualized with Liquid Fast Red (TA-125-AL, ThermoScientific). Slides were dried in the oven for 1 hour at 37°C and coverslipped with EcoMount (Biocare Medical) for microscopic examination. All intermediate washing steps were done in PBS, except for the visualization steps for which TBS was used. Except for the first secondary

antibody step, antibodies were diluted in PBS with 1% BSA (Sigma-Aldrich).
Quantification was performed in the lateral patellofemoral synovial lining and sub-lining of the knee joint, to avoid confounding influence of the medial surgery through the synovial tissue. Digital images of the unmixed colour spectra for each chromogen in the region of interest (ROI) were obtained with a Nuance multispectral imaging system (40x magnification). Macrophage subtypes were analysed using ImageJ 1.51n image analysis software. Colocalization of two or the three markers was calculated from the areal overlap between positivity for F4/80 and CD206 or iNOS or both. Data are expressed as percentage positivity for a label or combination of labels within the ROI.

Statistical analysis

Statistical analysis was performed using IBM SPSS software (v25.0, IBM SPSS Inc., Chicago, IL, USA). Assumptions of normality were tested with the Shapiro-Wilk's W test and checked graphically based on the residuals. Levene's test was used to assess homogeneity of variances. Mann-Whitney U-test was used for comparison between groups of metabolic parameters, (immuno)histopathological scores and monocyte percentages per time point. Wilcoxon matched-pairs signed rank test was used to compare changes over time in monocyte percentages within each group. Spearman rank correlation was used to test for associations. Two-sample t-testing was used to compare differences in lipid profiles. To account for the effect of time, delta values of eicosanoid levels between time points were used as input. The t-values for the eicosanoids were used for metabolic prioritisation in visualizing the metabolic network, as described previously6. In all analyses, a probability value < 0.05 was considered statistically significant. Unless stated otherwise, data are presented by the median with interquartile range (range between the 25th to 75th percentiles).

Supplemental Tables

Table S1. Flow cytometer setup.

Instrument: Becton Dickinson FACSCanto™ II						
Laser Lines	488 nm				633 nm	405 nm
Emission filters	780/60	670LP	585/42	530/30	660/20	450/50
Fluorochrome	PE/Cy7	PerCP	PE	Alexa Fluor 488	APC	Horizon V450

Table S2. Correlation analyses between synovial macrophage subsets and OA features. Two-tailed Spearman rank correlations between OA features and surface area positivity of the immunohistochemical macrophage markers in the knee joint. Abbreviations: r_s, Spearman's correlation coefficient; p, probability value. Bold font indicates statistically significant correlations between variables. Statistical significance level was set to $p<0.05$.

	OA score total		**OA score lateral**		**Osteophyte score**		**Synovitis score**	
	r_s	p	r_s	p	r_s	p	r_s	p
Positivity within synovial lining (%)								
F4/80	0,474	0,074	0,548	0,035	0,302	0,274	0,726	0,002
CD206	0,342	0,213	0,303	0,272	0,056	0,843	0,510	0,052
iNOS	0,435	0,105	0,454	0,089	0,193	0,490	0,713	0,003
Colocalization within synovial lining (%)								
F4/80 / CD206	0,399	0,141	0,517	0,048	0,372	0,172	0,702	0,004
F4/80 / iNOS	0,463	0,082	0,530	0,042	0,224	0,422	0,688	0,005
CD206 / iNOS	0,462	0,083	0,576	0,025	0,266	0,339	0,568	0,027
F4/80 / CD206 / iNOS	0,494	0,061	0,616	0,015	0,341	0,213	0,635	0,011
Positivity within F4/80+ fraction (%)								
CD206	0,114	0,685	0,075	0,789	0,206	0,461	0,110	0,695
iNOS	-0,027	0,924	0,032	0,909	-0,298	0,280	-0,109	0,700
CD206 / iNOS	0,449	0,093	0,510	0,052	0,307	0,265	0,172	0,540

Abbreviations: AF, Alexa Fluor; PE, phycoerythrin; Cy, cyanine; PerCP, peridinin chlorophyll protein complex; APC, allophycocyanin.
*Intracellular staining.

Supplemental Figures

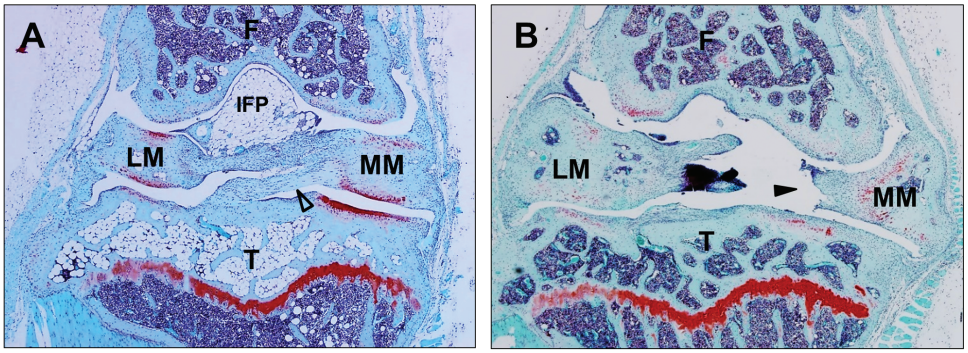


Figure S1. The success of the DMM surgery was assessed by histological analysis of the MMTL. Incomplete transection of the MMTL led to exclusion of the respective animal. A) Intact MMTL (open arrowhead) despite surgical intervention. B) Successful DMM intervention, showing frayed remains of MMTL at the medial meniscus (closed arrowhead). Original magnification ×10. Abbreviations: F, femur; T, tibia; LM, lateral meniscus; MM, medial meniscus; IFP, infrapatellar fat pad.

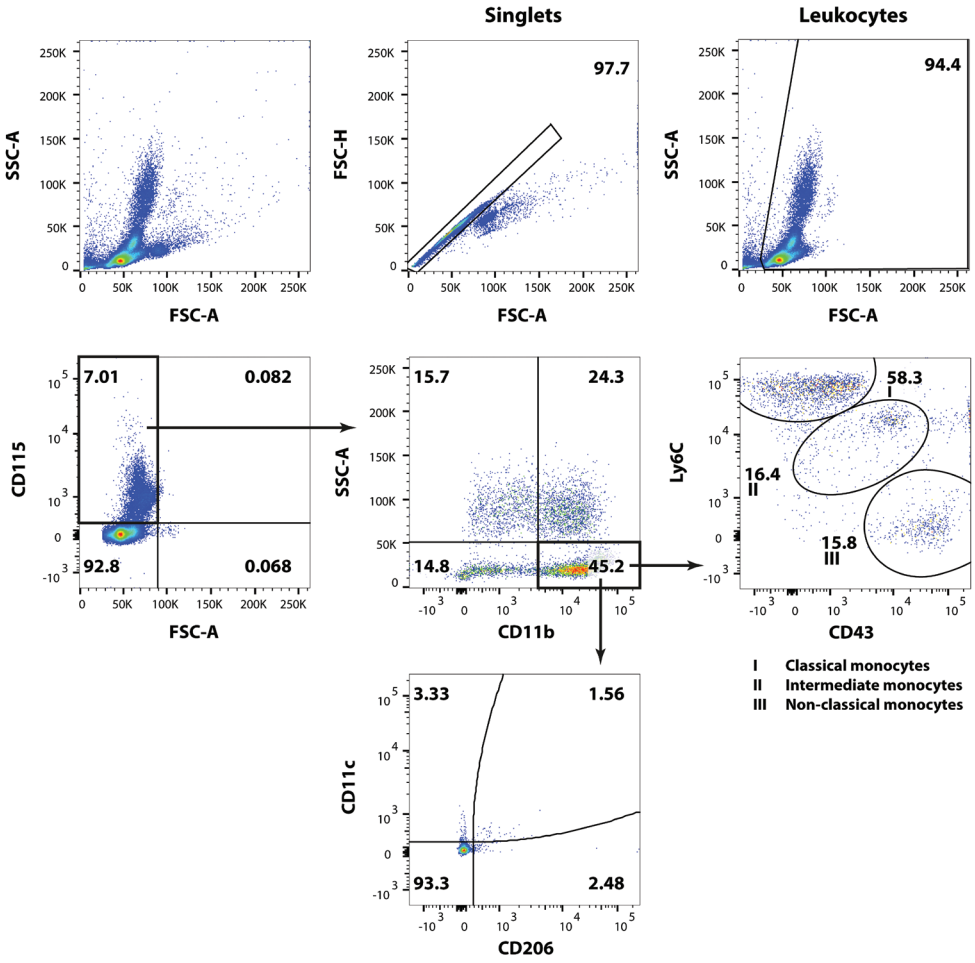


Figure S2. Flow cytometry gating strategy used to detect peripheral monocyte subpopulations. Cell clumps were gated out on a pulse geometry gate (FSC-H×FSC-A; "Singlets"), after which dead cells and debris were gated out according to size and scatter (SSC-A×FSC-A; "Leukocytes"). Positive selection for CD115 removed immature neutrophils and eosinophils. Monocytes were identified based on their size and CD11b expression. Monocyte populations of interest (I-III) were subsequently defined based on their expression of CD43 and Ly6C. Activation of circulating monocytes was assessed with CD206, which is involved in phagocytosis, and β2-integrin CD11c, which contributes to monocyte arrest on endothelial cells

References

1. Glasson SS, Blanchet TJ, Morris EA. The surgical destabilization of the medial meniscus (DMM) model of osteoarthritis in the 129/SvEv mouse. *Osteoarthritis Cartilage* 2007;15(9):1061-9. doi: 10.1016/j.joca.2007.03.006
2. Daans M, Luyten FP, Lories RJ. GDF5 deficiency in mice is associated with instability-driven joint damage, gait and subchondral bone changes. *Ann Rheum Dis* 2011;70(1):208-13. doi: 10.1136/ard.2010.134619 [published Online First: 2010/09/02]
3. Matthews DR, Hosker JP, Rudenski AS, *et al.* Homeostasis model assessment: insulin resistance and beta-cell function from fasting plasma glucose and insulin concentrations in man. *Diabetologia* 1985;28(7):412-9.
4. Glasson SS, Chambers MG, Van Den Berg WB, *et al.* The OARSI histopathology initiative - recommendations for histological assessments of osteoarthritis in the mouse. *Osteoarthritis Cartilage* 2010;18 Suppl 3:S17-23. doi: 10.1016/j.joca.2010.05.025
5. Wong A, Sagar DR, Ortori CA, *et al.* Simultaneous tissue profiling of eicosanoid and endocannabinoid lipid families in a rat model of osteoarthritis. *J Lipid Res* 2014;55(9):1902-13. doi: 10.1194/jlr.M048694
6. Casbas Pinto F, Ravipati S, Barrett DA, *et al.* A methodology for elucidating regulatory mechanisms leading to changes in lipid profiles. *Metabolomics* 2017;13(7):81. doi: 10.1007/s11306-017-1214-y [published Online First: 2017/06/10]



Chapter 4

Increased inflammation in the infrapatellar fat pad in a surgical mouse model of osteoarthritis upon high-fat feeding

Warmink K., Kozijn A.E., Bobeldijk I., Stoop R., Weinans H., Korthagen N.M.

Submitted for publication

Abstract

Background. Obesity is one of the greatest risk factors for osteoarthritis (OA) and evidence is accumulating that inflammatory mediators and innate immunity play an important role. The infrapatellar fat pad (IFP) could be a potential local source of inflammatory mediators in the knee. Here, we combine surgically induced joint damage with high-fat feeding in mice to investigate inflammatory responses in the IFP during OA development.

Methods. Mice (n=30) received either a low-fat diet (LFD), high-fat diet (HFD) for 18 weeks or switched diets (LFD>HFD) after 10 weeks. OA was induced by surgical destabilization of the medial meniscus (DMM) at week 10, contralateral knees served as sham controls. An additional HFD-only group (n=15) received no DMM.

Results. The most pronounced inflammation, characterized by macrophage crown-like structures (CLS), was found in HFD+DMM mice, with increased CLS/1000 adipocytes compared to HFD only (p=0.001) and LFD+DMM (p=0.005). The M1 macrophage marker iNOS increased significantly by DMM (p=0.04), while no change in M2 macrophage marker CD206 was observed. Fibrosis was minimal by HFD alone, but in combination with DMM there was a trend towards increased fibrosis.

Conclusions. These findings indicate that a high-fat diet alone does not trigger inflammation or fibrosis in the infrapatellar fat pad, but in combination with an extra damage trigger, like DMM, induces inflammation, fibrosis and a pro-inflammatory M1 macrophage shift in the infrapatellar fat pad. These data suggest that HFD provides a priming effect on the infrapatellar fat pad and that combined actions bring the joint in a metabolic state of progressive OA.

Introduction

Obesity is one of the greatest risk factors for osteoarthritis (OA) and evidence is accumulating that inflammatory mediators and innate immunity play an important role in obesity-related OA[1, 2]. Adipose tissue is nowadays viewed as an important and complex endocrine organ, containing macrophages and releasing many inflammatory factors that can act both locally and systemically. Well-known adipose factors include cytokines like interleukin-1 and tumor necrosis factor alpha and adipokines such as resistin, adiponectin and leptin[3]. A systematic review showed that the risk of developing hand OA is higher in people with obesity, providing strong evidence for a systemic component in obesity-related OA, as mechanical stress cannot explain the increased OA risk of non-weightbearing joints[4]. However, unraveling the disease process of OA and the causality of obesity or metabolic syndrome in this process remains challenging because of the complex multifactorial nature of OA[5].

OA is considered to be a whole joint disease, where cartilage, bone, synovium, menisci, ligaments, muscles and the joint capsule are all involved[6, 7]. The infrapatellar fat pad (IFP) or Hoffa's fat pad was proposed as an additional tissue that is involved in the pathogenesis of knee OA[8]. The IFP is an adipose tissue depot located within the articular capsule of the knee and thereby a potential local source of inflammatory mediators. The IFP is vascularized, well innervated, and consists mainly of adipocytes, fibroblasts and immune cells8, 9. Adipokines produced by adipocytes are found in the synovial fluid of OA patients and the leptin concentration is known to correlate with OA severity[10, 11]. The role of the IFP in the development of OA is still unclear, as both protective and harmful effects of the IFP and cell subsets in the IFP have been reported[12]. The secretion of several inflammatory mediators was found to be significantly higher in the IFP from OA patients, when compared to subcutaneous adipose tissue from the same patient[13]. These data suggest that there could be a role for the IFP during the development of OA, as a secretory organ releasing inflammatory mediators into the knee joint. However, research done on human IFP is mostly from end-stage OA patients undergoing knee arthroplasty and it might therefore misrepresent the true effect of the IFP in the disease process.

The release of pro-inflammatory cytokines by adipose tissue increases in obesity and is known to be primarily caused by nonfat cells9. Approximately 5% of all cells in adipose depots of both mice and humans are macrophages, but during obesity the percentage of macrophages increases, up to 50% of total cells[14]. In the healthy situation, macrophage populations in adipose tissue consist mainly of anti-inflammatory CD206-positive M2 type macrophages[15, 16]. However, in obesity, fat depots throughout the body, but especially abdominal fat, show a switch to a pro-inflammatory M1 macrophage phenotype, characterized by the production of several factors of which inducible nitric

oxide synthase (iNOS) is one[17]. Next to the switch in macrophage phenotype, adipose inflammation in obesity is often accompanied by tissue fibrosis[18] and an increase in adipocyte size, which reflects the metabolic cell stress[19]. When hypertrophic adipocytes die, macrophages will surround the dying cell and thereby form a crown-like structure (CLS)[20, 21]. The CLS count in histological sections is a good indication of the inflammatory state of the IFP and macrophage infiltration the inflamed adipose tissue. In human end-stage OA the macrophage phenotype in the IFP is found to be predominantly anti-inflammatory and CD206-positive[22], but there are indications that the IFP may have a pro-inflammatory contribution in the earlier phase of the disease process[12, 23].
Although long-term feeding of high-caloric diets consistently induces metabolic syndrome in rodents, diet-induced cartilage degradation proved variable in such models[24]. It seems that an additional trigger is needed to induce or accelerate diet-induced OA progression in the joint[25, 26]. We hypothesize a similar effect will be observed regarding inflammatory responses in the IFP, and that inflammation and OA induction is small upon high-fat feeding alone, but will be accelerated in combination with an extra trigger. Therefore, we employed a surgical model of OA by destabilization of the medial meniscus (DMM). We compared mice with injury-induced OA on a high-fat (HFD) or low-fat diet (LFD) with mice on a HFD alone. The inflammatory responses of the IFP to the destabilization trigger in a metabolically loaded system was investigated.

Materials and methods

Experimental design

Experimental groups were formed by 30 male wild-type C57BL/6J mice (Charles River Laboratories) that received a diet low-fat diet (LFD, 10% kcal from fat; cat# D12450B, Research Diets, Inc., New Brunswick, USA) or high-fat diet (HFD, 45% kcal from fat; cat# D12451, Research Diets, Inc.) for 18 weeks combined with surgical destabilization of the medial meniscus (DMM) at week 10. The 30 mice were randomized into 3 groups; high-fat diet (HFD+DMM group), low-fat diet (LFD+DMM group) and a third group that switched from a LFD to a HFD after 10 weeks (LFD>HFD+DMM group). An additional control group consisted of 15 male wild-type C57BL/6J mice taken from another study[27] that received the same HFD (cat# D12451, Research Diets, Inc.) without any surgical intervention (HFD-only group) for 38 weeks. This prolonged study duration ensured OA development in this mild model. Albeit from another litter and the time period of this HFD-only group was approximately twice as long, we felt that this additional control group could provide important information on the effects of diet in addition to contralateral sham-operated control knees from the HFD+DMM group. All mice started at 12 weeks of age and were fed *ad libitum*. Mice were housed

in open polycarbonate cages (Type II L) with 2-3 animals per cage. Cages were set up in temperature-controlled (21 ± 0.5°C) and humidity-controlled (45 ± 2%) rooms, with 15 air changes/hour under filtered positive pressure ventilation. Mice were maintained under standard conditions with a 12 h light-dark cycle (beginning at 07:00 UTC+1). All experiments were approved by the institutional Animal Care and Use Committee of TNO and were in compliance with European Community specifications regarding the use of laboratory animals (European Directive 2010/63/EU).

Surgical intervention

In the groups that received surgical intervention, OA was induced by destabilization of the medial meniscus as described previously [28]. In this procedure, the medial meniscotibial ligament (MMTL) of the right knee was transected to detach the medial meniscus from the tibial plateau and thereby causing knee instability. The left knee served as an internal control where sham surgery was performed. Surgery was performed under general anesthesia (isoflurane) and all mice received a subcutaneous injection of analgesia (Temgesic) 30 minutes before (0.05 mg/kg) and 4-6 hours after surgery (0.01 mg/kg). To prevent gnawing on the sutures analgesic treatment could be prolonged up to 3 days with 0.01 mg/kg Temgesic every 12 hours. Surgery was conducted on several consecutive days. Groups were equally divided over the days and time slots to avoid any influence on the outcome of this study.

Metabolic status and histological evaluation

Metabolic overload was monitored during the study, body weight and body composition (EchoMRI LLC, Houston, TX, USA) were assessed at regular intervals. EDTA samples were collected to determine fasted plasma total cholesterol, glucose and insulin levels. Insulin resistance index (HOMA-IR) was calculated according to the equation proposed by Matthews *et al*.[29], where HOMA-IR = glucose (mmol/L) x insulin (mU/L) / 22.5.

All knees were processed for histological evaluation. Articular cartilage degradation, osteophyte formation and synovitis were scored on Hematoxylin, Fast Green and Safranin-O stained 5um sections of the midcoronal region of each knee joint. The OARSI histopathology initiative scoring specifically designed for mouse was used as scoring system[30]. For all parameters we report the sum of the compartments as the total score, the patella compartments were not included in this study. In mice that received DMM surgery, histological sections from the front of the knee were used to check for successful MMTL transection. Based on an intact MMTL two HFD+DMM mice and 3 LFD+DMM mice were excluded from further analysis.

Hematoxylin phloxine saffron (HPS) stained sections of the joint including the IFP were used to determine the number of crown-like structures (CLS) per 1000 adipocytes. Picrosirius red stained sections were used to assess collagen levels in the IFP. For each

sample, the number of CLS and the level of sirius red staining was determined by using at least 3 individual coupes. CLS were counted blinded by two independent assessors, a CLS was defined by the presence of at least 4 nuclei, not originating from blood vessels, around one adipocyte combined with stained cytoplasm surrounding the adipocyte. The picrosirius red staining was quantified in ImageJ, using images that were converted to 8-bit with exclusion of background, and the percentage area of red staining was calculated. Number and size of adipocytes in the IFP was determined using the ImageJ Adiposoft plugin[31]. For each section three images were captured with an Olympus SC50 camera at 10x magnification and the average adipocyte number per μm^2 and average adipocyte size was determined.

Immunohistochemical assessment of macrophage subsets in the IFP

Knee joints from all groups were stained with chromogenic triple-labeling immunohistochemistry for M1 (iNOS) and M2 (CD206) macrophage subsets, based on a previously described method for human tissue[32]. Primary antibodies were applied for F4/80 to target murine macrophages (1:100, MF48000 BM8, Invitrogen), iNOS (1:400, ab136918 K13-A, Abcam) and CD206 (1:100, AF2535, R&D Systems). Heat-induced antigen retrieval was performed in the Dako PT Link System using the low pH Target Retrieval Solution (pH 6.0, Dako, CA, USA). First, primary antibodies against F4/80 and iNOS were incubated overnight at 4°C. Slides were blocked for endogenous peroxidase in 0.3% H_2O_2 for 15 min at room temperature, and incubated with alkaline phosphatase and horseradish peroxidase conjugated secondary antibodies (RALP525 L, Biocare Medical; ab97057, Abcam). Positive reactions were visualized with Ferangi Blue (FB813H, Biocare Medical) for iNOS and StayYellow (ab169561, Abcam) for F4/80. To inactivate preceding labels, slides were incubated with antibody elution buffer (100 mM glycine/NaOH, pH 10.0) for 1 hour at 50°C. Then, the primary antibody against CD206 was added for a 2-hour incubation at 37°C. Slides were washed and incubated with an AP alkaline phosphatase conjugated secondary antibody (ab6886, Abcam), which was visualized with Liquid Fast Red (TA-125-AL, ThermoScientific). Digital images of the unmixed colour spectra for each chromogen in the IFP were obtained with a Nuance multispectral imaging system (20x magnification). Macrophage subtypes were analyzed using ImageJ image analysis software (1.47v, Wayne Rasband, Bethesda, MD, USA). Colocalization of two or the three markers was calculated from the areal overlap between positivity for F4/80 and CD206 or iNOS or both. Data are expressed as percentage positivity for a label or combination of labels within the IFP or within the F4/80 macrophage population.

Statistics

Statistical analysis was performed using Prism (v7.04, GraphPad Software, La Jolla, CA, USA) and IBM SPSS software (v25.0, IBM SPSS Inc., Chicago, IL, USA). Normality was tested with the Shapiro-Wilk's W test and checked graphically. Statistical significance among different groups in normally distributed data was assessed using the one-way ANOVA with Tukey's multiple comparisons test. Non-normally distributed data was analyzed using the Kruskal-Wallis test with Dunn's multiple comparisons test. P-values ≤0.05 were considered statistically significant. Graphs and error bars represent median +/- interquartile range (IQR), p-values in graphs are reported with asterisks where p≤0.05 is *, p≤0.01 is **, p≤0.001 is *** and p>0.05 is not significant (NS).

Results

Metabolic status and osteoarthritis development

The metabolic status of the mice was monitored during the study period. At initiation of the diet at 12 weeks of age the average cholesterol level and fat mass percentage were comparable between the four groups (p=0.571 and p=0.210, respectively). During the study period HFD feeding caused metabolic overload, reflected by an increase in body weight (Figure 1A) and fat percentage (Figure 1B), which was largest in the HFD groups. Similarly, cholesterol levels, insulin levels and glucose levels were elevated at end point in the two HFD groups compared to other groups (Table 1). Even though body composition at week 0 was not different, the HFD-only group did have a higher total body weight at the start of the study, likely related to the fact that they were from a different litter used in another study.

Cartilage degradation and osteophyte formation was histologically assessed in all knees. Cartilage degradation was most pronounced in HFD+DMM knees with a median [IQR] of 19.38 [15.06-20.94] versus 17.0 [10.31-23.13] in the LFD>HFD+DMM knees and 13.75 [8.0-20.0] in the LFD+DMM knees, the difference between HFD+DMM and LFD+DMM was statistically significant (p<0.05) (figure 1C). The HFD-only group, although 20 weeks older, had an OA score of 4.25 [3.71-5.44] which was comparable to internal sham surgery joints. Osteophyte formation was significantly increased in the HFD+DMM group compared to the LFD+DMM group (p=0.04) (Figure 1D). Both OA score and osteophytosis were considerably lower in contralateral knee joints (sham) and in knee joints from HFD-only mice (Figure 1 C,D).

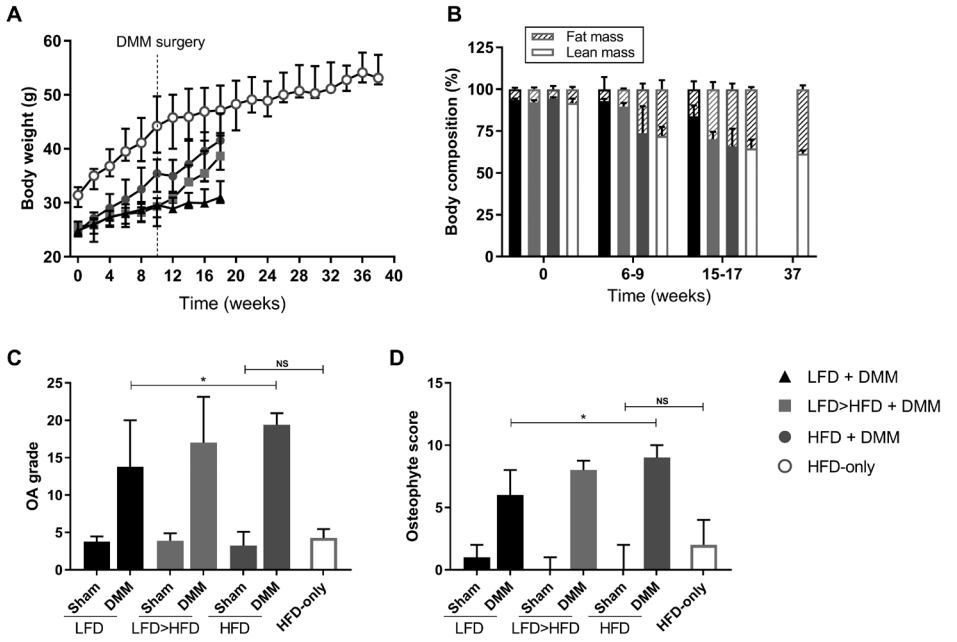


Figure 1. Metabolic and OA status of the mice. A) Body weight during the study period per study group. B) Body composition at several time points during the study, percentage of lean mass and fat mass are depicted. C) Summed OA score and D) osteophyte score at the end of the study period. Graphs and error bars represent median +/- interquartile range (IQR).

Synovitis and inflammation markers in the infrapatellar fat pad

Synovitis was increased in the knees that received DMM compared to internal sham controls and was most aggravated in the HFD+DMM group with a median [IQR] of 6.50 [5.25-8.50] (Figure 2A). The HFD-only group, receiving no additional intervention to induce OA apart from the 38-week HFD regimen, showed a synovitis score of 4.0 [4.0-6.0] that was significantly higher than the sham controls from the HFD+DMM group ($p<0.0001$). Adipose inflammation in the IFP, reflected by the number of CLS/1000 adipocytes, was low in the HFD-only group (2.41 [2.04-3.30] CLS/1000 adipocytes) and LFD+DMM group (1.82 [0.71-5.27] CLS/1000 adipocytes; Figure 2B). Only when OA was induced by DMM surgery in HFD-fed mice, a significant increase in CLS was observed (7.45 [1.11-15.62] CLS/1000 adipocytes) compared to HFD-only and LFD+DMM groups ($p<0.005$). Remarkably, contralateral joints of the HFD+DMM group also showed a trend towards increase in the amount of CLS (3.50 [2.43-9.48] CLS/1000 adipocytes). Adipocyte hypertrophy was distinct in groups receiving HFD compared with the LFD+DMM group ($p<0.001$) (Figure 2C + 2D).

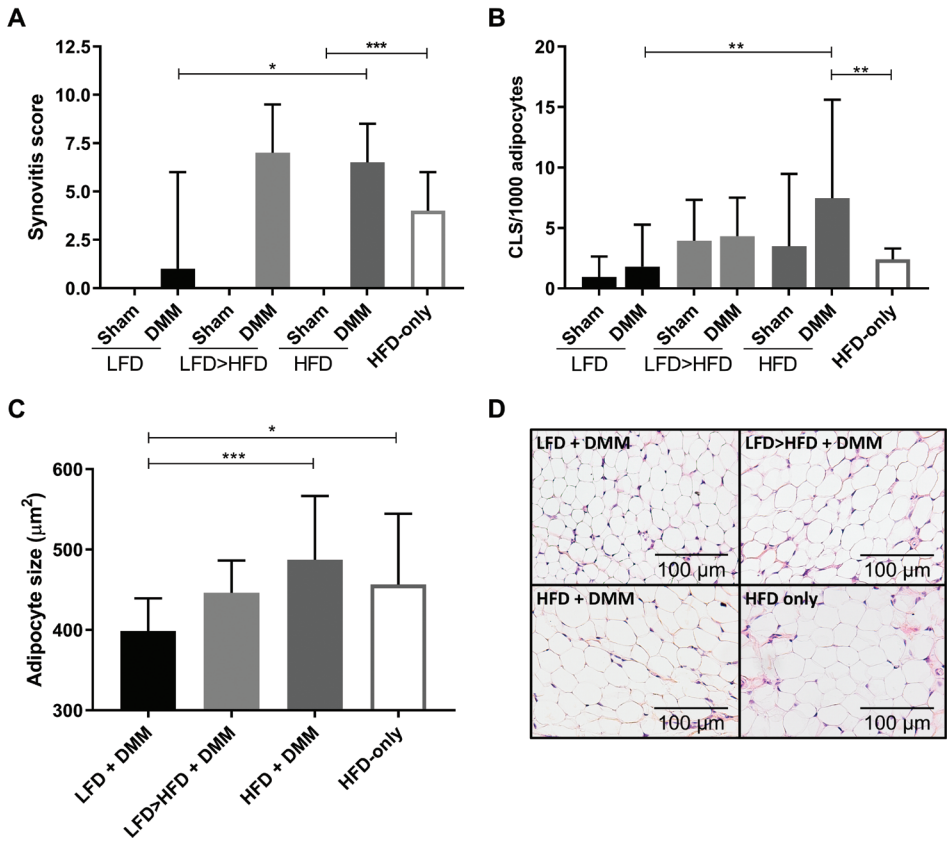


Figure 2. Markers of inflammation in the synovium and IFP. A) Histologically assessed synovitis score per group. B) Crown-like structure count in the IFP, expressed per 1000 adipocytes. C) The adipocyte size in the IFP, with D) representative images HPS stained IFP sections indicating the adipocyte size per group. Graphs and error bars represent median +/- interquartile range (IQR).

Macrophage phenotypes in the infrapatellar fat pad

To investigate the phenotype of macrophages in the IFP a triple immunohistochemistry staining was used to distinguish between pro-inflammatory M1 (F4/80+ and iNOS+) and anti-inflammatory M2 (F4/80+ and CD206+) macrophages (Figure S1). The pan macrophage marker F4/80 showed a positive surface area of 0.67% [0.49-1.14] in the IFP of the HFD-only group, compared to 1.18% [0.72-1.22] in the HFD+DMM group and 0.94% [0.68-1.25] in the LFD+DMM group, which were all not statistically different (Figure 3A). CD206 positivity in the IFP sections was low (<0.50%) and similar between groups, regardless of diet or DMM surgery (Figure 3B). The percentage of iNOS positive area was very low in the HFD-only group with 0.17% [0.11-0.23] but significantly higher

in DMM groups with a median of 0.54% [0.39-0.85] in the LFD+DMM group and 0.39% [0.27-0.42] in the HFD+DMM group (Figure 3C). When we evaluated colocalization of F4/80 with macrophage phenotype markers iNOS (M1) and CD206 (M2) showed no change in CD206-positive area between groups (Figure 3D). However, iNOS positivity within the total F4/80 area increased significantly, from 8.80% [5.80-11.83] in the HFD-only group to 13.68% [12.05-20.75] (p=0.04) and 13.40% [10.19-16.67] (p=0.07) in the LFD+DMM and HFD+DMM groups, respectively (Figure 3E). This indicates that DMM surgery provoked a relative increase in pro-inflammatory M1 macrophages in these mice.

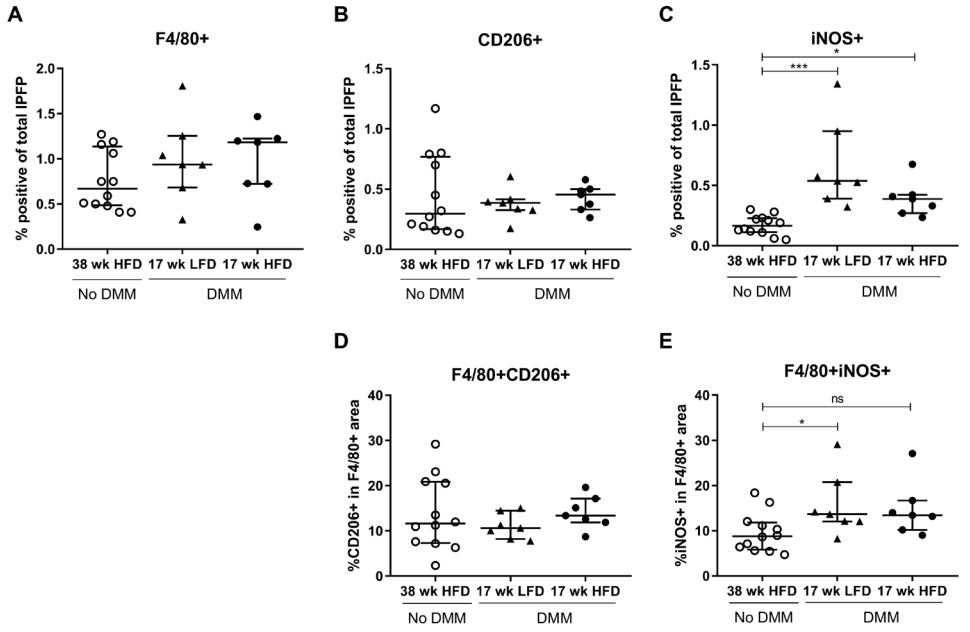


Figure 3. Macrophage phenotypes in the IFP. A) Percentage positive area of the pan macrophage marker F4/80, B) anti-inflammatory M2 macrophage marker CD206 and C) pro-inflammatory M1 macrophage marker iNOS in the total analyzed area of the IFP. D) Colocalization of F4/80 and CD206 and E) Colocalization of F4/80 and iNOS, both expressed as percentage of the total positive F4/80 area. Graphs and error bars represent median +/- interquartile range (IQR).

Fibrosis in the infrapatellar fat pad

To get an indication of the level of fibrosis in the IFP, collagen was stained using picrosirius red (Figure 4). The percentage of sirius red staining was lowest in the HFD-only group and significantly different from all the other groups (p<0.05), with a median [IQR] of 3.82% [2.61-4.71], indicating there is little collagen or fibrosis formation in these

fat pads. In the sham operated groups the level of collagen was similar, varying from 10.65% to 12.62%. The staining in the LFD+DMM group had a median positive area of 11.14% [9.44-25.47] and the LFD>HFD+DMM group had a slightly higher percentage of 17.67% [12.09-25.06]. The HFD+DMM group had the highest level of sirius red staining, with a median of 26.20% [14.10- 48.51], although it was not significantly different from other groups or the sham joint.

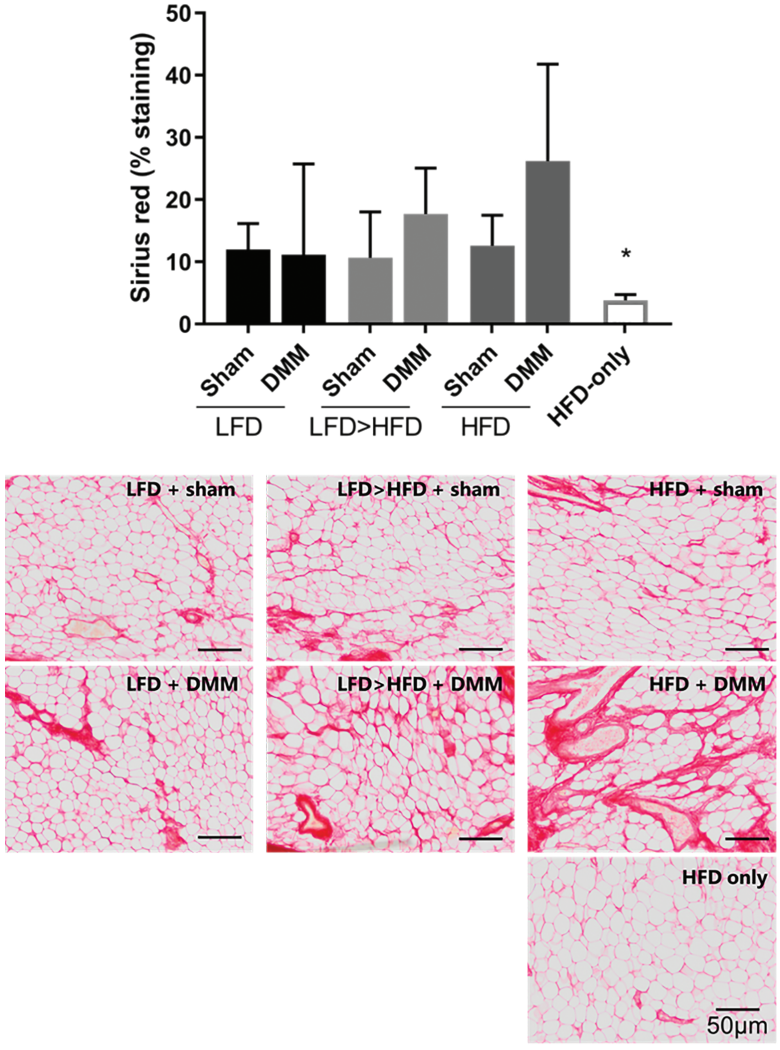


Figure 4. Fibrosis in the IFP. The percentage positive picrosirius red staining measured in the IFP sections, shown together with representative images of staining in the experimental groups. Graphs and error bars represent median +/- interquartile range (IQR).

Discussion

In this study we investigated the effects of high-fat feeding and DMM-induced OA on the metabolic load and innate immune response in the IFP. We found that DMM-induced OA in combination with HFD feeding increased IFP inflammation, characterized by an increase in CLS, and showed a trend towards increased fibrosis, characterized by picrosirius red staining. Long-term HFD feeding alone did not induce IFP inflammation or fibrosis, even though we did observe an increase in synovial inflammation after 38 weeks HFD. Interestingly, when DMM was applied, the contralateral (sham) joint also showed increased signs of IFP inflammation, although not significantly. Furthermore, we saw an significant increase in the adipocyte size from 400 to 500 micrometers comparing the LFD and HFD groups, however, this increase is modest compared to adipocyte enlargement usually observed in subcutaneous and visceral murine fat tissue depots in response to high-fat feeding[33]. As adipocyte size is an indicator of metabolic loading and inflammation[20], this finding, together with the low CLS count and little fibrosis in the HFD-only group, indicates that the IFP is less susceptible to develop inflammation in response to HFD than other fat depots such as intra-abdominal and subcutaneous fat. This finding is in line with a previous study reporting no pro-inflammatory M1 macrophage-mediated inflammation in the IFP of obese C57BL/6J mice prior to OA development[34]. However, we do observe changes in the IFP when an additional OA trigger is given in HFD animals, suggesting that there is a systemic priming effect of HFD on the IFP.

In response to obesity, macrophages in fat depots across the body are known to undergo a phenotype switch to pro-inflammatory M1 macrophages17. However, we did not find any changes in macrophage phenotype in the IFP associated with diet alone. We observed an increase in the pan macrophage marker F4/80 in groups that underwent DMM surgery but not in the (non DMM) HFD-only group. This increase in F4/80 was accompanied by a minor shift in macrophage phenotype, indicated by an increase in iNOS marker in the F4/80 positive area, suggesting an inflow of M1 macrophages to the IFP rather than polarization of resident M2 macrophages. This hypothesis is in line with the macrophage subsets found in human OA IFP, which is reported to be high in CD206+ cells compared to subcutaneous fat and compared to IFP of non-obese OA patients[22, 35]. Our findings indicate that HFD alone does not induce increased inflammation in the IFP as it does in other adipose depots in the body, but that an extra trigger, like DMM is needed before the IFP shows serious signs of inflammation or an increase in pro-inflammatory M1 macrophages. In a rat HFD groove model of OA where folate receptor expressing macrophages were imaged using SPECT/CT similar observations were made regarding macrophage activity in the total knee joint; when HFD was combined with mechanically induced cartilage damage a profound increase in macrophage activity

was observed[36]. Not only immune cells seem to react upon a trigger, several studies in rodents suggest that OA progression in animals with a metabolic phenotype is also accelerated upon mechanical or other stressors like gender, age and genetics[24, 25, 37].
The striking difference between the IFP and other adipose tissue in response to HFD in terms of inflammation and macrophages might be clarified by its unique anatomical location. In the knee joint the IFP is thought to function as a shock absorber[38], and its importance for knee function is substantiated by the preservation of the IFP under extreme starvation[39]. The IFP is known to be a fibrous adipose tissue type and has a greater stiffness compared to other adipose tissues, which is thought to be a result of the constant biomechanical stress[40, 41]. We observed a large difference in collagen levels in the IFP between the HFD+DMM group and the HFD only group, which is in agreement with previous literature findings that fibrotic processes in the human IFP are independent from BMI or obesity[42, 43]. We do see an increase in fibrosis in response to damage in the knee joint in an HFD environment as the highest values of Sirius red were observed when high fat feeding and DMM are combined. These findings contribute to the previously stated hypothesis that fibrosis in the IFP is not directly a result of obesity, but might be a tissue healing response in reaction to the injury that arises in the knee joint during OA[44]. Apparently, in a metabolically primed joint this effect is more pronounced.
The clinical relevance of changes in the human IFP during OA is under investigation. A recent study showed that volume change in the IFP measured by MRI is not associated with obesity but with cartilage degeneration[45]. This is in agreement with our finding that a HFD alone provokes little effect in the IFP, but additional cartilage damage induced by DMM does. Other studies have shown correlations between IFP volume, joint pain and joint inflammation in OA patients[46, 47]. On the other hand, there are also studies that showed a protective effect of IFP size on knee pain and cartilage defects[48, 49], possibly explained by the mechanism of shock absorption.
This study included a set of 15 mice that received HFD for an extended period of 38 weeks without DMM surgery to induce OA (HFD-only group)[27]. Differences found between the HFD+DMM and HFD-only group might be an underestimation, as the HFD-only group continued the diet 20 weeks longer compared to the DMM groups, possibly leading to a more aggravated state of OA and IFP inflammation than the state of the knee joint at 18 weeks of HFD-only. As this would result in an underestimation of the effects reported here, we consider our results to remain valid indicators for the effects of HFD and DMM on the inflammatory state of the IFP.
In summary, we found few signs of inflammation or fibrosis in the IFP due to high-fat feeding alone. We propose that metabolic overload primes adipocytes in the IFP for inflammation and cell stress upon a damaging trigger, as indicated by an increased amount of CLS and a trend towards more fibrosis upon surgical induction of OA. In this

provoked setting, inflammatory mediators excreted by adipocytes and M1 macrophages could contribute to the development of (metabolic) knee OA. However, in light of our results it seems unlikely that IFP inflammation can initiate OA development by obesity alone.

Acknowledgements
We are very grateful to Dr. Melina Daans for sharing her expertise and providing micro-surgical training to AK. We thank Jan Lindeman and Marlieke Geerts at the Leiden University Medical Center, Monica Tartjiono and Anne Schwerk for their help with the development of the triple chromogenic immunostaining for macrophages.

Authors' contributions
AK, IB and RS designed and performed the animal studies. AK and KW acquired and analyzed data. KW drafted the initial manuscript, all authors were involved in revising the manuscript. All authors read and approved the final manuscript.

Funding
This research was funded by the Dutch Research Council (NWO) domain Applied and Engineering Sciences (P15-23), the Netherlands Organization for Applied Scientific Research (TNO) and the European Union's Seventh Framework Programme for research, technological development and demonstration under grant agreement No. 305815-D-BOARD. The funders had no role in study design, data collection and analysis, decision to publish, or preparation of the manuscript.

Competing interests
The authors declare that they have no competing interest.

References

1. Goldring MB, Otero M. Inflammation in osteoarthritis. Curr Opin Rheumatol. 2011;23(5):471-8.
2. Kapoor M, Martel-Pelletier J, Lajeunesse D, Pelletier JP, Fahmi H. Role of proinflammatory cytokines in the pathophysiology of osteoarthritis. Nat Rev Rheumatol. 2011;7(1):33-42.
3. Kershaw EE, Flier JS. Adipose tissue as an endocrine organ. J Clin Endocrinol Metab. 2004;89(6):2548-56.
4. Yusuf E, Nelissen RG, Ioan-Facsinay A, Stojanovic-Susulic V, DeGroot J, van Osch G, *et al.* Association between weight or body mass index and hand osteoarthritis: a systematic review. Ann Rheum Dis. 2010;69(4):761-5.
5. Musumeci G, Aiello FC, Szychlinska MA, Di Rosa M, Castrogiovanni P, Mobasheri A. Osteoarthritis in the XXIst century: risk factors and behaviours that influence disease onset and progression. Int J Mol Sci. 2015;16(3):6093-112.
6. Poole AR. Osteoarthritis as a whole joint disease. HSS J. 2012;8(1):4-6.
7. Hunter DJ, Felson DT. Osteoarthritis. BMJ. 2006;332(7542):639-42.
8. Clockaerts S, Bastiaansen-Jenniskens YM, Runhaar J, Van Osch GJ, Van Offel JF, Verhaar JA, *et al.* The infrapatellar fat pad should be considered as an active osteoarthritic joint tissue: a narrative review. Osteoarthritis Cartilage. 2010;18(7):876-82.
9. Fain JN. Release of interleukins and other inflammatory cytokines by human adipose tissue is enhanced in obesity and primarily due to the nonfat cells. Vitam Horm. 2006;74:443-77.
10. Schaffler A, Ehling A, Neumann E, Herfarth H, Tarner I, Scholmerich J, *et al.* Adipocytokines in synovial fluid. JAMA. 2003;290(13):1709-10.
11. Ku JH, Lee CK, Joo BS, An BM, Choi SH, Wang TH, *et al.* Correlation of synovial fluid leptin concentrations with the severity of osteoarthritis. Clin Rheumatol. 2009;28(12):1431-5.
12. Ioan-Facsinay A, Kloppenburg M. An emerging player in knee osteoarthritis: the infrapatellar fat pad. Arthritis Res Ther. 2013;15(6):225.
13. Klein-Wieringa IR, Kloppenburg M, Bastiaansen-Jenniskens YM, Yusuf E, Kwekkeboom JC, El-Bannoudi H, *et al.* The infrapatellar fat pad of patients with osteoarthritis has an inflammatory phenotype. Ann Rheum Dis. 2011;70(5):851-7.
14. Weisberg SP, McCann D, Desai M, Rosenbaum M, Leibel RL, Ferrante AW, Jr. Obesity is associated with macrophage accumulation in adipose tissue. J Clin Invest. 2003;112(12):1796-808.
15. Nawaz A, Aminuddin A, Kado T, Takikawa A, Yamamoto S, Tsuneyama K, *et al.* CD206(+) M2-like macrophages regulate systemic glucose metabolism by inhibiting proliferation of adipocyte progenitors. Nat Commun. 2017;8(1):286.
16. Gordon S. Alternative activation of macrophages. Nat Rev Immunol. 2003;3(1):23-35.
17. Castoldi A, Naffah de Souza C, Camara NO, Moraes-Vieira PM. The Macrophage Switch in Obesity Development. Front Immunol. 2015;6:637.
18. Datta R, Podolsky MJ, Atabai K. Fat fibrosis: friend or foe? JCI Insight. 2018;3(19).

19. Choe SS, Huh JY, Hwang IJ, Kim JI, Kim JB. Adipose Tissue Remodeling: Its Role in Energy Metabolism and Metabolic Disorders. Front Endocrinol (Lausanne). 2016;7:30.
20. Skurk T, Alberti-Huber C, Herder C, Hauner H. Relationship between adipocyte size and adipokine expression and secretion. J Clin Endocrinol Metab. 2007;92(3):1023-33.
21. Cinti S, Mitchell G, Barbatelli G, Murano I, Ceresi E, Faloia E, *et al.* Adipocyte death defines macrophage localization and function in adipose tissue of obese mice and humans. J Lipid Res. 2005;46(11):2347-55.
22. Bastiaansen-Jenniskens YM, Clockaerts S, Feijt C, Zuurmond AM, Stojanovic-Susulic V, Bridts C, *et al.* Infrapatellar fat pad of patients with end-stage osteoarthritis inhibits catabolic mediators in cartilage. Ann Rheum Dis. 2012;71(2):288-94.
23. Iwata M, Ochi H, Hara Y, Tagawa M, Koga D, Okawa A, *et al.* Initial responses of articular tissues in a murine high-fat diet-induced osteoarthritis model: pivotal role of the IPFP as a cytokine fountain. PLoS One. 2013;8(4):e60706.
24. Kozijn AE, Gierman LM, van der Ham F, Mulder P, Morrison MC, Kuhnast S, *et al.* Variable cartilage degradation in mice with diet-induced metabolic dysfunction: food for thought. Osteoarthritis Cartilage. 2018;26(1):95-107.
25. de Visser HM, Mastbergen SC, Kozijn AE, Coeleveld K, Pouran B, van Rijen MH, *et al.* Metabolic dysregulation accelerates injury-induced joint degeneration, driven by local inflammation; an in vivo rat study. J Orthop Res. 2018;36(3):881-90.
26. Mooney RA, Sampson ER, Lerea J, Rosier RN, Zuscik MJ. High-fat diet accelerates progression of osteoarthritis after meniscal/ligamentous injury. Arthritis Res Ther. 2011;13(6):R198.
27. Kozijn AE, Tartjiono MT, Ravipati S, van der Ham F, Barrett DA, Mastbergen SC, *et al.* Human C-reactive protein aggravates osteoarthritis development in mice on a high-fat diet. Osteoarthritis Cartilage. 2019;27(1):118-28.
28. Culley KL, Dragomir CL, Chang J, Wondimu EB, Coico J, Plumb DA, *et al.* Mouse models of osteoarthritis: surgical model of posttraumatic osteoarthritis induced by destabilization of the medial meniscus. Methods Mol Biol. 2015;1226:143-73.
29. Matthews DR, Hosker JP, Rudenski AS, Naylor BA, Treacher DF, Turner RC. Homeostasis model assessment: insulin resistance and beta-cell function from fasting plasma glucose and insulin concentrations in man. Diabetologia. 1985;28(7):412-9.
30. Glasson SS, Chambers MG, Van Den Berg WB, Little CB. The OARSI histopathology initiative - recommendations for histological assessments of osteoarthritis in the mouse. Osteoarthritis Cartilage. 2010;18 Suppl 3:S17-23.
31. Galarraga M, Campion J, Munoz-Barrutia A, Boque N, Moreno H, Martinez JA, *et al.* Adiposoft: automated software for the analysis of white adipose tissue cellularity in histological sections. J Lipid Res. 2012;53(12):2791-6.
32. van Dijk RA, Rijs K, Wezel A, Hamming JF, Kolodgie FD, Virmani R, *et al.* Systematic Evaluation of the Cellular Innate Immune Response During the Process of Human Atherosclerosis. J Am Heart Assoc. 2016;5(6).
33. Mulder P, Morrison MC, Wielinga PY, van Duyvenvoorde W, Kooistra T, Kleemann R. Surgical removal of

inflamed epididymal white adipose tissue attenuates the development of non-alcoholic steatohepatitis in obesity. Int J Obes (Lond). 2016;40(4):675-84.
34. Barboza E, Hudson J, Chang WP, Kovats S, Towner RA, Silasi-Mansat R, *et al.* Profibrotic Infrapatellar Fat Pad Remodeling Without M1 Macrophage Polarization Precedes Knee Osteoarthritis in Mice With Diet-Induced Obesity. Arthritis Rheumatol. 2017;69(6):1221-32.
35. Harasymowicz NS, Clement ND, Azfer A, Burnett R, Salter DM, Simpson A. Regional Differences Between Perisynovial and Infrapatellar Adipose Tissue Depots and Their Response to Class II and Class III Obesity in Patients With Osteoarthritis. Arthritis Rheumatol. 2017;69(7):1396-406.
36. de Visser HM, Korthagen NM, Muller C, Ramakers RM, Krijger GC, Lafeber F, *et al.* Imaging of Folate Receptor Expressing Macrophages in the Rat Groove Model of Osteoarthritis: Using a New DOTA-Folate Conjugate. Cartilage. 2018;9(2):183-91.
37. Datta P, Zhang Y, Parousis A, Sharma A, Rossomacha E, Endisha H, *et al.* High-fat diet-induced acceleration of osteoarthritis is associated with a distinct and sustained plasma metabolite signature. Sci Rep. 2017;7(1):8205.
38. Saddik D, McNally EG, Richardson M. MRI of Hoffa's fat pad. Skeletal Radiol. 2004;33(8):433-44.
39. Smillie IS. Diseases of the Knee Joint. . London: Churchill Livingstone; 1980.
40. Macchi V, Porzionato A, Sarasin G, Petrelli L, Guidolin D, Rossato M, *et al.* The Infrapatellar Adipose Body: A Histotopographic Study. Cells Tissues Organs. 2016;201(3):220-31.
41. Fontanella CG, Carniel EL, Frigo A, Macchi V, Porzionato A, Sarasin G, *et al.* Investigation of biomechanical response of Hoffa's fat pad and comparative characterization. J Mech Behav Biomed Mater. 2017;67:1-9.
42. Bastiaansen-Jenniskens YM, Wei W, Feijt C, Waarsing JH, Verhaar JA, Zuurmond AM, *et al.* Stimulation of fibrotic processes by the infrapatellar fat pad in cultured synoviocytes from patients with osteoarthritis: a possible role for prostaglandin f2alpha. Arthritis Rheum. 2013;65(8):2070-80.
43. Eymard F, Pigenet A, Citadelle D, Tordjman J, Foucher L, Rose C, *et al.* Knee and hip intra-articular adipose tissues (IAATs) compared with autologous subcutaneous adipose tissue: a specific phenotype for a central player in osteoarthritis. Ann Rheum Dis. 2017;76(6):1142-8.
44. Ioan-Facsinay A, Kloppenburg M. Osteoarthritis: Inflammation and fibrosis in adipose tissue of osteoarthritic joints. Nat Rev Rheumatol. 2017;13(6):325-6.
45. Masaki T, Takahashi K, Hashimoto S, Ikuta F, Watanabe A, Kiuchi S, *et al.* Volume change in infrapatellar fat pad is associated not with obesity but with cartilage degeneration. J Orthop Res. 2018.
46. Cowan SM, Hart HF, Warden SJ, Crossley KM. Infrapatellar fat pad volume is greater in individuals with patellofemoral joint osteoarthritis and associated with pain. Rheumatol Int. 2015;35(8):1439-42.
47. Ballegaard C, Riis RG, Bliddal H, Christensen R, Henriksen M, Bartels EM, *et al.* Knee pain and inflammation in the infrapatellar fat pad estimated by conventional and dynamic contrast-enhanced magnetic resonance imaging in obese patients with osteoarthritis: a cross-sectional study. Osteoarthritis Cartilage. 2014;22(7):933-40.

48. Cai J, Xu J, Wang K, Zheng S, He F, Huan S, *et al.* Association Between Infrapatellar Fat Pad Volume and Knee Structural Changes in Patients with Knee Osteoarthritis. J Rheumatol. 2015;42(10):1878-84.
49. Han W, Cai S, Liu Z, Jin X, Wang X, Antony B, *et al.* Infrapatellar fat pad in the knee: is local fat good or bad for knee osteoarthritis? Arthritis Res Ther. 2014;16(4):R145.

Table S1. Overview of metabolic parameters per study group before start of the diet and at endpoint of each study. Data are presented as mean values ± SD.

	Before diet				t= 18 weeks			t = 38 weeks
	LFD + DMM	LFD>HFD + DMM	HFD + DMM	HFD only	LFD + DMM	LFD>HFD + DMM	HFD + DMM	HFD only
Body weight (g)	25.2 ± 1.77	25.1 ± 1.82	24.9 ± 1.75	31.1 ± 2.32	31.4 ± 1.99	38.8 ± 3.14	40.06 ± 6.94	47.6 ± 4.50
Cholesterol (mM)	2.01 ± 0.14	1.95 ± 0.30	2.08 ± 0.08	1.99 ± 0.27	2.40 ± 0.99	3.46 ± 1.17	3.99 ± 0.84	4.59 ± 1.25
Fat mass (g)	1.49 ± 0.29	1.81 ± 0.41	1.37 ± 0.34	2.38 ± 1.19	4.52 ± 1.91	11.2 ± 3.42	12.48 ± 4.67	20.3 ± 2.74
Lean mass (g)	21.5 ± 1.41	21.0 ± 1.59	21.1 ± 1.44	27.6 ± 1.87	25.4 ± 1.72	26.5 ± 1.79	26.60 ± 2.33	32.6 ± 1.83
Glucose (mmol/L)	11.4 ± 0.82	10.3 ± 1.37	11.4 ± 1.01	10.1 ± 1.69	9.90 ± 1.81	12.6 ± 2.01	12.92 ± 3.01	11.1 ± 1.58
Insulin (ug/ml)	0.52 ± 0.17	0.55 ± 0.18	0.35 ± 0.14	1.06 ± 0.76	1.52 ± 1.18	2.95 ± 1.41	4.05 ± 2.18	15.3 ± 8.04
HOMA-IR	7.26 ± 2.70	9.96 ± 11.9	3.57 ± 2.08	12.4 ± 10.7	15.8 ± 7.77	39.7 ± 22.2	62.79 ± 39.9	193.1 ± 104.7

Supplemental Tables

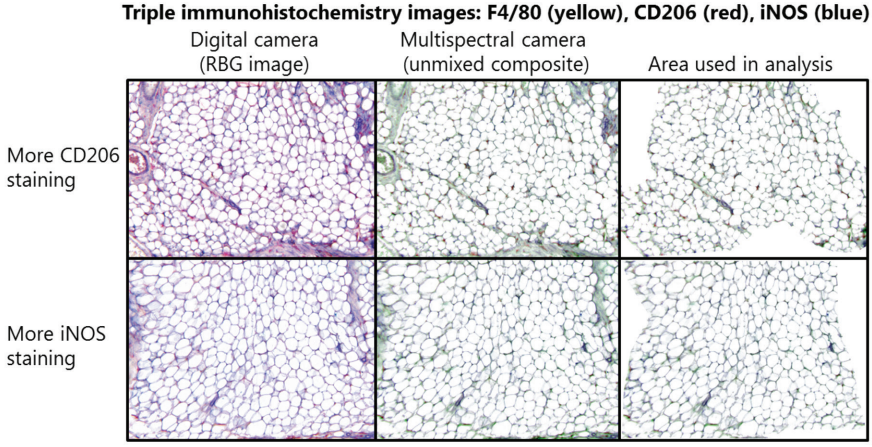


Figure S1. Analysis of triple immunohistochemistry images. Representative images of several steps in the analysis of the immunohistochemistry staining. Two individual samples are shown; one with relatively more CD206 and one with relatively more iNOS. By eye, colour differences are best observed in the image taken with a normal digital camera. To quantify the individual chromogen signal and possible colocalization the multispectral camera images were used, as shown in the middle panel. Blood vessels and other (non-fat) tissues were excluded as much as possible in the image used for the final analysis.



Chapter 5

Human C-reactive protein aggravates osteoarthritis development in mice on a high-fat diet

Kozijn A.E., Tartjiono M.T., Ravipati S., van der Ham F., Barrett D.A., Mastbergen S.C., Korthagen N.M., Lafeber F.P.J.G., Zuurmond A.M., Bobeldijk I., Weinans H., Stoop R.

Published as:
Kozijn A.E., Tartjiono M.T., Ravipati S., van der Ham F., Barrett D.A., Mastbergen S.C., Korthagen N.M., Lafeber F.P.J.G., Zuurmond A.M., Bobeldijk I., Weinans H., Stoop R.
Human C-reactive protein aggravates osteoarthritis development in mice on a high-fat diet.
Osteoarthritis Cartilage. 2019 Jan;27(1):118-128.

Abstract

Background. C-reactive protein (CRP) levels can be elevated in osteoarthritis (OA) patients. In addition to indicating systemic inflammation, it is suggested that CRP itself can play a role in OA development. Obesity and metabolic syndrome are important risk factors for OA and also induce elevated CRP levels. Here we evaluated in a human CRP (hCRP)-transgenic mouse model whether CRP itself contributes to the development of 'metabolic' OA.

Methods. Metabolic OA was induced by feeding 12-week-old hCRP-transgenic males (hCRP-tg, n = 30) and wild-type littermates (n = 15) a 45 kcal% high-fat diet (HFD) for 38 weeks. Cartilage degradation, osteophytes and synovitis were graded on Safranin O-stained histological knee joint sections. Inflammatory status was assessed by plasma lipid profiling, flow cytometric analyses of blood immune cell populations and immunohistochemical staining of synovial macrophage subsets.

Results. Male hCRP-tg mice showed aggravated OA severity and increased osteophytosis compared with their wild-type littermates. Both classical and non-classical monocytes showed increased expression of CCR2 and CD86 in hCRP-tg males. HFD-induced effects were evident for nearly all lipids measured and indicated a similar low-grade systemic inflammation for both genotypes. Synovitis scores and synovial macrophage subsets were similar in the two groups.

Conclusions. Human CRP expression in a background of HFD-induced metabolic dysfunction resulted in the aggravation of OA through increased cartilage degeneration and osteophytosis. Increased recruitment of classical and non-classical monocytes might be a mechanism of action through which CRP is involved in aggravating this process. These findings suggest interventions selectively directed against CRP activity could ameliorate metabolic OA development.

Introduction

Osteoarthritis (OA) is a progressive joint disease of partially unknown aetiology that is characterised by focal loss of articular cartilage. In humans the most significant factor contributing to OA is overweight, leading to an OA phenotype here referred to as 'metabolic OA'. In recent years there has been increasing emphasis on the systemic, metabolic components involved in the development and progression of this OA phenotype[1-3]. There is mounting evidence that metabolic overload and related systemic inflammatory mediators are associated with OA development and progression. This led to the recognition of a clinically distinct OA phenotype, termed metabolic OA[4]. Especially the systemic low-grade chronic inflammation, which is strongly associated to metabolic overload[5], is thought to play an important role in the local development and progression of metabolic OA[3 4].

Metabolic overload-induced systemic inflammation as seen in humans can be induced by prolonged high-fat diet (HFD) feeding in small animal models and has been shown to aggravate metabolic OA development in these models[6]. We have previously demonstrated in various obesity-prone mouse strains that HFD feeding alone does not necessarily lead to aggravated articular cartilage degradation and suggested that an additional trigger besides high-caloric feeding is necessary to evoke metabolic OA[7]. In a study by Gierman *et al.*[8], this human C-reactive protein-transgenic (hCRP-tg) strain was used to easily monitor the systemic inflammatory status of the mice via the general inflammation marker CRP. Aggravated OA pathology was observed in hCRP-tg male mice fed with a HFD (45 kcal% energy from fat) compared with chow diet. As these mice received a HFD without an additional trigger, it is conceivable that CRP itself might have triggered the aggravated OA pathology. Moreover, low-grade inflammation proved more important than mechanical overload in the development of HFD-induced metabolic OA in the hCRP-tg mouse[8]. Anti-inflammatory intervention with either cholesterol-lowering rosuvastatin or PPARγ agonist rosiglitazone showed significant suppression of both OA development as well as plasma CRP levels, supporting the importance of inflammation in metabolic OA pathogenesis.

CRP involvement has also been suggested in human OA pathogenesis. Systemic CRP levels are significantly elevated in OA patients compared with healthy controls and have been reported to relate with clinical features and radiographic severity[9-12]. The population-based Chingford study confirmed these findings and the authors suggested that CRP levels in early OA can be used as a predictive marker for disease progression[13]. In patients with advanced OA, systemic CRP levels reflected local joint inflammation14 or pain15 rather than radiographic OA. The latter finding was corroborated by a recent meta-analysis of 32 studies, where CRP levels were significantly associated with pain and decreased physical function but not radiographic OA[16]. In contrast, others demonstrated no association between CRP levels and OA severity after adjustment for

body mass – including the follow-up of the Chingford study[17-20]. These contradictory results between studies have clouded the association between CRP levels and OA pathology.
In our present study, we aimed to elucidate the role of CRP in HFD-induced OA pathogenesis. Male hCRP-tg mice were compared with their wild-type male littermates on a HFD to infer whether the expression of CRP contributed to diet-induced OA aggravation. OA features like osteophyte formation and synovitis were determined to investigate involvement with different aspects of OA pathology. Systemic lipid profiles, blood immune cell populations and synovial macrophage subsets were evaluated to assess whether hCRP-tg mice had a more proinflammatory status relative to their wild-type littermates.

Materials and methods

A detailed methods section is available at the end of this Chapter.

Mice and experimental design

The experiment was carried out in male human CRP-transgenic (hCRP-tg, n=30) and male wild-type littermates (n=15) on a C57BL/6J background. Metabolic OA was induced by switching the diet of the mice from standard chow to a high-fat diet (HFD, 45 kcal% from fat; cat# D12451, Research Diets Inc., New Brunswick, USA) at 12 weeks of age. Both groups received the HFD for a consecutive period of 38 weeks. The experiment was approved by the institutional Animal Care and Use Committee of TNO and was in compliance with ARRIVE guidelines and European Community specifications regarding the use of laboratory animals.

Analysis of metabolic dysfunction and osteoarthritis

Metabolic dysfunction was monitored at regular interval during the study period by assessing body weight gain, changes in body composition (EchoMRI LLC, Houston, TX, USA), fasted plasma total cholesterol, glucose and insulin levels. Fasted plasma CRP levels were determined by sandwich ELISA (cat.no. DY1707, R&D Systems, USA). Insulin resistance index (HOMA-IR) was calculated according to the equation proposed by Matthews *et al.*[21]: HOMA-IR = (glucose (mmol/L) × insulin (mU/L)) / 22.5.
Articular cartilage degradation, osteophyte formation and synovitis were scored on coronal 5µm knee joint sections, stained with Haematoxylin, Fast Green and Safranin-O, according to OARSI histopathology initiative recommendations for the mouse[22]. For all grades, we report the sum of the medial and lateral compartments as the total score. Please see Supplemental Methods for more details.

Lipid and oxylipin analyses in fasted plasma

Samples were stored at -80°C before analysis. General lipid profiles were determined at time points t=0 weeks, t=4 days after HFD switch (peak in hCRP plasma levels) and t=38 weeks. Oxylipin profiling was performed at t=0, 14 and 38 weeks, due to deficient sample volumes at the intermediate blood collection at t=4 days. Sample volumes of 5µl and 50µl were aliquoted from each fasted plasma sample for general lipid/free fatty acids (FFA) analysis and oxylipin analysis, respectively. Please refer to the Supplemental Methods for a more detailed method description. The lipidomic datasets analysed during the current study are also stored in a phenotype database repository and are available by signing up via https://dashin.eu/interventionstudies/. After receiving credentials and logging in, the study can be accessed via https://dashin.eu/interventionstudies/study/show/39162914 or by searching the study code (hCRP_in_mouse) or study title (Human C-reactive protein aggravates osteoarthritis development in mice on a high-fat diet).

Immunophenotyping of peripheral cell populations by flow cytometry

Peripheral myeloid and lymphoid populations were analysed by flow cytometry at three different time points (t=2/11/37 weeks). Peripheral blood (5 drops/animal) was drawn via tail incision using lithium heparin-coated Microvette tubes. Cell-surface staining was performed with the myeloid and lymphoid antibody panels shown in Tables 1 and 2. Pooled samples were used for unstained, single-stained and FMO controls to determine background levels of staining. Data were acquired with a 3-laser FACSCanto™ II flow cytometer (Becton Dickinson) (Table S2) and analysed using FlowJo v10.2 (Treestar Inc., USA). Cell populations of interest were gated according to the gating strategies as depicted in Figures S3 and S4, to obtain their population frequencies. Baseline population frequencies were determined in age-matched hCRP-tg (n=5) and wild-type (n=4) males from later litters and were not included in the statistical analysis (shown here in grey). Detailed descriptions are included in the Supplemental Methods.

Table 1. Antibody panel used for the analysis of peripheral myeloid subpopulations.

Marker	Fluorochrome	Dilution	Clone	Manufacturer	Catalogue number
CCR2	FITC	1:100	475301	R&D Systems	FAB5538F
MHCII	PE	1:100	M5/114.15.2	BD Biosciences	557000
CD11c	PE/Cy7	1:100	N418	eBioscience	25-0114
GR1	PerCP/Cy5.5	1:100	RB6-8C5	BD Biosciences	552093
CD86	APC	1:100	GL1	BD Biosciences	558703
F4/80	APC/Cy7	1:200	BM8	BioLegend	123118
CD11b	Horizon V450	1:100	M1/70	BD Biosciences	560455

Abbreviations: FITC, fluorescein isothiocyanate; PE, phycoerythrin; Cy, cyanine; PerCP, peridinin chlorophyll protein complex; APC, allophycocyanin.

Table 2. Antibody panel used for the analysis of peripheral lymphoid subpopulations.

Marker	Fluorochrome	Dilution	Clone	Manufacturer	Catalogue number
CD8a	FITC	1:100	53-6.7	BD Biosciences	553031
CD4	PE	1:100	RM4-4	eBioscience	12-0043-83
CD62L	PE/Cy7	1:100	MEL-14	eBioscience	25-0621-82
CD45	PerCP/Cy5.5	1:100	30-F11	BD Biosciences	550994
CD25	APC	1:100	PC61.5	eBioscience	17-0251-81
CD3e	APC/Cy7	1:200	145-2C11	BD Biosciences	557596
CD19	Horizon V450	1:1000	1D3	BD Biosciences	560375

Abbreviations: FITC, fluorescein isothiocyanate; PE, phycoerythrin; Cy, cyanine; PerCP, peridinin chlorophyll protein complex; APC, allophycocyanin.

Immunohistochemical evaluation of macrophage subsets in the knee

Knee joints from both groups were stained with chromogenic triple-labelling immunohistochemistry (IHC) for M1 and M2 macrophage subsets, based on a previously described method for human tissue[23]. Primary antibodies targeted murine macrophages (F4/80, 1:100, MF48000 (BM8), Invitrogen), M1 macrophages (iNOS, 1:400, ab136918 (K13-A), Abcam) and M2 macrophages (CD206, 1:100, AF2535, R&D Systems). Quantification was performed in the lateral patellofemoral synovial lining of the knee joint. Digital images of the unmixed colour spectra for each chromogen in the region of interest (ROI) were obtained with a Nuance multispectral imaging system (40x magnification). Macrophage subtypes were analysed using ImageJ 1.51n image analysis software. Colocalization of two or the three markers was calculated from the areal overlap between positivity for F4/80 and CD206 or iNOS or both. Data are expressed as percentage positivity for a label or combination of labels within the ROI or within the $F4/80^+$ macrophage population. Please see Supplemental Methods for more details.

Statistical analysis

Statistical analysis was performed using Prism (v7.01, GraphPad Software, La Jolla, CA, USA) and IBM SPSS software (v25.0, IBM SPSS Inc., Chicago, IL, USA). Please refer to the statistical analysis section in the Supplemental Methods for a more detailed description.

Results

Increased cartilage degeneration and osteophytosis in hCRP-tg mice

To assess whether human CRP itself plays a role in the development of metabolic OA, male hCRP-tg mice were compared with their wild-type male littermates on a HFD. Chow controls were not included in our study, as previous work by our group[8] has shown that hCRP-tg male mice on a HFD had significantly higher OA grades than mice on chow.

Increases in body weight due to fat accumulation, plasma cholesterol and insulin resistance index (HOMA-IR) reflect a state of metabolic dysfunction in both hCRP-tg and wild-type mice (Figure S1). Expression of CRP was validated at the protein level in fasted plasma from hCRP-tg males, whereas wild-type controls were negative. HFD feeding induced changes at the CRP protein level as observed before[8]. Directly after diet switch, HFD provoked a steep increase in CRP levels in hCRP-tg males followed by a gradual decrease over the course of the study (Figure S2A).

Human CRP-tg males showed increased articular cartilage fibrillations and vertical clefts with loss of surface lamina (Figure 1A,B). Cartilage erosion was only seen at the lateral knee compartments and almost exclusively occurred in the hCRP-tg group. Total OA scores demonstrated a significant difference between both groups, with a median [interquartile range] of 4.25 [3.72-5.44] in wild-type vs. 6.00 [4.69-7.26] in hCRP-tg males, $p<0.01$, $d=0.818$, 95%CI [0.06-0.57] (Figure 1B). This difference in severity between groups was primarily visible at the lateral side of the knee joint with 2.38 [1.69-3.10] in wild-type vs. 4.00 [2.82-5.00] in hCRP-tg, $p<0.01$, $d=1.066$, 95%CI [0.16-0.69].

Osteophyte formation was distinctly more present in hCRP-tg mice (3.00 [2.00-5.00]) compared with wild-type controls (2.00 [1.00-4.00]. Figure 1C), $p=0.03$, $d=0.46$, 95%CI [-0.12-0.68]. Synovitis scores were comparable between both groups (Figure 1D), with $p=0.28$, $d=0.10$, 95%CI [-0.32-0.44].

The relative individual induction of CRP levels at 4 days after diet switch did not associate with the individual OA grades at end point (Figure S2B), unlike observed before[8]. Individual OA grades reflecting cartilage degeneration did not associate to the individual osteophyte and synovitis scores (Figure S2C,D). Changes in CRP levels within the hCRP-tg group showed no association to osteophyte or synovitis scores (data not shown).

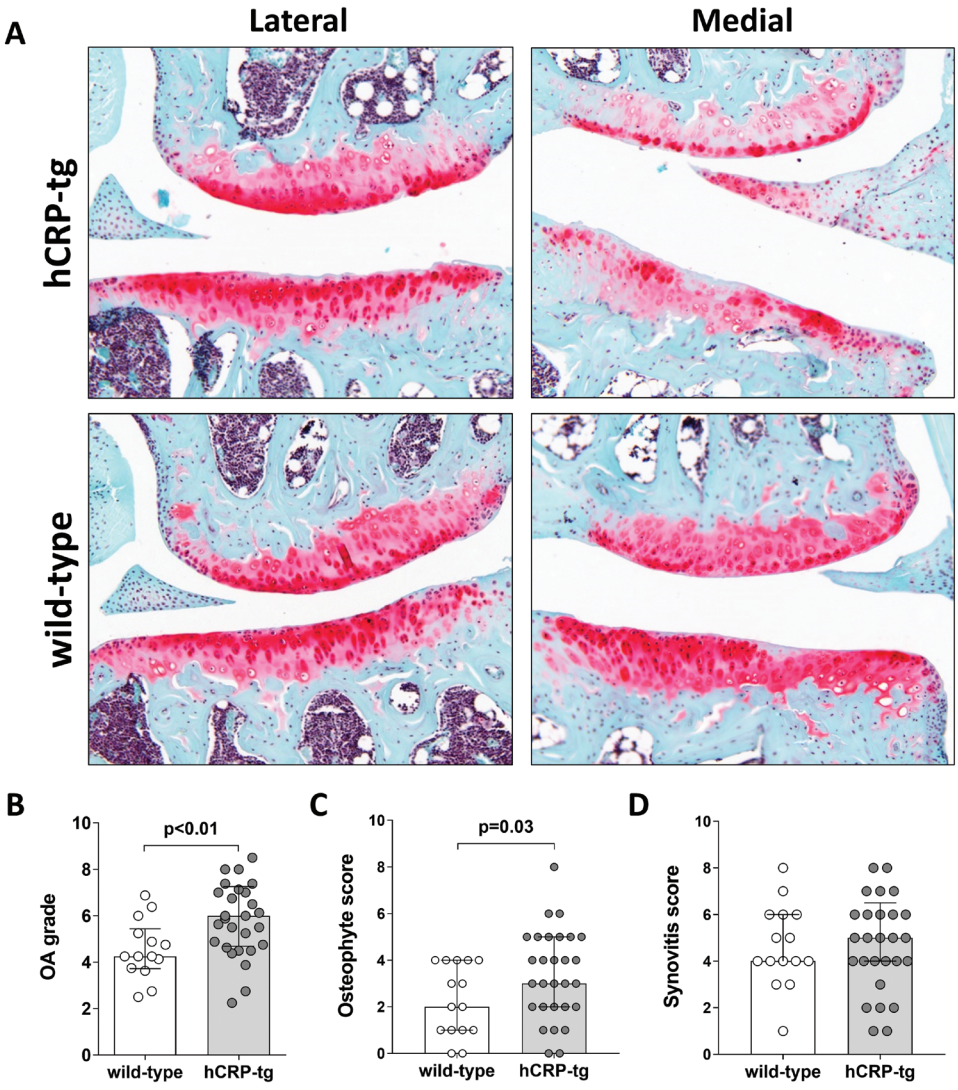


Figure 1 HFD feeding aggravates OA progression in hCRP-tg mice. A) Representative coronal sections of the lateral and medial tibiofemoral compartments, stained with Fast-Green/Safranin-O, from hCRP-tg and wild-type littermates fed a HFD. Chow controls were not included in our study, but hCRP-tg males are known to not develop OA on a feeding regime of 38 weeks[8]. Magnification for all microphotographs was 40×. B) Summed histopathological scores for the tibiofemoral knee compartments of the hCRP-tg and wild-type groups. C) Total osteophyte scores showing the individual summed score for the tibiofemoral knee compartments for each animal per study group. D) Total synovitis scores showing the individual summed score for the tibiofemoral knee compartments for each animal per study group. B-D) Scoring was performed according to OARSI histopathology recommendations for the mouse[22]. Data are presented as group medians (indicated by bars) with IQR (error bars).

Lipid metabolism comparable between genotypes

Strong diet-induced effects were observed for nearly all measured lipids, showing predominantly increased concentrations in plasma over time. Uni- and multivariate statistical analyses revealed no differences in general lipid and oxylipin profiles between hCRP-tg and wild-type males, neither per time point nor over time (data not shown). Furthermore, none of the measured lipids correlated with OA severity within the hCRP-tg group. Lysophosphatidylcholines (LPC) to phosphatidylcholines (PC) ratio, as a general indicator of inflammatory status and possible predictor of advanced knee OA in humans[24], dropped shortly after HFD switch (hCRP-tg: from 0.83 [0.62-1.10] to 0.70 [0.38-0.80]; wild-type: from 0.86 [0.75-0.93] to 0.69 [0.57-0.83]) and remained constant afterward. Genotypes demonstrated no major differences in individual PC or LPC levels, as represented by the PC/LPC pairs in Figure 2A. Similarly, the switch to HFD was directly reflected in a decline of the sums of omega-6 as well as omega-3 fatty acids (FFA) as a percentage of total FFA in both groups. However, both groups showed significant increases in total omega-3 FFA at end-point, while total omega-6 FFA levels remained constant (data not shown). This was reflected in the omega-6/omega-3 FFA ratio, another lipid marker of general inflammatory state, which decreased significantly over time with no differences between groups (data not shown). Individual oxylipin changes were similar between genotypes. The arachidonic acid (AA) metabolite 5,6-epoxyeicosatrienoic acid (5,6-EET) and its stable hydrolysis product 5,6-dihydroxyeicosatrienoic acid (5,6-DHET) increased over time (Figure 2B). Oxidized linoleic acid (LA) metabolites showed a decrease over time, as represented by 13-hydroxyoctadecadienoic acid (13-HODE, Figure 2B). The DHA-metabolite 17-hydroxy docosahexaenoic acid (17-HDHA) increased over time (Figure 2B).

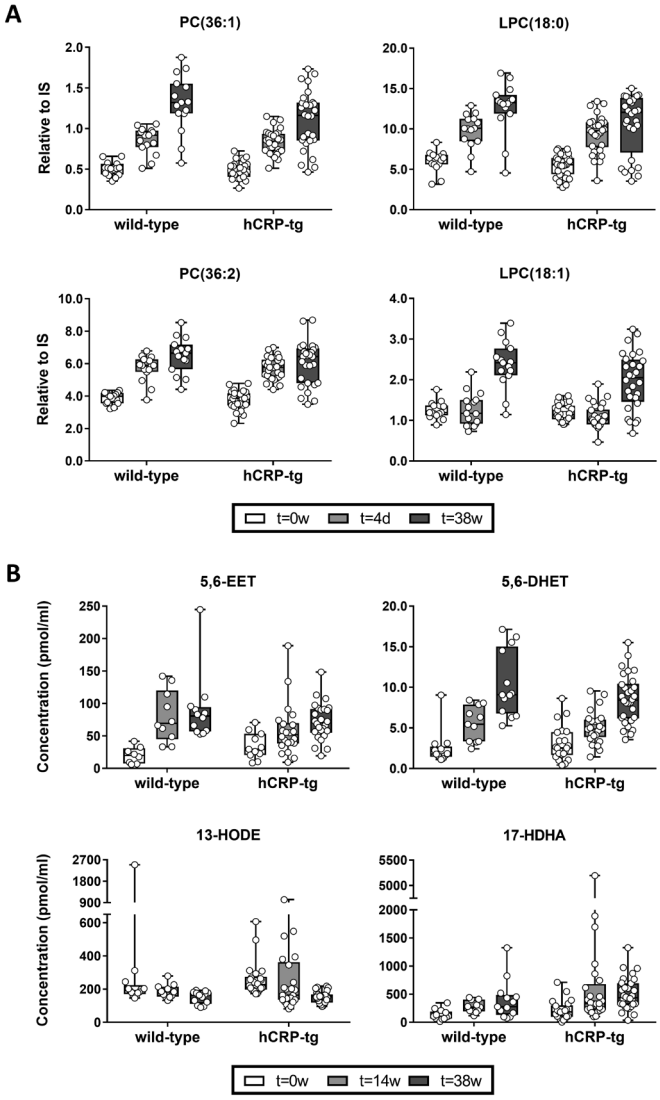


Figure 2 Transgenic and wild-type hCRP males show similar plasma lipid profiles on a HFD. A) Representative PC/LPC pairs show increases in fasted plasma levels in both study groups during the HFD regimen. B) Representative oxylipins from the three most important oxylipin substrates (i.e. AA, LA and DHA) demonstrate distinct concentration changes in fasted plasma during the HFD regimen. Boxplots show boxes extending from the 25th to 75th percentiles containing the median (middle line), with error bars down to the minimum and up to the maximum value. The individual value for each animal is plotted as a dot superimposed on the graph. IS, internal standard; PC, phosphatidylcholine; LPC, lysophosphatidylcholine; EET, epoxyeicosatrienoic acid; DHET, dihydroxyeicosatrienoic acid; HODE, hydroxyoctadecadienoic acid; HDHA, hydroxy docosahexaenoic acid; AA, arachidonic acid; LA, linoleic acid; DHA, docosahexaenoic acid.

Increased monocyte activation in hCRP-tg mice on a HFD

Peripheral myeloid and lymphoid populations were analysed by flow cytometry at three different time points (t = 2, 11 and 37 weeks) to evaluate the direct and prolonged systemic effects of HFD feeding on immune status (Figures S3 and S4). Baseline population frequencies were determined in age-matched hCRP-tg (n=5) and wild-type (n=4) males from later litters and were not included in the statistical analysis (shown in Figure 3A in grey).

HFD feeding induced similar immune reactivity within lymphocyte populations of hCRP-tg and wild-type males (data not shown), but triggered distinct changes in the circulating monocyte populations of these groups. Firstly, HFD feeding nearly doubled the total percentage of circulating $CD11b^+$ monocytes in both groups (30.43±5.26 at week 2 vs. 53.85±10.35 at week 37, Figure 3A). Secondly, the hCRP-tg mice showed significant upregulation of activated non-classical $GR\text{-}1^{low}$ monocytes expressing both the integrin CD11c and chemokine receptor CCR2 after two weeks of HFD feeding (Figure 3B, p=0.02, *d*=0.82, 95%CI [0.70-6.33]). Co-expression of the lymphocyte activation antigen CD86 on GR-1lowCCR2+ monocytes was elevated upon long-term HFD feeding, with hCRP-tg males showing a significantly increased co-expression compared with wild-type controls (Figure 3C (p=0.02, *d*=0.79, 95%CI [0.73-8.07]) and Figure 3D (p=0.02, *d*=0.82, 95%CI [0.79-7.39])). Correspondingly, percentages of $GR\text{-}1^{low}$ monocytes without CCR2 expression were significantly decreased in hCRP-tg males compared with wild-types at 2 weeks (data not shown). Over time, hCRP-tg mice showed an increase in activated classical $GR\text{-}1^{high}CCR2^+CD86^+$ monocytes compared with wild-type controls (Figure 3E, p=0.04, *d*=0.71, 95%CI [0.06-1.64]).

To evaluate the association between genotype and OA development on the changes in circulating immune cell populations, linear mixed modelling was used (Figure S5). In hCRP-tg mice the percentages of $CD11b^+$ leukocytes were associated with lateral OA severity, while in wild-type littermates this correlation was inversed. Correspondingly, $CD11b^-$ cell populations significantly decreased with increasing lateral OA severity in hCRP-tg mice and vice versa for wild-type controls. The hCRP-tg genotype was also significantly associated with higher percentages of both classical $CD11b^+GR\text{-}1^{high}$ and non-classical $CD11b^+GR\text{-}1^{low}$ monocytes with increasing lateral OA severity. Wild-type controls showed an inverse relationship between these monocyte subsets and lateral OA severity.

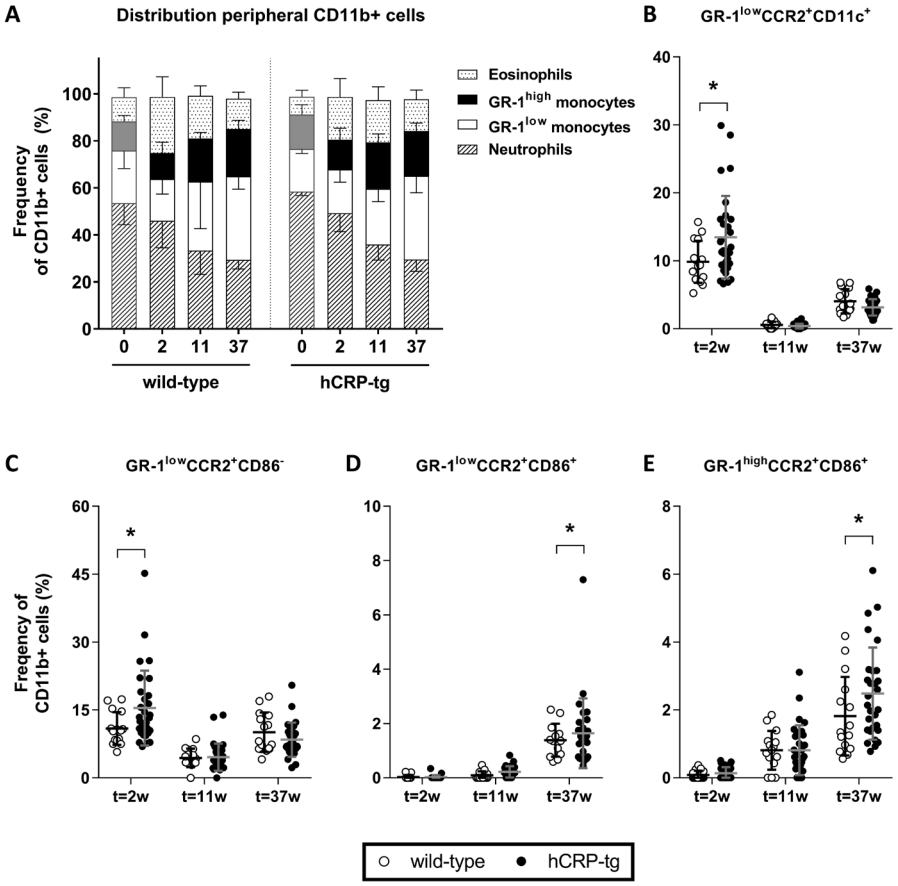


Figure 3 Increased activation of classical and non-classical monocytes in hCRP-tg mice. A) Distribution of peripheral CD11b+ immune cells shows HFD-mediated monocytosis in both groups over time. Baseline population frequencies were determined in age-matched hCRP-tg (n=5) and wild-type (n=4) males from later litters and were not included in the statistical analysis (shown here in grey). B) GR-1low non-classical monocytes showed an increase in CCR2 and CD11c expression upon 2 weeks of HFD feeding, which was significantly elevated in hCRP-tg compared with wild-type mice. C-D) GR-1^{low} non-classical monocytes expressing CCR2 upregulated the lymphocyte activation antigen CD86 after long-term HFD feeding (37 weeks), with hCRP-tg males showing higher co-expression of these activation markers compared with wild-type controls. E) GR-1^{high} classical monocytes co-expressing CCR2 and CD86 increase over time and were significantly more present in hCRP-tg compared with wild-type males at t=37 weeks. Data are presented as group means (indicated by bars) with SD (error bars). *p<0.05 compared with wild-type controls.

Human CRP has no effect on synovial macrophage accumulation and phenotype shift

As systemic CRP levels have been found to reflect local joint inflammation in patients with advanced OA[14], knee joints were evaluated for the local presence of M1 and M2 macrophage subsets in the synovial lining layer. Macrophages were detected by the pan-macrophage marker F4/80 and subsets were discriminated by colocalization of inducible nitric oxide synthase (iNOS) for M1 macrophages and the mannose receptor (CD206) for M2 macrophages.

Overall, both upon microscopical evaluation and image analysis, there were no significant differences found for synovial macrophage populations between genotypes (Fig 4A). Univariate testing hinted towards increased CD206 positivity and CD206/iNOS colocalization in knee joints from hCRP-tg males ($p=0.122$ and $p=0.183$ respectively, MWU-test; Fig 4B).

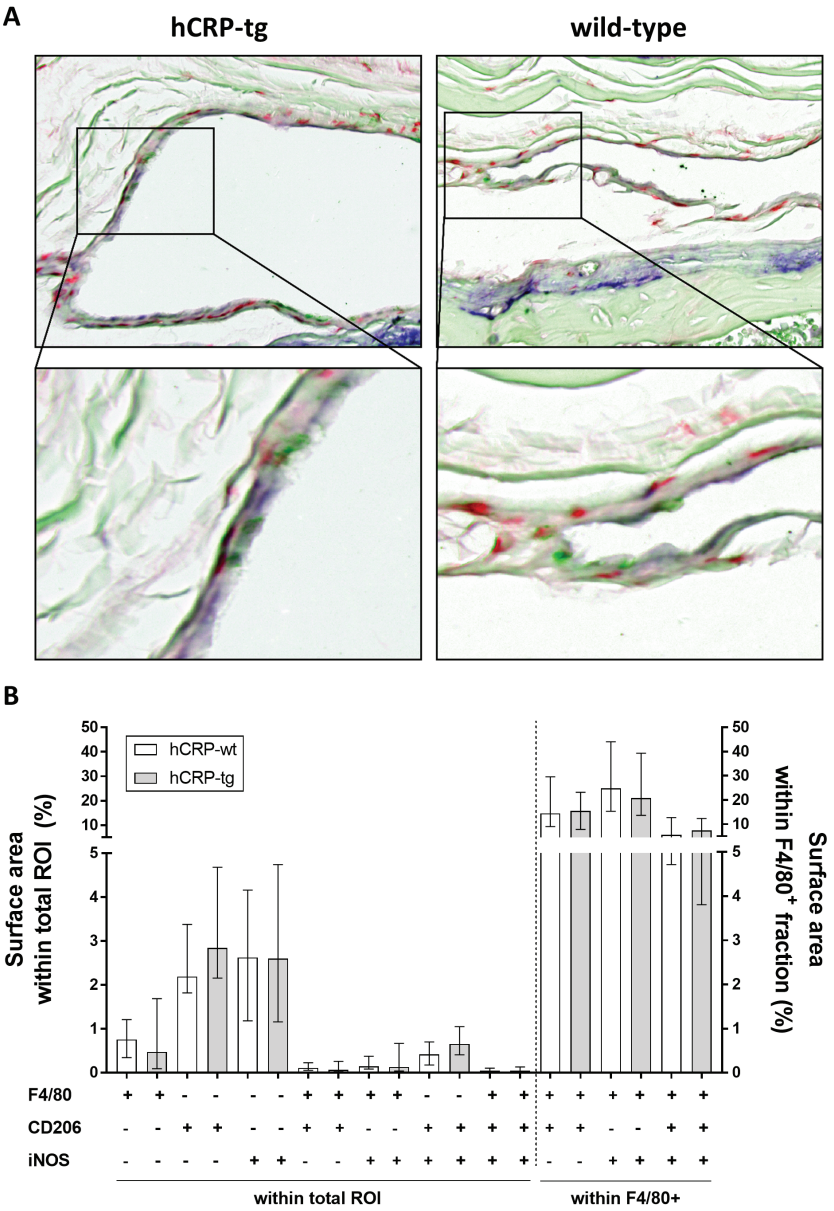


Figure 4 Human CRP has no effect on synovial macrophage accumulation and subsets. A) Representative unmixed spectral images of the lateral patellofemoral synovial lining (ROI) showing pan-macrophage marker F4/80 (green), M1 subset marker iNOS (blue) and M2 subset marker CD206 (magenta) positivity. Magnification for the top microphotographs was 40×. B) Percentage of the surface area within the ROI or within the F4/80$^+$ cell fraction for hCRP-tg and wild-type mice, showing no CRP-induced shift in macrophage numbers and phenotypes. Data are presented as group medians (indicated by bars) with IQR (error bars).

Discussion

High CRP levels found in metabolic syndrome patients have been suggested to actively contribute to inflammatory morbidities and related increased cardiovascular and diabetic risks[25]. In the current study we demonstrate that hCRP-tg mice developed more severe OA compared with their wild-type controls under the same HFD regime. Although obesity-related low-grade systemic inflammation is recognized as a contributing factor in metabolic OA pathogenesis, associations between CRP levels and OA features rendered contradictory results between cohort studies. Here we show that hCRP-tg mice exhibit increased cartilage degradation and osteophytosis, but not increased synovitis. The latter is generally seen as a typical inflammatory component of OA, which may partly underlie the conflicting findings in the different cohort studies. Our study, in which the expression of CRP was the only variable, implicates CRP as an independent trigger to aggravate HFD-induced OA development.

The positive association between metabolic syndrome and CRP levels in humans26 and the exacerbation of metabolic disorders in hCRP-tg mice[8 27 28] suggest CRP is more than merely an inflammation marker in metabolic disorders. In hCRP-tg mice, as in humans, the CRP protein is synthesized by hepatocytes only and is regulated at the transcriptional level[29]. Confirming previous observations[8], HFD feeding evoked a direct and prolonged rise in plasma CRP levels in hCRP-tg males from our study, indicative of a systemic inflammatory status. Possibly, CRP induces cascades that are not raised in wild-type C57BL/6J mice or amplifies the activation of inflammatory pathways that are not triggered by HFD alone.

While a widely used clinical marker of general inflammation, the physiological functions of human CRP remain to be fully elucidated and can be pro- or anti-inflammatory depending on the situation. One major route of action is the involvement of CRP in innate immunity through the opsonisation of pathogens or dying cells and subsequent activation and modulation of complement via binding to C1q[30]. Even though no added effect to synovitis severity was observed, an increased inflammatory pathway because of CRP signalling still seems likely as osteophyte formation is linked to inflammation[31 32]. It is well possible that CRP is driving a specific inflammatory pathway that is associated with osteophyte development. Angiogenesis at the osteochondral junction could be such a process, which has been demonstrated to lead to endochondral ossification and the formation of osteophytes[33]. Human CRP has been shown to upregulate vascular growth factor (VEGF) expression[34], a driver of neovascularization which is expressed by hypertrophic chondrocytes and synovial macrophages, and VEGF inhibition is suggested as a treatment strategy for OA[35]. Involvement of synovial macrophages is not supported by our results, but perhaps hypertrophic chondrocytes can play a role under the experimental conditions applied.

Inflammation is closely linked to lipid metabolism, a conjunction particularly noticeable in metabolic diseases. As obesity and metabolic syndrome are important risk factors for OA and induce elevated CRP levels in patients, we postulated that obese hCRP-tg males might demonstrate a more proinflammatory lipid profile compared to their controls. Indeed, HFD-induced effects were evident for nearly all lipids measured and indicated low-grade systemic inflammation. However, these changes were not significantly different between genotypes nor correlated to any of the observed OA features. It is possible that the added effect of CRP at the individual lipid level was overshadowed by the profuse systemic influence of the HFD itself.

Alternatively, it is arguable that CRP could have affected OA development locally. This is supported by de Visser *et al.* in a rat model of metabolic OA, where local changes in synovial fluid oxylipin concentrations were not equally translated into systemic changes for the same oxylipins measured in plasma[36]. A route through which CRP could be involved in lipid-driven local cartilage changes is via OA-induced upregulation and activation of phospholipase A2 (PLA2) enzymes by chondrocytes. PLA2 enzymes are able to dissociate pentameric CRP to its pathogenic monomeric (m)CRP subunits[37]. Increased PLA2 activity has been demonstrated in the synovial fluid of OA patients and animal models of OA[38-40]. Devoid of synovial fluid samples, we attempted to explore PLA2 activity in our lipidomic data from fasted plasma samples. Unfortunately, systemic lipid concentrations rendered some conflicting results concerning PLA2 activity. As PLA2 enzymes mainly convert PC to LPC, the decrease in systemic LPC/PC ratio in our HFD-fed mice suggests a lower activation of PLA2. Hydrolysis of PC to LPC by PLA2 enzymes produces a free fatty acid, which is frequently the omega-6 fatty acid arachidonic acid (ARA)[41]. In this respect, the observed increase in omega-6/omega-3 FFA ratio substantiates decreasing PLA2 activity. However, the increases in ARA and its metabolites point to an increased activation of PLA2. Combined enzymatic activities of PLA2 enzymes and cyclooxygenase (COX)-2 generate prostaglandins from ARA and members of this pathway have been implicated in OA pathogenesis[42 43]. Although sample volumes were insufficient to measure prostaglandin E2 (PGE2) levels, we did observe an increase in prostaglandin PGD2 concentration over time – further corroborating increased PLA2 activity. Clearly, the in vivo effects of the lipid metabolism on the inflammatory milieu is complex and circulating lipids do not provide the best read-out in our current model.

The physiological role of CRP may be just as complex, with its multiple active isoforms and manifold physiological functions in various biological systems. Even though CRP predates the adaptive immune system by millions of years, it was found to bridge innate with adaptive immunity by binding to Fcγ receptors on immune cells like monocytes[44]. Both hCRP-tg and wild-type mice showed expansion of the systemic monocyte fraction upon HFD feeding, consistent with previous findings[45]. However, we found that hCRP-tg

monocytes expressed more activation markers like CD11c, CCR2 and CD86. The integrin CD11c was predominantly expressed by activated CD11b^{+}GR-1^{low}CCR2^{+} monocytes, which are known to upregulate CD11c as an adhesive ligand during monocyte recruitment in shear flow[46]. This suggests that non-classical, patrolling GR-1^{low} monocytes were more actively recruited to the tissues of hCRP-tg mice compared with wild-type controls. In addition, hCRP-tg mice showed an increase in activated CD11b^{+}GR-1^{high}CCR2^{+}CD86^{+} classical monocytes, indicative of an enhanced inflammatory state. This latter observation might be linked to metabolic OA development, as the increased percentages of CD11b^{+} immune cells and monocyte subsets in the hCRP-tg genotype were positively associated with increasing lateral OA severity. Wild-type controls showed inverse associations, strengthening the involvement of CRP in the activation of these immune populations.

The systemic activation of myeloid cells was not reflected in the knee joint, where synovial macrophage subsets were comparable between hCRP-tg and wild-type littermates. This is consistent with the similar synovitis scores found in both groups. Our findings add to recent reports on HFD-induced OA in mice on a C57BL/6J background, where macrophage depletion aggravated cartilage degeneration following injury[47] and resident adipose tissue macrophages retained their M2-like phenotype in the infrapatellar fat pad[48]. Together, these findings emphasize the persistence and therefore the importance of local macrophage populations in regulating homeostasis in the osteoarthritic knee joint. The combination of monocyte recruitment and unchanged resident macrophage populations in our study show similarities to observations in a mouse model of inflammatory arthritis[49]. Here, tissue-resident synovial macrophages showed no changes in phenotype or number and expressed markers of M2 polarization over the course of arthritis. However, the authors showed that non-classical monocytes recruited from circulation orchestrated the initiation and resolution of joint inflammation by differentiating into M1 and M2 macrophages respectively. Perhaps the hint towards an overall increase in CD206 expression in the synovium indicates monocyte presence, as activated monocytes are able to upregulate CD206 expression[50]. This monocytic plasticity and the role of human CRP herein warrants further research in the context of metabolic OA.

Although the functional involvement of CRP in OA pathogenesis remains uncertain, our study shed some light on the biological processes involved. This uncertainty is inherent to the gain-of-function model we employed, as overexpression phenotypes often fail to faithfully reflect the physiological function(s) of a protein[51]. A loss-of-function model would have provided more straightforward interpretable results. However, unlike human CRP, mouse CRP is a minor acute-phase reactant and is synthesized in only trace amounts[52 53]. Human CRP, when transferred into mice, behaves as it does in man: its expression is highly inducible and tissue-specific[29]. We believe that this significant

difference in the transcriptional control of CRP synthesis in humans and mice justifies the use of our model for studying human CRP. Still, extrapolation from mouse to man requires caution. Validation of our findings on peripheral monocyte subsets in obese OA patients with high and low CRP levels is required to confirm the role CRP in OA pathogenesis. An additional potential limitation of our study is that chow controls were not included in our study, as we focused on CRP involvement in OA and previous work by our group has shown that HFD feeding in hCRP-tg males led to severe OA development compared with chow-fed hCRP-tg males[8].

The present study implicates CRP as an independent trigger for the aggravation of metabolic OA by increasing cartilage degeneration and osteophytosis. Increased recruitment of classical and non-classical monocytes might be a mechanism of action through which CRP is involved in aggravating this process. Based on our data, involvement of CRP in lipid metabolism and synovial macrophage activation seems unlikely. Although the mechanism of action for CRP involvement in OA is not yet resolved, it is clear that we are selling CRP short when solely considering it a general systemic inflammation marker in metabolic OA. Our findings suggest that interventions selectively directed against CRP activity could ameliorate metabolic OA development.

Acknowledgements

We thank Marjolein van Rotterdam for the technical and operational aspects of the animal facilities. We thank Sabina Bijlsma, Carina de Jong-Rubingh and Eric Schoen for their continued statistical support. We thank Jan Lindeman and Marlieke Geerts at the Leiden University Medical Center and for their help with the development of the triple chromogenic immunostaining for macrophages. We thank Anne Schwerk for her enthusiastic assistance concerning the histological part of the research. The authors acknowledge that due to space limitations only a subselection of references is included in this manuscript.

Authors' contributions

AEK, AMZ, IB and RS have designed the experiment. AEK, MT, FC, RS, FH, JB and JB have carried out experimental procedures. AEK has been the primary person responsible for writing the manuscript. HMV, SCM, AMZ, DAB, FPJL, IB, RS, AM and HW were involved in drafting the work or revising it critically for important intellectual content. All authors approved the final version to be published.

Funding

This manuscript was supported by funding from the Netherlands Organization for Applied Scientific Research (TNO) and the European Union's Seventh Framework Programme for research, technological development and demonstration under grant

agreement No. 305815-D-BOARD. Funders did not have any additional role in the study design, data collection and analysis, decision to publish or preparation of the manuscript.

Competing interests

The authors declare that they have no conflict of interest.

References

1. Pottie P, Presle N, Terlain B, Netter P, Mainard D, Berenbaum F. Obesity and osteoarthritis: more complex than predicted! *Ann Rheum Dis* 2006;65(11):1403-5. doi: 10.1136/ard.2006.061994
2. Velasquez MT, Katz JD. Osteoarthritis: another component of metabolic syndrome? *Metab Syndr Relat Disord* 2010;8(4):295-305. doi: 10.1089/met.2009.0110
3. Thijssen E, van Caam A, van der Kraan PM. Obesity and osteoarthritis, more than just wear and tear: pivotal roles for inflamed adipose tissue and dyslipidaemia in obesity-induced osteoarthritis. *Rheumatology (Oxford)* 2015;54(4):588-600. doi: 10.1093/rheumatology/keu464
4. Wang X, Hunter D, Xu J, Ding C. Metabolic triggered inflammation in osteoarthritis. *Osteoarthritis Cartilage* 2015;23(1):22-30. doi: 10.1016/j.joca.2014.10.002
5. Hotamisligil GS. Inflammation and metabolic disorders. *Nature* 2006;444(7121):860-7. doi: 10.1038/nature05485
6. Berenbaum F, Griffin TM, Liu-Bryan R. Review: Metabolic Regulation of Inflammation in Osteoarthritis. *Arthritis Rheumatol* 2017;69(1):9-21. doi: 10.1002/art.39842
7. Kozijn AE, Gierman LM, van der Ham F, Mulder P, Morrison MC, Kuhnast S, et al. Variable cartilage degradation in mice with diet-induced metabolic dysfunction: food for thought. *Osteoarthritis Cartilage* 2018;26(1):95-107. doi: 10.1016/j.joca.2017.10.010
8. Gierman LM, van der Ham F, Koudijs A, Wielinga PY, Kleemann R, Kooistra T, et al. Metabolic stress-induced inflammation plays a major role in the development of osteoarthritis in mice. *Arthritis Rheum* 2012;64(4):1172-81. doi: 10.1002/art.33443
9. Hanada M, Takahashi M, Furuhashi H, Koyama H, Matsuyama Y. Elevated erythrocyte sedimentation rate and high-sensitivity C-reactive protein in osteoarthritis of the knee: relationship with clinical findings and radiographic severity. *Ann Clin Biochem* 2016;53(Pt 5):548-53. doi: 10.1177/0004563215610142
10. Sanchez-Ramirez DC, van der Leeden M, van der Esch M, Roorda LD, Verschueren S, van Dieen JH, et al. Elevated C-reactive protein is associated with lower increase in knee muscle strength in patients with knee osteoarthritis: a 2-year follow-up study in the Amsterdam Osteoarthritis (AMS-OA) cohort. *Arthritis Res Ther* 2014;16(3):R123. doi: 10.1186/ar4580
11. Lee YC, Lu B, Bathon JM, Haythornthwaite JA, Smith MT, Page GG, et al. Pain sensitivity and pain reactivity in osteoarthritis. *Arthritis Care Res (Hoboken)* 2011;63(3):320-7. doi: 10.1002/acr.20373
12. Punzi L, Ramonda R, Oliviero F, Sfriso P, Mussap M, Plebani M, et al. Value of C reactive protein in the assessment of erosive osteoarthritis of the hand. *Ann Rheum Dis* 2005;64(6):955-7. doi: 10.1136/ard.2004.029892
13. Spector TD, Hart DJ, Nandra D, Doyle DV, Mackillop N, Gallimore JR, et al. Low-level increases in serum C-reactive protein are present in early osteoarthritis of the knee and predict progressive disease. *Arthritis Rheum*

1997;40(4):723-7.doi:10.1002/1529-0131(199704)40:4<723::AID-ART18>3.0.CO;2-L
14. Pearle AD, Scanzello CR, George S, Mandl LA, DiCarlo EF, Peterson M, et al. Elevated high-sensitivity C-reactive protein levels are associated with local inflammatory findings in patients with osteoarthritis. *Osteoarthritis Cartilage* 2007;15(5):516-23. doi: 10.1016/j.joca.2006.10.010
15. Sturmer T, Brenner H, Koenig W, Gunther KP. Severity and extent of osteoarthritis and low grade systemic inflammation as assessed by high sensitivity C reactive protein. *Ann Rheum Dis* 2004;63(2):200-5.
16. Jin X, Beguerie JR, Zhang W, Blizzard L, Otahal P, Jones G, et al. Circulating C reactive protein in osteoarthritis: a systematic review and meta-analysis. *Ann Rheum Dis* 2015;74(4):703-10. doi: 10.1136/annrheumdis-2013-204494
17. Kerkhof HJ, Bierma-Zeinstra SM, Castano-Betancourt MC, de Maat MP, Hofman A, Pols HA, et al. Serum C reactive protein levels and genetic variation in the CRP gene are not associated with the prevalence, incidence or progression of osteoarthritis independent of body mass index. *Ann Rheum Dis* 2010;69(11):1976-82. doi: 10.1136/ard.2009.125260
18. Davis CR, Karl J, Granell R, Kirwan JR, Fasham J, Johansen J, et al. Can biochemical markers serve as surrogates for imaging in knee osteoarthritis? *Arthritis Rheum* 2007;56(12):4038-47. doi: 10.1002/art.23129
19. Engstrom G, Gerhardsson de Verdier M, Rollof J, Nilsson PM, Lohmander LS. C-reactive protein, metabolic syndrome and incidence of severe hip and knee osteoarthritis. A population-based cohort study. *Osteoarthritis Cartilage* 2009;17(2):168-73. doi: 10.1016/j.joca.2008.07.003
20. Livshits G, Zhai G, Hart DJ, Kato BS, Wang H, Williams FM, et al. Interleukin-6 is a significant predictor of radiographic knee osteoarthritis: The Chingford Study. *Arthritis Rheum* 2009;60(7):2037-45. doi: 10.1002/art.24598
21. Matthews DR, Hosker JP, Rudenski AS, Naylor BA, Treacher DF, Turner RC. Homeostasis model assessment: insulin resistance and beta-cell function from fasting plasma glucose and insulin concentrations in man. *Diabetologia* 1985;28(7):412-9.
22. Glasson SS, Chambers MG, Van Den Berg WB, Little CB. The OARSI histopathology initiative - recommendations for histological assessments of osteoarthritis in the mouse. *Osteoarthritis Cartilage* 2010;18 Suppl 3:S17-23. doi: 10.1016/j.joca.2010.05.025
23. van Dijk RA, Rijs K, Wezel A, Hamming JF, Kolodgie FD, Virmani R, et al. Systematic Evaluation of the Cellular Innate Immune Response During the Process of Human Atherosclerosis. *J Am Heart Assoc* 2016;5(6) doi: 10.1161/JAHA.115.002860
24. Zhang W, Sun G, Aitken D, Likhodii S, Liu M, Martin G, et al. Lysophosphatidylcholines to phosphatidylcholines ratio predicts advanced knee osteoarthritis. *Rheumatology (Oxford)* 2016;55(9):1566-74. doi: 10.1093/rheumatology/kew207
25. Devaraj S, Singh U, Jialal I. Human C-reactive protein and the metabolic syndrome. *Curr Opin Lipidol* 2009;20(3):182-9. doi: 10.1097/MOL.0b013e32832ac03e
26. Voils SA, Cooper-DeHoff RM. Association between high sensitivity C-reactive protein and metabolic syndrome in subjects completing the

National Health and Nutrition Examination Survey (NHANES) 2009-10. *Diabetes Metab Syndr* 2014;8(2):88-90. doi: 10.1016/j.dsx.2014.04.021
27. Tanigaki K, Vongpatanasin W, Barrera JA, Atochin DN, Huang PL, Bonvini E, et al. C-reactive protein causes insulin resistance in mice through Fcgamma receptor IIB-mediated inhibition of skeletal muscle glucose delivery. *Diabetes* 2013;62(3):721-31. doi: 10.2337/db12-0133
28. Kaneko H, Anzai T, Nagai T, Anzai A, Takahashi T, Mano Y, et al. Human C-reactive protein exacerbates metabolic disorders in association with adipose tissue remodelling. *Cardiovasc Res* 2011;91(3):546-55. doi: 10.1093/cvr/cvr088
29. Ciliberto G, Arcone R, Wagner EF, Ruther U. Inducible and tissue-specific expression of human C-reactive protein in transgenic mice. *EMBO J* 1987;6(13):4017-22.
30. Marnell L, Mold C, Du Clos TW. C-reactive protein: ligands, receptors and role in inflammation. *Clinical immunology* 2005;117(2):104-11. doi: 10.1016/j.clim.2005.08.004
31. Schett G. Joint remodelling in inflammatory disease. *Ann Rheum Dis* 2007;66 Suppl 3:iii42-4. doi: 10.1136/ard.2007.078972
32. Blom AB, van Lent PL, Holthuysen AE, van der Kraan PM, Roth J, van Rooijen N, et al. Synovial lining macrophages mediate osteophyte formation during experimental osteoarthritis. *Osteoarthritis Cartilage* 2004;12(8):627-35. doi: 10.1016/j.joca.2004.03.003
33. Mapp PI, Walsh DA. Mechanisms and targets of angiogenesis and nerve growth in osteoarthritis. *Nat Rev Rheumatol* 2012;8(7):390-8. doi: 10.1038/nrrheum.2012.80
34. Chen J, Gu Z, Wu M, Yang Y, Zhang J, Ou J, et al. C-reactive protein can upregulate VEGF expression to promote ADSC-induced angiogenesis by activating HIF-1alpha via CD64/PI3k/Akt and MAPK/ERK signaling pathways. *Stem Cell Res Ther* 2016;7(1):114. doi: 10.1186/s13287-016-0377-1
35. Hamilton JL, Nagao M, Levine BR, Chen D, Olsen BR, Im HJ. Targeting VEGF and Its Receptors for the Treatment of Osteoarthritis and Associated Pain. *J Bone Miner Res* 2016;31(5):911-24. doi: 10.1002/jbmr.2828
36. de Visser HM, Mastbergen SC, Ravipati S, Barrett DA, Welsing PM, Chapman V, et al. Quantification of systemic and local lipid-derived inflammatory mediators in a rat OA model. *Osteoarthritis and Cartilage* 2017;25(Supplement 1):S98-S99. doi: 10.1016/j.joca.2017.02.158
37. Thiele JR, Habersberger J, Braig D, Schmidt Y, Goerendt K, Maurer V, et al. Dissociation of pentameric to monomeric C-reactive protein localizes and aggravates inflammation: in vivo proof of a powerful proinflammatory mechanism and a new anti-inflammatory strategy. *Circulation* 2014;130(1):35-50. doi: 10.1161/CIRCULATIONAHA.113.007124
38. Kortekangas P, Aro HT, Nevalainen TJ. Group II phospholipase A2 in synovial fluid and serum in acute arthritis. *Scand J Rheumatol* 1994;23(2):68-72.
39. Panula HE, Lohmander LS, Ronkko S, Agren U, Helminen HJ, Kiviranta I. Elevated levels of synovial fluid PLA2, stromelysin (MMP-3) and TIMP in early osteoarthrosis after tibial valgus osteotomy in young beagle dogs. *Acta Orthop Scand* 1998;69(2):152-8.
40. Valdes AM, Loughlin J, Timms KM, van Meurs JJ, Southam L, Wilson

SG, et al. Genome-wide association scan identifies a prostaglandin-endoperoxide synthase 2 variant involved in risk of knee osteoarthritis. *Am J Hum Genet* 2008;82(6):1231-40. doi: 10.1016/j.ajhg.2008.04.006
41. Balsinde J, Winstead MV, Dennis EA. Phospholipase A(2) regulation of arachidonic acid mobilization. *FEBS Lett* 2002;531(1):2-6.
42. Bar-Or D, Rael LT, Thomas GW, Brody EN. Inflammatory Pathways in Knee Osteoarthritis: Potential Targets for Treatment. *Curr Rheumatol Rev* 2015;11(1):50-58. doi: 10.2174/1573397111666150522094131
43. Dave M, Amin AR. Yin-Yang regulation of prostaglandins and nitric oxide by PGD2 in human arthritis: reversal by celecoxib. *Immunol Lett* 2013;152(1):47-54. doi: 10.1016/j.imlet.2013.04.002
44. Du Clos TW, Mold C. C-reactive protein: an activator of innate immunity and a modulator of adaptive immunity. *Immunol Res* 2004;30(3):261-77. doi: 10.1385/IR:30:3:261
45. Beliard S, Le Goff W, Saint-Charles F, Poupel L, Deswaerte V, Boucharechas L, et al. Modulation of Gr1low monocyte subset impacts insulin sensitivity and weight gain upon high-fat diet in female mice. *Int J Obes (Lond)* 2017 doi: 10.1038/ijo.2017.179
46. Wu H, Gower RM, Wang H, Perrard XY, Ma R, Bullard DC, et al. Functional role of CD11c+ monocytes in atherogenesis associated with hypercholesterolemia. *Circulation* 2009;119(20):2708-17. doi: 10.1161/CIRCULATIONAHA.108.823740
47. Wu CL, McNeill J, Goon K, Little D, Kimmerling K, Huebner J, et al. Conditional Macrophage Depletion Increases Inflammation and Does Not Inhibit the Development of Osteoarthritis in Obese Macrophage Fas-Induced Apoptosis-Transgenic Mice. *Arthritis Rheumatol* 2017;69(9):1772-83. doi: 10.1002/art.40161
48. Barboza E, Hudson J, Chang WP, Kovats S, Towner RA, Silasi-Mansat R, et al. Profibrotic Infrapatellar Fat Pad Remodeling Without M1 Macrophage Polarization Precedes Knee Osteoarthritis in Mice With Diet-Induced Obesity. *Arthritis Rheumatol* 2017;69(6):1221-32. doi: 10.1002/art.40056
49. Misharin AV, Cuda CM, Saber R, Turner JD, Gierut AK, Haines GK, 3rd, et al. Nonclassical Ly6C(-) monocytes drive the development of inflammatory arthritis in mice. *Cell reports* 2014;9(2):591-604. doi: 10.1016/j.celrep.2014.09.032
50. Dias-Melicio LA, Fernandes RK, Rodrigues DR, Golim MA, Soares AM. Interleukin-18 increases TLR4 and mannose receptor expression and modulates cytokine production in human monocytes. *Mediators Inflamm* 2015;2015:236839. doi: 10.1155/2015/236839
51. Sochalska M, Tuzlak S, Egle A, Villunger A. Lessons from gain- and loss-of-function models of pro-survival Bcl2 family proteins: implications for targeted therapy. *FEBS J* 2015;282(5):834-49. doi: 10.1111/febs.13188
52. Whitehead AS, Zahedi K, Rits M, Mortensen RF, Lelias JM. Mouse C-reactive protein. Generation of cDNA clones, structural analysis, and induction of mRNA during inflammation. *Biochem J* 1990;266(1):283-90.
53. Szalai AJ, McCrory MA. Varied biologic functions of C-reactive protein: lessons learned from transgenic mice. *Immunol Res* 2002;26(1-3):279-87. doi: 10.1385/IR:26:1-3:279

Supplemental Materials and methods

Experimental animals and housing

The experiment was carried out in male human CRP-transgenic (hCRP-tg, n=30) and male wild-type littermates (n=15) on a C57BL/6J background. Males were chosen over females because hCRP-tg males express higher levels of CRP and are more prone to develop metabolic OA[1 2]. Group sizes were determined based on variance obtained from historical data, in which the power analysis for lipid profiling was leading. In turn, estimated effect size and variation of these data will be used to estimate the required sample size for future studies. Mice were obtained from the in-house breeding colony (TNO Metabolic Health Research, Leiden, The Netherlands) at our specific pathogen-free (SPF) animal facility. The hCRP-tg mice carry the hCRP transgene engineered in the laboratory of Dr. Ulrich Rüther[3] and were repeatedly backcrossed to become C57BL/6J congenic. The transgene is a 31-kb fragment of human DNA containing the CRP gene, with the CRP promoter and all the known CRP regulatory elements at the 5' flanking region and a CRP pseudogene at the 3' flanking region[4]. Genotyping was performed by polymerase chain reaction using genomic DNA from ear punches. Age at the start of the study was 12 weeks. Mice were housed in open polycarbonate cages (Type II L) with 2-3 animals/cage. Cages were set up in temperature-controlled (21 ± 0.5°C) and humidity-controlled (45 ± 2%) rooms, with 15 air changes/hour under filtered positive pressure ventilation. Mice were maintained under standard conditions with a 12 h light-dark cycle (beginning at 07:00 UTC+1) and monitored twice a day. The experiment was approved by the institutional Animal Care and Use Committee of TNO and was in compliance with ARRIVE guidelines and European Community specifications regarding the use of laboratory animals.

Experimental design

Metabolic OA was induced by switching the diet of the mice from standard chow to a high-fat diet (HFD, 45 kcal% from fat; cat# D12451, Research Diets Inc., New Brunswick, USA) at 12 weeks of age. Both groups received the HFD for a consecutive period of 38 weeks. During the study period, the diets were stored frozen (-20°C) and refreshed weekly. Mice had access to autoclaved water and food ad libitum. One hCRP-tg mouse died after 34 weeks in the study and was excluded from data analysis.

Assessment of metabolic dysfunction

To monitor metabolic dysfunction, body weights (every other week) and changes in body composition (t = 0/6/15/25/37 weeks) by EchoMRI LLC (Houston, TX, USA) were determined during the entire study period. At regular intervals (t = 0/6/14/22/30/38 weeks) EDTA plasma samples were collected by tail vein incision after a 4-5 hour fasting period. Total cholesterol was determined by enzymatic assay (No. 11491458216,

Roche Diagnostics Nederland BV, The Netherlands) directly upon plasma collection according to manufacturer's instructions. Residual plasma was stored at -80ºC. Fasted plasma CRP, glucose and insulin levels were measured for all time points at once. CRP levels were determined by sandwich ELISA (cat.no. DY1707, R&D Systems, USA). Glucose levels were determined by the hexokinase method using commercial reagents (cat.no. 2319 and 2942, InstruChemie, The Netherlands; cat.no. G6918, Sigma-Aldrich, The Netherlands). Insulin levels were determined using an ELISA for mouse insulin (cat.no. 10-1113-01, Mercodia, Sweden). Insulin resistance index (HOMA-IR) was calculated according to the equation proposed by Matthews et al.5: HOMA-IR = (glucose (mmol/L) × insulin (mU/L)) / 22.5.

Histopathology of the knee

Knee joints were harvested, fixed in a 10% formalin neutral buffered solution (Sigma-Aldrich, The Netherlands) for 24 hours, decalcified in Kristensen's solution, dehydrated and embedded in paraffin. Serial coronal 5 µm sections were collected throughout the joint at 60 µm intervals and stained with Weigert's Hematoxylin, Fast Green and Safranin-O. Two representative sections from the midcoronal region of each knee joint were evaluated for OA severity, using the OARSI histopathology initiative scoring system for the mouse6. Grading was performed by two independent observers who were blinded for group assignment. The joint was scored at 6 locations: femoral condyles and tibial plateaus at the lateral and medial sides, trochlear groove and the patella (score 0-6 per compartment). Due to incomplete patellar scores for some mice, we report the sum of the medial and lateral scores as the total tibiofemoral cartilage degeneration score (maximum total score 24). Osteophyte formation and synovitis were scored separately on the same sections according to the 0-3 scoring paradigm recommended by the OARSI histopathology initiative6: 0 is normal, 1 = mild, 2 = moderate and 3 = severe changes. We report the sum of the medial and lateral compartments as the total score (maximum total score 12). One wild-type mouse was not scored for any OA feature due to technical difficulties and was excluded from any analysis concerning OA scores.

Lipid and oxylipin analyses in fasted plasma

Samples were stored at -80°C before analysis. General lipid profiles were determined at time points t=0 weeks, t=4 days after HFD switch (peak in hCRP plasma levels) and t=38 weeks. Oxylipin profiling was performed at t=0, 14 and 38 weeks, due to deficient sample volumes at the intermediate blood collection at t=4 days.

Five µl of fasted plasma was extracted with isopropanol containing several internal standards (IS) (C17:0 lysophosphatidylcholine, di-C12:0 phosphatidylcholine, tri-C17:0 glycerol ester, C17:0 cholesterol ester, C17:0 ceramide d31-C16:0 fatty acid and d33-C17:0

fatty acid). The extract was split into two parts, one part was derivatised for analysis of free fatty acids and polar lipids, the second part was processed further without derivatisation for the analysis of neutral lipids (TG, ChE, ...). FFA (after derivatization) and polar lipids were separated on a Waters Aquity BEH C8 column [150 x 2.1 mm, 1.7 µm, temperature (T) = 50°C] using a mobile phase gradient from 98% mobile phase A [0.1% formic acid in water] to 100% mobile phase B (0.1% formic acid in acetonitrile:IPA 6:4) in 25,5 min with a flow of 0.5 ml/min. Mass detection was carried out using electrospray ionization in the positive mode (heater capillary temperature 300°C, spray voltage 4 kV, scan range m/z 202-1000). Injection volume was 2 µl. Neutral lipids were separated on a Waters Aquity BEH phenyl column (100 x 2.1 mm, 1.7 µm; T = 60°C) using a mobile phase gradient from 40% mobile phase A [5% methanol in 0.1% formic acid, 10 mM NH_4Ac] to 100% mobile phase B (100% methanol containing 0.1% formic acid , 2 mM NH_4Ac) in 13 min with a flow of 0.4 ml/min. Mass detection was carried out using atmospheric pressure chemical ionization in the positive mode (heater capillary temperature 150°C, vaporizer temperature 260°C, spray current 6µA, scan range m/z 300–1,200). Injection volume was 3 µl. All measurements were performed in randomized order and a quality control (QC) sample (NIST human plasma reference sample) was measured between every 10 samples during the analysis procedure for performance control. Identification was based on (relative) retention times and accurate mass of the lipids. More than 200 individual lipids were reported. Concentrations of complex lipids were determined relative to internal standards of the respective compound classes, i.e., for LPC, PC, TG, Cer, and ChE. Exceptions were made for DG, which were reported relative to C17:0 Cer, and for SPM, which were reported relative to C17:0 LPC. Analysis of the fatty acids extracts was performed according to the method described by Pettinella et al.7, which involves derivatization of fatty acids with quaternary ammonium, allowing an analysis of fatty acid derivatives in the positive mode and the discrimination of n-3 and n-6 fatty acids. Lysophosphatidylcholines (LPC) to phosphatidylcholines (PC) ratio was calculated by dividing the sum of all measured LPC by the sum of all measured PC. Due to deficient sample volumes not permitting a separate measurement of total fatty acid composition, the omega-6/omega-3 FFA ratio was approximated based on the non-esterified fatty acids that were measured.

For oxylipin analysis, sample volumes of 50 µl were aliquoted from each fasted plasma sample. Internal standards (10µl of PGF2a-EA-d4 (2.49µM), 10µl of AA-d8 (1µM), 10µl of PGD2-d4 (1µM), 10µl of 15-HETE-d8 (7.6µM) were added to each sample or blank sample (MilliQ water), along with 2µl of formic acid (98% v/v) and 5µl butylhydroxytoluene. Sample preparation and analysis was performed based on the method described by Wong et al.[8]. In summary, lipids were extracted by SPE, separated using HPLC and detected using mass spectrometry in multiple reaction monitoring mode. Pooled QC samples (human plasma) were interspaced approximately after every 14 study samples

to monitor the method performance. A total of 23 oxylipins were quantified, using appropriate standards. Concentrations were calculated using fully extracted calibration standards for each of the analytes.

Immunophenotyping of peripheral cell populations

Peripheral myeloid and lymphoid populations were analysed by flow cytometry at three different time points (t=2/11/37 weeks). Baseline values were determined in age-matched hCRP-tg (n=5) and wild-type (n=4) males from later litters. As such, these measurements were excluded from statistical analysis.

Peripheral blood (5 drops/animal) was drawn via tail incision using lithium heparin-coated Microvette tubes. Following erythrocyte lysis, cells were washed and resuspended in staining buffer (phosphate buffered saline solution with 2%newborn calf serum, PBS-NBCS). Cells were then divided into two samples and transferred to V-bottom 96-wells plates, washed and blocked with 50µl normal mouse serum for 15 minutes at room temperature. Cell-surface staining was performed with the myeloid and lymphoid antibody panels shown in Tables 1 and 2. Anti-CD16/CD32 monoclonal antibody (clone 2.4G2, dilution 1:50, cat#553141, BD Biosciences, USA) was added to the antibody mix to reduce non-specific antibody binding. Staining incubation was performed in PBS-NBCS for 30 minutes at 4ºC. Pooled samples were used for unstained, single-stained and FMO controls. Data acquisition was performed with a 3-laser FACSCanto™ II flow cytometer using the FACSDiva Software (Becton Dickinson) (Supplemental Table S1). Cytometer Setup and Tracking beads and CompBeads antibody-capturing particles (both BD Biosciences) were used to standardize instrument and compensation settings, respectively. Flow cytometry data were analysed using FlowJo v10.2 (Treestar Inc., USA). Cell clumps were gated out on a pulse geometry gate (FSC-H×FSC-A). Debris sized <25K were excluded on low angle (forward scatter, FSC) vs. 90º angle (side scatter, SSC; "live" gate). Cell populations of interest were subsequently gated according to the gating strategies as depicted in Supplemental Figures S2 and S3, to obtain their population frequencies.

Immunohistochemical evaluation of synovial macrophages

Knee joints from both groups were stained with chromogenic triple-labelling immunohistochemistry (IHC) for M1 and M2 macrophage subsets, based on a previously described method for human tissue9. Primary antibodies targeted murine macrophages (F4/80, 1:100, MF48000 (BM8), Invitrogen), M1 macrophages (iNOS, 1:400, ab136918 (K13-A), Abcam) and M2 macrophages (CD206, 1:100, AF2535, R&D Systems). The first section of each slide served as a negative control to which no primary antibodies were applied. Slides were deparaffinized with xylene for 5 min and rehydrated through graded alcohols to DI water. Heat-induced antigen retrieval was

performed in the Dako PT Link System using the low pH Target Retrieval Solution (pH 6.0, Dako, CA, USA). After washing, primary antibodies against F4/80 and iNOS were added for overnight incubation at 4°C. Slides were washed the next day, blocked in 0.3% H_2O_2 for 15 min at RT, and incubated with appropriate AP- and HRP-conjugated secondary antibodies (RALP525 L, Biocare Medical; ab97057, Abcam). Positive reactions were visualized with Ferangi Blue (FB813H, Biocare Medical) for iNOS and StayYellow (ab169561, Abcam) for F4/80. To inactivate preceding labels, slides were incubated with antibody elution buffer (100 mM glycine/NaOH, pH 10.0) for 1 hour at 50°C. Following a washing step, primary antibody against CD206 was added for a 2-hour incubation at 37°C. Slides were washed and incubated with an appropriate AP-conjugated secondary antibody (ab6886, Abcam), which was visualized with Liquid Fast Red (TA-125-AL, ThermoScientific). Slides were dried in the oven for 1 hour at 37°C and coverslipped with EcoMount (Biocare Medical) for microscopic examination. All intermediate washing steps were done in PBS, except for the visualization steps for which TBS was used. Except for the first secondary antibody step, antibodies were diluted in PBS with 1% BSA (Sigma-Aldrich).

Quantification was performed in the lateral patellofemoral synovial lining of the knee joint, here referred to as the region of interest (ROI). Digital images of the unmixed colour spectra for each chromogen in the ROI were obtained with a Nuance multispectral imaging system (40x magnification). Macrophage subtypes were analysed using ImageJ 1.51n image analysis software. After selection of the ROI by hand, positivity of each label was measured as a percentage of the ROI surface area. Positivity for CD206 and iNOS was also evaluated within the $F4/80^+$ cell fraction using the same method. Colocalization of two or three markers was calculated from the areal overlap between positivity for F4/80 and CD206 or iNOS or both. Data are expressed as the surface area percentage of a label or combination of labels within the ROI or within the $F4/80^+$ macrophage population.

Statistical analysis

Assumptions of normality were tested with the Shapiro-Wilk's W test and checked graphically based on the residuals. Levene's test was used to assess homogeneity of variances. Data analysed using parametric t-testing are presented as mean ± standard deviation (SD). Data analysed using non-parametric tests are presented by the median with interquartile range (range between the 25th to 75th percentiles). Effect sizes (d) were calculated using Hedges g and reported with corresponding 95% confidence intervals (CI). Results were evaluated by including and excluding outliers (defined as more than two SD from the mean). As inclusion of the outliers did not change statistical differences between groups, all outliers were included. Non-parametric Mann-Whitney U-test was used for comparison of metabolic parameters, lipid concentrations per

time point and (immuno)histopathological scores between groups. Non-parametric Spearman rank correlation was used to test for associations. Differences in lipid profiles were analysed by a multivariate approach: PCA was used to examine for any clustering trends, followed by supervised PLS-DA analysis to better examine differences in the underlying lipidomic profiles of both groups.

Prevalences of the various cell populations were expressed as percentage of a reference population. In many instances, the range in these percentages was such that an assumption of a constant absolute standard deviation was not warranted. For this reason, all data were log-transformed prior to analysis. This transformation turns data with constant relative standard deviation into data with a constant absolute standard deviation, thereby permitting the application of well-known statistical methods such as linear mixed models. The log-transformed data was analysed using a sequence of mixed models with mouse as a random factor, week as a within-subject factor and OA scores as well as genotype [diet] as between-subject factors or variables. The models used were: 1) a model including the main effects of genotype, week and the OA scores and the interaction effects between genotype and week (1 interaction term), genotype and OA scores (4 interaction terms) and week and OA scores (4 interaction terms), 2) a model including the main effects of genotype, week and the OA scores and the interaction effect between genotype and week, 3) a model including the main effects of genotype and week and the interaction effect between genotype and week. The first model was used to assess p-values for the interaction effects between genotype and OA scores and week and OA scores, the second model was used to assess the p-values of OA scores under the assumption that there are no interaction terms involving these scores. Finally, the third model was used to assess the p-values for genotype, week and the genotype by week interaction. For parameters with statistically significant effects involving genotype or OA scores ($p < 0.01$), a backward elimination procedure was applied so that the final models for the respective parameters only include statistically significant effects. Interpretation and quantification of the statistically significant effects are based on these models. In all other analyses, a p-value <0.05 was considered statistically significant.

Supplemental Figures

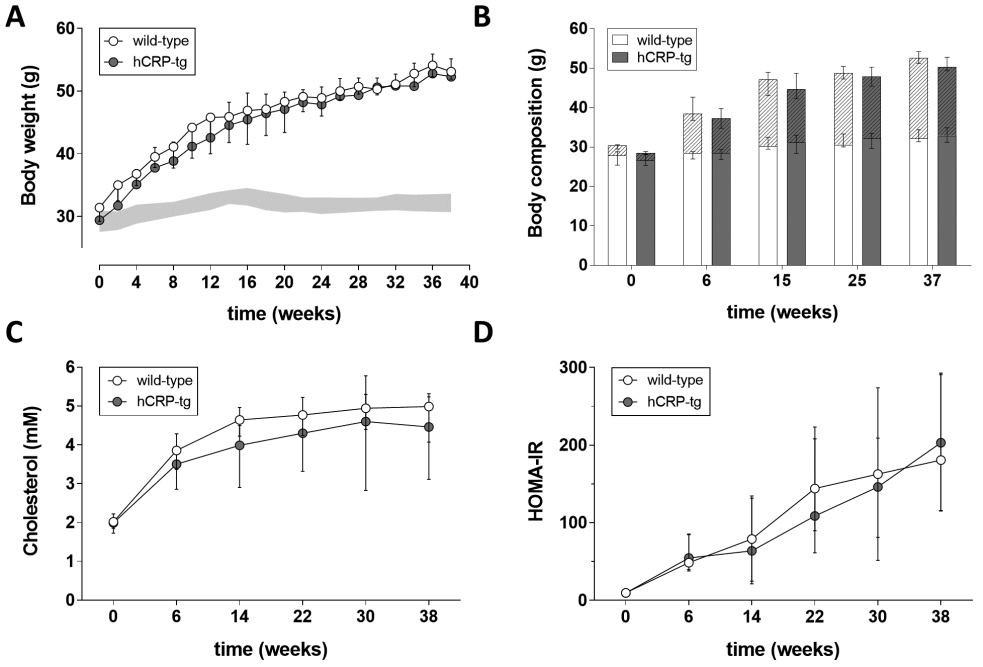


Figure S1. Increases in body weight due to fat accumulation, cholesterol and insulin resistance index (HOMA-IR) reflect a state of metabolic dysfunction in both hCRP-tg and wild-type mice. A) Body weights of both groups during the study period. Grey line represents body weight gain (median ± IQR) for chow-fed hCRP-tg mice over 38 weeks, as determined in a previously published study8. B) Body composition represented by lean mass (filled bars) and fat mass (striped bars) at various time points. C) Total fasting cholesterol levels (mmol/L) during the course of the study. D) Elevated HOMA-IR due to prolonged HFD-induced increases in fasting insulin and glucose levels. Data are presented as group medians (indicated by symbols or bars) with IQR (error bars).

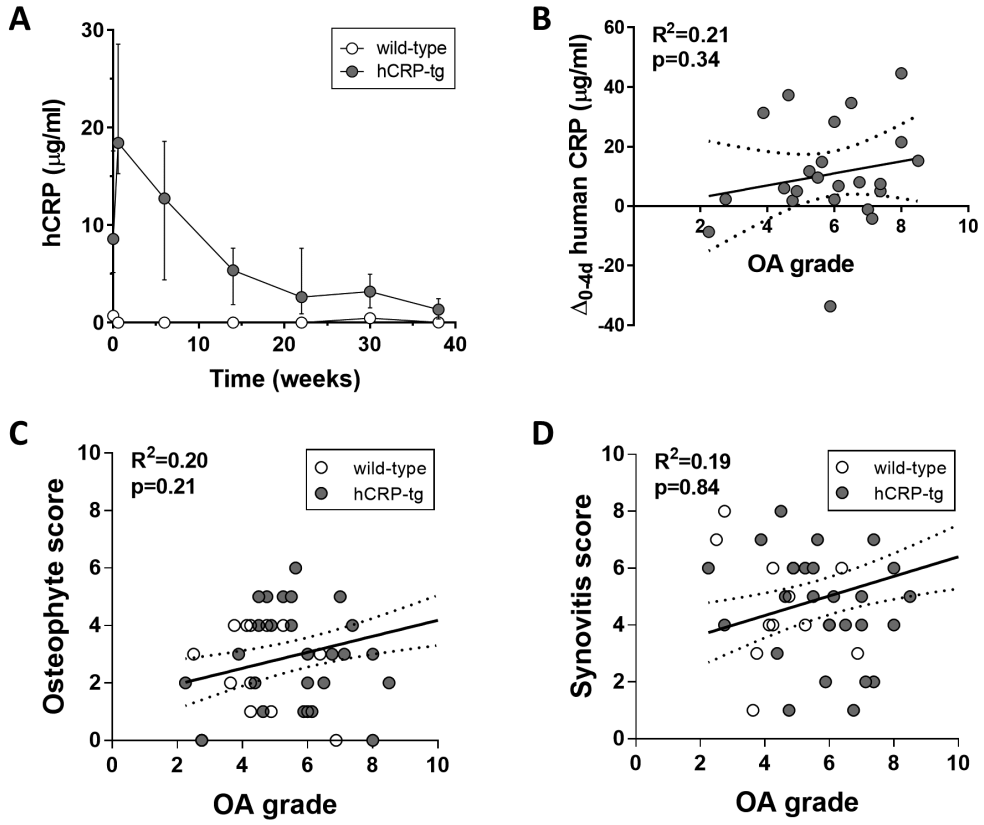


Figure S2. Human CRP levels and associations with end point OA grades. A) Human CRP levels in hCRP-tg and wild-type males during the course of the study. Values presented are the median ± IQR. B) Relative individual induction of human CRP plasma levels after 4 days on HFD show no association with total OA scores at end point. Total OA scores do not associate with osteophyte (C) and synovitis (D) scores at end point either.

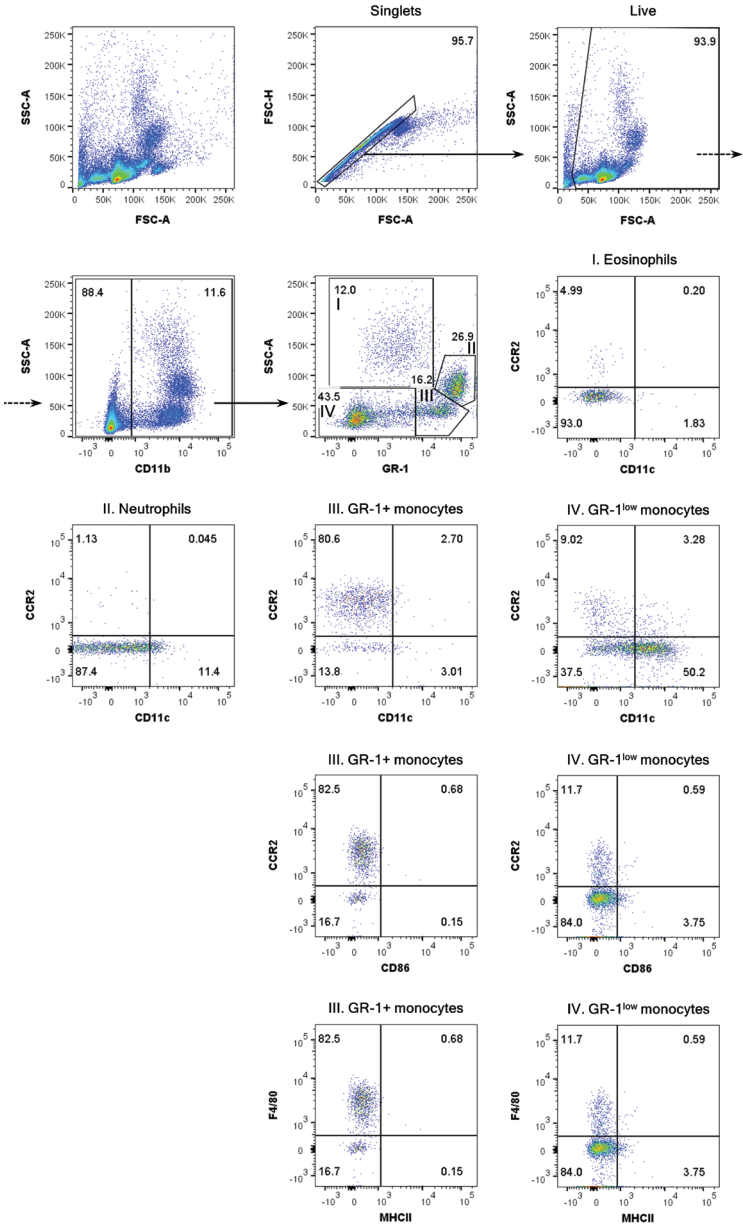


Figure S3. Gating strategy used to detect peripheral myeloid populations. Cell clumps were gated out on a pulse geometry gate (FSC-H×FSC-A; Singlets) and cells were subsequently gated according to size and scatter to eliminate dead cells and debris from analysis (SSC-A×FSC-A; "Live" gate). CD11b+ myeloid cells were defined and divided into 4 major subpopulations based on their size and expression of GR-1: I. Eosinophils, II. Neutrophils, III. GR-1+ monocytes and IV. GR-1-low monocytes. Subpopulations were subsequently assessed for their expression of activation markers.

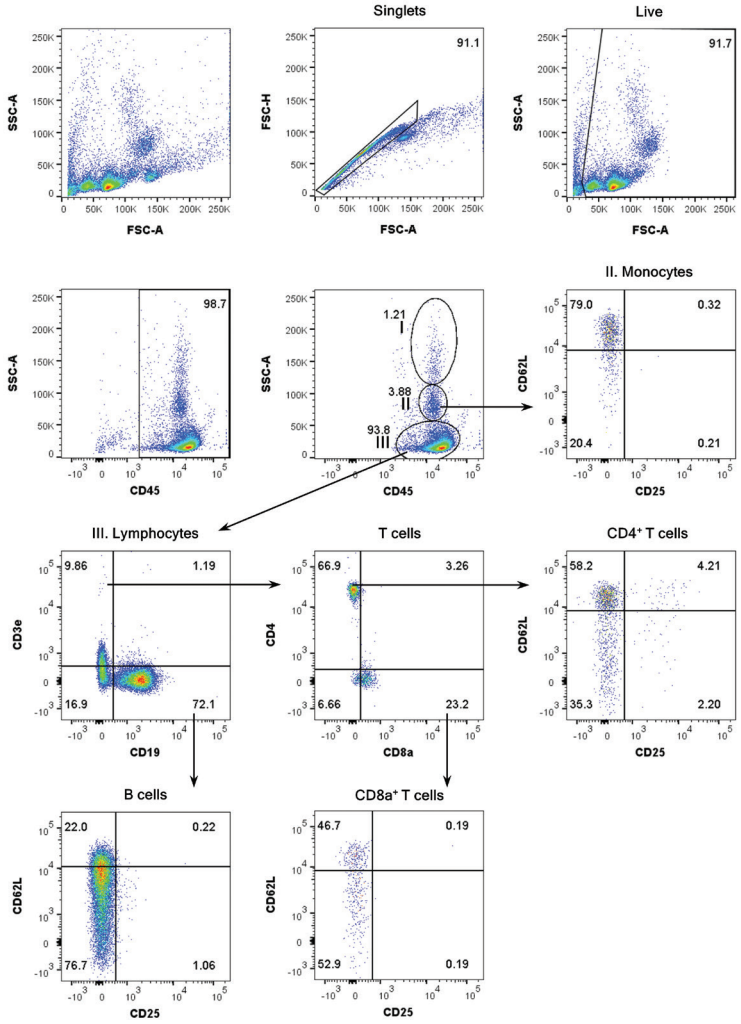


Figure S4. Gating strategy used to detect peripheral lymphoid populations. Cell clumps were gated out on a pulse geometry gate (FSC-H×FSC-A; Singlets) and cells were subsequently gated according to size and scatter to eliminate dead cells and debris from analysis (SSC-A×FSC-A; "Live" gate). CD45+ leukocytes were defined and divided into 3 major subpopulations based on their size: I. Granulocytes, II. Monocytes, III. Lymphocytes. T and B cells from the lymphocyte population were discriminated based on their surface expression of CD3ε and CD19, respectively. T cells were further characterized by their surface expression of CD4 and CD8a. All subpopulations were assessed for their expression of activation markers CD62L and CD25.

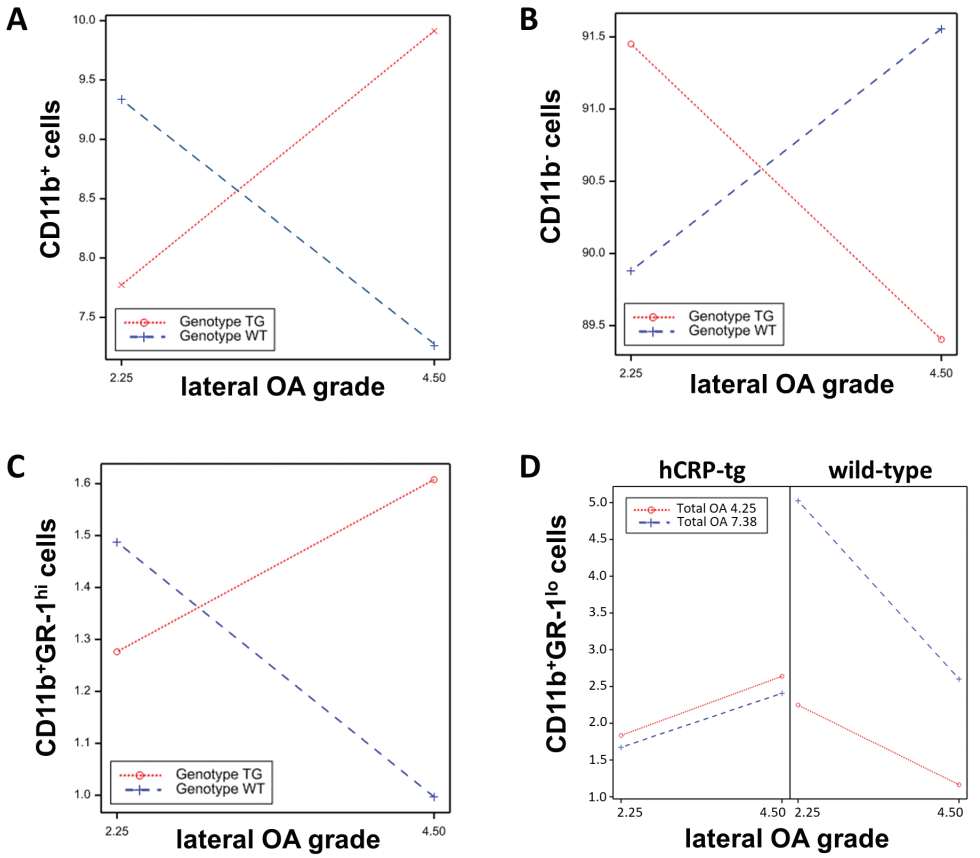


Figure S5. Correlations between genotype and OA development on the changes in circulating immune cell populations. A) Percentages of CD11b^{+} leukocytes were associated with lateral OA severity in hCRP-tg males, while in wild-type littermates this correlation was inversed. B) CD11b- cell populations significantly decreased with increasing lateral OA severity in hCRP-tg mice and vice versa for wild-type controls. The hCRP-tg genotype was also significantly associated with higher percentages of both classical CD11b^{+}GR-1^{hi} (C) and non-classical CD11b^{+}GR-1^{lo} (D) monocytes with increasing lateral OA severity. Wild-type controls showed an inverse relationship between these monocyte subsets and lateral OA severity.

Supplemental Tables

Table S1. List of the analysed free fatty acids.

Chain	Compound
C12:0	Lauric acid
C14:0	Myristic acid
C14:1	Myristoleic acid
C16:0	Palmitic acid
C16:1	(cis-)9-palmitoleic acid
C16:2	Hexadecadienoic acid
C18:0	Stearic acid
C18:1	Oleic acid
C18:2(ω-6)	Linoleic acid
C18:3(ω-3)	α-Linolenic acid
C18:3(ω-6)	γ-Linolenic acid
C20:0	Arachidic acid
C20:1	Gondoic acid
C20:2	11,14-eicosadienoic acid
C20:3(ω-3+6)	11,14,17-eicosatrienoic acid
C20:3(ω-9)	Mead acid
C20:4(ω-6)	Arachidonic acid
C20:5	5,8,11,14,17-eicosapentaenoic acid
C22:0	Behenic acid
C22:1	(cis-)erucic acid
C22:2	13,16-docosadienoic acid
C22:3	13,16,19-docosatrienoic acid
C22:4(ω-6)	7Z,10Z,13Z,16Z-docosatetraenoic acid
C22:5(ω-3)	7,10,13,16,19-docosapentaenoic acid
C22:5(ω-6)	4,7,10,13,16-docosapentaenoic acid
C22:6(ω-3)	4,7,10,13,16,19-docosahexaenoic acid
C24:0	Lignoceric acid

Table S2. Flow cytometer setup.

Instrument: Becton Dickinson FACSCanto™ II							
Laser lines	488 nm				633 nm		405 nm
Emission filters	780/60	670LP	585/42	530/30	780/60	660/20	450/50
Fluorochrome	PE/Cy7	PerCP/Cy5.5	PE	FITC	APC/Cy7	APC	Horizon V450

Supplemental References

1. Gierman LM, van der Ham F, Koudijs A, Wielinga PY, Kleemann R, Kooistra T, et al. Metabolic stress-induced inflammation plays a major role in the development of osteoarthritis in mice. *Arthritis Rheum* 2012;64(4):1172-81. doi: 10.1002/art.33443
2. Whitehead AS, Zahedi K, Rits M, Mortensen RF, Lelias JM. Mouse C-reactive protein. Generation of cDNA clones, structural analysis, and induction of mRNA during inflammation. *Biochem J* 1990;266(1):283-90.
3. Ciliberto G, Arcone R, Wagner EF, Ruther U. Inducible and tissue-specific expression of human C-reactive protein in transgenic mice. *EMBO J* 1987;6(13):4017-22.
4. Ciliberto G, Pizza MG, Arcone R, Dente L. DNA sequence of a pseudogene for human C-reactive protein. *Nucleic Acids Res* 1987;15(14):5895.
5. Matthews DR, Hosker JP, Rudenski AS, Naylor BA, Treacher DF, Turner RC. Homeostasis model assessment: insulin resistance and beta-cell function from fasting plasma glucose and insulin concentrations in man. *Diabetologia* 1985;28(7):412-9.
6. Glasson SS, Chambers MG, Van Den Berg WB, Little CB. The OARSI histopathology initiative - recommendations for histological assessments of osteoarthritis in the mouse. *Osteoarthritis Cartilage* 2010;18 Suppl 3:S17-23. doi: 10.1016/j.joca.2010.05.025
7. Pettinella C, Lee SH, Cipollone F, Blair IA. Targeted quantitative analysis of fatty acids in atherosclerotic plaques by high sensitivity liquid chromatography/tandem mass spectrometry. *J Chromatogr B Analyt Technol Biomed Life Sci* 2007;850(1-2):168-76. doi: 10.1016/j.jchromb.2006.11.023
8. Wong A, Sagar DR, Ortori CA, Kendall DA, Chapman V, Barrett DA. Simultaneous tissue profiling of eicosanoid and endocannabinoid lipid families in a rat model of osteoarthritis. *J Lipid Res* 2014;55(9):1902-13. doi: 10.1194/jlr.M048694
9. van Dijk RA, Rijs K, Wezel A, Hamming JF, Kolodgie FD, Virmani R, et al. Systematic Evaluation of the Cellular Innate Immune Response During the Process of Human Atherosclerosis. *J Am Heart Assoc* 2016;5(6) doi: 10.1161/JAHA.115.002860



Chapter 6

Intensive therapeutic lowering of cholesterol does not affect progression of diet-induced osteoarthritis in a translational dyslipidemia model

van Gemert Y., Kozijn A.E., Pouwer M.G., Kruisbergen N.N.L., van den Bosch M.H.J., Blom A.B., Pieterman E.J., Weinans H., Stoop R., Princen H.M.G., van Lent P.L.E.M.

Awaiting submission for publication

Abstract

Background. High systemic cholesterol levels have been associated with osteoarthritis (OA) development. Therefore, cholesterol lowering by statins has been suggested as a potential treatment. We investigated whether therapeutic high-intensive cholesterol-lowering attenuated OA development in dyslipidemic APOE*3Leiden.CETP mice.

Methods. Female mice (n=13-16 per group) were fed a Western-type diet (WTD) for 38 weeks. After 13 weeks, mice were divided into a baseline group and 5 groups receiving WTD alone or with treatment: atorvastatin alone, combined with PCSK9 inhibitor alirocumab and/or ANGPTL3 inhibitor evinacumab. Knee joints were analysed for cartilage degradation, synovial inflammation and ectopic bone formation using histology. Aggrecanase activity in articular cartilage and synovial S100A8 expression were determined as markers of degradation/regeneration and inflammation.

Results. Cartilage degradation was significantly increased in WTD-fed mice, but cholesterol-lowering strategies did not ameliorate cartilage destruction. This was supported by comparable aggrecanase activity and S100A8 expression in all treatment groups. Synovitis and ectopic bone formation were comparable between groups and independent of cholesterol levels.

Conclusions. Intensive therapeutic cholesterol lowering did not attenuate progression of cartilage degradation in WTD-fed APOE*3Leiden.CETP mice. We propose that inflammation is a key feature here and therapeutic cholesterol-lowering strategies may still be promising for OA patients presenting both dyslipidemia and inflammation.

Introduction

Hypercholesterolemia, or increased systemic levels of low-density lipoprotein cholesterol (LDL-C) subtypes, is a shared cardiometabolic risk factor associated with cardiovascular disease (CVD) and osteoarthritis (OA)[1]. Still, epidemiological studies are divided over the relationship between both conditions. A recent meta-analysis found a significantly increased prevalence and risk of overall CVD in OA patients compared to non-OA controls[2], while others did not observe this association[3]. It is unclear how high systemic LDL-C levels, characteristic for CVD, influence OA pathology. Increased total cholesterol levels were recently associated with increased risk of generalized OA[1], while others found no association with LDL-C or total cholesterol[4] and even describe protective effects of high-density lipoprotein cholesterol (HDL-C). Use of statins, a class of drugs often prescribed to lower LDL-C levels, was associated with reduced incidence and progression of knee OA in some studies[5 6], while not in others[7 8]. Also in hand OA, often associated with inflammation, statin use did not affect disease incidence[9]. Although pathophysiological grounds for a causal relationship between OA and CVD have not yet been established in humans, common cardiometabolic risk factors may indicate shared biochemical pathways.

The efficacy of cholesterol-lowering treatments on OA incidence and progression can be evaluated in a more controlled manner in preclinical models. We and others have demonstrated that cholesterol-supplemented Western-type diet (WTD) feeding aggravated OA features in the knee joint[10-12]. APOE*3Leiden.CETP mice, a translational model for human lipoprotein metabolism that responds to lipid-lowering drugs in a human-like manner[13 14], showed increased articular cartilage degradation on a cholesterol-rich WTD[10]. High cholesterol levels provoked synovial activation and ectopic bone formation in a collagenase-induced OA model[11]. Hypercholesterolemia triggered OA development through oxidative stress and chondrocyte apoptosis12. Atorvastatin treatment ameliorated OA outcome in these models[10 12]. These observations indicate that pathophysiological processes resulting from increased cholesterol load may contribute to OA pathogenesis.

In this study we investigated whether therapeutic high-intensive cholesterol lowering attenuates OA progression in APOE*3Leiden.CETP mice fed a cholesterol-supplemented WTD. We employed incremental lipid-lowering interventions using atorvastatin alone or combined with alirocumab, a monoclonal antibody against proprotein convertase subtilisin/kexin type 9 (PCSK9)[15], and/or the novel evinacumab, a monoclonal antibody against angiopoietin-like 3 (ANGPTL3)[13]. We evaluated the effects of cholesterol loading and lowering on cartilage degradation, ectopic bone formation and synovial activation.

Materials and Methods

Please refer to the end of this Chapter for a detailed methods section.

Results

Increased cartilage degradation in APOE*3Leiden.CETP mice fed a cholesterol-supplemented WTD

As previously observed[10], cholesterol-supplemented WTD feeding coincided with a mild but significant increase in cartilage degeneration after 38 weeks (WTD, 7.8 ± 1.9) compared to 13 weeks (baseline, 3.8 ± 1.8; 2.1-fold increase, p=0.001; Figure 1A,C). Cartilage degradation was mainly observed at the lateral tibia and femur (Figure S1A). Proteolytic activity in the cartilage, as a measure of matrix degradation, was determined by quantification of NITEGE neo-epitopes[16]. NITEGE staining in articular cartilage was significantly increased at 38 weeks in WTD-fed mice compared to baseline controls (p=0.01; Figure 1B,D).

Therapeutic cholesterol lowering does not ameliorate cartilage degradation in knee joints of dyslipidemic mice

Systemic cholesterol levels were determined to assess the effectiveness of standard and high-intensive cholesterol-lowering treatments. All treatments induced an intervention-dependent gradual decrease of cholesterol levels over the course of the study, the combination treatments being most effective (Figure 1E,F). The decrease in systemic cholesterol levels coincided with a reduced body weight gain in the treated groups compared to WTD controls (Figure S2). Analysis of lipoprotein profiles showed that all treatments induced a significant reduction of VLDL/LDL cholesterol whereas no differences in HDL levels were observed (Figure 1G). This decline in cholesterol levels did not attenuate the progression of cartilage destruction in the treatment groups as compared to WTD controls (Figure 1A,C). Moreover, NITEGE staining was significantly increased in WTD-fed mice receiving double or triple treatment (AA, p=0.001; AE, p=0.05; AAE, p=0.01; Figure 1B,D).

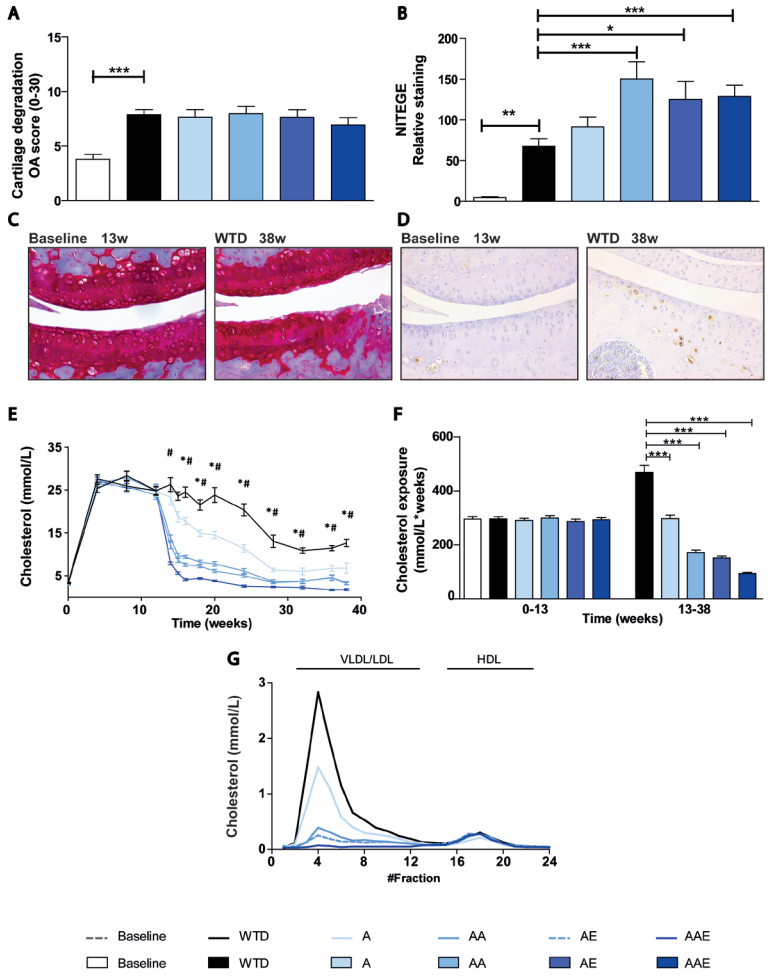


Figure 1. Cholesterol-lowering interventions do not ameliorate cartilage degradation in dyslipidemic mice. APOE*3Leiden.CETP mice received a Western Type Diet for 38 weeks. Data depicted in figure 2E-G are given as background information and have been published previously by Pouwer *et al*[18]. describing the effects on the progression of atherosclerosis. A) Cartilage degradation was determined using histological analysis and revealed a significant increase in cartilage degeneration after 38 weeks of WTD-feeding compared to baseline controls. B) Immunohistochemical analysis of NITEGE staining revealed a significant increase in WTD-fed mice receiving double or triple treatment (AA, p=0.001; AE, p=0.05; AAE, p=0.01). C,D) Representative pictures of cartilage degradation and NITEGE staining (20x magnification). E) WTD feeding significantly increased systemic cholesterol levels and all cholesterol-lowering treatments induced a significant gradual reduction in systemic cholesterol levels. F) Plasma total cholesterol exposure confirmed an intervention-dependent decrease over the course of the study. G) Cholesterol-lowering interventions resulted in a significant decrease of VLDL/LDL (fractions 4-15) levels while no changes in HDL (fraction 16-24) levels were observed. Abbreviations: A= atorvastatin, AA= atorvastatin + alirocumab, AE= atorvastatin + evinacumab, AAE= atorvastatin + alirocumab + evinacumab. n=13-16 per group. * p<0.001 WTD versus A, # P <0.001 WTD versus AA, AE and AAE in figure 1E; * p < 0.05, ** p < 0.01, ***p < 0.001 versus WTD.

Modulation of systemic cholesterol levels does not affect synovial inflammation or ectopic bone formation

Previously, we reported that high systemic cholesterol levels aggravated synovial inflammation and ectopic bone formation in collagenase-induced OA[11]. Therefore, we examined the effect of therapeutic cholesterol-lowering therapies on these OA features. All groups developed minor synovial inflammation, which was independent of systemic cholesterol levels (Figure 2A,C). The alarmin S100A8, a marker for activated macrophages[17], also showed minor expression in the synovial lining and was comparable in all groups (Figure 2D). Finally, we determined whether high plasma cholesterol promoted ectopic bone formation in this model. The total number of osteophytes per knee joint and the maturation stage remained comparable between all groups upon reduction of systemic cholesterol levels (Figure 2B). Most osteophytes occurred at the anterior side of the medial femoral condyle (Figure 2E).

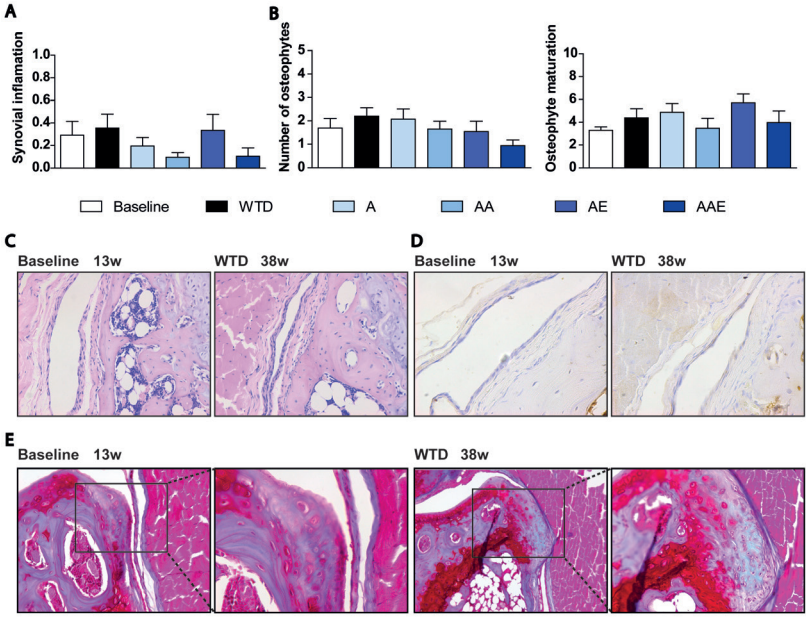


Figure 2. No effect of lowering systemic cholesterol on synovial inflammation and ectopic bone formation. APOE*3Leiden.CETP mice received a Western Type Diet for 38 weeks. A) Synovial inflammation was determined using an arbitrary score (0-2) and was independent of cholesterol levels. Ectopic bone formation and maturation stage were determined after 13 and 38 weeks of WTD-feeding on Safranin-O/FastGreen-stained sections. B) No differences were observed in the total number of osteophytes as well as maturation between all different groups. C) Representative pictures of synovial inflammation (20x magnification). D) Sections were stained for the alarmin S100A8, which was only expressed to a minor extent in the synovium. E) Representative pictures of ectopic bone formation (Left panel: 20x magnification, right panel: 40x magnification). Abbreviations: A=atorvastatin, AA=atorvastatin + alirocumab, AE= atorvastatin + evinacumab, AAE= atorvastatin + alirocumab + evinacumab.

Discussion

The association of CVD with OA has become increasingly recognized and understanding their interrelationship is imperative for improving therapeutic approaches. Cholesterol, with its crucial role in CVD, could be a potential link. Our study demonstrates that therapeutic cholesterol-lowering therapies proved insufficient in reducing progression of cartilage degradation, in contrast to earlier findings with prophylactic cholesterol lowering[10]. Ectopic bone formed independent of systemic cholesterol levels, while aggrecanase activity was increased after cholesterol-lowering treatment. The absence of synovial activation suggests a minor role of joint inflammation in our model. Taken together, our findings demonstrate that therapeutic cholesterol lowering does not slow the progression of cartilage degradation in dyslipidemic APOE*3Leiden. CETP mice.

This is the first study to show the effects of novel, therapeutic cholesterol-lowering interventions on the progression of cartilage degradation. Compared to previous studies10, the translational and clinical value is improved by the therapeutic experimental design. The APOE*3Leiden.CETP strain has high translatability in lipoprotein metabolism and metabolic diseases, showing human-like responses to hypolipidemic treatments[13 14]. In this study, diet-induced dyslipidemia was distinct and manifested itself in cartilage degradation as well as atherosclerosis development[18]. The cholesterol-lowering interventions successfully reduced atherosclerosis progression[18] while cartilage degeneration progressed despite of therapy, suggesting differential involvement of pathophysiological pathways. Although OA and atherosclerosis may share overlapping vascular and inflammatory pathophysiological processes[2], the role of an impaired lipid metabolism and the effects of cholesterol-lowering therapies on OA progression in humans remain unclear. A systematic literature review and meta-analysis revealed a clear association between dyslipidemia and OA, suggesting that lipid disturbances could be a risk factor for OA[19]. Yet results from clinical studies have been diverse, showing beneficial[5 6] or no[7-9] effects of statin use on OA incidence or progression. Different methods of analysis, effect of treatment or the lack of patient stratification could explain the observed difference between clinical studies.

Regarding the effects of statin use on OA incidence and progression, our collective results seem to indicate that statins can be beneficial pre-onset10 but cannot modify disease course. This divergent effectiveness suggests that other mechanisms, additional to lipoprotein disturbances, are important in cholesterol-induced OA pathogenesis. Systemic dyslipidemia may induce a lipid imbalance within the synovial fluid of OA patients that could irreversibly affect chondrocyte homeostasis. Although we were unable to investigate in detail the mechanistic pathways involved in cartilage pathophysiology, we have analysed the activity of catabolic mediators in the cartilage matrix. Important catabolic mediators involved in cartilage degradation are aggrecanases and matrix metalloproteases (MMPs). Both cleave aggrecan at a specific site, leaving behind the

neo-epitopes NITEGE and VDIPEN, respectively[16]. VDIPEN-epitopes are expressed during advanced cartilage degradation. NITEGE-epitopes are expressed during early cartilage degradation and have also been observed during regeneration of proteoglycan content in articular cartilage. In this study, NITEGE staining increased after 38 weeks of WTD feeding compared to baseline controls. Cholesterol-lowering treatments resulted in a significant increase in NITEGE staining. As no difference in cartilage degradation was observed, we propose that the observed aggrecanase activity could indicate a more active repair mechanism after cholesterol-lowering treatment, possibly protecting against cartilage degradation after prolonged cholesterol exposure.

As inflammatory involvement is increasingly recognized in OA, cholesterol-lowering treatments that have pleiotropic immunomodulatory effects – such as statins and anti-PCSK9 antibodies – may be beneficial for OA patients in multiple ways. We have previously reported that high systemic cholesterol levels enhanced ectopic bone formation and synovial activation during inflammatory collagenase-induced OA via local inflammatory processes11. Ectopic bone formation was enhanced via the activation of transforming growth factor β (TGF-β) and synovial activation via the alarmin S100A8/A9, a marker for activated macrophages11. In contrast, we observed little ectopic bone formation or macrophage activation in our current study, both of which were independent of systemic cholesterol levels as well. These findings imply that local inflammation is required for LDL-driven OA pathology. Local inflammation occurs in approximately 50% of the OA patients and has been associated with the development of joint pathology. Inflammation is essential for the oxidation of LDL, which is taken up by the synovial lining cells and drives joint pathology via pro-inflammatory mechanisms[20].

In conclusion, our results show that cholesterol-supplemented WTD feeding disturbed lipoprotein metabolism and coincided with increased cartilage degradation in APOE*3Leiden.CETP mice. Therapeutic, high-intensive cholesterol-lowering interventions did not attenuate the progression of cartilage degradation and had no effect on ectopic bone formation and synovial activation. We propose that local inflammation is a prerequisite in cholesterol-induced OA pathology. Therapeutic cholesterol-lowering strategies may still be promising for OA patients presenting both dyslipidemia and joint inflammation.

Acknowledgements

The authors would like to thank Nanda Keijzer, Nicole Worms, Erik Offerman, Annet Sloetjes and Birgitte Walgreen for their excellent technical assistance.

Authors' contributions

MGP, EJP and HMGP have designed the study. MGP, EJP, AEK and YG have carried out

experimental procedures. YG and AEK have been the primary persons responsible for writing the manuscript. NNLK, MHJB, ABB, EJP, HW, RS, HMGP and PLEML were involved in drafting the work or revising it critically for important intellectual content. All authors approved the final version to be published. The authors acknowledge that due to space limitations only a subselection of references is included in this manuscript.

Funding

This manuscript was supported by funding from the Dutch Arthritis Foundation (Grant number 17-1-404 and LLP-22) and Regeneron Pharmaceuticals, by an allowance for TKI-LSH from the Ministry of Economic Affairs in the Netherlands, the Netherlands Organization for Applied Scientific Research (TNO) research program "Preventive Health Technologies", the Dutch Arthritis Foundation under grant agreement n°17-1-404, and the European Union Seventh Framework Programme under grant agreement n°305815 (EU FP7/2007-2013; HEALTH.2012.2.4.5-2; D-BOARD: Novel Diagnostics and Biomarkers for Early Identification of Chronic Inflammatory Joint Diseases).

Competing interests

Alirocumab (Praluent®) and Evinacumab (REGN1500) are developed by Regeneron Pharmaceuticals and Evinacumab is currently in clinical trials. JG and VG are employees of Regeneron Pharmaceuticals and EJP, RS and HMGP are employees of TNO.

References

1. Buchele G, Gunther KP, Brenner H, et al. Osteoarthritis-patterns, cardio-metabolic risk factors and risk of all-cause mortality: 20 years follow-up in patients after hip or knee replacement. *Sci Rep* 2018;8(1):5253. doi: 10.1038/s41598-018-23573-2
2. Hall AJ, Stubbs B, Mamas MA, et al. Association between osteoarthritis and cardiovascular disease: Systematic review and meta-analysis. *Eur J Prev Cardiol* 2016;23(9):938-46. doi: 10.1177/2047487315610663 [published Online First: 2015/10/16]
3. Hoeven TA, Leening MJ, Bindels PJ, et al. Disability and not osteoarthritis predicts cardiovascular disease: a prospective population-based cohort study. *Ann Rheum Dis* 2015;74(4):752-6. doi: 10.1136/annrheumdis-2013-204388 [published Online First: 2014/01/05]
4. Garcia-Gil M, Reyes C, Ramos R, et al. Serum Lipid Levels and Risk Of Hand Osteoarthritis: The Chingford Prospective Cohort Study. *Sci Rep* 2017;7(1):3147. doi: 10.1038/s41598-017-03317-4 [published Online First: 2017/06/11]
5. Clockaerts S, Van Osch GJ, Bastiaansen-Jenniskens YM, et al. Statin use is associated with reduced incidence and progression of knee osteoarthritis in the Rotterdam study. *Ann Rheum Dis* 2012;71(5):642-7. doi: 10.1136/annrheumdis-2011-200092 [published Online First: 2011/10/13]
6. Veronese N, Koyanagi A, Stubbs B, et al. Statin use and knee osteoarthritis outcomes: A longitudinal cohort study. *Arthritis Care Res (Hoboken)* 2018 doi: 10.1002/acr.23735 [published Online First: 2018/08/26]
7. Michaelsson K, Lohmander LS, Turkiewicz A, et al. Association between statin use and consultation or surgery for osteoarthritis of the hip or knee: a pooled analysis of four cohort studies. *Osteoarthritis Cartilage* 2017;25(11):1804-13. doi: 10.1016/j.joca.2017.07.013 [published Online First: 2017/08/02]
8. Riddle DL, Moxley G, Dumenci L. Associations between statin use and changes in pain, function and structural progression: a longitudinal study of persons with knee osteoarthritis. *Ann Rheum Dis* 2013;72(2):196-203. doi: 10.1136/annrheumdis-2012-202159 [published Online First: 2012/11/23]
9. Burkard T, Hugle T, Layton JB, et al. Risk of Incident Osteoarthritis of the Hand in Statin Initiators: A Sequential Cohort Study. *Arthritis Care Res (Hoboken)* 2018;70(12):1795-805. doi: 10.1002/acr.23616 [published Online First: 2018/06/10]
10. Gierman LM, Kuhnast S, Koudijs A, et al. Osteoarthritis development is induced by increased dietary cholesterol and can be inhibited by atorvastatin in APOE*3Leiden.CETP mice--a translational model for atherosclerosis. *Ann Rheum Dis* 2014;73(5):921-7. doi: 10.1136/annrheumdis-2013-203248
11. de Munter W, van den Bosch M, Slöetjes A, et al. High LDL levels lead to increased synovial inflammation and accelerated ectopic bone formation during experimental osteoarthritis. *Osteoarthritis and cartilage* 2016;24(5):844-55.
12. Farnaghi S, Prasadam I, Cai G, et al. Protective effects of mitochondria-targeted antioxidants and statins on cholesterol-induced osteoarthri-

tis. *FASEB J* 2017;31(1):356-67. doi: 10.1096/fj.201600600R
13. Dewey FE, Gusarova V, Dunbar RL, et al. Genetic and Pharmacologic Inactivation of ANGPTL3 and Cardiovascular Disease. *N Engl J Med* 2017;377(3):211-21. doi: 10.1056/NEJMoa1612790 [published Online First: 2017/05/26]
14. Pouwer MG, Heinonen SE, Behrendt M, et al. The APOE3-Leiden Heterozygous Glucokinase Knockout Mouse as Novel Translational Disease Model for Type 2 Diabetes, Dyslipidemia, and Diabetic Atherosclerosis. *Journal of Diabetes Research* 2019;2019
15. Schwartz GG, Steg PG, Szarek M, et al. Alirocumab and cardiovascular outcomes after acute coronary syndrome. *New England Journal of Medicine* 2018;379(22):2097-107.
16. van Meurs JB, van Lent PL, Holthuysen AE, et al. Kinetics of aggrecanase- and metalloproteinase-induced neoepitopes in various stages of cartilage destruction in murine arthritis. *Arthritis Rheum* 1999;42(6):1128-39. doi:10.1002/1529-0131(199906)42:6<1128::AID-ANR9>3.0.CO;2-2 [published Online First: 1999/06/12]
17. van Lent PL, Blom AB, Schelbergen RF, et al. Active involvement of alarmins S100A8 and S100A9 in the regulation of synovial activation and joint destruction during mouse and human osteoarthritis. *Arthritis & Rheumatism* 2012;64(5):1466-76.
18. Pouwer MG, Pieterman EJ, Worms N, et al. Triple Treatment With Alirocumab and Evinacumab on Top of Atorvastatin Regresses Lesion Size and Improves Plaque Phenotype in APOE* 3Leiden. CETP Mice. *Circulation* 2018;138(Suppl_1):A12966-A66.
19. Baudart P, Louati K, Marcelli C, et al. Association between osteoarthritis and dyslipidaemia: a systematic literature review and meta-analysis. *RMD open* 2017;3(2):e000442.
20. de Munter W, Geven EJ, Blom AB, et al. Synovial macrophages promote TGF-beta signaling and protect against influx of S100A8/S100A9-producing cells after intra-articular injections of oxidized low-density lipoproteins. *Osteoarthritis Cartilage* 2017;25(1):118-27. doi: 10.1016/j.joca.2016.07.020 [published Online First: 2016/08/16]

Supplemental Methods and materials

Study design

We refer to Pouwer et al[18] for a more detailed description of experimental design, treatments and sample size calculations.

Animals

The experiment was carried out in female APOE*3Leiden.CETP transgenic mice on a C57BL/6 background (8-12 weeks of age), obtained from the in-house breeding colony (TNO Metabolic Health Research, Leiden, The Netherlands). Groups consisted of 13-16 animals. Initial groups included more mice to account for autoantibody development against the human monoclonal evinacumab. The development of auto-antibodies was determined and autoantibody-positive mice were excluded from all analyses The experiment was approved by the institutional Animal Care and Use Committee of TNO and were in compliance with European Community specifications regarding the use of laboratory animals.

Diet and treatments

Metabolic OA was induced by switching the diet of the mice from standard chow to WTD with 0.30% cholesterol and 15% saturated fat. At t=13 weeks, mice were divided in 6 groups that matched based on age, body weight, plasma total cholesterol (TC), plasma total triglycerides (TG) and cholesterol exposure (mmol/L*weeks). Sixteen mice were sacrificed as the baseline control group and the other 5 groups continued to receive WTD alone or with treatment for 25 weeks. Treatments comprised atorvastatin (4-10 mg/kg/d; concentrations based on food intake), atorvastatin and alirocumab (10 mg/kg), atorvastatin and evinacumab (25 mg/kg) or atorvastatin, alirocumab and evinacumab. Atorvastatin (mixed in the diet) and dietary cholesterol concentrations were adapted during the study to reach the non-HDL-C lowering goal of 1 mM (Figure 1). Alirocumab and evinacumab were administered by weekly subcutaneous injections.

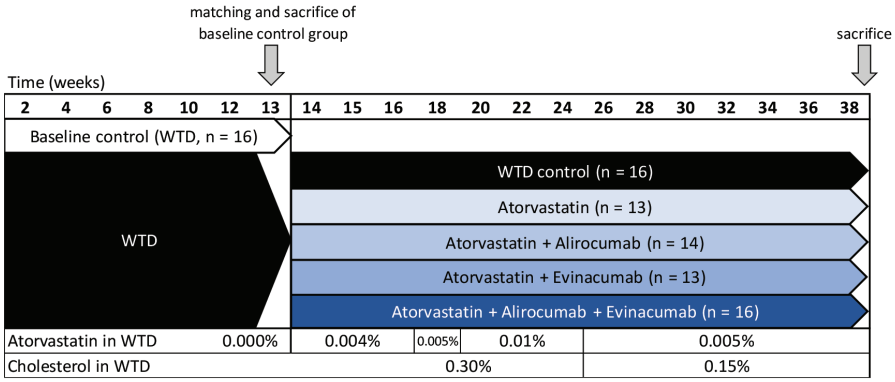


Figure 1. Schematic overview of the experimental study design.

Assessment of metabolic dysfunction

Plasma cholesterol levels were monitored throughout the study period. Peripheral blood (5 drops/animal) was drawn via tail incision using EDTA-coated tubes (Sarstedt) after 4h of food deprivation and by heart punction at sacrifice. Total cholesterol was determined with an enzymatic assay (Roche Diagnostics) according to manufacturer's instructions and total cholesterol exposure was calculated as mmol/L*weeks. For lipoprotein profiles, pooled plasma of each group was fractionated using an Äkta FPLC system (Pharmacia) and analyzed for their cholesterol-containing fractions.

Histological analysis

Murine knee joints were fixed in formalin and decalcified using formic acid. Subsequently, the joints were embedded in paraffin and cut in 7µm sections. Sections were stained using Safranin-O/Fast Green and Hematoxylin/Eosin for histological analysis. Cartilage damage in the joint was quantified using a more detailed version of the OARSI scoring system, as described previously[14] (0 = no damage, 30 = maximal damage). Five sections were scored and averaged per joint after blinding. Osteophyte formation and maturation were determined using an arbitrary scoring system as described previously[15]. Ten different locations were scored for osteophyte formation and maturation on both the medial and lateral side of the joint. Synovial inflammation was scored using three sections per joint and a scoring range from 0-2 (0 = no inflammation, 1 = mild inflammation, 2 = moderate inflammation; Figure S3).

Immunohistochemistry

For immunohistochemical analysis, knee joint sections were deparaffinized and endogenous peroxidase blocking was performed using H_2O_2 in methanol. Antigen retrieval was performed in citrate buffer pH 6.0. Sections were stained with polyclonal antibodies against S100A8 (kindly provided by Thomas Vogl, Institute of Immunology, University of Muenster, German), NITEGE (kindly provided by John Mort, Shriners

Hospital for Children, Montreal, Canada) or non-relevant rabbit IgG control (R&D systems). Biotinylated anti-rabbit IgG was used as a secondary antibody. Subsequently, sections were stained with avidin-streptavidin-peroxidase (Elite kit, Vector Laboratories) and diaminobenzidine (Sigma-Aldrich) was used for visualization of peroxidase staining. Counterstaining was performed using haematoxylin (Merck). NITEGE staining was determined using the Leica Application Suite (Leica Microsystems), three sections were scored and averaged per joint in the superficial non-calcified layer of articular cartilage. Positive staining area was corrected for the total area that was analyzed. NITEGE staining was determined in a blinded fashion.

Statistical analysis

Statistical analysis was performed using SPSS Statistics Data Editor (IBM). Differences between groups were analyzed using a parametric One-Way ANOVA followed by a 2-sided Dunnett's Multiple Comparison test. Due to a non-Gaussian distribution, Mann-Whitney U-test was used for comparison between groups for the synovitis scores. P-values below 0.05 were considered significant. Results are expressed as mean ± SEM.

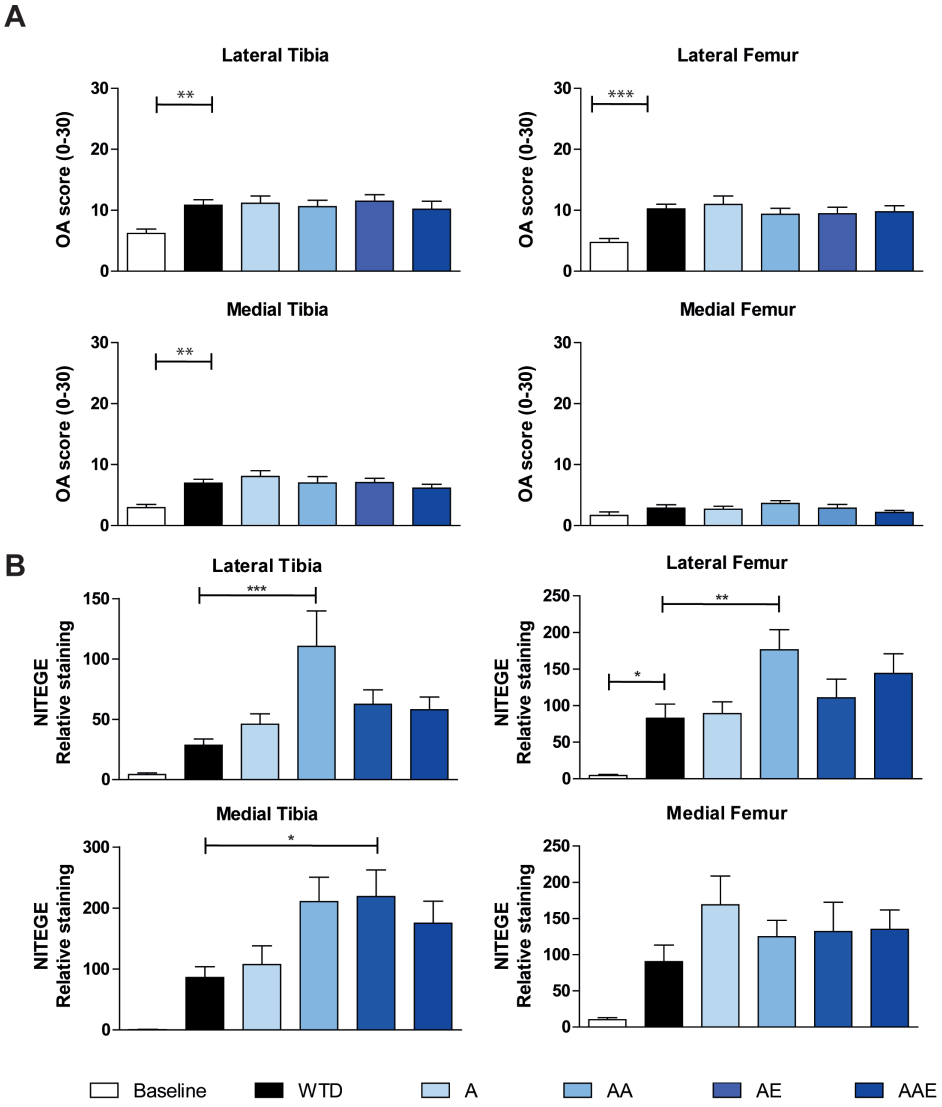


Figure S1. Overview of OA severity scores and relative NITEGE staining per cartilage compartment. A) Sections were stained using Safranin-O/Fast Green for histological analysis. Cartilage damage in the joint was quantified using a detailed version of the OARSI score (0 = no damage, 30 = maximal damage). Five sections were scored and averaged per joint. A significant increase in cartilage degradation was observed between baseline and WTD at the LT, LF and MT side of the joint. B) Immunohistochemical analysis of NITEGE staining revealed significant differences in aggrecanase activity after cholesterol-lowering treatments at the LT, LF and MT side of the joint. A= atorvastatin, AA = atorvastatin + alirocumab, AE= atorvastatin + evinacumab, AAE= atorvastatin + alirocumab + evinacumab. n=13-16 per group. * $P < 0.05$, ** $P < 0.01$, ***$P < 0.001$.

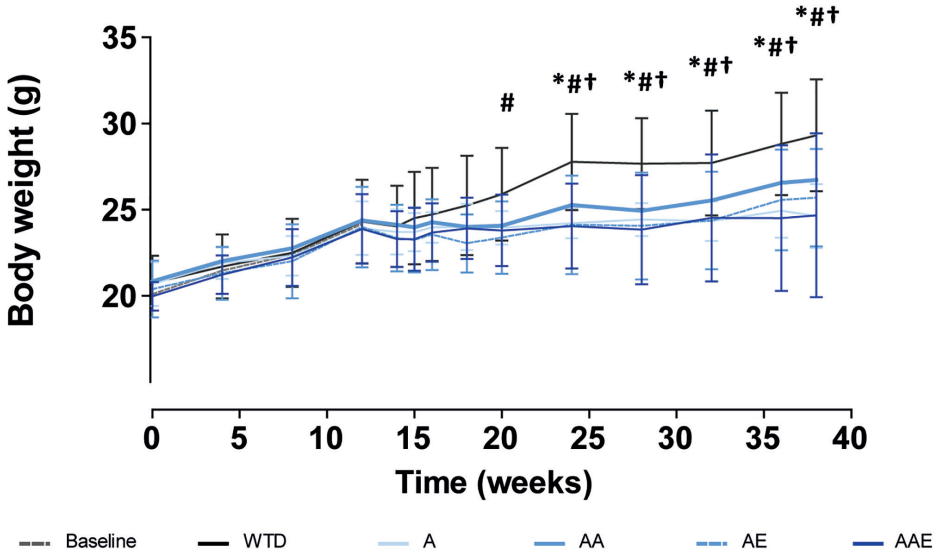


Figure S2. Administration of different cholesterol-lowering interventions resulted in a reduced body weight gain. Abbreviations: A = atorvastatin, AA= atorvastatin + alirocumab, AE= atorvastatin + evinacumab, AAE= atorvastatin + alirocumab + evinacumab. n=13-16 per group. * P<0.001 WTD versus A, # P <0.001 WTD versus AA, AE and AAE, † P <0.001 WTD versus AAE.

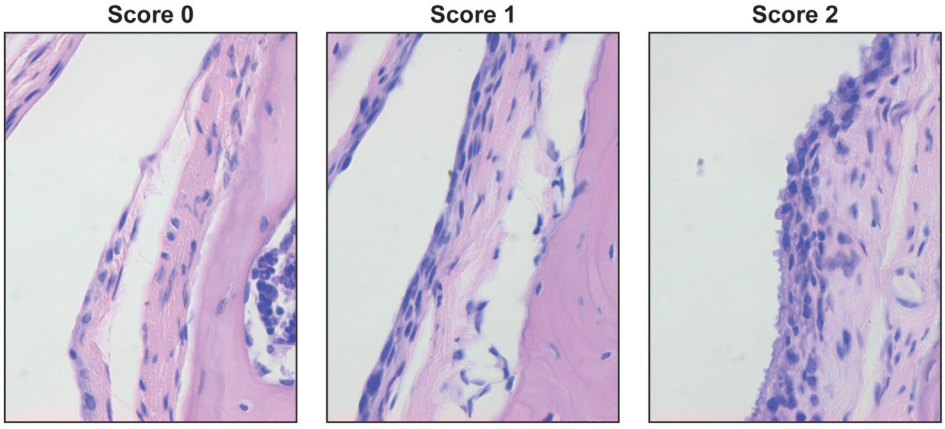
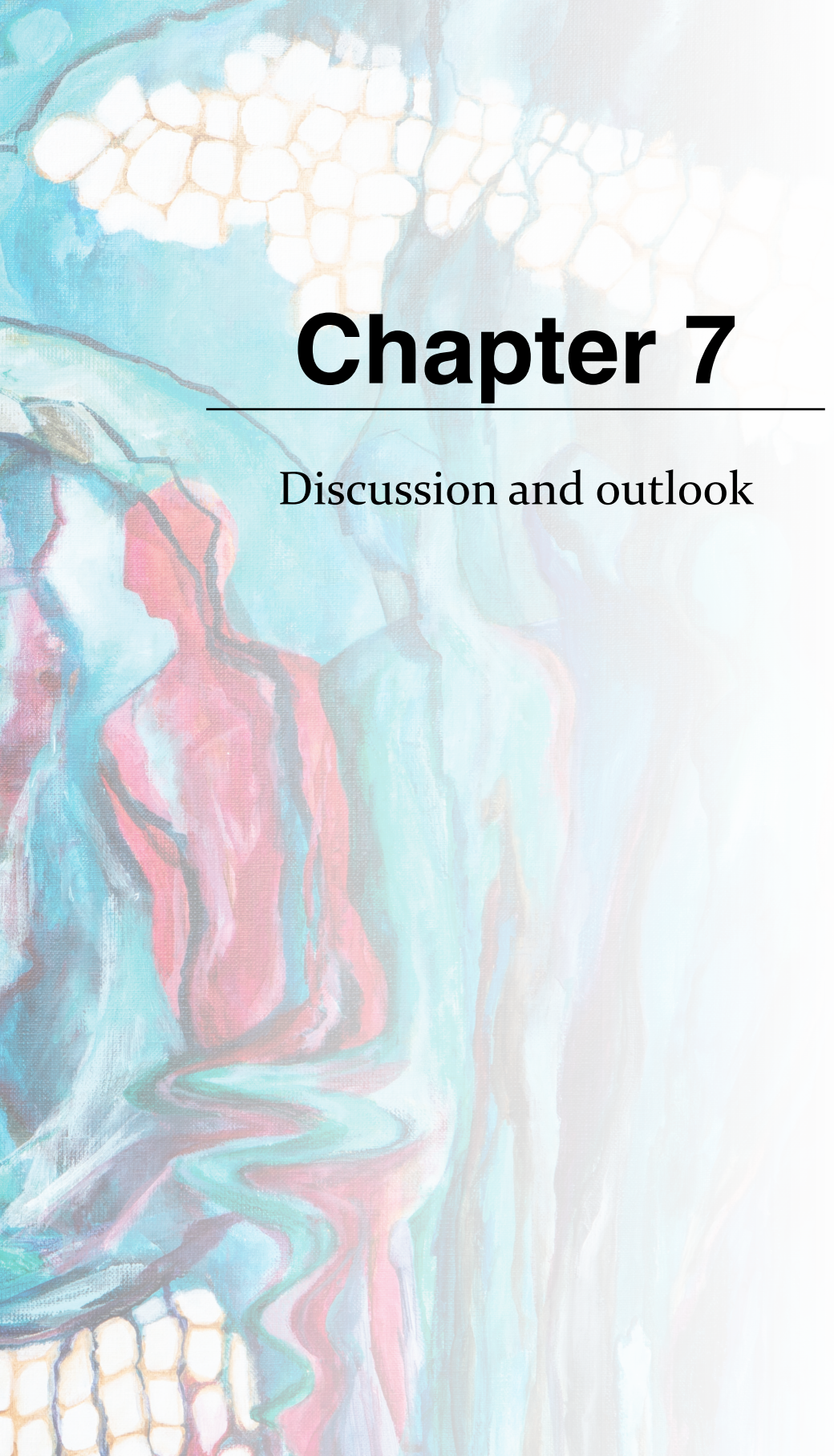


Figure S3. Synovial inflammation scoring system. Synovial inflammation was quantified by evaluating synovial thickening and cell infiltration in the synovial lining using H&E stained sections of the joint. Synovial inflammation was scored using an arbitrary score of 0-2 (0 = no inflammation, 1 = mild inflammation, 2 = moderate inflammation), three sections were scored per joint.





Chapter 7

Discussion and outlook

Metabolic and inflammatory pathways share many evolutionary interactions and their comprehensive interrelationship underlies many contemporary metabolic diseases, like metabolic osteoarthritis (OA). The balance between both systems is delicate and needs to be properly maintained. Plasticity and adaptability of the cells and the pathways involved in both metabolism and immunity ensures the host to deal with challenges like overfeeding and infection. However, persistent stimuli can drive either system to become locked in an alternative, harmful stable state. We found that long-term consumption of a high-caloric diet will lead to metabolic overload such as obesity or dyslipidemia, but does not necessarily result in aggravated degradation of articular cartilage. Although we showed that high-fat feeding alone could unquestionably aggravate OA progression (*Figure 2, Chapter 3*), we propose that an additional trigger is necessary to evoke OA onset in a metabolically compromised subject. Data presented in this thesis support this hypothesis, demonstrating a role for simultaneous dysregulation of systemic lipid metabolism and inflammatory mediators like C-reactive protein (CRP) and peripheral blood monocytes. Moreover, we showed that therapeutic treatment of just one of these systems, through lowering systemic cholesterol levels, proved insufficient in halting OA progression.

Osteoarthritis and nutrition: food for thought

Emerging evidence suggests that metabolic syndrome (MetS) is associated with an increased risk of OA. This has led to the introduction of the term 'metabolic OA' for the MetS-associated subtype of OA[1], although the validity of this subtype is still under debate[2]. One or multiple components of MetS can be associated with OA, with obesity being the greatest modifiable risk factor[3]. Overweight and obesity are defined as 'abnormal or excessive fat accumulation that presents a risk to health' according to the World Health Organization. As obesity is the consequence of a sustained positive energy balance over time, considerable research has been devoted assessing the effects of nutrition. Nevertheless, it is as yet unclear whether excessive food intake in general or an excess of specific foods or nutrients plays a major role in the development of obesity. Epidemiological evidence suggests that excessive fat consumption promotes the development of obesity, with a direct relationship between the amount of dietary fat and the degree of obesity[4]. The same can be observed in preclinical animal models, where high-fat diets (≥40% of energy from fat) provided ad libitum to sedentary animals reliably produce increases in energy intake, body fat gain, and obesity[5]. The C57BL/6J strain is most thoroughly examined in the context of metabolic OA, as the obese state observed in these mice closely parallels the metabolic adaptations seen in human disease pathogenesis[6]. Using mice on a C57BL/6J background, we have assessed the potential of various high-caloric diets on inducing metabolic OA (Chapter 2-5). Although the manifestation of a metabolic phenotype was consistently confirmed,

articular cartilage degradation was rarely observed. The results presented in this thesis suggest that diet plays a role in exacerbating OA progression, but an additional trigger is needed to evoke OA.

These results prompt a difficult discussion, as it touches on the foundation of the obesity-induced OA model as introduced by Silberberg and Silberberg in the 1950s[7]: nutrition. In our experience, inducing obesity and metabolic dysregulation in male C57BL/6J mice takes 10-12 weeks of HFD feeding, with 45% of energy from fat. OA development is mild in the diet-induced model, therefore also referred to as a "spontaneous" OA model by some. Consequently, the slowly progressive disease requires at least two- to threefold longer study duration compared to chemically or surgically induced models. Even though this period is significantly shorter compared with ageing OA models (≥1 year of age in mice), ageing processes cannot be ruled out in the development of diet-induced OA. Control diets will account for ageing effects but are equally questionable in their effects on articular cartilage, as undefined chow control diets add great variability: the micro- and macronutrient content of chow differs markedly from the defined diets and the natural ingredients of chow are subject to seasonal changes. Usually, as in the work presented in this thesis, control diets are well-defined and differ from study diets predominantly in one macronutrient: in the case of high-fat diets, the fat surplus is often proportionally replaced by carbohydrates in control diets. Donovan et al. recently showed that this simplistic approach might backfire when studying OA development, with dietary fat and sucrose content conveying independent effects on OA pathology in mice8. Here, a low-fat low-sucrose control diet demonstrated substantially more severe joint pathology compared with the 'standard' low-fat high-sucrose control diet in male C57BL/6J mice, without inducing differences in body mass or body fat[8]. It must be noted here that the authors focused on early-stage OA pathology, as the mice received diet treatment for 20 weeks in total. An explorative study at TNO Metabolic Health Research has also shown significant differences between defined low-fat control diets from different manufacturers in male mice on a C57BL/6J background, in terms of body weight gain and metabolic dysfunction (M.C.M. Morrison, R. Kleemann, 2017; data not published). In a rat study performed by our group, using the same defined diets as the mouse study of *Chapter 3*, control rats unexpectedly gained significant body weight – hinting towards different digestive physiology for different species and strains. These observations highlight the complex interplay of macronutrients on metabolic dysregulation and point to a major role for the gastrointestinal (GI) tract in inducing these metabolic changes.

The GI tract, the key interface between ingested nutrients and the body, has been mainly researched in the context of NSAID-induced toxicity in the OA field[9,10]. Yet, considering its four primary functions (digestion, absorption, excretion and protection), it seems inevitable that the GI tract plays a role in obesity-induced OA. An essential part of the GI

tract for performing its functions is the microbiome: a myriad of microorganisms within the gastric lumen tailored to the individual, which aid in digestion and nutrient uptake and is directly influenced by diet[11,12]. Owing to recent technological advances it is now understood that the intestinal microbiota is especially vital to metabolic homeostasis and host health, as perturbations in intestinal microbiota (termed dysbiosis) have been associated with the pathogenesis of both intestinal and extra-intestinal disorders like obesity[13,14]. Correlational evidence is also emerging for a potential relationship between dysbiosis and metabolic OA onset[15]. The fact that many of the risk factors for metabolic OA show overlap with microbiome dysbiosis, such as ageing, gender, obesity and quality of nutrients intake[16], is a writing on the wall. Preclinical models fed a HFD have demonstrated quantitative and qualitative microbiome alterations[17] and evidence is accumulating that these changes might be related to OA pathology[18]. Recently, trauma-induced OA was found to be less severe in germ-free mice (i.e. devoid of all microorganisms) than in specific pathogen-free mice (i.e. harbouring gut microbiota)[19], also pointing to a role for the microbiome in OA pathology. In a small set of OA patients, the presence of synovial and systemic bacterial membrane component lipopolysaccharide (LPS) and LPS-binding factor (LPB) have recently been associated with the presence of activated macrophages in the knee, radiographic OA severity and joint symptoms20. Endogenous LPS is continually produced within the gut by the death of Gram-negative bacteria and is absorbed into intestinal capillaries to be transported by lipoproteins[21]. High-fat diets enhance translocation of the bacterial LPS from the microbiome into the bloodstream, initiating obesity and insulin resistance[21]. However, due to the correlational nature of these observations[16], unravelling the exact mechanism of the relationship between intestinal microbiota and OA is required to support the hypothesis that OA pathology can be microbiota-driven.

Metabolic osteoarthritis, metabolism, and immunity

The pivotal mutualistic relationship between the host and the microbiome extends beyond metabolic functions, as millions of years of co-evolution have rendered adaptations to the host immune system to preserve this symbiotic relationship while containing the microbiota[22]. During the past decades, it has become clear that inflammation is a key feature of metabolic syndrome and its associated comorbidities, like obesity[23]. We (Chapter 3-5)[24] and others[25,26] have demonstrated that low-grade, systemic inflammation is also involved in metabolic OA pathology. Diet, especially fat, has been identified as a strong modulator of the microbiota14. Accumulating data from both human and animal studies demonstrate that intestinal microbes can affect host lipid metabolism through multiple direct and indirect biological mechanisms[27]. Lipids are potent modulators of both innate and adaptive immunity as well and the

increased intake of dietary saturated fatty acids (SFA) is thought to link obesity and OA[28]. Eicosanoids, or oxylipins, are the lipid mediators best known for their pivotal role in inflammation29. We performed lipidomic analyses to detect adaptations over time in the systemic lipid and eicosanoid profiles in our obesity-induced OA models (Chapter 3 and 5). In humans, the association of lipid abnormalities with tissue pathology in OA cartilage was already made in the 1990s[30]. A recent systematic literature review and meta-analysis revealed that dyslipidemia occurs twofold more in individuals with than without OA, pointing to lipid disturbances as a risk factor for OA[31]. Despite plasma volume limitations and volume demands of the lipidomic assay, we were able to observe a shift in eicosanoid metabolism towards the cytochrome P450 (CYP450) pathway (Figure 3, Chapter 3). HFD feeding induced increased systemic levels of the eicosanoid precursor arachidonic acid (AA), a n-6 polyunsaturated fatty acid that can trigger a pro-inflammatory cascade. The observed increase in systemic levels of dihydroxyeicosatrienoic acids (DHETs) pointed to an increased AA hydroxylation by the enzyme soluble epoxide hydrolase (sEH) in the CYP450 pathway. These results suggest that systemic changes, triggered by HFD-induced metabolic dysregulation, aggravate OA progression by modulating the eicosanoid metabolism via sEH.

Soluble EH is expressed in adipose tissue[32–34], hepatocytes[32,33], and pancreatic islets[34–36] and has been suggested to be involved in the homeostasis of metabolic diseases[37]. Altered CYP-expression and increased sEH-generated DHET levels have also been observed in obese murine models of metabolic syndrome[38–40]. Interestingly, due to its phosphatase activities, sEH can regulate cholesterol levels[37,41], another risk factor for metabolic OA (Chapter 6). In accordance with these findings, pharmacological inhibition of sEH ameliorated metabolic syndrome[33,42]. A similar dysregulation of CYP-mediated eicosanoid metabolism has been observed in patients with cardiovascular disease, a metabolic condition that shares pathophysiological similarities with OA[43] for which sEH inhibitors (sEHi) have shown promising therapeutic effects[44]. Although the effectiveness of sEHi treatment is not yet researched in OA patients, a recent study positively associated increases in synovial fluid levels of sEH-generated DHET with knee OA and radiographic progression[45] – suggesting a link between eicosanoid metabolism and OA pathogenesis as well.

Due to their immune modulatory capacity[46], it is conceivable that eicosanoids mediate the link between metabolism and immunity in metabolic OA. Infiltration of immune cells like monocytes in the OA synovium lies at the basis of synovitis[47,48]. Immune infiltration in the OA synovium primarily reflects migration rather than local proliferation[49,50] and eicosanoids could play an important role in this process. Although initially considered inactive EET degradation products, DHET have been reported to promote CCL2-mediated monocyte chemotaxis in vivo, leading to an increased recruitment of monocytes into tissues[51]. DHET were also shown to be able to restore

sEHi-blocked human monocyte migration in vitro[51], verifying specificity and the crucial role DHET play in monocyte recruitment. The fact that DHET specifically promote monocyte chemotaxis via the CCL2/CCR2 signalling axis is particularly interesting, since this signalling axis was found to preferentially mediate monocyte trafficking and promote inflammation and tissue damage in OA[48]. We observed expansion and activation of circulating non-classical monocyte subpopulations (Chapter 3 and 5) consistent with reports in obese[52,53] and OA patients[54], respectively. Especially striking was the increase in proinflammatory intermediate monocytes (Chapter 3), purportedly the main population to be perturbed in human disease conditions[55] including obesity[56]. As intermediate monocytes represent a transitional subset between classical and non-classical monocytes, the observed increase can indicate renewing of the non-classical monocyte pool by maturation of peripheral classical monocytes. However, the intermediate subpopulation is also known to reflect disease activity in rheumatoid arthritis patients[57]. Moreover, monocyte chemotaxis receptor CCR2 expression on circulating intermediate monocytes was recently found to correlate positively with serum TNF levels and pain in women with knee OA[54]. This is in line with the previous finding that synovial fluid (but not serum) levels of CCL2 (CCR2 ligand, also referred to as MCP-1), correlated with pain and physical disability in OA[58]. Therefore, the increase in circulating intermediate monocytes can alternatively indicate involvement of this subset in metabolic OA pathogenesis.

In addition to monocyte expansion, we also observed distinct activation of the circulating non-classical monocyte subpopulation during metabolic OA progression (Chapter 3 and 5), pointing to monocyte recruitment to tissues. Activated monocytes may develop into macrophages upon tissue entry, differentiating into either a proinflammatory M1 or a pro-resolving (anti-inflammatory) M2 macrophage phenotype. We investigated the local effects of HFD feeding on M1 and M2 macrophage subsets in the synovium and the infrapatellar fat pad (IPFP) (Chapter 3-5). Increased numbers of adipose tissue macrophages and their polarization towards a proinflammatory profile greatly contributes to the low-grade systemic inflammation in obesity as well as OA[59]. Lipids play an important role in macrophage polarization, as recently evidenced by the involvement of the eicosanoid PGE2 in switching from the M1 to M2 macrophage polarization state and resolution of inflammation[60]. However, the HFD-induced systemic activation of myeloid cells was not reflected by a local polarization towards the M1 macrophage subset in the knee joint, as the synovia and IPFP of HFD-fed mice showed a mixed pattern of both M1 and M2 macrophage markers (Chapter 3-5). Interestingly, the combination of HFD with knee injury (DMM) triggered increased iNOS deposition in both the synovium and IPFP (Chapter 3-5). In the IPFP, this coincided with an increase in crown-like structures – a hallmark of adipose inflammation (Chapter 4). Our findings are in line with results from clinical[61,62] and murine[63–65] studies showing

that resident macrophages retain their M2-like phenotype while displaying a pro-inflammatory cytokine profile. Together, these findings emphasize the persistence and therefore importance of local macrophage populations in regulating homeostasis in the OA knee joint of mice.

Apart from their most known potential to differentiate into macrophages, monocytes exert a plethora of other functions in acute and chronic inflammatory diseases. In arthritic conditions, intermediate and non-classical monocytes have a significantly increased potential to differentiate into osteoclasts[66–68]. Osteoclasts are specialized bone cells that mediate bone resorption and are thought to participate in OA pathophysiology[69,70]. Interestingly, a selective expansion of the intermediate monocyte subset has also been reported for arthritic conditions[71,72], suggesting that in particular this subset may be involved in OA pathogenesis via this route. The process of bone remodelling is likely coupled to the process of angiogenesis, which are both enhanced in pathologic conditions[73,74], where osteoclastogenesis is thought to stimulate angiogenesis[75]. Angiogenesis is another feature of OA, which leads to ossification and is driven by proangiogenic factors like vascular growth factor (VEGF)[76,77]. The intertwining of these processes fits with the aggravated metabolic OA progression in our hCRP-tg mice (Chapter 5), as human C-reactive protein (CRP) has been shown to upregulate VEGF expression[78]. As reviewed in Chapter 5, CRP is positively associated with BMI in humans[79] and could be involved in lipid-driven local cartilage changes via OA-induced upregulation and activation of phospholipase A2 (PLA2) enzymes[80,81]. In OA patients too, a recent meta-analysis revealed that hs-CRP levels were modestly higher in OA than controls and associated with increased pain and decreased physical function[26]. Moreover, as a modulator of innate and adaptive immunity, CRP promotes monocyte chemotaxis both directly and indirectly[82]: completing the circle back to our observations that both the numbers of circulating monocytes and the level of monocyte activation increased in our HFD-induced OA models (Chapter 3 and 5). This enumeration aptly showcases the interdependence of different biological processes, harbouring internal autocrine and paracrine loops, and reflects the complexity of metabolic OA pathogenesis.

The close interactions between metabolism and immunity are increasingly appreciated and have led to the exciting new field of 'immunometabolism'[83]: unravelling the molecular links between metabolic processes and immune signalling pathways to understand immunity in both health and metabolic disease. Metabolic changes induced by overfeeding, or by specific diets, can impact the immune system in a complex organ-specific manner – explaining why the unfocused treatment of changing a diet and increasing physical exercise ameliorates OA progression. Immune cells possess the ability to respond to environmental signals and exhibit a wide variety of distinct functional fates[12]. The functional plasticity of immune cells is paralleled by their

profound metabolic reprogramming capabilities, matching the cells' function, lifespan and bioenergetic requirements during consecutive transitions from inactive to active state. For example, this was recently corroborated by the discovery of an alternative metabolic pathway in natural killer (NK) cells that supports NK cell activation[84,85]. These recent findings convincingly demonstrate that systemic metabolism influences cellular metabolism, thus shaping the immune response. Taken together with the research presented in this thesis, changes in lipid metabolism could underlie the observed monocyte activation in the context of metabolic OA. In particular, we propose that sEH and its products could represent an intersection of metabolic and inflammatory pathways through which microbial signals (e.g. LPS) can regulate both metabolism and immunity, much like the eicosanoid-driven host-pathogen interaction[86,87]. This metabolic link may ultimately be exploited to treat metabolic OA, however, given the plethora of interacting physiological pathways involved, we have to acknowledge that single-target drugs or general medication is at least difficult but probably impossible to design.

Metabolic osteoarthritis: is the whole worse than the sum of its parts?

This thesis contributes to the view that the whole is worse than the sum of its parts in metabolic OA. The different parts (e.g. cartilage damage, adipose stress, systemic inflammation, pain) amplify each other via the various interconnections and feed-forward loops in these systems, thus chronically worsening disease progression. Elaborating on this reasoning, it is not farfetched to propose that OA development in one joint may increase the risk of OA development in other joints. OA frequently affects multiple joints in an individual[88], but involvement of multiple joints is relatively understudied and has not been extensively characterized epidemiologically[89]. Nevertheless, it is conceivable that locally induced mediators can enter the circulation and damage or at least prime other joints. In Chapter 4 for example, the sham-operated knee joints of mice fed a HFD showed a slight increase in crown-like structures in the IPFP compared with LFD-fed mice, suggesting a systemic process. However, this hypothesis is difficult to substantiate with our data, as we cannot eliminate the impact of sham-surgery. Future preclinical studies with surgical models (like DMM) should compare inflammation-related metabolic OA features in the operated knee with the non-operated knee and other non-operated joints in the same mouse, performing sham surgery in a separate group of age and sex-matched mice, to investigate the possibility of a metabolic OA feed-forward loop at joint level. In humans, further epidemiological research is needed to determine whether having OA in a single joint increases the risk of multiple joint OA (MJOA). Soon to be published findings from the Johnston County Osteoarthritis (JoCo OA) Study, a community-based prospective cohort, suggest that MJOA is highly prevalent in the population and relates to a high disease

burden[89]. Though the high mean age (72 years) and BMI (31 kg/m^2) of this particular sample prohibits generalisation below the age of 55, the unexpectedly high percentage of MJOA in this population may indicate that single-joint OA can indeed progress to MJOA. If true, this would cause another shift in our understanding of OA aetiology and progression: from an articular cartilage-centered to a whole-joint disease, could the metabolic OA phenotype actually be a whole-body disease (Figure 1)? The concept of metabolic OA as a whole-body disease would definitely impact current practice, as it would make early diagnosis even more pressing and change treatment methodology due to the additional need to prevent spread to other joints.

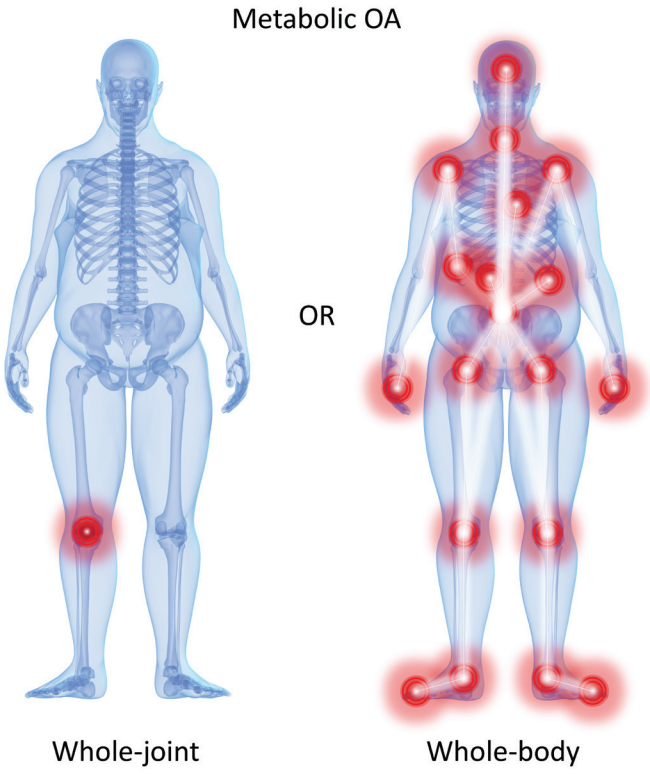


Figure 1. Thesis-driven hypothesis: from an articular cartilage-centered to a whole-joint disease, could the metabolic OA phenotype be a whole-body disease? The intestinal microbiota is especially vital to metabolic homeostasis and host health, as perturbations in intestinal microbiota (termed dysbiosis) have been associated with the pathogenesis of both intestinal and extra-intestinal disorders like obesity. Correlational evidence is emerging for a potential relationship between dysbiosis and metabolic OA onset, as described in this chapter, raising the question whether and how dysbiosis can impact metabolic OA pathology.

In conclusion, we have obtained deeper insight into the complexity and biological mechanisms involved in metabolic OA. Our major finding was the need for an additional trigger on top of diet-induced metabolic dysfunction to disturb the homeostatic balance between immune cells and articular cartilage. Dietary modulation remains the basis for treatment of metabolic diseases like metabolic OA, likely signifying an essential role for the GI tract and its microbiome. We show that high-fat feeding alone induces a proinflammatory environment by shifting eicosanoid metabolism towards the CYP450 pathway, increasing monocyte numbers and activation, and increasing synovial iNOS deposition in HFD-fed mice. Understanding the proinflammatory priming effect of high-fat feeding and how it exacerbates OA progression offers important opportunities to intervene, as the intertwining of metabolic and inflammatory pathways involved may provide for synergistic effects in restoring homeostasis. This thesis suggests sEH and its DHET metabolites as potential treatment targets to provide therapeutic benefit in OA. Thanks to eicosanoid involvement in microbial communication as well as host metabolism and immunity[86,87], sEH and its products could represent an intersecting target for which treatment effects could be synergistically induced in all three systems (microbiome, metabolism and immunity).

Disease, by definition, is disruption of homeostasis. In its attempts to restore homeostasis, inflammation might enforce and perpetuate metabolic changes in a persistent stimulus and possibly drive the system to become locked in an alternative, harmful stable state. This thesis proposes that in metabolic OA, a changed eicosanoid metabolism along with a heightened inflammatory state (e.g. increased CRP) releases mediators into circulation that induce non-classical monocyte activation as well as their infiltration into tissues. Local inflammation likely induces factors (e.g. iNOS) that contribute to maintain systemic activation, resulting in a chronic pathological state. Building on this framework, we propose to change the concept of OA as a whole-joint disease to OA as a whole-body disease, at least for the metabolic OA subtype, in which the joint is susceptible to signals that can originate outside the joint.

References

1. Zhuo, Q., Yang, W., Chen, J. & Wang, Y. Metabolic syndrome meets osteoarthritis. *Nat. Rev. Rheumatol.* **8**, 729–737 (2012).
2. Li, S. & Felson, D. T. What Is the Evidence to Support the Association Between Metabolic Syndrome and Osteoarthritis? A Systematic Review. *Arthritis Care Res.* **71**, 875–884 (2019).
3. King, L. K., March, L. & Anandacoomarasamy, A. Obesity & osteoarthritis. *Indian J. Med. Res.* **138**, 185–193 (2013).
4. Golay, A. & Bobbioni, E. The role of dietary fat in obesity. *Int. J. Obes. Relat. Metab. Disord. J. Int. Assoc. Study Obes.* **21 Suppl 3**, S2-11 (1997).
5. Buettner, R., Schölmerich, J. & Bollheimer, L. C. High-fat Diets: Modeling the Metabolic Disorders of Human Obesity in Rodents*. *Obesity* **15**, 798–808 (2007).
6. Wang, C.-Y. & Liao, J. K. A Mouse Model of Diet-Induced Obesity and Insulin Resistance. in *mTOR* (ed. Weichhart, T.) vol. 821 421–433 (Humana Press, 2012).
7. Silberberg, M. & Silberberg, R. Degenerative joint disease in mice fed a high-fat diet at various ages. *Exp. Med. Surg.* **10**, 76–87 (1952).
8. Donovan, E. L., Lopes, E. B. P., Batushansky, A., Kinter, M. & Griffin, T. M. Independent effects of dietary fat and sucrose content on chondrocyte metabolism and osteoarthritis pathology in mice. *Dis. Model. Mech.* **11**, dmm034827 (2018).
9. Wallace, J. L. Polypharmacy of osteoarthritis: the perfect intestinal storm. *Dig. Dis. Sci.* **58**, 3088–3093 (2013).
10. Scarpignato, C. *et al.* Safe prescribing of non-steroidal anti-inflammatory drugs in patients with osteoarthritis--an expert consensus addressing benefits as well as gastrointestinal and cardiovascular risks. *BMC Med.* **13**, 55 (2015).
11. Monteiro, M. P. & Batterham, R. L. The Importance of the Gastrointestinal Tract in Controlling Food Intake and Regulating Energy Balance. *Gastroenterology* **152**, 1707-1717.e2 (2017).
12. Buck, M. D., Sowell, R. T., Kaech, S. M. & Pearce, E. L. Metabolic Instruction of Immunity. *Cell* **169**, 570–586 (2017).
13. Carding, S., Verbeke, K., Vipond, D. T., Corfe, B. M. & Owen, L. J. Dysbiosis of the gut microbiota in disease. *Microb. Ecol. Health Dis.* **26**, (2015).
14. Marchesi, J. R. *et al.* The gut microbiota and host health: a new clinical frontier. *Gut* **65**, 330–339 (2016).
15. Szychlinska, M. A., Di Rosa, M., Castorina, A., Mobasheri, A. & Musumeci, G. A correlation between intestinal microbiota dysbiosis and osteoarthritis. *Heliyon* **5**, e01134 (2019).
16. Courties, A., Berenbaum, F. & Sellam, J. The Phenotypic Approach to Osteoarthritis: A Look at Metabolic Syndrome-Associated Osteoarthritis. *Joint Bone Spine* S1297319X18304445 (2018) doi:10.1016/j.jbspin.2018.12.005.
17. He, C. *et al.* High-Fat Diet Induces Dysbiosis of Gastric Microbiota Prior to Gut Microbiota in Association With Metabolic Disorders in Mice. *Front. Microbiol.* **9**, (2018).
18. Guss, J. D. *et al.* The effects of metabolic syndrome, obesity, and the gut microbiome on load-induced osteoarthritis. *Osteoarthritis Cartilage* **27**, 129–139 (2019).

19. Ulici, V. *et al.* Osteoarthritis induced by destabilization of the medial meniscus is reduced in germ-free mice. *Osteoarthritis Cartilage* **26**, 1098–1109 (2018).
20. Huang, Z. Y., Stabler, T., Pei, F. X. & Kraus, V. B. Both systemic and local lipopolysaccharide (LPS) burden are associated with knee OA severity and inflammation. *Osteoarthritis Cartilage* **24**, 1769–1775 (2016).
21. Cani, P. D. *et al.* Metabolic Endotoxemia Initiates Obesity and Insulin Resistance. *Diabetes* **56**, 1761–1772 (2007).
22. Hooper, L. V., Littman, D. R. & Macpherson, A. J. Interactions Between the Microbiota and the Immune System. *Science* **336**, 1268–1273 (2012).
23. Saltiel, A. R. & Olefsky, J. M. Inflammatory mechanisms linking obesity and metabolic disease. *J. Clin. Invest.* **127**, 1–4.
24. Gierman, L. M. *et al.* Metabolic stress-induced inflammation plays a major role in the development of osteoarthritis in mice. *Arthritis Rheum.* **64**, 1172–1181 (2012).
25. Hotamisligil, G. S. Inflammation and metabolic disorders. *Nature* **444**, 860–867 (2006).
26. Wang, X., Hunter, D., Xu, J. & Ding, C. Metabolic triggered inflammation in osteoarthritis. *Osteoarthritis Cartilage* **23**, 22–30 (2015).
27. Ghazalpour, A., Cespedes, I., Bennett, B. J. & Allayee, H. Expanding role of gut microbiota in lipid metabolism: *Curr. Opin. Lipidol.* **27**, 141–147 (2016).
28. Sekar, S. *et al.* Saturated fatty acids induce development of both metabolic syndrome and osteoarthritis in rats. *Sci. Rep.* **7**, 46457 (2017).
29. Araújo, A. C., Wheelock, C. E. & Haeggström, J. Z. The Eicosanoids, Redox-Regulated Lipid Mediators in Immunometabolic Disorders. *Antioxid. Redox Signal.* **29**, 275–296 (2018).
30. Lippiello, L., Walsh, T. & Fienhold, M. The association of lipid abnormalities with tissue pathology in human osteoarthritic articular cartilage. *Metabolism.* **40**, 571–576 (1991).
31. Baudart, P., Louati, K., Marcelli, C., Berenbaum, F. & Sellam, J. Association between osteoarthritis and dyslipidaemia: a systematic literature review and meta-analysis. *RMD Open* **3**, e000442 (2017).
32. De Taeye, B. M. *et al.* Expression and Regulation of Soluble Epoxide Hydrolase in Adipose Tissue. *Obesity* **18**, 489–498 (2010).
33. Liu, Y. *et al.* Inhibition of Soluble Epoxide Hydrolase Attenuates High-Fat-Diet–Induced Hepatic Steatosis by Reduced Systemic Inflammatory Status in Mice. *PLoS ONE* **7**, e39165 (2012).
34. Bettaieb, A. *et al.* Soluble Epoxide Hydrolase Deficiency or Inhibition Attenuates Diet-induced Endoplasmic Reticulum Stress in Liver and Adipose Tissue. *J. Biol. Chem.* **288**, 14189–14199 (2013).
35. Enayetallah, A. E., French, R. A., Barber, M. & Grant, D. F. Cell-specific Subcellular Localization of Soluble Epoxide Hydrolase in Human Tissues. *J. Histochem. Cytochem.* **54**, 329–335 (2006).
36. Luo, P. *et al.* Inhibition or Deletion of Soluble Epoxide Hydrolase Prevents Hyperglycemia, Promotes Insulin Secretion, and Reduces Islet Apoptosis. *J. Pharmacol. Exp. Ther.* **334**, 430–438 (2010).
37. Xu, X. *et al.* The Role of Cytochrome P450 Epoxygenases, Soluble Epoxide Hydrolase, and Epoxyeicosatrienoic Acids in Metabolic Diseases. *Adv. Nutr. Int. Rev. J.* **7**, 1122–1128 (2016).

38. Zha, W. *et al.* Functional characterization of cytochrome P450-derived epoxyeicosatrienoic acids in adipogenesis and obesity. *J. Lipid Res.* **55**, 2124–2136 (2014).
39. Wang, W. *et al.* Lipidomic profiling of high-fat diet-induced obesity in mice: Importance of cytochrome P450-derived fatty acid epoxides: Lipidomics of Obesity. *Obesity* **25**, 132–140 (2017).
40. Wang, W. *et al.* Lipidomic profiling reveals soluble epoxide hydrolase as a therapeutic target of obesity-induced colonic inflammation. *Proc. Natl. Acad. Sci.* **115**, 5283–5288 (2018).
41. Imig, J. D. & Hammock, B. D. Soluble epoxide hydrolase as a therapeutic target for cardiovascular diseases. *Nat. Rev. Drug Discov.* **8**, 794–805 (2009).
42. Iyer, A. *et al.* Pharmacological Inhibition of Soluble Epoxide Hydrolase Ameliorates Diet-Induced Metabolic Syndrome in Rats. *Exp. Diabetes Res.* **2012**, 1–11 (2012).
43. Fernandes, G. S. & Valdes, A. M. Cardiovascular disease and osteoarthritis: common pathways and patient outcomes. *Eur. J. Clin. Invest.* **45**, 405–414 (2015).
44. Theken, K. N. *et al.* Evaluation of cytochrome P450-derived eicosanoids in humans with stable atherosclerotic cardiovascular disease. *Atherosclerosis* **222**, 530–536 (2012).
45. Valdes, A. M. *et al.* Omega-6 oxylipins generated by soluble epoxide hydrolase are associated with knee osteoarthritis. *J. Lipid Res.* **59**, 1763–1770 (2018).
46. Dennis, E. A. & Norris, P. C. Eicosanoid Storm in Infection and Inflammation. *Nat. Rev. Immunol.* **15**, 511–523 (2015).
47. Rahmati, M., Mobasheri, A. & Mozafari, M. Inflammatory mediators in osteoarthritis: A critical review of the state-of-the-art, current prospects, and future challenges. *Bone* **85**, 81–90 (2016).
48. Raghu, H. *et al.* CCL2/CCR2, but not CCL5/CCR5, mediates monocyte recruitment, inflammation and cartilage destruction in osteoarthritis. *Ann. Rheum. Dis.* **76**, 914–922 (2017).
49. Lopes, E. B. P., Filiberti, A., Husain, S. A. & Humphrey, M. B. Immune Contributions to Osteoarthritis. *Curr. Osteoporos. Rep.* **15**, 593–600 (2017).
50. Bernardini, G., Benigni, G., Scrivo, R., Valesini, G. & Santoni, A. The Multifunctional Role of the Chemokine System in Arthritogenic Processes. *Curr. Rheumatol. Rep.* **19**, 11 (2017).
51. Kundu, S. *et al.* Metabolic products of soluble epoxide hydrolase are essential for monocyte chemotaxis to MCP-1 in vitro and in vivo. *J. Lipid Res.* **54**, 436–447 (2013).
52. Rogacev, K. S. *et al.* Monocyte heterogeneity in obesity and subclinical atherosclerosis. *Eur. Heart J.* **31**, 369–376 (2010).
53. Poitou, C. *et al.* $CD14^{dim}$ $CD16^{+}$ and $CD14^{+}$ $CD16^{+}$ Monocytes in Obesity and During Weight Loss: Relationships With Fat Mass and Subclinical Atherosclerosis. *Arterioscler. Thromb. Vasc. Biol.* **31**, 2322–2330 (2011).
54. Loukov, D., Karampatos, S., Maly, M. R. & Bowdish, D. M. E. Monocyte activation is elevated in women with knee-osteoarthritis and associated with inflammation, BMI and pain. *Osteoarthritis Cartilage* **26**, 255–263 (2018).
55. Wong, K. L. *et al.* The three human monocyte subsets: implications for health and disease. *Immunol. Res.*

53, 41–57 (2012).
56. Stansfield, B. K. & Ingram, D. A. Clinical significance of monocyte heterogeneity. *Clin. Transl. Med.* **4**, 5 (2015).
57. Tsukamoto, M., Suzuki, K., Seta, N. & Takeuchi, T. Increased circulating CD14brightCD16+ intermediate monocytes are regulated by TNF-α and IL-6 axis in accordance with disease activity in patients with rheumatoid arthritis. *Clin. Exp. Rheumatol.* **36**, 540–544 (2018).
58. Li, L. & Jiang, B.-E. Serum and synovial fluid chemokine ligand 2/ monocyte chemoattractant protein 1 concentrations correlates with symptomatic severity in patients with knee osteoarthritis. *Ann. Clin. Biochem.* **52**, 276–282 (2015).
59. Castoldi, A., Naffah de Souza, C., Câmara, N. O. S. & Moraes-Vieira, P. M. The Macrophage Switch in Obesity Development. *Front. Immunol.* **6**, (2016).
60. Manferdini, C. *et al.* Adipose stromal cells mediated switching of the pro-inflammatory profile of M1-like macrophages is facilitated by PGE2: in vitro evaluation. *Osteoarthritis Cartilage* **25**, 1161–1171 (2017).
61. Daghestani, H. N., Pieper, C. F. & Kraus, V. B. Soluble Macrophage Biomarkers Indicate Inflammatory Phenotypes in Patients With Knee Osteoarthritis: Macrophage Markers in OA. *Arthritis Rheumatol.* **67**, 956–965 (2015).
62. de Jong, A. J. *et al.* Lack of high BMI-related features in adipocytes and inflammatory cells in the infrapatellar fat pad (IFP). *Arthritis Res. Ther.* **19**, 186 (2017).
63. Misharin, A. V. *et al.* Nonclassical Ly6C– Monocytes Drive the Development of Inflammatory Arthritis in Mice. *Cell Rep.* **9**, 591–604 (2014).
64. Wu, C.-L. *et al.* Conditional Macrophage Depletion Increases Inflammation and Does Not Inhibit the Development of Osteoarthritis in Obese Macrophage Fas-Induced Apoptosis-Transgenic Mice: CONDITIONAL MACROPHAGE DEPLETION IN MaFIA-TRANSGENIC MICE. *Arthritis Rheumatol.* **69**, 1772–1783 (2017).
65. Barboza, E. *et al.* Profibrotic Infrapatellar Fat Pad Remodeling Without M1 Macrophage Polarization Precedes Knee Osteoarthritis in Mice With Diet-Induced Obesity. *Arthritis Rheumatol.* **69**, 1221–1232 (2017).
66. Chiu, Y. G. *et al.* CD16 (FcRγIII) as a potential marker of osteoclast precursors in psoriatic arthritis. *Arthritis Res. Ther.* **12**, R14 (2010).
67. Durand, M. *et al.* Monocytes from patients with osteoarthritis display increased osteoclastogenesis and bone resorption: The In Vitro Osteoclast Differentiation in Arthritis study. *Arthritis Rheum.* **65**, 148–158 (2013).
68. Puchner, A. *et al.* Non-classical monocytes as mediators of tissue destruction in arthritis. *Ann. Rheum. Dis.* annrheumdis-2018-213250 (2018) doi:10.1136/annrheumdis-2018-213250.
69. Geurts, J. *et al.* Elevated marrow inflammatory cells and osteoclasts in subchondral osteosclerosis in human knee osteoarthritis: MARROW INFLAMMATORY CELLS IN OSTEOARTHRITIS. *J. Orthop. Res.* **34**, 262–269 (2016).
70. Bertuglia, A. *et al.* Osteoclasts are recruited to the subchondral bone in naturally occurring post-traumatic equine carpal osteoarthritis and may contribute to cartilage degradation. *Osteoarthritis Carti-*

lage **24**, 555–566 (2016).
71. Rossol, M., Kraus, S., Pierer, M., Baerwald, C. & Wagner, U. The CD14 ^{bright} CD16+ monocyte subset is expanded in rheumatoid arthritis and promotes expansion of the Th17 cell population: Monocyte Subset Promotes Th17 Cell Expansion in RA. *Arthritis Rheum.* **64**, 671–677 (2012).
72. Tsukamoto, M. *et al.* CD-14brightCD16+ intermediate monocytes are induced by interleukin-10 and positively correlate with disease activity in rheumatoid arthritis. *Arthritis Res. Ther.* **19**, 28 (2017).
73. Cackowski, F. C. *et al.* Osteoclasts are important for bone angiogenesis. *Blood* **115**, 140–149 (2010).
74. Cui, Y. *et al.* EPC -derived exosomes promote osteoclastogenesis through Lnc RNA - MALAT 1. *J. Cell. Mol. Med.* **23**, 3843–3854 (2019).
75. Cackowski, F. C. & Roodman, G. D. Perspective on the Osteoclast: An Angiogenic Cell? *Ann. N. Y. Acad. Sci.* **1117**, 12–25 (2007).
76. Mapp, P. I. & Walsh, D. A. Mechanisms and targets of angiogenesis and nerve growth in osteoarthritis. *Nat. Rev. Rheumatol.* **8**, 390–398 (2012).
77. Hamilton, J. L. *et al.* Targeting VEGF and Its Receptors for the Treatment of Osteoarthritis and Associated Pain: TARGETING VEGF AND VEGFRs FOR TREATMENT OF OSTEOARTHRITIS AND PAIN. *J. Bone Miner. Res.* **31**, 911–924 (2016).
78. Chen, J. *et al.* C-reactive protein can upregulate VEGF expression to promote ADSC-induced angiogenesis by activating HIF-1α via CD64/PI3k/Akt and MAPK/ERK signaling pathways. *Stem Cell Res. Ther.* **7**, 114 (2016).
79. Choi, J., Joseph, L. & Pilote, L. Obesity and C-reactive protein in various populations: a systematic review and meta-analysis: Obesity and CRP in various populations *J. Choi* et al. *Obes. Rev.* **14**, 232–244 (2013).
80. Thiele, J. R. *et al.* Dissociation of pentameric to monomeric C-reactive protein localizes and aggravates inflammation: in vivo proof of a powerful proinflammatory mechanism and a new anti-inflammatory strategy. *Circulation* **130**, 35–50 (2014).
81. Ganova, P., Gyurkovska, V., Belenska-Todorova, L. & Ivanovska, N. Functional complement activity is decisive for the development of chronic synovitis, osteophyte formation and processes of cell senescence in zymosan-induced arthritis. *Immunol. Lett.* **190**, 213–220 (2017).
82. Sproston, N. R. & Ashworth, J. J. Role of C-Reactive Protein at Sites of Inflammation and Infection. *Front. Immunol.* **9**, 754 (2018).
83. Rathmell, J. C. Metabolism and autophagy in the immune system: immunometabolism comes of age. *Immunol. Rev.* **249**, 5–13 (2012).
84. Assmann, N. *et al.* Srebp-controlled glucose metabolism is essential for NK cell functional responses. *Nat. Immunol.* **18**, 1197–1206 (2017).
85. Pearce, E. J. & Pearce, E. L. Driving immunity: all roads lead to metabolism. *Nat. Rev. Immunol.* **18**, 81–82 (2018).
86. Noverr, M. C., Erb-Downward, J. R. & Huffnagle, G. B. Production of Eicosanoids and Other Oxylipins by Pathogenic Eukaryotic Microbes. *Clin. Microbiol. Rev.* **16**,

517–533 (2003).
87. Tsitsigiannis, D. I. & Keller, N. P. Oxylipins as developmental and host–fungal communication signals. *Trends Microbiol.* **15**, 109–118 (2007).
88. Nelson, A. E., Smith, M. W., Golightly, Y. M. & Jordan, J. M. "Generalized osteoarthritis": A systematic review. *Semin. Arthritis Rheum.* **43**, 713–720 (2014).
89. Gullo, T. R. *et al.* Defining multiple joint osteoarthritis, its frequency and impact in a community-based cohort. *Semin. Arthritis Rheum.* **48**, 950–957 (2019).





Summary
Nederlandse samenvatting
Dankwoord
Curriculum vitae
List of abbreviations

Summary

The present thesis aims to investigate how metabolic overload contributes to the pathophysiology of knee OA. It has become increasingly recognized that aberrations in metabolism and immunity play a critical role in OA pathogenesis, especially in the 'metabolic OA' subtype. We explored the role of these independent yet intertwined processes using state-of-the-art lipidomic and cellular approaches in mouse models of diet-induced OA. **Chapter 2** presents an overview of twelve preclinical studies in which mice received various high-caloric dietary regimens at variable duration. The diet-induced osteoarthritis model was evaluated for its robustness and repeatability by comparing OA features observed in these experiments. From this comprehensive overview we deduced that diet-induced metabolic overload per se does not necessarily lead to aggravated articular cartilage degradation. Two out of twelve studies demonstrated aggravated cartilage degradation compared with controls. These studies were performed in mouse strains transgenic for human proteins involved either in inflammation (human C-reactive protein (hCRP) mice) or lipoprotein metabolism (ApoE*3Leiden.CETP mice). We therefore suggest that an additional trigger, other than high-caloric feeding alone, is necessary to evoke metabolic OA.

To evaluate whether nutritional fat could indeed aggravate OA progression, low- and high-fat feeding was combined with a mild mechanical stressor (**Chapter 3**). OA onset was induced by microsurgical destabilization of the medial meniscus (DMM) in C57BL/6J mice. This post-traumatic OA (PTOA) model is low invasive and sufficiently sensitive to study subtle changes in disease progression by mild triggers like genetic background and diet. High-fat diet (HFD) feeding indeed increased OA severity in this model and our findings point to a role for both lipid dysregulation and monocyte activation in disease pathogenesis. Based on these results, we suggest that these systemic factors might contribute to a diet-induced proinflammatory environment that enables aggravation of cartilage degeneration.

To unravel the effects of a dysregulated lipid metabolism on the inflammatory state, we studied the development of metabolic inflammation both locally and systemically. In **Chapter 4**, an extension of the studies described in Chapters 3 and 5, we focussed on the inflammatory status of the infrapatellar fat pad (IFP) during OA progression. Evidence is emerging that the IFP can be a potential local source of inflammatory mediators in the knee and hence contribute to OA progression. The most pronounced adipose inflammation, characterized by crown-like structures, was found in mice that received a HFD on top of a microsurgical trigger (DMM). We observed a significantly increased deposition of the proinflammatory macrophage marker iNOS due to DMM surgery, but found no change in pro-resolving macrophage marker CD206. Adipose fibrosis was minimal, but DMM intervention seemed to induce a trend towards increased fibrosis. These data suggest that HFD provides a priming effect on the IFP and that combined

actions of HFD feeding and a cartilage damage trigger (like DMM) bring the joint in a metabolic state of progressive OA.

Next, we addressed the involvement of the innate immune system in the development of diet-induced OA. For this we provided male mice from a human C-reactive protein (hCRP) knock-in strain with an HFD for 38 weeks (**Chapter 5**). We demonstrated that hCRP-tg mice developed more severe OA compared with their wild-type controls under the same HFD regimen. The expression of human CRP being the only variable, this finding implicates CRP as an independent trigger to aggravate HFD-induced OA development. Increased recruitment of classical and non-classical monocytes might be a mechanism of action through which CRP is involved in aggravating this process.

To expand on the outcomes of Chapters 3 and 5, in **Chapter 6** we assessed the contribution of elevated plasma cholesterol levels to the severity of diet-induced OA. Cholesterol is involved in lipid metabolism as well as inflammation and is described to aggravate OA progression. Novel high-intensive cholesterol-lowering strategies were evaluated for their efficacy in halting or reducing aggravation of pre-existent, diet-induced OA. We observed insignificant effects of therapeutic cholesterol-lowering on OA features and suggest that cholesterol-lowering treatments alone are probably not effective in preventing progression of pre-existent OA. We suggest that the absence of inflammation in this model might explain the reduced effectiveness of cholesterol lowering, which bears implications for the clinical setting.

Chapter 7 contains the general discussion, where the major findings of this thesis are placed into the context of the current status of the field. Here, we discuss the implications of findings described in this thesis and propose to view the metabolic OA subtype as a whole-body disease instead of a whole-joint disease.

Nederlandse samenvatting

Dit proefschrift heeft zich erop gericht om beter inzicht te krijgen in de bijdrage van metabole overbelasting aan het verloop van knieartrose (OA). Het wordt steeds meer erkend dat afwijkingen in metabolisme en immuniteit een cruciale rol spelen in de ontwikkeling van OA, vooral in het subtype gedefinieerd als 'metabole OA'. We onderzochten de rol van deze onafhankelijke, maar met elkaar verweven processen met behulp van state-of-the-art lipidomische en cellulaire technieken in muismodellen met dieet-geïnduceerde OA. **Hoofdstuk 2** presenteert een overzicht van twaalf preklinische studies waarin muizen verschillende hoogcalorische dieetregimes kregen in experimenten van variabele duur. Het dieet-geïnduceerde OA model werd geëvalueerd op zijn robuustheid door de verscheidene OA kenmerken te vergelijken die in deze experimenten werden waargenomen. Uit dit uitgebreide overzicht hebben we afgeleid dat dieet-geïnduceerde metabole overbelasting op zichzelf niet noodzakelijkerwijs leidt tot toegenomen kraakbeenschade. Twee van de twaalf studies toonden een significante verslechtering van het gewrichtskraakbeen in vergelijking met controles. Deze studies werden uitgevoerd in muizenstammen die transgeen zijn voor menselijke eiwitten die betrokken zijn bij ontsteking (muizen met humaan C-reactief proteïne (hCRP)) of bij het lipoproteïnemetabolisme (ApoE*3Leiden.CETP-muizen). We opperen daarom dat een extra trigger, naast hoogcalorisch eten, nodig is om metabole OA op te wekken.
Om te evalueren of een vetrijke voeding inderdaad de ontwikkeing van OA kan verergeren, werd vetarm en vetrijk eten gecombineerd met een milde mechanische stressor (**Hoofdstuk 3**). OA werd geïnduceerd door microchirurgische destabilisatie van de mediale meniscus (DMM) in wildtype C57BL/6J muizen. Dit posttraumatische OA (PTOA) model is laag invasief en voldoende gevoelig om subtiele veranderingen in ziekteprogressie te bestuderen door milde triggers zoals genetische achtergrond en dieet. Vetrijke voeding (HFD) verhoogde inderdaad de ernst van de kraakbeenschade in dit model en onze bevindingen wijzen op een rol voor zowel ontregeling van lipiden als activatie van monocyten bij de progressie van OA. Op basis van deze resultaten stellen wij voor dat deze systemische factoren kunnen bijdragen aan een door voeding geïnduceerde ontsteking die verergering van kraakbeenschade mogelijk maakt.
Om de effecten van een ontregeld lipidenmetabolisme op de ontstekingsstatus te ontrafelen, hebben we de ontwikkeling van metabole ontsteking zowel lokaal (in het kniegewricht) als systemisch (in het bloed) bestudeerd. In **Hoofdstuk 4**, een uitbreiding van de studies beschreven in hoofdstukken 3 en 5, hebben we ons gericht op de ontstekingsstatus van het lichaam van Hoffa (infrapatellar fat pad, IFP) tijdens de ontwikkeling van OA. Er zijn aanwijzingen dat de IFP een potentiële lokale bron van ontstekingsmediatoren in de knie kan zijn en daarom kan bijdragen aan de progressie van OA. De meest uitgesproken vetontsteking, gekenmerkt door 'kroonachtige structuren'

(crown-like structures, CLS), werd gevonden bij muizen die een vetrijk dieet kregen bovenop een microchirurgische trigger (DMM). We zagen een aanzienlijk verhoogde afzetting van de macrofaag marker iNOS als gevolg van DMM-chirurgie, duidend op ontsteking, maar vonden geen verandering in de ontstekingsremmende macrofaag marker CD206. Vetfibrose was minimaal, maar de chirurgische DMM ingreep leek een trend naar verhoogde fibrose te veroorzaken. Deze data suggereren dat een vetrijk dieet IFP metabolisch gezien 'oplaadt' en dat de combinatie van vetrijke voeding en een trigger voor kraakbeenschade (zoals DMM) het gewricht in een metabole staat van progressieve OA brengen.

Vervolgens hebben we de betrokkenheid van het aangeboren immuunsysteem bij de ontwikkeling van dieet-geïnduceerde OA onderzocht. Hiervoor hebben we mannelijke muizen van een humaan C-reactieve proteïne (hCRP) knock-in stam gedurende 38 weken voorzien van een vetrijk dieet (**Hoofdstuk 5**). We toonden aan dat hCRP-transgene muizen een ernstiger verloop van OA ontwikkelden in vergelijking met hun wildtype-controles op hetzelfde vetrijke dieet. Aangezien het tot expressie brengen van het humaan CRP de enige variabele was tussen beide studiegroepen, impliceert deze bevinding dat humaan CRP als een onafhankelijke trigger kan dienen om dieet-geïnduceerde OA te verergeren. Toegenomen werving van klassieke en niet-klassieke monocyten kan een mechanisme zijn waarop humaan CRP betrokken is bij het verergeren van OA.

Om de resultaten van hoofdstukken 3 en 5 uit te breiden, hebben we in **Hoofdstuk 6** de bijdrage geëvalueerd van verhoogde plasma cholesterolwaarden aan de ernst van dieet-geïnduceerde OA. Cholesterol is zowel betrokken bij het lipidenmetabolisme als bij ontsteking en is beschreven OA ontwikkeling te verergeren. Nieuwe, hoog-intensieve cholesterolverlagende strategieën werden geëvalueerd op hun werkzaamheid bij het stoppen of verminderen van de progressie van reeds bestaande, door het dieet-geïnduceerde OA. We hebben onbeduidende effecten waargenomen van therapeutische cholesterolverlagers op kraakbeenschade en suggereren dat cholesterolverlagende behandelingen alleen waarschijnlijk niet effectief zijn in het voorkomen van progressie van reeds bestaande OA. Wellicht verklaart de afwezigheid van ontsteking in dit model de verminderde effectiviteit van de cholesterolverlaging.

Hoofdstuk 7 bevat de algemene discussie, waarin de belangrijkste bevindingen van dit proefschrift in de context van de huidige kennis en ontwikkelingen in het artrose veld worden geplaatst. Hier bespreken we de implicaties van bevindingen beschreven in dit proefschrift en stellen we voor om het metabole OA subtype te zien als een aandoening van het hele lichaam.

Dankwoord

Tijdens het uitvoeren van mijn PhD traject en het schrijven van mijn proefschrift ben ik tweemaal bevallen – alles bij elkaar genomen voelt deze prestatie als de derde bevalling. Ik heb ontzettend veel geleerd gedurende deze periode, ook dankzij mijn bijzondere positie waardoor ik mijn onderzoek zowel bij TNO in Leiden als bij het UMC Utrecht kon uitvoeren. Het was soms pittig, met ups en downs, en ik heb dan ook erg veel te danken aan de steun van geweldige collega's en andere mensen om mij heen. Iedereen die heeft bijgedragen aan dit proefschrift, direct of indirect, wil ik graag op deze plaats bedanken – en een aantal hieronder in het bijzonder.

Geachte prof. dr. Weinans, beste Harrie, je kon mij altijd meeslepen in je aanstekelijke enthousiasme en geweldige passie voor het vak. Onze communicatie liet soms te wensen over, maar ik wist dat ik altijd op jou kon rekenen en dat waardeer ik enorm. Heel erg bedankt voor de energie die je in mij en mijn onderzoek gestoken hebt en voor je vertrouwen.

Geachte prof. dr. Lafeber, beste Floris, een typische professor, voor zover die bestaan natuurlijk, wie er plezier in schepte advocaat van de duivel te spelen en met zo kort mogelijke antwoorden communiceerde. Ik heb erg veel geleerd van jouw kijk op onderzoek doen, met één been in de kliniek en één op het lab, en wil je daar ontzettend voor bedanken. Ik vond het mooi dat je naast je professionele rol ook los durfde te zijn en heb veel gelachen om je humor.

Geachte dr. Stoop, beste Reinout, met jou heb ik toch wel de hechtste band opgebouwd; ontzettend bedankt voor je nimmer aflatende begeleiding en hulp, ook in het lab, jij bent cruciaal geweest voor mijn PhD traject. Daarnaast denk ik ook met veel plezier terug aan onze gezamenlijke fietstochten en culinaire uitspattingen buiten het werk om. Ik hoop dat ik je nog veel zal blijven zien, aan de fysieke afstand tussen onze woningen kan het in ieder geval niet liggen!

Geachte dr. Bobeldijk, beste Ivana, je kreeg mij in je schoot geworpen bij je nieuwe baan als projectleider bij TNO MHR en hebt deze verantwoordelijkheid gracieus opgepakt. Ik voelde mij op mijn gemak bij jou, kon altijd bij je binnenlopen en vond je andere kijk op mijn onderzoek waardevol. Bedankt voor de fijne tijd en in het bijzonder het leuke Keystone congres samen.

Geachte dr. Mastbergen, beste Simon, hoewel je niet officieel een co-promotor van mij was, voelde dat in de praktijk toch zo. Je was wat dat betreft een man met twee gezichten voor mij: bedankt voor je adviezen met betrekking tot mijn onderzoek, maar ook voor je bijdrage aan de leuke sfeer bij onze uitjes buiten het werk om.

Geachte dr. Zuurmond, beste Anne-Marie, jij was één van de redenen voor mij om toch opnieuw aan een PhD traject te beginnen. Bedankt voor de begeleiding en tijd die

je mij hebt gegeven, ook nadat je aan je nieuwe baan begonnen was.

Dear members of the **D-BOARD consortium**, many thanks for the interesting meetings and for constructively thinking along with our research. **Dear Ferran, Srini, Dave** and **Vicky**, thank you for your collaboration and for sharing your expertise in the field of lipidomics, the results of which have become an integral part to my thesis. Prof. Dear **Ali**, it was always 'gezellig' with you! Thank you for everything, and in particular for your contribution to Chapter 3.

Behdad, Parisa, en alle overige collega's van de afdeling Orthopedie, bedankt voor de constructieve meetings en jullie input op mijn onderzoek!

Huub, D-BOARD collega, het was fijn om samen met jou op te kunnen trekken. Veel succes met je verdere carrière in de orthopedie! Reumatologie kamergenoten, **Thijmen, Nick, Jelena, Maartje, Lize, Eefje, Bart, Xavier, Astrid**, de maandagen waren dankzij jullie altijd een feestje. Bedankt voor het plezier op de werkvloer en zeker ook daarbuiten, tijdens onze stedentrips! Nicoline, bedankt voor jouw aanvullende begeleiding op het gebied van macrofagen en voor de leuke uitjes die je hebt georganiseerd – voor mij en het Weinans team! En niet onbelangrijk: dankzij jou en **Kelly** konden mijn IFP samples toch nog geanalyseerd en gepubliceerd worden, daar ben ik jullie beiden ontzettend dankbaar voor! **Paco**, bedankt voor je hulp bij de ingewikkeldere statistische analyses. **Katja, Arno, Kim, Marion, Anne-Karien**, en alle overige Reumatologie collega's, bedankt voor jullie input tijdens de meetings waar ik veel van opgestoken heb en voor de fijne tijd bij jullie op de afdeling!

TNO MHR collega's, de geweldige sfeer bij ons op de afdeling was één van de redenen voor mij om dit PhD traject te starten. Graag wil ik jullie allemaal ontzettend bedanken voor de fijne tijd, en in het bijzonder:
Lobke, bedankt voor jouw voorwerk en de duidelijke overdracht, daar heb ik veel aan gehad. **Frits**, mijn rots in de branding, zonder jouw vrijwillige hulp was mijn PhD traject een heel stuk lastiger, zo niet onmogelijk, geweest – ik ben jou ontzettend dankbaar voor je hulp bij het ontkalken, het scoren, je adviezen, je hulp met de confocal microscoop en wat al niet meer. Wat ben ik blij dat jij vandaag naast mij staat als paranimf! **Erik**, wandelende histologie encyclopedie, ik prijs me gelukkig dat ik van jou dit vak geleerd kreeg – bedankt voor alles, ook (of misschien vooral?) voor je oneindige gemopper en hoekige humor. **Wim**, bedankt voor de leuke momenten binnen en buiten het lab en voor het net missen van mijn hoofd toen die schuimspaan enthousiast uit het handvat schoot. **Christa** en **Joline**, ervaren muizenchirurgen, bedankt voor jullie adviezen omtrent het opereren en de nazorg van mijn proefdieren.

Pascalle, als proefdierdeskundige heb ik veel aan jouw kennis en ervaring gehad bij het ontwerpen en aanvragen van mijn dierproeven. **Suzan, Marjolein** en **Renate**, bedankt voor de goede zorg en hulp omtrent mijn proefdieren. **Anne**, we hebben helaas kort samengewerkt, maar jouw immunohistologische kennis en vaardigheden hebben een enorme impact gehad op deze thesis. Heel erg bedankt voor je toewijding op dit vlak en voor de gezellige lunchwandelingen. **Stephan**, in het onderzoek doen zit het niet altijd mee; ik ben blij dat jij tijdens je laatste stage toch ontdekte dat dit niet de carrière voor jou was. Bedankt voor je inzet en het werk dat je gedaan kreeg, ik wens je het beste! **Monica**, dankzij jouw positieve instelling, incasseringsvermogen en enorme doorzettingsvermogen heb je geweldige resultaten en twee terechte co-auteurschappen behaald. Ik was trots te horen dat je nu een prachtige baan als analist gekregen hebt bij Frits op de afdeling en ik wens je een geweldige carrière verder!
Collega TNOIO's, **Susan, Rob, Wen, Petra, Martine** en **Marianne**, jullie hebben mij helpen groeien; ontzettend bedankt voor de gezelligheid in en om het lab en voor jullie ondersteuning (zowel praktisch als mentaal). **Hans**, jouw kennis van het atherosclerose veld is onmiskenbaar en bewonderenswaardig. Bedankt voor je uitstapje naar het artrose veld, waar jouw begeleiding en fijne samenwerking leidde tot Hoofdstuk 6! **Elsbet**, jij toverde altijd een lach op mijn gezicht; alles wat jij voor mij en de afdeling gedaan hebt valt onmogelijk samen te vatten in één zin. Heel erg bedankt voor je positiviteit, het delen van je kennis, je hulp en adviezen met betrekking tot mijn onderzoek, de fijne samenwerking die leidde tot Hoofdstuk 6, de hilarische woordspelingen en natuurlijk de gezelligheid!
Coen, een fijnere manager dan jij had ik me in die tijd niet kunnen wensen. Bedankt voor de kansen die je mij gegeven hebt als analist bij MHR en voor het behouden van de goede sfeer op de afdeling ondanks het zware weer waar we in zaten. **Han**, ik had een bijzondere positie als de enige overgebleven werknemer die aan artrose werkte, maar daar heb jij als manager nooit een punt van gemaakt. Bedankt voor het meedenken en faciliteren van de nodige accountverlengingen, dat heeft me erg geholpen.

Lieve familie, vrienden en vriendinnen, bedankt voor jullie interesse in mijn werk, maar vooral ook voor de ontspanning en afleiding. **Malou** en **Eva**, PhD lotgenoten, bij jullie vond ik de steun die ik nergens anders kon vinden: bedankt voor jullie vriendschap en het delen van ervaringen, de reality checks en voor jullie onvoorwaardelijke steun met betrekking tot mijn PhD traject. Ik ben ontzettend trots en blij, **Malou**, met jou aan mijn zijde als paranimf! Lieve **Ebeneters, Ebenhaezers, EbenhIJsers** (en ga zo maar door), bij jullie vond ik de ontspanning die ik af en toe hard nodig had – ik kijk met veel plezier terug op onze weekenden en vakanties samen en hoop dat er nog vele zullen volgen! Lieve **Jay**, ik wil jou ontzettend bedanken voor het ontwerpen van de prachtige kaft van mijn boekje! Lieve **Kim**, we spreken elkaar niet zo regelmatig meer

als vroeger, maar je blijft mijn allerbeste vriendin. Jij hebt een onmiskenbare stempel op mijn leven gedrukt en daar ben ik je voor altijd dankbaar voor. Lieve **Thijs**, ik vind het fijn nog steeds contact met jou te hebben, ook al wonen we elk aan de andere kant van Nederland. Bedankt voor alle fijne telefoongesprekken! Lieve **Rik** en **Martine**, jullie vriendschap betekent veel voor mij en ik hoop dat we nog vele jaren lichtjesfeesten zullen blijven vieren. Het was geen makkelijke opdracht om een kunstwerk te maken over mijn PhD project, **Martine**, maar jij hebt daar een geweldige invulling aan gegeven – ontzettend bedankt voor deze kroon op mijn werk! Lieve **Linde**, mijn eerste Voorschotense vriendin, bedankt voor jouw vriendschap! Ik hoop dat wij en onze meiden elkaar nog veel zullen blijven zien!

Lieve **Johnny, Monique, Freek** en **Renée**, een fijnere schoonfamilie kan ik me haast niet wensen. Bedankt voor jullie interesse in mijn onderzoek, maar vooral ook voor de steun daarnaast, welke alleen door familie geboden kan worden!
Lieve **Martijn, Annemieke, Laurens** en **Céline**, hoe heerlijk was het dat wij tegelijkertijd aan het grote avontuur van het starten van een gezin begonnen! Jullie hebben het jullie misschien nooit gerealiseerd, maar ik heb erg veel aan jullie gehad en ik ben ontzettend blij met jullie als familie!
Lieve **pap en mam**, ik weet niet waar ik moet beginnen jullie te bedanken. Jullie hebben me een mooie jeugd gegeven en dragen nog dagelijks bij aan het welzijn in ons leven. Voor jullie is nooit iets teveel en ik weet dat ik altijd op jullie terug kan vallen. Heel veel dank voor jullie liefde, aanmoediging en onvoorwaardelijke steun over de jaren.

Lieve **Lara** en **Ella**, jullie zijn de allerliefste, leukste en knapste dochters van de hele wereld en veel belangrijker voor mij dan dit boekje! Ik ben ontzettend trots op jullie en kan niet wachten tot jullie zusje zich aandient.
Lieve **Peter Paul**, jij bent mijn alles en ik weet zeker dat ik zonder jou hier niet had gestaan vandaag. Ik ben zo trots op en gelukkig met wat wij samen opgebouwd hebben. Bedankt voor al je liefde, steun en relativering: zonder jou was dit boekje er nooit gekomen. Bedankt ook voor de mooie momenten die we samen mee hebben mogen maken – ik hoop dat er nog vele zullen volgen. Met jou kan ik de wereld aan!

Curriculum vitae

Anne Elisabeth Kozijn was born on the 17th of November 1985 in Apeldoorn, The Netherlands. After obtaining her high school diploma at the Stedelijk Gymnasium Apeldoorn in 2004, she attended Wageningen University to study Biotechnology. During the broad BSc phase of this study she discovered that her interest lay primarily in the biomedical sciences and organised her MSc Biotechnology around this perspective. She dedicated the last year of her MSc study to the completion of two immunology-oriented scientific internships, at the Department of Cell Biology and Immunology of Wageningen University and at the Faculty of Medical Sciences from the Newcastle University. Here, she participated in a research project from the Musculoskeletal Research Group on the mechanisms underlying modulation of human Th17 responses in rheumatoid arthritis which resulted in her first publication. This scientific internship motivated her to continue doing research by means of a PhD track. She graduated from Wageningen University in January 2010. From March 2010 onwards she worked as a PhD candidate on the mechanisms behind tolerance induction to gluten within a celiac disease research program at the Laboratory of Pediatrics, division Gastroenterology and Nutrition, at the Erasmus Medical Centre under guidance of her promotor dr. Janneke Samsom. She ceased this PhD track in May 2012 and started as a research assistant at the Metabolic Health Research (MHR) Unit of the Netherlands Organisation of Applied Scientific Research (TNO). At the same department, in collaboration with the Orthopaedics and Reumatology Departments of University Medical Centre Utrecht (UMCU), she started her PhD on biomarkers in osteoarthritis in July 2013. She was guided by her promotors prof. dr. ir. Harrie Weinans (Orthopaedics, UMCU) and prof. dr. Floris Lafeber (Rheumatology, UMCU) and her co-promotors dr. Anne-Marie Zuurmond (TNO MHR) and later dr. Reinout Stoop (TNO MHR) and dr. Ivana Bobeldijk-Pastorova (TNO MHR). The overall aim of this research was to explore how metabolic overload contributes to the pathophysiology of knee osteoarthritis and the results of this research are presented in this thesis.

List of abbreviations

AA	Arachidonic acid (in Chapter 6 only: Atorvastatin + Alirocumab treatment)
AAALAC	Association for Assessment and Accreditation of Laboratory Animal Care
AAE	Atorvastatin + Alirocumab + Evinacumab treatment (Chapter 6)
ACL	Anterior cruciate ligament
ADAMTS	A disintegrin and metalloproteinase with thrombospondin motifs protein family
AE	Atorvastatin + Evinacumab treatment (Chapter 6)
AF	Alexa Fluor
ANGPTL3	Angiopoietin-like 3
ANOVA	Analysis of variance
AP	Alkaline phosphatase
APC	Allophycocyanin
APOE	Apolipoprotein E
APOC1	Apolipoprotein C1
ARA	Arachidonic acid
ARRIVE	Animal Research: Reporting of In Vivo Experiments
BMI	Body mass index
BSA	Bovine serum albumin
CCL	CC chemokine ligand
CD	Cluster of differentiation
Cer	Ceramides
CETP	Cholesteryl ester transfer protein
ChE	Cholesterol ester
CI	Confidence interval
CLS	Crown-like structures
COX	Cyclooxygenase
CRP	C-reactive protein
CVD	Cardiovascular disease
Cy	Cyanine
CYP	Cytochrome P450
DAMP	Danger-associated molecular pattern
DG	Diacylglycerols
DHA	Docosahexaenoic acid
DHET	Dihydroxyeicosatrienoic acid
DMM	Destabilization of the medial meniscus

EDTA	Ethylenediaminetetraacetic acid
EET	Epoxyeicosatrienoic acid
EH	Epoxide hydrolase
ELISA	Enzyme-linked immunosorbent assay
FACS	Fluorescence Activated Cell Sorting
FELASA	Federation of European Laboratory Animal Science Associations
FFA	Free fatty acids
FFPE	Formalin-fixed paraffin-embedded
FITC	Fluorescein isothiocyanate
FMO	Fluorescence minus one
FSC	Forward scatter
GI tract	Gastrointestinal tract
GM-CSF	Granulocyte-macrophage colony-stimulating factor
GR-1	Antibody against Ly-6G/Ly-6C
hCRP	Human C-reactive protein
HDHA	Hydroxy docosahexaenoic acid
HDL	High-density lipoprotein
HDL-C	High-density lipoprotein-associated cholesterol
HETE	Hydroxyeicosatetraenoic acid
HFD	High-fat diet (45%kcal from fat)
HODE	Hydroxyoctadecadienoic acid
HOMA-IR	Insulin resistance index
HPS	Hematoxylin phloxine saffron
HRP	Horse radish peroxidase
IDL	Intermediate-density lipoprotein
IFP	Infrapatellar fat pad (Hoffa's fat pad)
IHC	Immunohistochemistry
IL	Interleukin
iNOS	Inducible nitric oxide synthase
IPFP	Infrapatellar fat pad (Hoffa's fat pad)
IQR	Interquartile range
IS	Internal standard
LA	Linoleic acid
LDL	Low-density lipoprotein
LDLr	Low-density lipoprotein receptor
LFD	Low-fat diet (10%kcal from fat)
LOX	Lipoxygenase
LPB	Lipopolysaccharide-binding factor
LPC	Lysophosphatidylcholine

LPS	Lipopolysaccharide
LTF	Lateral tibiofemoral compartment of the knee joint
MAC	Membrane attack complex
MCP-1	Monocyte chemoattractant protein-1
MFD	Mid-fat diet (30%kcal from fat)
MHCII	Major histocompatibility complex class II
MJOA	Multiple joint osteoarthritis
MMP	Metalloproteinase
MMTL	Medial meniscotibial ligament
MRI	Magnetic resonance imaging
MTF	Medial tibiofemoral compartment of the knee joint
MUFA	Monounsaturated fatty acid
MWU	Mann–Whitney U test
NAFLD	Non-alcoholic fatty liver disease
NASH	Nonalcoholic steatohepatitis
NBCS	New-born calf serum
NGF	Nerve growth factor
NK cell	Natural killer cell
NS	Not significant
NSAID	Nonsteroidal anti-inflammatory drug
OA	Osteoarthritis
OARSI	Osteoarthritis Research Society International
oxLDL	Oxidized low-density lipoprotein
OxoODE	Oxooctadecadienoic acid
PBL	Peripheral blood leukocytes
PBS	Phosphate-Buffered Saline
PC	Phosphatidylcholine
PCA	Principal component analysis
PCSK9	Proprotein convertase subtilisin/kexin type 9
PE	Phycoerythrin
PerCP	Peridinin Chlorophyll Protein Complex
PGH2	Prostaglandin H2
PGE2	Prostaglandin E2
PLA2	Phospholipase A2
PLS-DA	Partial least squares discriminant analysis
PTOA	Post-traumatic osteoarthritis
PUFA	Polyunsaturated fatty acid
QC	Quality control
RA	Rheumatoid arthritis

ROI	Region of interest
RT	Room temperature
SD	Standard deviation
sEH	Soluble epoxide hydrolase
sEHi	Soluble epoxide hydrolase inhibitor
SEM	Standard error of the mean
SFA	Saturated fatty acids
SPF	Specific-pathogen-free
SPM	Sphingomyelin
SSC	Side scatter
T cell	Type of lymphocyte which develops in the thymus gland
TBS	Tris-buffered saline
TG	Triglycerides
TGF-β	Transforming growth factor β
TLR	Toll-like receptor
TNF-α	Tumor necrosis factor α
TNFR	Tumor necrosis factor receptor
VEGF	Vascular growth factor
VHFD	Very-high-fat diet (60%kcal from fat)
VLDL	Very-low-density lipoprotein
WTD	Western-type diet

